UTEC ME 85-014

Fifth Semi-Annual Report

to the

National Aeronautics and Space Administration

on

Grant NAG-1-283

ACOUSTIC PROPAGATION IN A THERMALLY STRATIFIED ATMOSPHERE

by

W. K. Van Moorhem

Mechanical and Industrial Engineering Department

University of Utah

Salt Lake City, Utah 84112

February 7, 1985

ABSTRACT

This report describes the activities during the fifth six month period of the investigation of acoustic propagation in the atmosphere with a realistic temperature profile. Progress has been achieved in two major directions: comparisons between the lapse model and experimental data taken by NASA during the second tower experiment, and development of a model propagation in an inversion. Data from the second tower experiment became available near the end of 1984 and some comparisons have been carried out, but this work is not complete. Problems with the temperature profiler during the experiment have produced temperature profiles that are difficult to fit to the assumed variation of temperature with height, but in cases where reasonable fits have been obtained agreement between the model and the experiments are close. The major weaknesses in the model appear to be the presence of discontinuities in some regions, the low sound levels predicted near the source height, and difficulties with the argument of the Hankel function being outside the allowable range. Work on the inversion model has progressed slowly, and the rays for that case are discussed along with a simple energy conservation model of sound level enhancement in the inversion case.

INTRODUCTION

During the past six months work on grant NAG-1-283 has progressed in several directions: the lapse case model has become operational and is being used to make comparisons with the propagation data obtained in the second tower experiment in October, 1984, and with data collected by Willshire and Shepherd using a wind turbine as a source; modeling of the inversion case is underway and is expected to be completed in the Spring or early Summer of 1985. Completion of the lapse case models was carried out by two Master's students, Alex Cheng and Yiping Ma. Cheng [1] used the saddle point method to carry out an approximate inversion of the Hankel transformed solution as was presented in the previous semi-annual report [2]. His work is mainly concerned with the region inside the shadow boundary and his results show the usual interference pattern. He did, however, use the approach of Sachs and Silbert [3] to avoid the singularity occuring at the shadow boundary in the saddle point approximation and this approach allows the solution to be extended into the shadow region. Ma [4] used approximate contour integration to extend the solution deep into the shadow region and to investigate the contribution of the surface wave to the total solution in the lapse case.

The total model using both of these results shows all of the characteristics of the empirical model of Wiener and Keast [5]: a region of increasing excess attenuation beyond the shadow boundary extending to a distance beyond the boundary of the same order of magnitude as the distance from the source to the boundary, followed by a region of nearly constant excess attenuation. The model often shows an overshoot in excess attenuation in the area where the increasing excess attenuation region merges with the region of "constant" excess attenuation. This overshoot is also seen in Weiner and Keast's data [5]. The model actually shows a slowly increasing excess attenuation (as $r^{1/2}$) in the "constant" region in the empirical model. When the data of the second tower experiment became available[6], comparison shifted to those results and to data obtained from the wind turbine in Medicine Bow, Montana in the Spring of 1984. This data was obtained from Shepherd [7]. Failure of a set of temperature sensors on the meteorological tower during the tower experiment has caused a difficulty in curve fitting the assumed form for the temperature profile to the actual data but some work on this comparison has been completed and more is underway at present.

Work on the inversion case has progressed very slowly due to the need to complete the lapse case and begin comperison with the experimental data. However, the equations of the rays have been developed and geometry of this ray diagram is understood. This proved to be an extremely important point in the lapse model, and realization of the need to understand this geometry in detail will undoubtedly prove to be very helpful in this case.

The second section of this report describes the results obtained from the lapse model to date. The inversion model is described in the third section of the report. Finally, the plans for the final six months of the grant are discussed in the fourth section. Copies of both theses in which the models were developed are included in the appendix along with a copy of the Acoustical Society of America paper describing the plane wave solution discussed in the previous Semi-Annual Report [2].

RESULTS FROM THE LAPSE MODEL

The model developed for the lapse temperature gradient case has been described in the Fourth Semi-Annual report [2], but at the time of preparation of that report the model had not been used sufficiently to allow any general conclusions to be drawn. At present the model is being used to analyze the data of the second tower experiment that was conducted at NASA-Wallops in the Fall of 1984 [6]. Only a small amount of the data collected during that experiment has been modeled at present and it is desirable to first consider a comparison with the empirical model of Wiener and Keast[5]. During their experiments Wiener and Keast did not attempt to measure either wind or temperature gradient and, thus, the comparisons are crude ones, but they at least allow us to look at some results of the model.

Figure 1 presents a comparison between the empirical model of Wiener and Keast [5] and results calculated by Ma [4] as part of his M.S. thesis. Considering that the actual data of Wiener and Keast shows a scatter of typically ±10 dB as indicated by the shadowed region, the model prediction is extremely good. The "overshooting" that the model predicts at distances slighlty greater then 1000 m also appears to be in the data of Wiener and Keast (see Figure 2 of [5]). The fact that a model which does not contain the effects of turbulence can produce a "saturating" of the excess attenuation well into the shadow region is very interesting as this effect has often been ascribed to turbulent scattering. Mathematically, the saturating is the result of carrying out the integration for the inversion of the Hankel transformation, through an approximation, for a receiver in the shadow zone. The exponentially decaying effect of rays tangent to the boundary produce the rapid decay near the boundary, but the effect of rays with a complex angle of propagation (as $z \to \infty$) produce this effect and no physical explanation has been given at present.

The model has also been used to investigate the effects of surface waves under lapse conditions. Ma[4] found that surface waves are less likly to occur under lapse conditions than under isothermal ones. For example, for a geometric configuration of the source and receiver with a fixed surface impedence where a surface wave will occur in the isothermal case, it may or may not occur in the lapse case, and if it does not occur in the isothermal case, it will not

occur in the lapse case. In addition, when a surface wave does occur, it is significant mainly in the region of rapid decay just beyond the shadow. Closer to the source, the much stronger direct and reflected waves dominate, and further from the source, the exponential decay of the surface wave weakens it significantly below the "saturation" value of the sound level in the shadow. More discussion of these results is given by Ma [4].

Figure 2 shows the temperature profiles obtained during run 4B, record 12, of the second tower experiment [6] with a source height of 11.26m and a source-receiver distance of 154.3m (507.75 ft.). Also shown in that figure are five attempts to fit the experimental data. Two of these were least-square fits, one to the entire data set, and the second to the lower four data points. The other three fits were obtained by subjectively choosing the three parameters to obtain reasonable values. Both of the least-square fits gave peculiar values of these parameters. Using the lower four data points resulted in an extremely large value of alpha and very flat profile near the ground and an extremely large value of temperature at the ground. With the entire set of data a very small value of alpha was obtained.

Only the large alpha case of the least-square fits could be calculated due to problems in the model and the results are shown in Figure 3 and 4 for 500 Hz and 1000 Hz respectively. The solid line is the result of the model, the experimental data is circled, and the broken line is the Weiner and Keast model, which is just the simple source level in this case. The fact that the broken line does not show an abrupt decrease at small heights indicates that the shadow boundary has not been reached in this case. Peak levels in the interference pattern in the 500 Hz case are in good agreement but the location of the maxima and minima do not agree. In the 1000 Hz case the model predicts peak values about 5 dB lower than the data and again the location of maxima and minima are not in agreement. Investigation of the ray diagram temperature parameters seems to indicate that it is unlikely that this data was taken near the shadow boundary. Similar comments can be made about Figures 5 to 10 which are calculated with the subjective fits to the data.

Figures 11 and 12 are a comparison of the data of the experiment and the model for run 9B, record 27 in the same geometric configuration as the previous case. Here only the least-square fit has been used and the data was clearly taken near the shadow boundary. In the

500 Hz case the model overpredicts the levels while in the 1000 Hz case agreement is quite good.

Attempts to model lower sources have shown that the dip in the values predicted by the model near the source height (see the Fourth Semi-annual report [2]) is a failure of the model and further work is needed. In addition it is clear that in future experiments at least one additional temperature sensor is needed closer to the ground to allow good curve fitting of the data.

Attempts to model the situation existing in the wind turbine data [7] have been frustrated by the high source location (40 to 120 m) which has caused the argument of the Hankel functions used in the model to be outside the allowable limits of the NASA supplied program. This problem was discussed by Cheng [1] but no solution was given. It appears that the model will have to be modified to analytically allow cancellation of two terms in the model as opposed to simply calculating the values and allowing the cancellation to occur in the numerical results. This modification has not yet been undertaken, but some preliminary work has been carried out to identify the source of the problem.

INVERSION PROBLEM

Work on the inversion problem has been progressing very slowly due to completing the lapse model and the need to carry out comparisons with the experimental data in that case. The author will be only teaching half time during the spring quarter and a significant amount of work is expected to be accomplished. At present the ray equations have been developed and interpreted. This is the necessary first step to developing the model as it gives both mathematical and physical insight into the mathematical questions that develop while developing the actual solution to the wave equation. Lack of appreciation of this important point caused considerable problems with the lapse model. The ray model also yields some interesting results by itself as is described below.

The rays are obtained by use of an acoustic form of Snell's law

$$\frac{\cos\theta(z)}{a(z)} = \frac{\cos\theta_s}{a(s)} \tag{1}$$

where z is the height above the ground of an arbitrary point and s is the height of the source, θ is the angle the ray makes with respect to the horizontal direction, and a is the speed of sound. From (1) one can calculate the slope of the rays as

$$\frac{dz}{dr} = \pm \left[\frac{Az + B}{Cz + D}\right]^{1/2} \tag{2}$$

after substituting the assumed temperature profile,

$$T = T_\infty + \frac{\Delta T}{1 + \alpha z} \tag{3}$$

into (1) where

$$A = \alpha[\,1 + \alpha s + \Delta T/T_\infty - (1 + \alpha s)\cos^2\theta_s\,] \tag{4}$$

$$B = [\,1 + \alpha s + \Delta T/T_\infty - (1 + \alpha s)(1 + \Delta T/T_\infty)\cos^2\theta_s\,] \tag{5}$$

$$C = \alpha\,(1 + \alpha s)\cos^2\theta_s \tag{6}$$

and

$$D = (\,1 + \Delta T/T_\infty)\,(\,1 + \alpha s)\cos^2\theta_s \tag{7}$$

Equation (2) can then be integrated to obtain the ray paths.

In the case of an inversion ΔT is negative and A of equation (4) may be positive, negative or zero while the remaining functions, B, C, and D, are positive for θ_s and z corresponding to physically existing rays. When A is positive integration of (2) yields the function $F_1(\,\theta_s, z\,)$ defined by

$$F_1(\,z, \theta_s\,) = \frac{\sqrt{(Az+B)(Cz+D)}}{A} + \frac{E}{2A\sqrt{(AC)}}\,\mathrm{Tanh}^{-1}\left[\frac{A(Cz+D)}{C(Az+B)}\right]^{1/2} \tag{8}$$

where

$$E = AD - BC = \alpha\,\Delta T/T_\infty\,[\,1 + \alpha s + \Delta T/T_\infty](1 + \alpha s)\cos^2\theta_s \tag{9}$$

Note that this is very similar to the function defining the rays in the lapse case, [2]. The $A > 0$ case occurs for $\text{Cos}\,\theta_S \leq \text{Cos}\,\Theta$, where

$$\text{Cos}\,\Theta = \left[\frac{1 + \Delta T/T_\infty + \alpha s}{1 + \alpha s}\right]^{1/2}. \qquad (10)$$

and represents waves that are not refracted downward through a turning point and escape the trapping effect of the inversion.

When $\text{Cos}\,\theta_S = \text{Cos}\,\Theta$, $A = 0$ and integration of (2) yields

$$F_2(\theta_S, z) = \frac{2}{3C\sqrt{B}}\,(Cz + D)^{3/2}, \qquad (11)$$

and when $\text{Cos}\,\theta_S > \text{Cos}\,\Theta$ then $A < 0$ and integration of (2) gives

$$F_3(\theta_S, z) = \frac{\sqrt{[(Az + B)(Cz + D)]}}{A} + \frac{E}{A\sqrt{[-AC]}}\,\text{Tan}^{-1}\left[\frac{-A(Cz+D)}{C(Az+B)}\right]^{1/2} \qquad (12)$$

Using these functions the rays in the inversion case can be described. As in the lapse case several cases occur.

Rays propagating upward initially are given by

$$r = F_i(\theta_s, z) - F_i(\theta_s, s) \tag{13}$$

where i = 1,2, or 3 depending on the initial angle of the ray on leaving the source. Rays with i =1 do not have a turning point and go directly from the source to infinity. The i = 2 case rays have a turning point at infinity. The third case, i =3, are rays with a turning point at a finite height greater then the source height. The height of this turning point is given by

$$z_{tp} = - B/A. \tag{14}$$

and the horizontal location by

$$r_{tp} = - F_i(\theta_s, s). \tag{15}$$

Rays initially propagating downward are described by

$$r = F_i(\theta_s, s) - F_i(\theta_s, z) \tag{16}$$

for i = 1, 2, or 3. In all three cases the rays are reflected from the ground with the reflected waves given by

$$r = F_i(\theta_s, z) + F_i(\theta_s, s) - 2\,F_i(\theta_s, 0). \tag{17}$$

Again in the i =1 case the rays do not have a turning point, the i =2 case corresponds to rays with a turning point at infinity, and the i =3 rays have a turning point at a finite height greater than the source height and given by (14).

Any ray with a turning point then goes through a succession of reflections and turning points. The rays which were travelling upward initially are given by

$$r = - F_3(\theta_s, z) - F_3(\theta_s, s) - 2(n-1)\ F_3(\theta_s, 0) \qquad (18)$$

after they have been refracted downward. Here n is the number of turning points the wave has passed through. After reflection at the surface these rays are described by

$$r = F_3(\theta_s, z) - F_3(\theta_s, s) - 2n F_3(\theta_s, 0). \qquad (19)$$

For rays going downward initially

$$r = F_3(\theta_s, z) + F_3(\theta_s, s) - 2(n+1)\ F_3(\theta_s, 0) \qquad (20)$$

after reflection and

$$r = - F_3(\theta_s, z) + F_3(\theta_s, s) - 2n F_3(\theta_s, 0) \qquad (21)$$

after refraction at the turning point. Again n is the number of turning points a ray has passed through. Figure 13 is a typical plot of the rays using this solution.

This solution contains one unrealistic feature, there are rays that can propagate upward to

very large heights (infinity in the limit) before being refracted downward to effect the solution on the ground. Physically one would not expect such rays to exist in reality where the inversion would be replaced by a lapse condition at sufficient height above the ground. These rays reach the ground at very large distances from the source, however, having travelled an extremely long path length, thus one would assume that their influence on the t'al solution would be minimal.

Using this solution one can obtain an approximate result for the sound level enhancment at the ground by assuming energy is conserved between two bounding rays and comparing the isothermal rays to the rays for the inversion condition. The rays which are trapped in the inversion are defined by $-\Theta \leq \theta_S \leq \Theta$, where Θ is defined by (11) and is a small angle typically less then 10°. The acoustic intensity between this limiting ray, $\theta_S = \Theta$, and the ground can be approximated as

$$I = P^2 (2\pi r\, z(r))/\rho a \qquad (22)$$

where the term in parentheses is the area between the ground and the limiting ray. The height of this ray is z(r).

For an isothermal atmosphere the ray is defined by

$$z(r) = (\mathrm{Tan}\,\Theta)\, r + s \qquad (24)$$

and for the inversion case by solving (14) and (12) for z as a function of radius. Setting the intensities equal and solving for the ratio of the amplitudes of the acoustic pressure in the constant temperature and inversion cases yields

$$\frac{P_I^2}{P_C^2} = \frac{\left[\dfrac{\Delta T/T_\infty}{1 + \alpha s + \Delta T/T_\infty}\right]^{1/2} (\alpha r) + \alpha s}{\left[\dfrac{3\alpha r}{2}\sqrt{(\Delta T/T_\infty) + (1 + \alpha s + \Delta T/T_\infty)^{3/2}}\right]^{2/3} - 1 - \Delta T/T_\infty} \qquad (24)$$

and the enhancement in sound pressure level due to the inversion relative to the isothermal case is given by $10\ \mathrm{Log}(P_I^2/P_C^2)$. This function is plotted in Figures 14 to 17 for some typical parameters. In the limit of large radius (24) behaves like $r^{1/3}$ and the sound level enhancement like (10/3) Log (r) or about 1 dB/doubling of distance, thus the sound pressure level of a source in an inversion would be expected to decrease 5 dB/doubling of distance at large distances from the source based on this model. It should be realized that the ground has been assumed to be perfectly reflecting here and an absorbing ground would increase the decay rate.

Experimental data to compare to this simple model is scarce. Shepherd [7] reports a 6 dB/ doubling of distance. Wiener and Keast [5] show a positive excess attenuation in the downwind case, and thus a faster decay than the geometrical 6 dB/doubling of distance, thus the model is interesting but unsubstantiated.

FUTURE WORK

During the remaining six months of the current grant, work is planned for three main tasks: continued comparison between the existing lapse model and experimental data, this may require some modification in the model as discussed earlier, due to limits on the argument of the Hankel functions and to eliminate some of the discontinuities present in the current formulation; an attempt to use the fast fourier transform technique to invert the Hankel transformed solution, this will eliminate the discontinuities present in the present model and may be necessary in the inversion case where many rays can reach an observer location, and development of the inversion model, this model is partly worked out but has not been completed and has not been presented here. A paper is being prepared describing the ray solution to both the lapse and inversion problems. It is anticipated that this paper will form a foundation to develop both the lapse and inversion models in future papers. The author will be presenting a paper on this work at the Second Workshop on Long Range Acoustic Propagation in February, 1985, and has submitted an abstract of a paper to the Acoustical Society of America for presentation at the Spring meeting in 1985.

REFERENCES

1. Cheng, Alex, Sound Propagation from a Point Source in a Thermally Stratified Medium, M.S. Thesis, Mechanical and Industrial Engineering Department, University of Utah, Salt Lake City, Utah, 1985.
2. Yan Moorhem, W. K., Fourth Semi-Annual Report to the National Aeronautics and Space Administration on Grant NAG-1-283, UTEC ME 84-075, Mechanical and Industrial Engineering Department, University of Utah, Salt Lake City, Utah, 1984.
5. Secha, D. A., and Silbiger, A., "Focusing and Refraction of Harmonic Sound and Transient Pulses in a Stratified Media," J. Acoustical Society of America, 49, 824, 1971.
4. Ma, Y., Wave Propagation along a Finite Impedance Ground under a Lapse Temperature Condition, M.S. Thesis, Mechanical and Industrial Engineering Department, University of Utah, Salt Lake City, Utah, 1984.
5. Wiener, F. M., and Keast, D. N., "Experimental Study of the Propagation of Sound over Ground," J. Acoustical Society of America, 31, 724, 1959.
6. Willshire, W. L., Private Communication, NASA Langley Research Center, Hampton, Virginia, 1984.
7. Shepherd, K. P., Private Communication, Bionetics Corp., Hampton, Virginia, 1984.

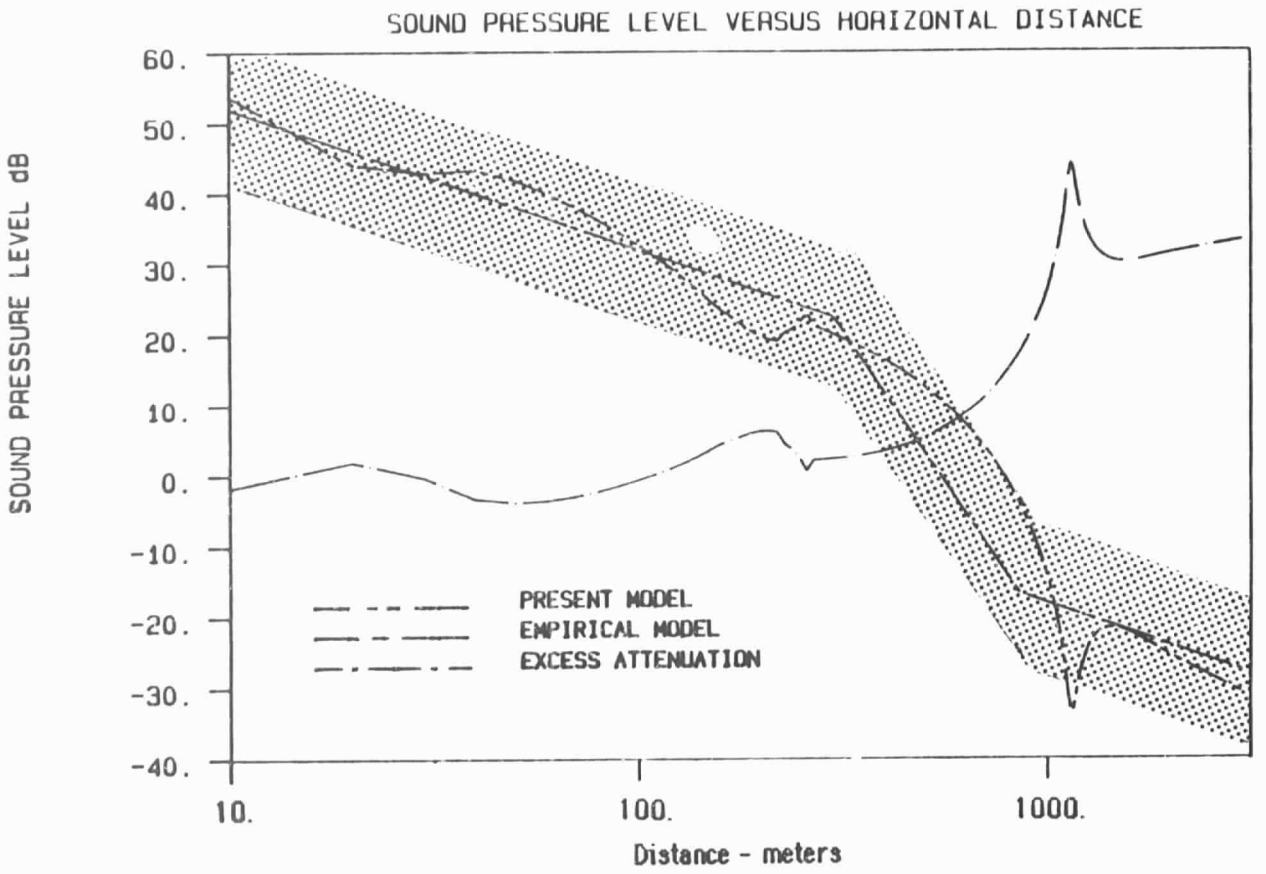

Figure 1. Sound pressure level versus horizontal distance for $\Delta T/T_\infty$ = .001, α = 3.5 m^{-1}, ω = 10,000 sec^{-1}, s = 3 m, and z = 1 m. The empirical model is due to Wiener and Keast [5] with ϕ_C = 180 °, and ϕ = 0° to simulate temperature gradient effects.

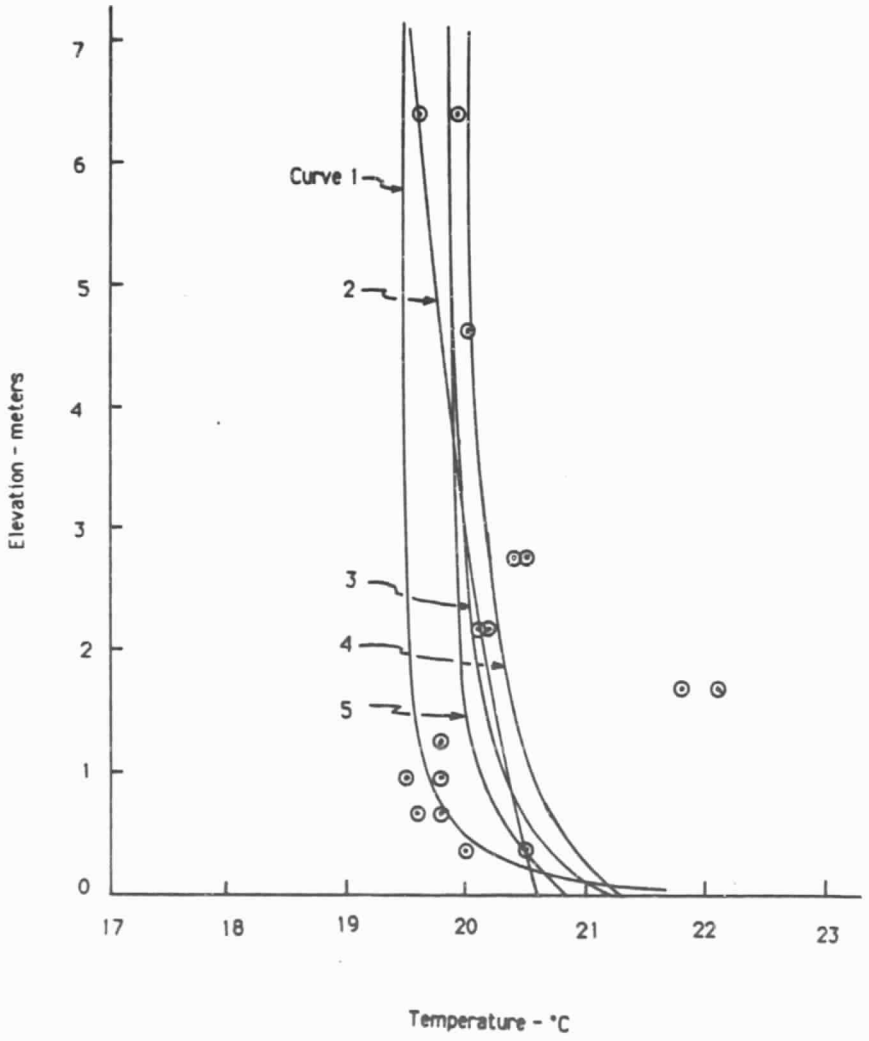

Figure 2. Temperature versus height from the second NASA tower experiment [6] record 12. Curve 1 is a least-square fit to the data at the four lowest heights, T_∞ = 19.4 °, ΔT = 6.6°, α = 21.1 m^{-1}. Curve 2 is a least-square fit to all data except that at 1.7 m, T_∞ = 17.7 °, ΔT = 2.6°, α = .1 m^{-1}. Curves 3 to 5 are subjective fits to the data set: T_∞ = 19.8 °, ΔT = 1.5 °, α = 2. m^{-1}; T_∞ = 19.8 °, ΔT = 1.5 °, α = 1. m^{-1}; T_∞ = 19.8 °, ΔT = 1.0 °, α = 2. m^{-1}.

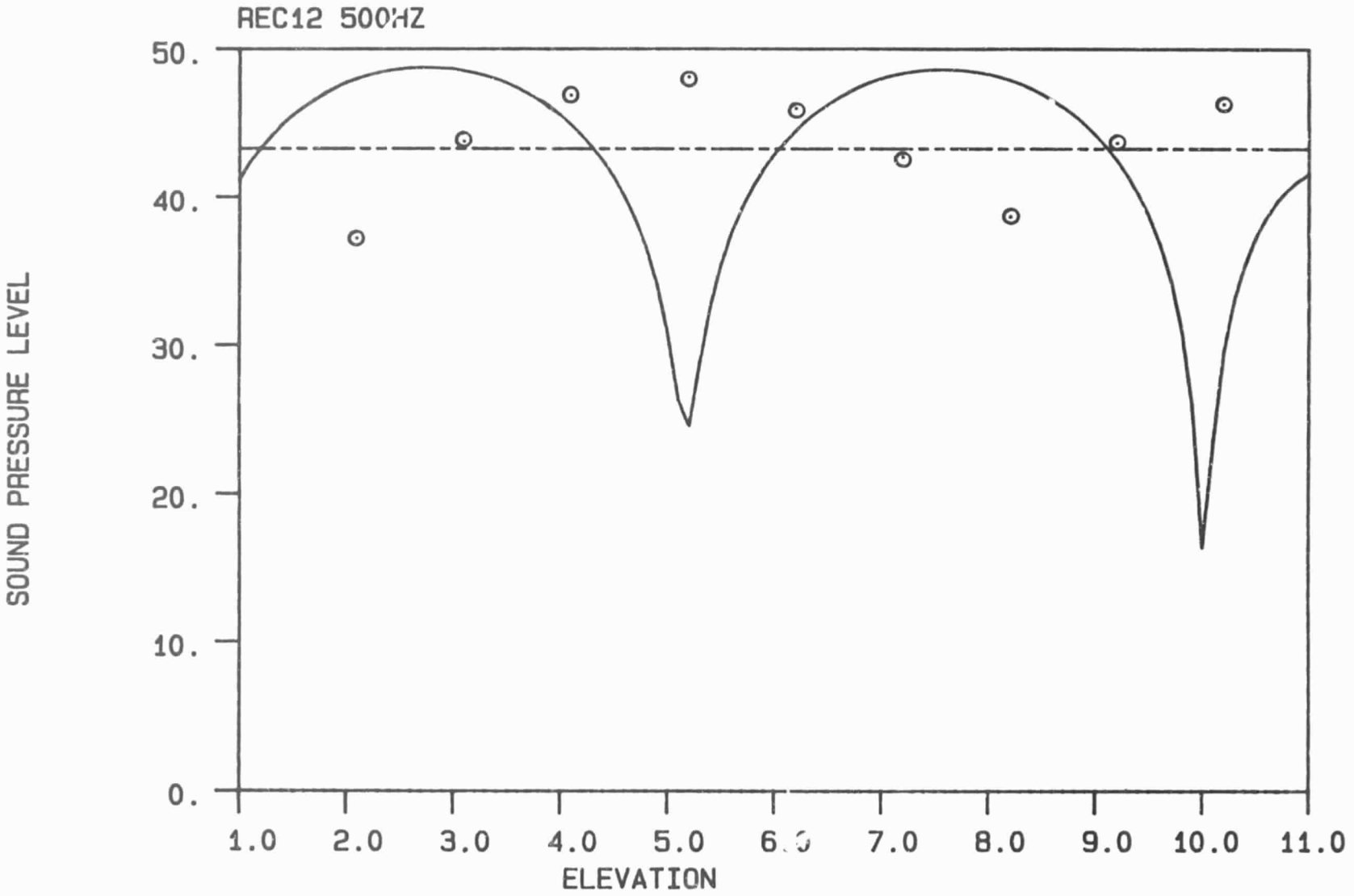

Figure 3. Sound Pressure versus height, record 12, s = 11.26 m, r = 154.3 m, and f = 500 Hz. Model results with T_∞ = 19.4 °, ΔT = 6.6°, and α = 21.1 m^{-1}.

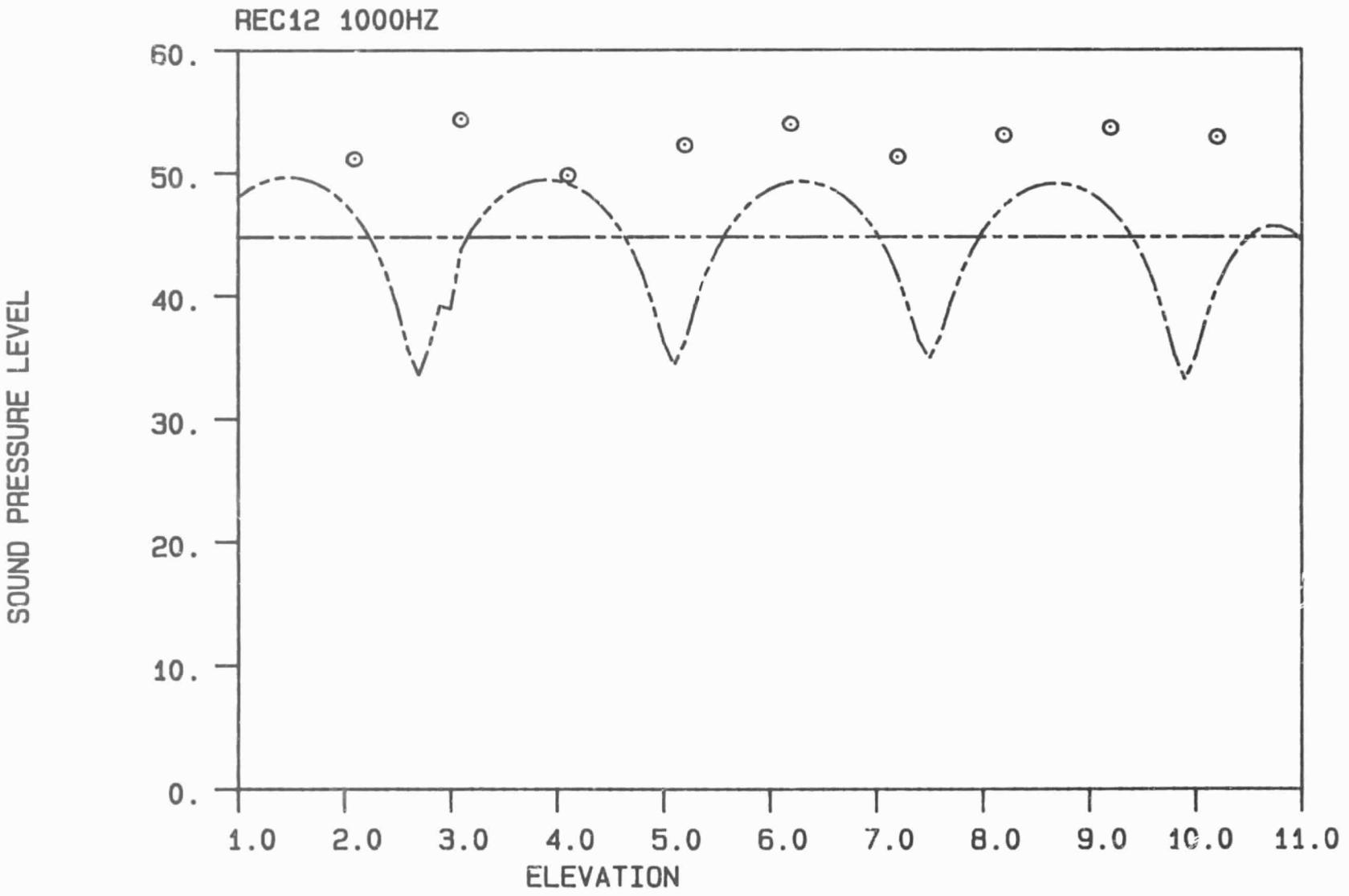

Figure 4. Sound Pressure versus height, record 12, s = 11.26 m, r = 154.3 m, and f = 1000 Hz. Model results with T_∞ = 19.4 °, ΔT = 6.6°, and α = 21.1 m^{-1}.

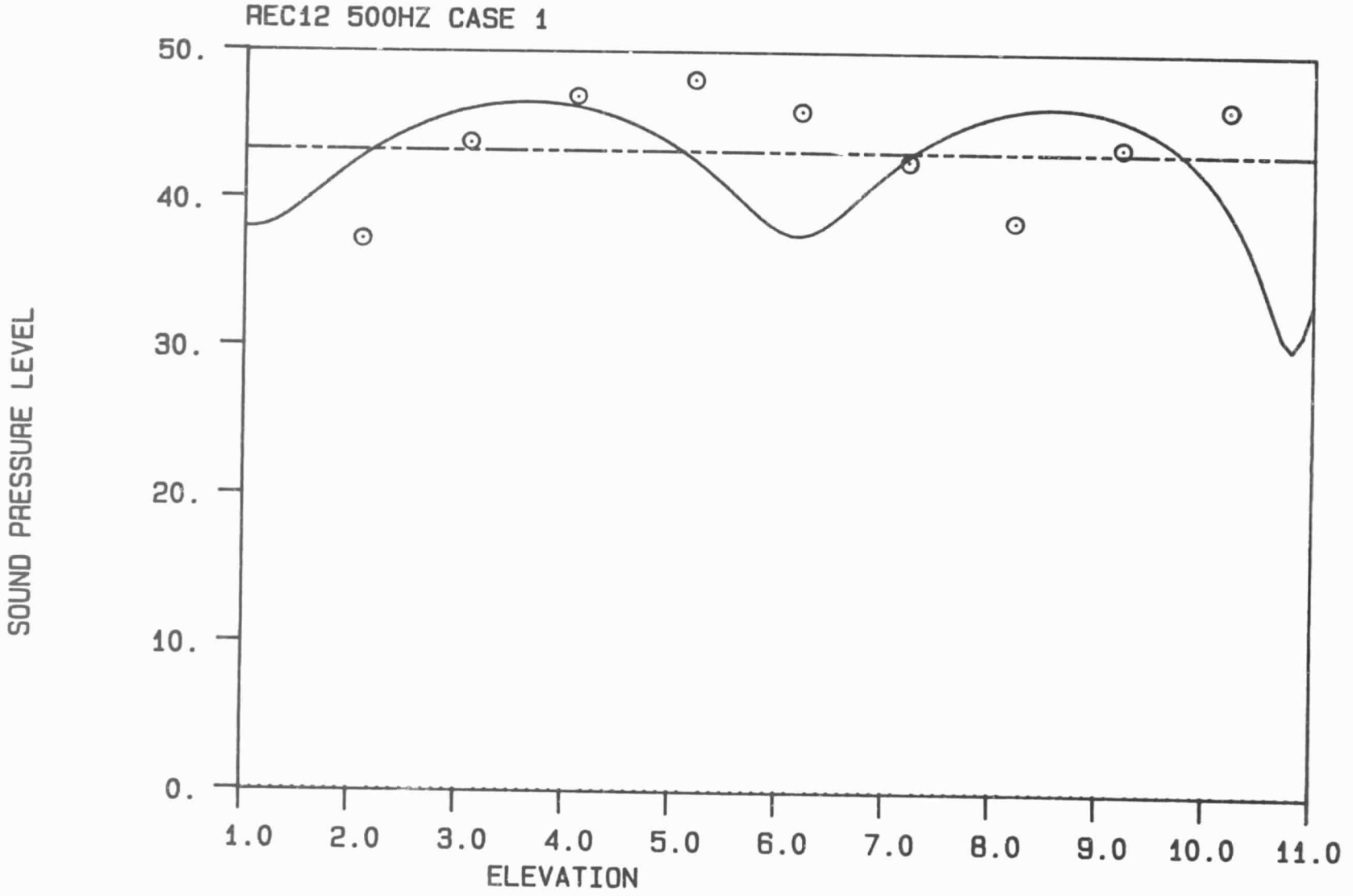

Figure 5. Sound Pressure versus height, record 12, s = 11.26 m, r = 154.3 m, and f = 500 Hz. Model results with T_∞ = 19.8 °, ΔT = 1.5 °, and α = 2. m^{-1}.

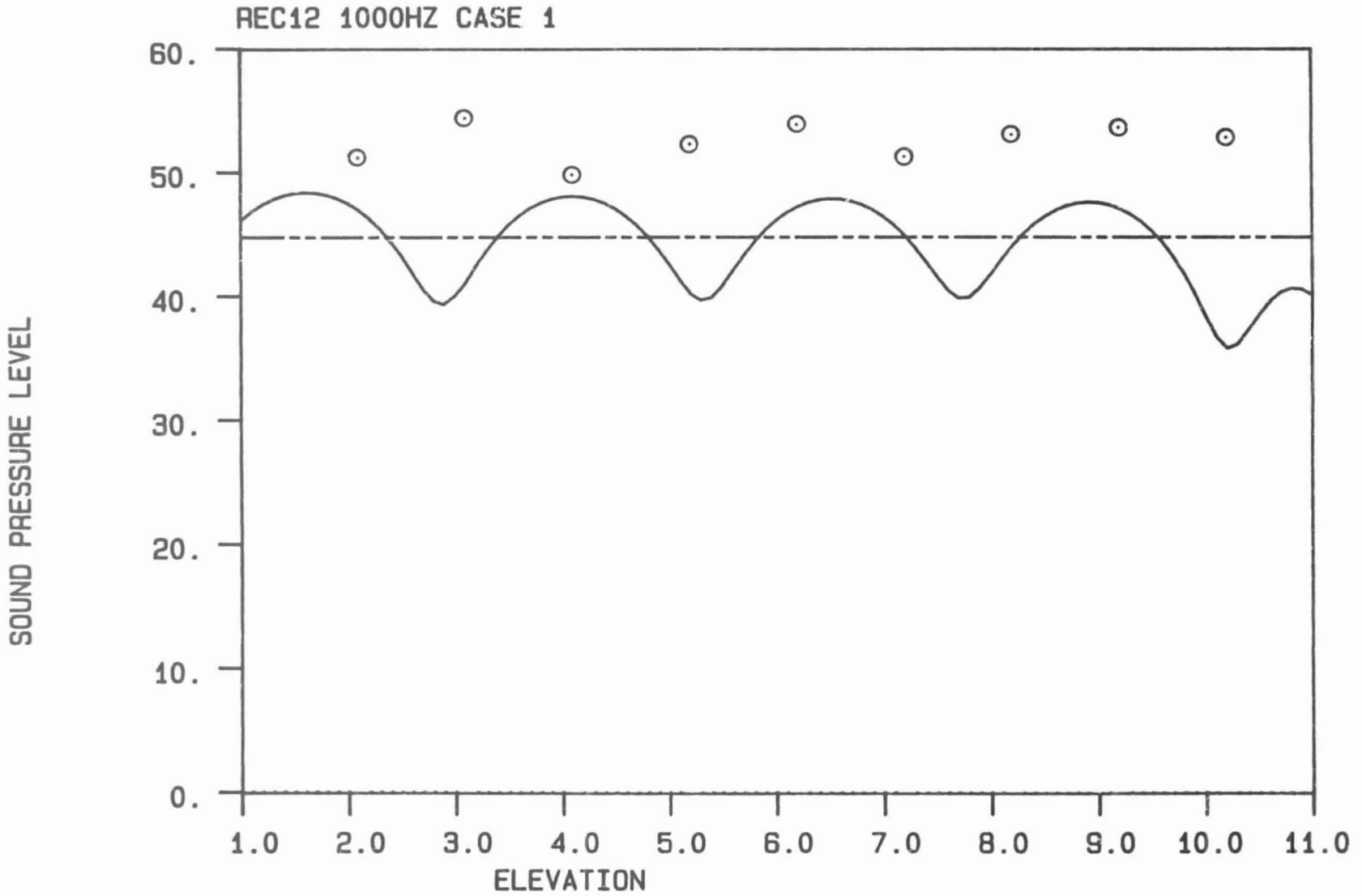

Figure 6. Sound Pressure versus height, record 12, s = 11.26 m, r = 154.3 m, and f = 1000 Hz. Model results with T_∞ = 19.8 °, ΔT = 1.5 °, and α = 2. m^{-1}.

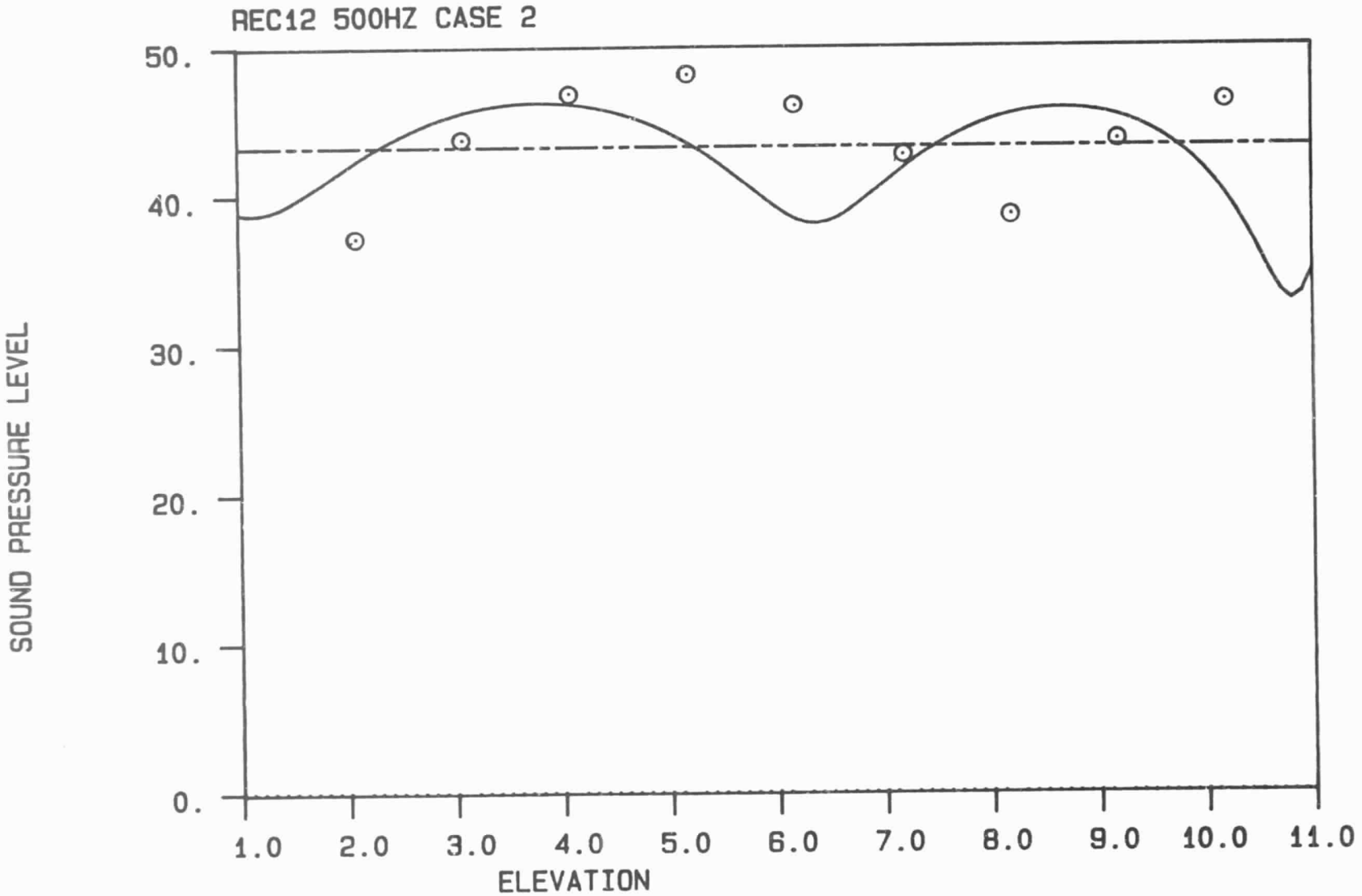

Figure 7. Sound Pressure versus height, record 12, s = 11.26 m, r = 154.3 m, and f = 500 Hz. Model results with T_∞ = 19.8 °, ΔT = 1.5 °, and α = 1. m^{-1}.

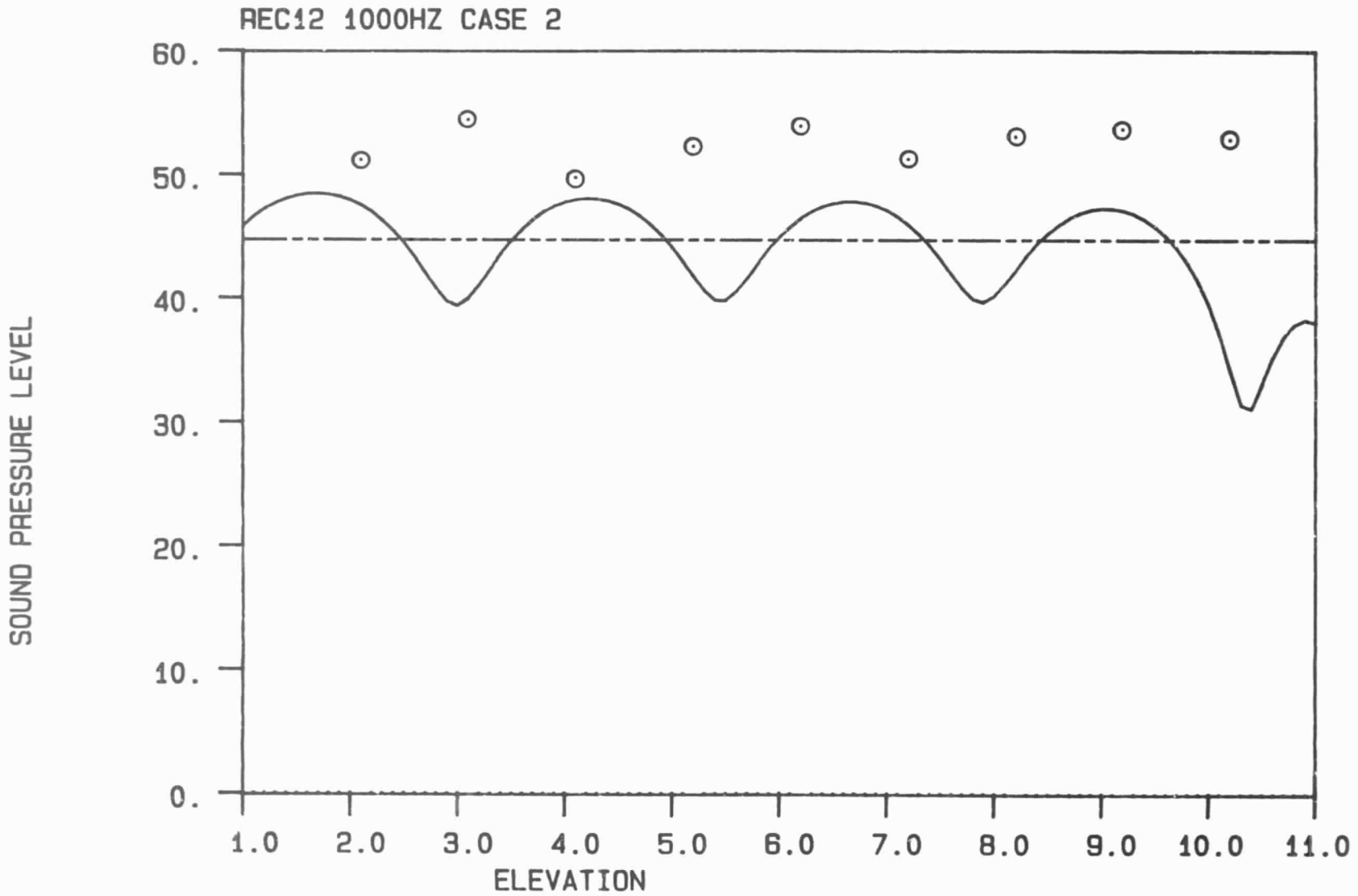

Figure 8. Sound Pressure versus height, record 12, s = 11.26 m, r = 154.3 m, and f = 1000 Hz. Model results with T_{∞} = 19.8 °, ΔT = 1.5 °, and α = 1. m^{-1}.

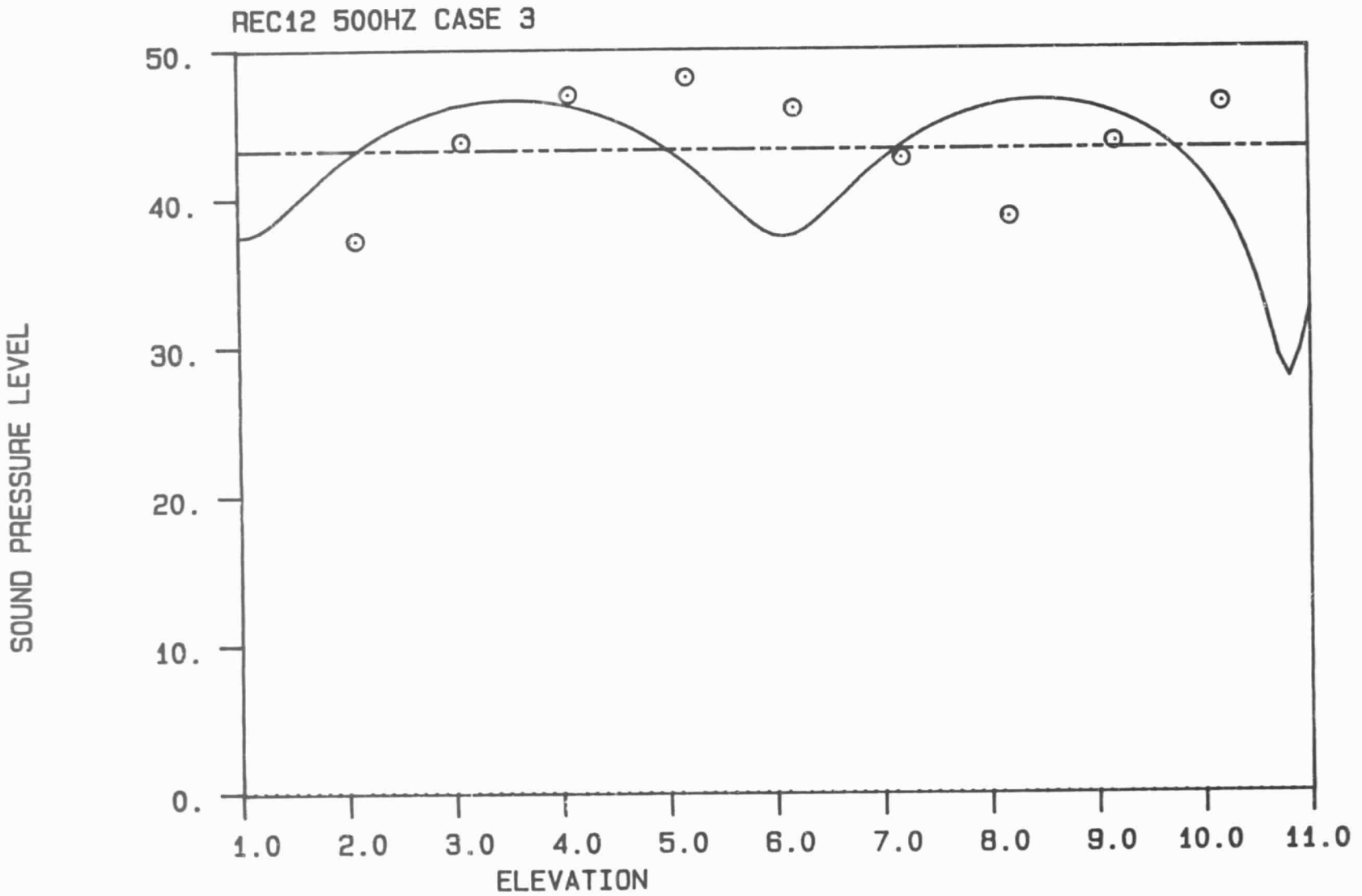

Figure 9. Sound Pressure versus height, record 12, s = 11.26 m, r = 154.3 m, and f = 500 Hz. Model results with T_∞ = 19.8 °, ΔT = 1.0 °, and α = 2. m^{-1}.

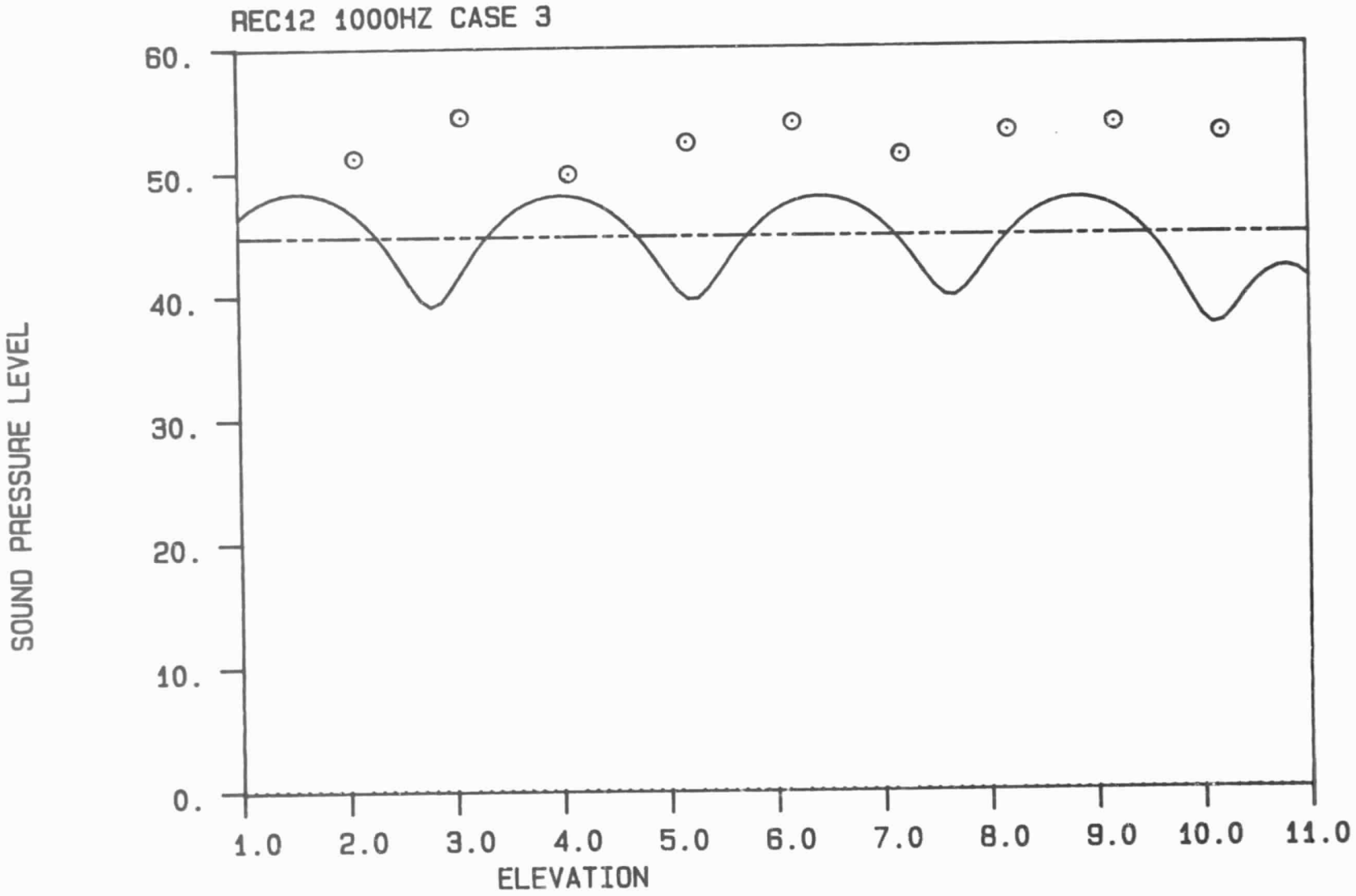

Figure 10. Sound Pressure versus height, record 12, s = 11.26 m, r = 154.3 m, and f = 1000 Hz. Model results with T_∞ = 19.8 °, ΔT = 1.5 °, and α = 2. m^{-1}.

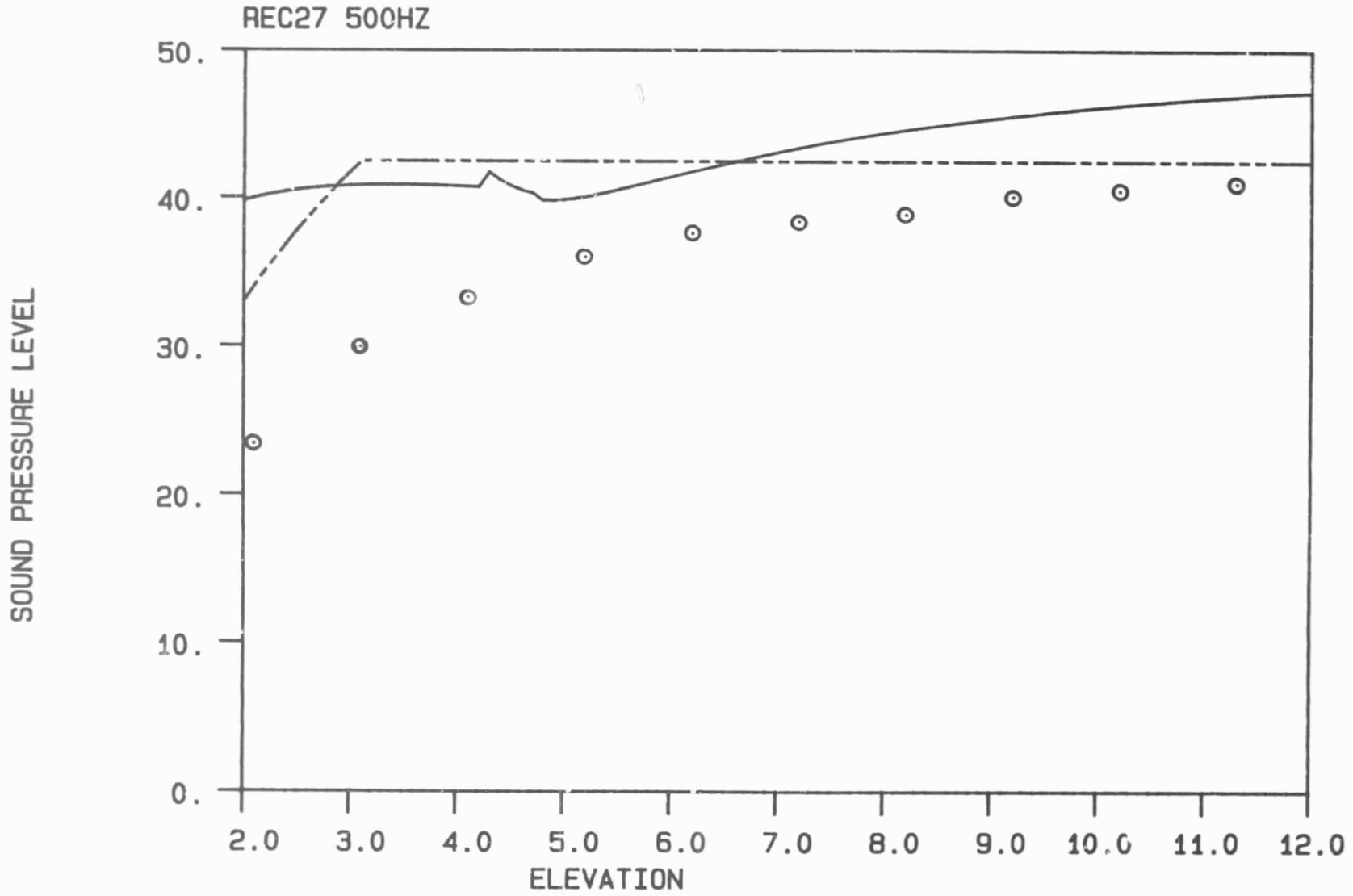

Figure 11. Sound Pressure versus height, record 27, s = 11.26 m, r = 154.3 m, and f = 500 Hz. Model results with T_∞ = 20.9°, ΔT = 12.43 °, and α = 20.10 m^{-1}.

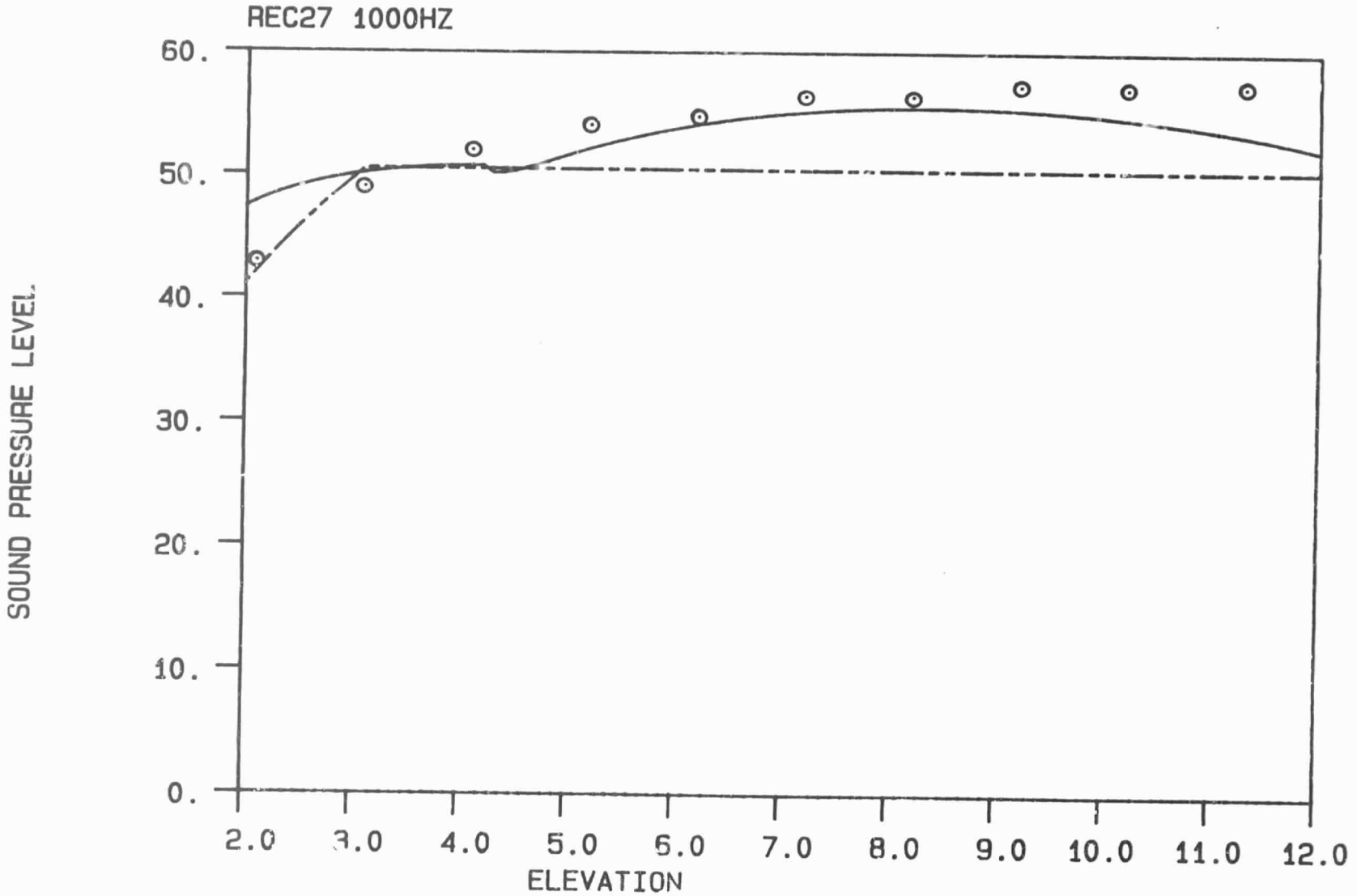

Figure 12. Sound Pressure versus height, record 27, s = 11.26 m, r = 154.3 m, and f = 1000 Hz. Model results with $T_\infty = 20.9°$, $\Delta T = 12.43°$, and $\alpha = 20.10\ m^{-1}$.

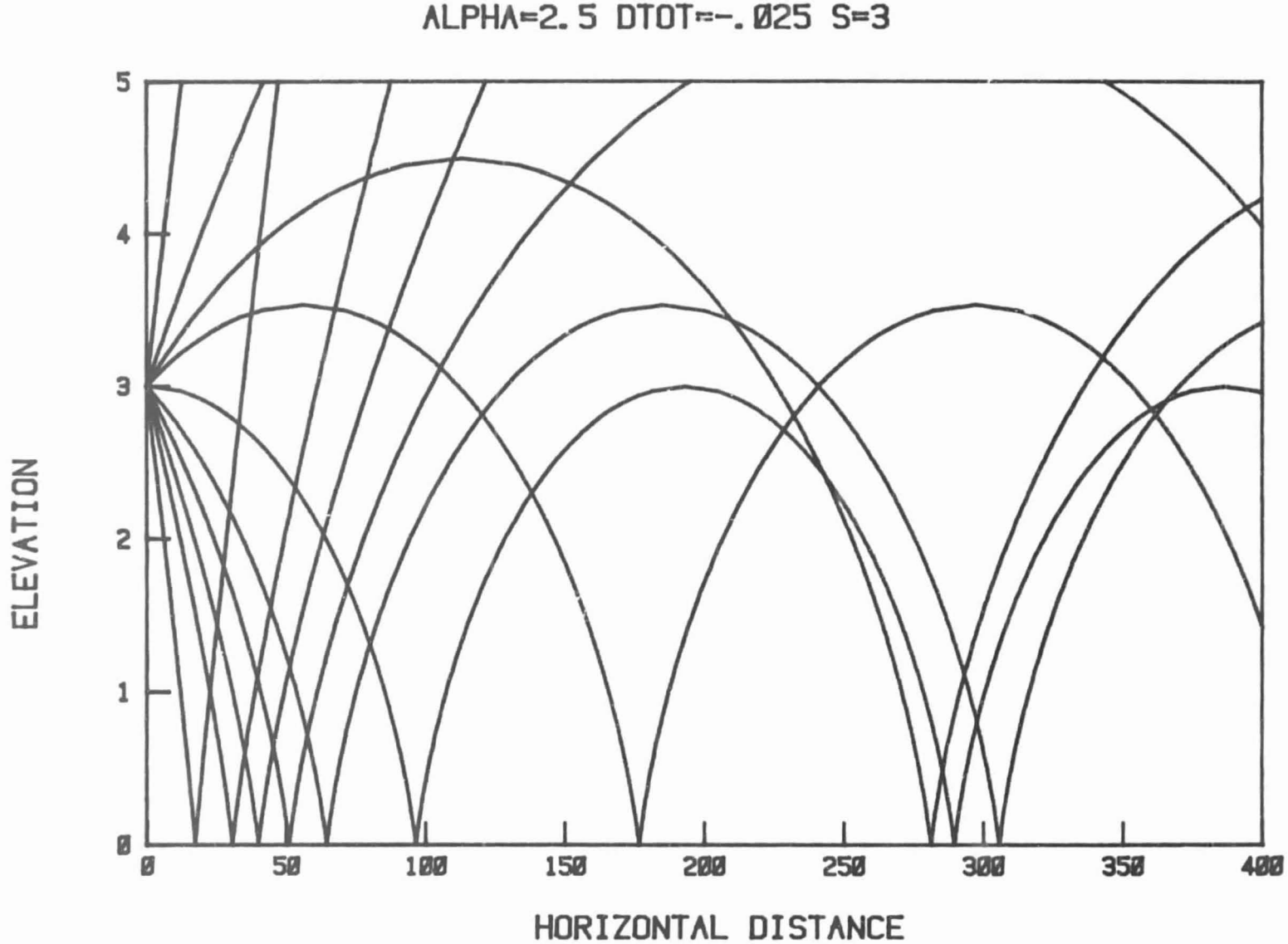

Figure 13. Ray diagram with $\Delta T/T_{\infty} = -.025$, $\alpha = 2.5\ m^{-1}$, and a source height of 3 m.

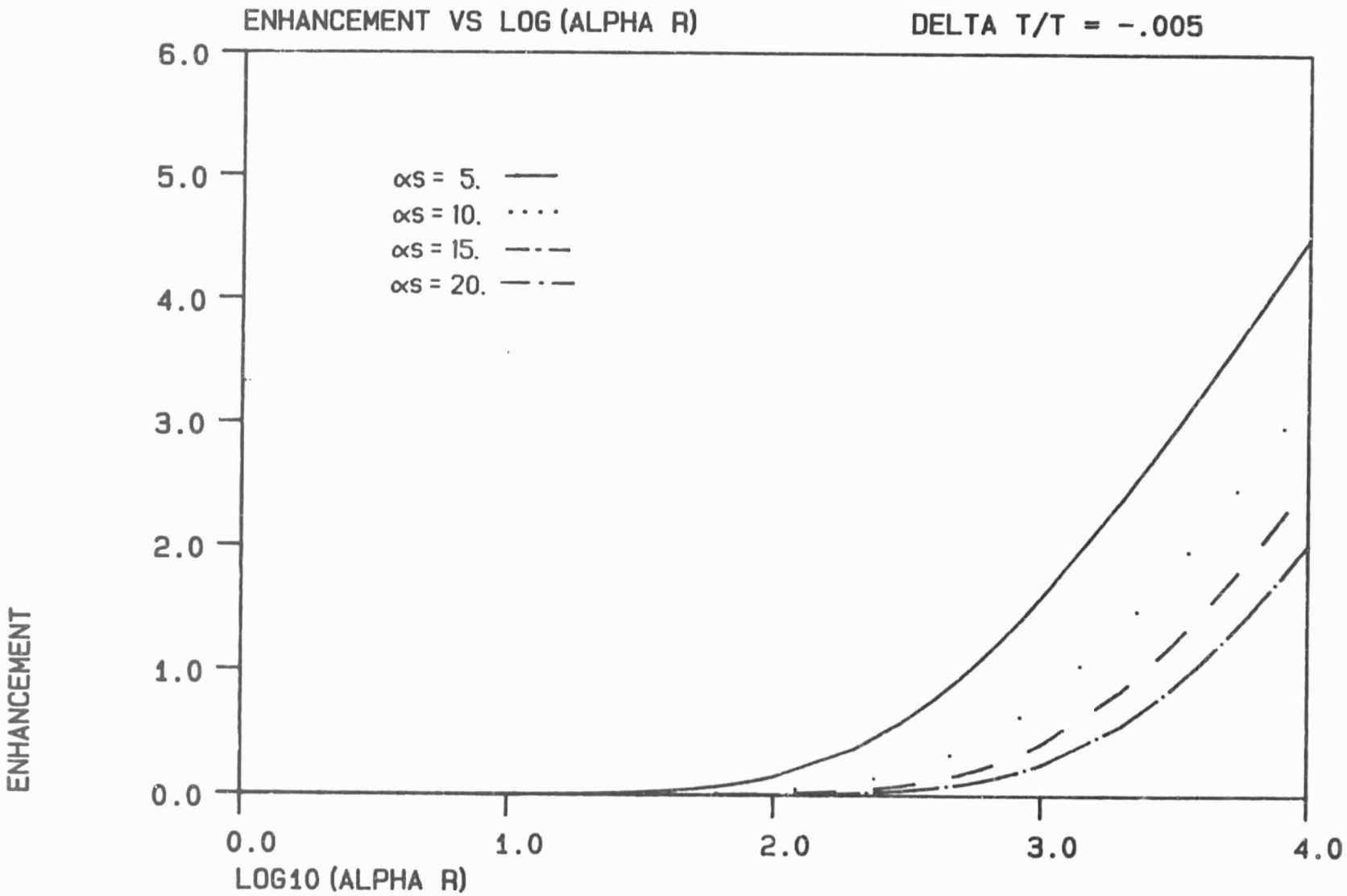

Figure 14. Sound level enhancement versus nondimensional distance for $\Delta T/T_{\infty} = -.005$ from the energy model.

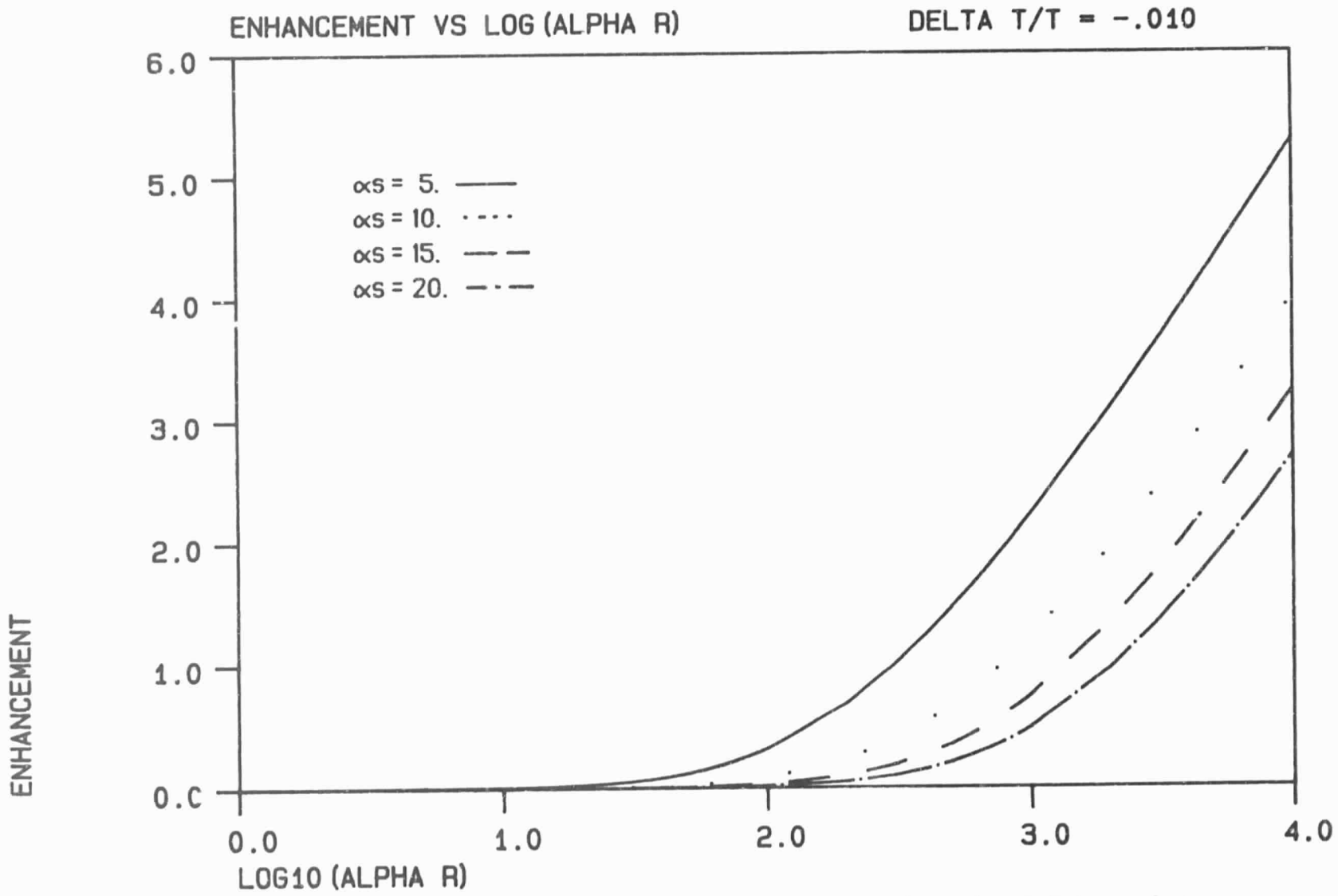

Figure 15. Sound level enhancement versus nondimensional distance for $\Delta T/T_{\infty} = -.010$ from the energy model.

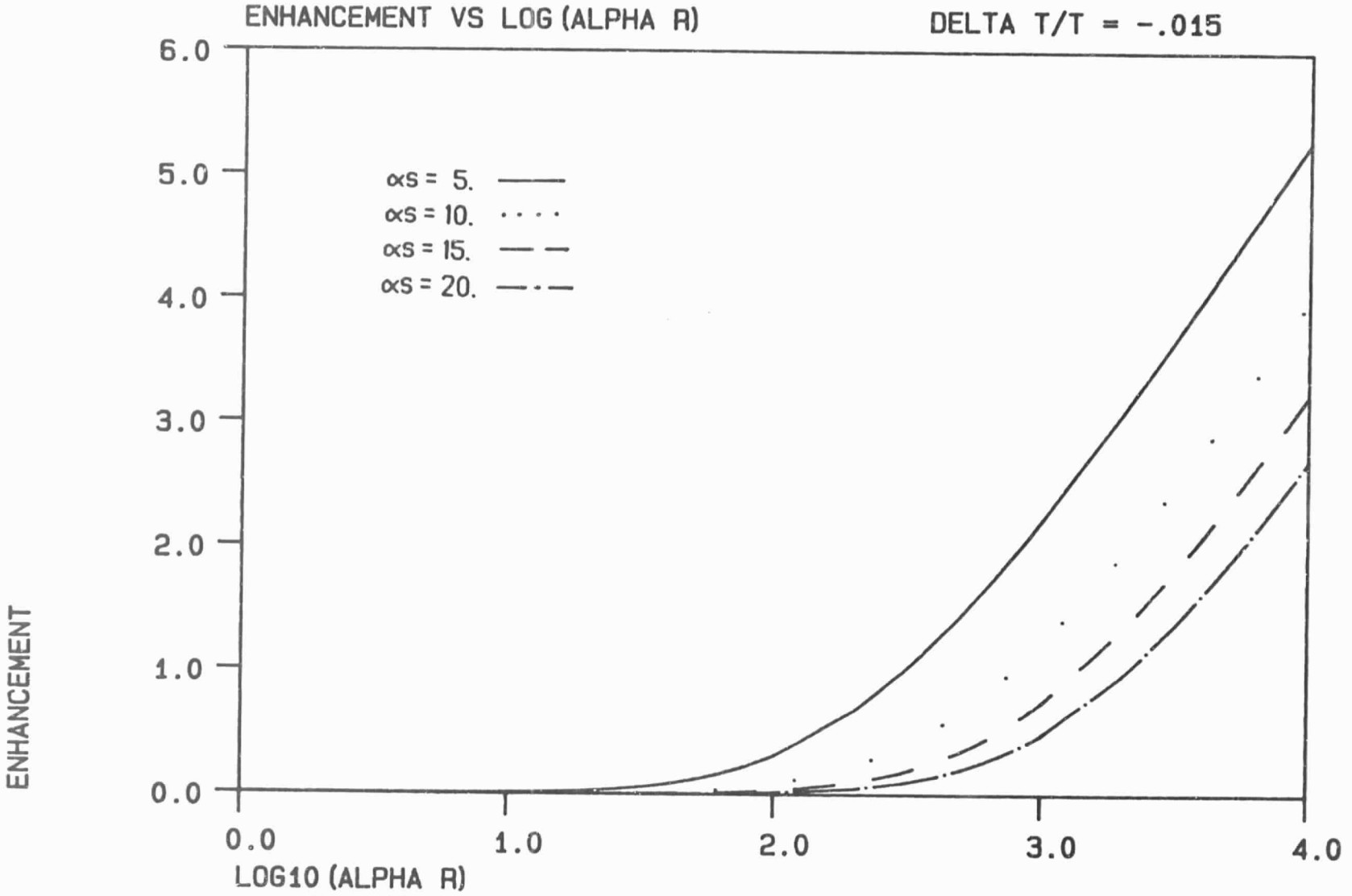

Figure 16. Sound level enhancement versus nondimensional distance for $\Delta T/T_\infty = -.015$ from the energy model.

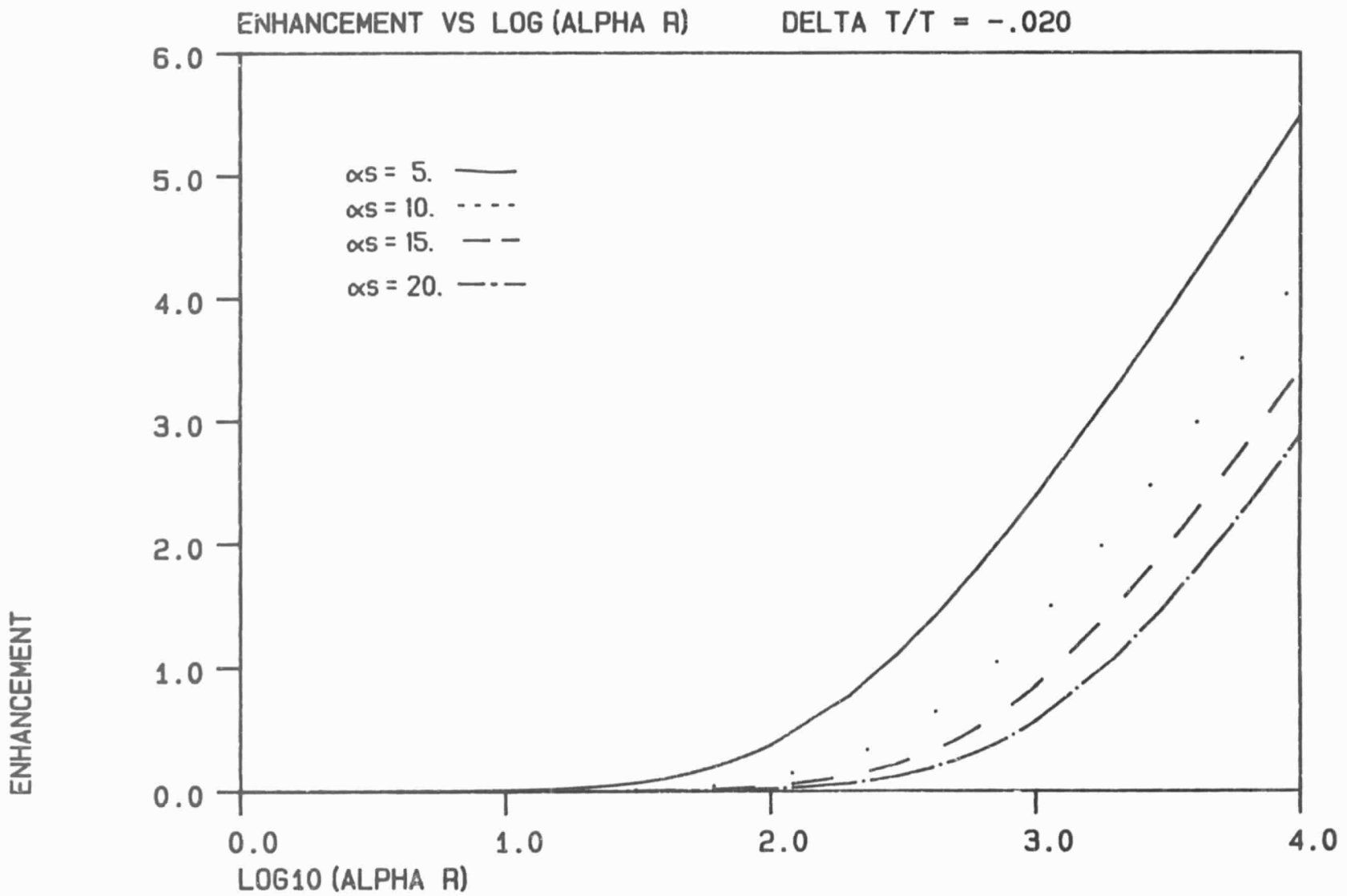

Figure 17. Sound level enhancement versus nondimensional distance for $\Delta T/T_\infty$ = -.020 from the energy model.

APPENDIX A

SOUND PROPAGATION FROM A POINT SOURCE IN A THERMALLY STRATIFIED MEDIUM

by

Alexander S.C. Cheng

A thesis submitted to the faculty of
The University of Utah
in partial fulfillment of the requirements for the degree of

Master of Science

in

Mechanical Engineering

Department of Mechanical and Industrial Engineering

The University of Utah

March 1985

ABSTRACT

A mathematical model for the propagation of acoustic waves from a point source in a thermally stratified medium has been developed. The temperature profile chosen is a model of a fully developed lapse condition and fits the limited amount of data available. This profile has a large vertical temperature gradient near the ground and asymptotically approaches a constant value high above the ground. C. I. Chessel's model for grass has been used to characterize the ground surface impedance.

The governing equation is a simple wave equation with a variable sound speed and a source term. A semi-analytical solution to the problem is obtained by using a Hankel transformation and the Saddle Point method to invert the transformation. Some of the steps are carried out numerically.

In the 'illuminated' region where geometrical rays can reach, an interference pattern occurs. And in the shadow region where no rays can enter according to the geometric acoustic, an exponentically decaying behavior is observed. The sound pressure level predicted in the present model is in good agreement with the empirical model formulated by Wiener and Keast.

TABLE OF CONTENTS

ACKNOWLEDGEMENTS

The author would like to express his appreciation to Dr. William K. Van Moorhem for his technical guidance and patience during the preparation of this thesis. I would also like to acknowledge the finanical sponsorship of NASA to make the completion of this work possible.

NOMENCLATURE

a	Sound speed
h_1, h_2	Modified Hankel functions
$H^{(1)}_{1/3}$, $H^{(2)}_{1/3}$	Hankel functions of 1/3 order
i	$\sqrt{-1}$
J_0	Bessel function of first kind
P	Pressure
q	Source strength constant
R	Reflection coefficient
r	Receiver radius
S	Specific entropy
s	Source height
T	Temperature
t	Time
V	Velocity
W	Component of velocity along z axis
Z	Normal impedance
z	Receiver height
α	Temperature variation parameter
β	Hankel transform variable
δ	Dirac delta function
ΔT	Temperature change between $z = 0$ and $z = \infty$
θ	Incidence angle
ρ	Density

ξ	Arbitrary independent variable
ω	Circular frequency

Subscripts

M	Mean values existing without an acoustic disturbance
o	Evaluated at z = 0
∞	Evaluated at z ∞

Superscripts

'	Variables with acoustic disturbation

CHAPTER I

INTRODUCTION

The study of sound propagation has a long and intriguing history, and is of increased importance due to the needs of the modern society. With the increased population density and continuing expansion of air traffic, jet aircraft noise has become one of the major issues in environment noise control. Its impact on the airport community has led to the strict noise certification requirements imposed by the Federal Aviation Agency (FAA), which is the major impetus for acquiring a better understanding of outdoor sound propagation.

A great deal of progress has been made towards understanding the mechanisms associated with the propagation of sound in the atmosphere. Four major factors are found to be significant and have been the major areas in recent research. They are the atmospheric absorption, reflection from the ground surface, scattering by turbulence, and refraction by wind and temperature gradients in the atmosphere. Each of these effects is described briefly in the following except the last case, refraction due to temperature inhomogeneity in the atmosphere, which is the subject of this discussion and will be examined thoroughly.

The absorption of acoustic energy during propagation through the atmosphere has been investigated for many years. Three mechanisms have proven to be the major contributors. The first one, classical absorption, is caused by the transport process of classical physics (shear

viscosity, thermal conductivity, mass diffusion, and thermal diffusion). The second is the absorption caused by rotational relaxation of the molecules in air [1]. The third mechanism is due to vibrational relaxation of oxygen and nitrogen molecules. It was the discovery of the latter factor that produced agreement between the predicted absorption and measured data [2]. Although further investigation at low frequencies and lower humidity is desirable, it appears that the atmospheric absorption is a considerably well-understood phenomenon.

The reflection of waves at a ground surface modeled by a finite, nonzero normal impedance surface has proven to be a complicated and intriguing subject. Several models of the ground surface and different mathematical methods and approximations have been presented in a pletlora of papers on this subject. The 'local reacting' model of the surface is the most common and widely used in current practice, and in general the solution to the wave equation consists of four terms. The first term represents the wave travelling directly from the source to the receiver without contacting the ground. The second term represents the reflected wave which appears to originate at an image source below the ground. The third term is generally referred to as a ground wave because it produces a strong signal near the ground as in the propagation of electromagnetic waves above the earth. This term becomes dominant when the receiver is far from the source and near the ground surface, where the direct and reflected wave terms cancel. The fourth term, whose exact physical nature is still obscure, represents a 'surface wave' [3]. It originates from the mathematics in the wave equation solution, and behaves as a disturbance in the air propagating cylindrically outward and decaying exponentially with height. This

disturbance only occurs under some combinations of source-receiver geometry and values of the surface impedance. This modeling of the ground reflection is found to have a good agreement with the measurements conducted by Lawhead and Ruduick [4], provided that an appropriate normal impedence of the ground surface is available. Chessel's model of the ground [5], which allows the impedance to be calculated from a flow resistance, coupled with the type of model described above gives reasonable predictions of the reflection phenomenon.

Turbulence scattering, perhaps the least understood mechanism for outdoor sound propagation, is believed to be responsible for the sharp spikes in the measurements of an acoustic signal which has propagated a long distance. It is due to the wind velocity and temperature fluctuations which cause secondary sound waves to spread out from the original path of the sound wave in a variety of directions. Several theoretical models pertaining to this subject have been considered over the past century. However, none of these theories totally explains the mechanisms associated with turbulence that result in the attenuation of sound and that can be used for a reliable prediction.

Refraction is the bending of sound rays caused by gradual changes in the propagation speed of a sound wave. The variation of sound speed in the atmosphere is brought about principally by vertical gradients of temperature and wind velocity. Since the sound speed is proportional to the square root of the temperature, the vertical variation in temperature will cause a change in sound speed with height so that the wave front is moving at different speeds for various heights. This causes the wave to turn and is known as refraction. Similarly, wind gradients cause portions of the wave front to move faster as seen by

vectorially adding the wind speed and sound wave speed. The resultant propagation speed is not constant with height, so again refraction occurs. There are two types of refractions, upward and downward. The upward refraction is caused by the temperature lapse condition when temperature decreases with increasing height, or when the sound propagates in the opposite direction of wind. Conversely, the downward refraction is due to the temperature inversion, when temperature increases with height, or when the sound propagates as the same direction of wind. The major acoustic effect in refraction is the production of a refractive shadow zone, where, according to the ray picture (geometric acoustics) no sound may enter. The detailed measurements of Parkin and Scholes [6] concluded that refraction due to vertical gradients of wind and temperature in practice produces equivalent acoustic effects. However, these results are based on a relatively little information on the temperature condition: it is being described as lapse, neutral or inversion only, and thus provides no insight on the quantity of each individual factor. It is the purpose of this paper to investigate primarily on the subject of the temperature inhomogeneity in the atmosphere.

The atmosphere is not isothermal under normal conditions. During the daytime hours, radiation from the sun heats up the air in contact with the ground by means of conduction, and the atmosphere is typically warmer near the ground surface and a lapse condition exists. As the sun sets, the surface of the earth cools by radiation. This cools the air adjacent to the earth's surface and an inversion temperature gradient results. The former condition, a lapse condition with temperature decreases with height, is of primary interest in the present

work. Although these regions of strong temperature gradients extend, at maximum, a few meters above the ground, many acoustic sources and receivers are also in this range of elevation.

The influence of temperature homogeneities on sound propagation has been the subject of numerous theoretical studies. Quantitive modeling of refraction caused by sound speed gradients has been carried out over the past several years, particularly in connection with underwater acoustics [7], but little work has been done directly related to the atmospheric problem. There are two closely related approaches that have been used, ray-tracing and a direct solution of the wave equation. Ray tracing provides a qualitative picture of sound behavior in the present of temperature gradient, but determination of the actual sound levels is considerably more complicated, particularly in the regions usually referred to as caustics or convergence zones, where the sound is being focused. Also, this method gives no information about the behavior in the shadow region. Direct solution of the wave equation with a variable sound speed has been undertaken by Pekaris [8], Pridmore-Brown and Ingard [9], Tolstoy [10] and others mainly with the aim of determining the behavior in the shadow region.

A model is being developed by Van Moorhem [11] to apply to the atmospheric case. This work is different from the previous ones in that a physically realistic temperature profile and a finite impedance boundary condition are used to describe the ground surface. The propagation of plane waves has already been considered by Landheim [12]. The point source problem, which is considerably more complex, but is closer to a realistic application, is considered here. Physically, determining the point source solution is nothing more than the summing

of the plane wave solutions over all possible wave incidence angles. However, this summing process, or integration, is expressed as an inverse Hankel transformation which poses a complicated mathematical problem; and no exact solution can be obtained with the existing knowledge. It is at this point this investigation began. A direct numerical integration could be carried out, but it would require a great deal of computation and is therefore not a practical low cost prediction scheme. Another alternative is by employing approximation methods; it is essential and indeed the only approach that can lead to an semi-analytic solution to our problem. This approach has the advantage over the numerical evaluation in that it is more useful for understanding the solution physically, although perhaps not for accuracy.

The entire development of techniques for evaluating the formal solution is based on an approximation schemes in which the Hankel functions are being replaced by their asymptotic expansions. By doing so, the original problem is put into a form so that the Saddle Point method [13] becomes applicable, although some modifications are necessary. This approach has been used successfully in the isothermal problem and in underwater acoustics and would appear useful here. This method will be described in more detail in the following chapters.

The purpose of this thesis, thus, is to numerically implement this model with a computer program. With the required information given, such as the strength and the frequency of the sound source, this program is to predict the sound level received in any particular location in the atmosphere. The work is begun with a general description of how the temperature inhomogeneity affects sound propagation. This is done with the ray tracing method and will be described in

Chapter II. Chapter III discusses the governing equation and its formal solution as obtained by Van Moorhem [11]. Chapter IV describes the analytical approach to the inverse Hankel transformation using the approximation (Saddle Point) method. The results and conclusions are discussed in the following chapters. Plots with different parameters are generated to give an overall depiction of the relative sound magnitude versus height in the physical space and also the results are compared with the empirical model performed by Weiner and Keast. A complete list of the program and its usage is given in the appendix.

CHAPTER II

RAY TRACING

The direction of wave propagation can be represented by rays which are lines perpendicular to the wave fronts. Despite the fact that this ray representation only provides a qualitative picture of the sound behavior in an inhomogenous medium, and the wave nature of sound is completely excluded, it explains some of the physical characteristics of the results obtained from the wave equation in the later chapters.

The location of rays emanating from a source at a height s above a plane surface in a thermally stratified medium can be obtained through the Snell's Law [14]. The vertical temperature profile employed here is

$$T(z) = T_{\infty} + \frac{\Delta T}{1 + \alpha z} \tag{1}$$

which allows a large gradient near the ground (z = 0), but asympototically approaches a constant high above the ground. In the present case, ΔT is a positive value which describes a lapse condition that generally exists during the daylight hours. For a perfect gas, the speed of sound is given by

$$a = \sqrt{\gamma R T} \quad . \tag{2}$$

Substituting (2) into (1) yields

$$a^2(z) = a_\infty^2 \left(1 + \frac{\Delta T}{T_\infty} \cdot \frac{1}{1 + \alpha z}\right) . \tag{3}$$

Snell's law requires that

$$\frac{\cos \theta(z)}{a(z)} = \text{constant} \tag{4}$$

where $\theta(z)$ is the angle between the ray and the horizontal in the present case. The constant can be evaluated by letting $\theta(s)$ be the initial angle of a sound ray propagating out at the source location, and $a(s)$ is the sound speed at the source height. Notice that the constant varies according to the $\theta(s)$ chosen, and thus represents rays with different initial angles. So, for a ray with an initial angle $\theta(s)$, the corresponding angle $\theta(z)$ with the horizontal at a height z is

$$\cos \theta(z) = \frac{a(z)}{a(s)} \cos \theta(s) \quad . \tag{5}$$

With this relationship, between the local and the initial angle of incident, we can then trace the slopes of a particular ray at different locations. The slope of a ray is

$$\frac{dz}{dr} = \tan \theta(z) \quad , \tag{6}$$

and by expressing the tangent in term of cosine

$$\tan \theta(z) = \pm \sqrt{\frac{1}{\cos^2 \theta(z)} - 1} \tag{7}$$

we obtain

$$\frac{dz}{dr} = \pm \sqrt{\frac{a^2(s)}{a^2(z)} \frac{1}{\cos^2\theta(s)} - 1} \quad . \tag{8}$$

The choice of the sign depends on whether the ray is propagating upward or downward as it leaves the source. Substituting the expressions for a(z) in (3) and rearranging the terms yield

$$\frac{dz}{dr} = \pm \sqrt{\frac{AZ + B}{CZ + D}} \tag{9}$$

where

$$\begin{aligned} A &= \alpha \left(1 + \alpha s + \Delta T/_T - (1 + \alpha s) \cos^2\theta(s)\right) \\ B &= 1 + \alpha s + \Delta T/_T - (1 + \alpha s)\left(1 + \Delta T/_T\right) \cos^2\theta(s) \\ C &= \alpha (1 + \alpha s) \cos^2\theta(s) \\ D &= \left(1 + \Delta T/_T\right)(1 + \alpha s) \cos^2\theta(s) \ . \end{aligned} \tag{10}$$

The next task is to evaluate the horizontal distance as a function of height. This is done by integrating (9) which gives rise to four different types of rays with four corresponding equations given by:

(1) $r = F(z,\theta(s)) - F(s,\theta(s))$ (11)

for rays propagating upward from the source.

(2) $r = F(s,\theta(s)) - F(z,\theta(s))$ (12)

for rays propagating downward from the source.

(3) $r = F(z,\theta(s)) + F(s,\theta(s)) - 2F(0,\theta(s))$ (13)

for rays propagating downward initially and reflected upward at the surface .

$$(4)\quad r = F(z,\theta(s)) + F(s,\theta(s)) \tag{14}$$

for rays propagating downward initially and refracted upward without reaching the surface. The function $F(z,\theta(z))$ resulting from the integration of (9) is given by

$$F(z,\theta(s)) = \frac{\sqrt{(AZ + B)(CZ + D)}}{A} + \frac{AD - BC}{2A\sqrt{AC}} \ln\left(\frac{1 + \phi}{1 - \phi}\right) \tag{15}$$

where

$$\phi = \frac{C\,(AZ + B)}{A\,(CZ + D)} \quad .$$

These four types of rays are shown in Figure 1. With this ray tracing technique, it can be seen from the figure that the physical space is divided into seven different regions. Except for region 7, each of them is characterized by a combination of two types of rays. As is shown in Figure 1, regions 1 and 3 are both characterized by the direct and reflected waves, except that the former has the direct wave travelling upward while the latter is travelling downward. Region 5 is made up of reflected and refracted waves. It is to be stressed at this point that, at least from a mathematical stand point, there exist two kinds of refracted waves. Care must be taken to distinguish them because, as we will see in the later section, their mathematical solutions for the sound pressure are different by a 90° phase angle. Physically, they are determined by whether the refracted wave has or has not reached the caustic before it arrives at the receiver's loca-

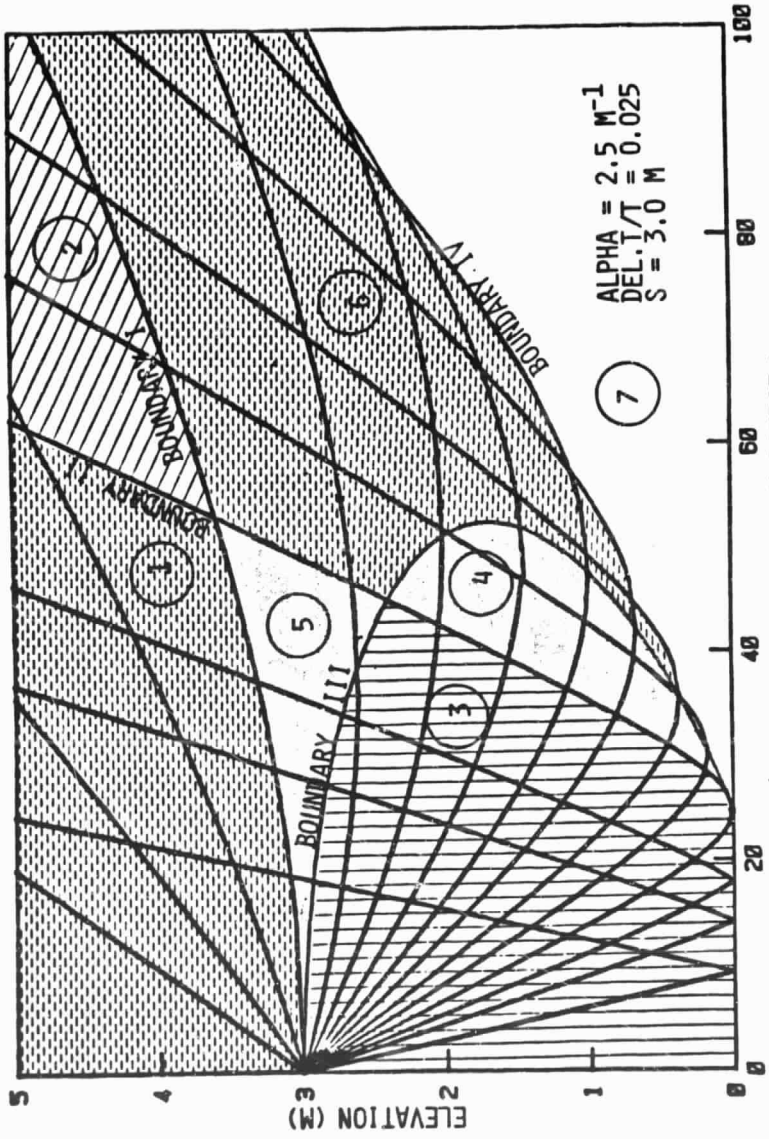

Figure 1. Ray diagram for sound propagation in the presence of temperature gradient.

tion. The refracted wave in region 5 belongs to the latter kind. Regions 2 and 4 are identical to 1 and 3 except that the reflected wave has been replaced by a refracted wave: the one that has reached the caustic before it entered the region. Region 6, which is bounded by the caustic, consists of both kinds of refracted waves. It follows that at any locations, except that in the shadow region, the receiver is always reached by two different sound rays identified by their initial angle $\theta(s)$ at the source. This phenomenon, as we will see in the the following sections, contributes a great deal of insight to the physical interpretation of the mathematical solution of sound propagation from a point source.

CHAPTER III

FORMAL SOLUTION OF THE POINT SOURCE PROBLEM

This chapter summarizes the formal solution as obtained by Van Moorhem [11]. Sound propagation can usually be regarded as a small acoustic disturbance to the atmosphere's ambient state. Even in a thermally stratified atmosphere, its physical behavior is still governed by the linear acoustic wave equations but with a variable sound speed. Assuming there are no viscous or body forces exerted on the medium, the continuity and momentum equations become

$$\frac{\partial \rho}{\partial t} + \nabla \cdot (\rho V) = Q \tag{16}$$

where Q is the source term and

$$\frac{\partial V}{\partial t} + V \cdot \nabla V = -\frac{1}{\rho} \nabla P \tag{17}$$

where ρ, V, and P are the physical variables: density, velocity and pressure, respectively.

Since the ambient state is thermally inhomogenous, the equations of state for the atmosphere become [15]

$$P = P(\rho, S) \tag{18}$$

and

$$\frac{DS}{Dt} = 0 \tag{19}$$

where S is the specific entropy of the air particle.

For a small acoustic disturbance, the physical variables can be expressed as the sum of their time mean and their fluctuating parts. Thus assuming

$$\begin{aligned} P &= P_M + P'(r,z,t) \\ \rho &= \rho_M(z) + \rho'(r,z,t) \\ V &= V'(r,z,t) \\ S &= S_M(z) \end{aligned} \tag{20}$$

where the quantities with subscript M represent the time mean atmospheric condition and are functions of only height above the ground with the exception of pressure which is assumed constant throughout the atmosphere. Also, the medium is assumed to be at rest ($V_M = 0$). P', ρ', and V' represent the acoustic perturbation and always assumed small compared to their corresponding time mean or ambient values. Substituting Equation (20) into Equations (16) through (19) and neglecting the products of the second order terms, the governing equations become

$$\frac{\partial P'}{\partial t} + \rho_M \nabla V' + V' \nabla \rho_M = Q \tag{21}$$

$$\frac{\partial V}{\partial t} + \frac{1}{\rho_M} \nabla \rho' = 0 \tag{22}$$

$$\frac{\partial P'}{\partial t} + V' \nabla P_M = a_M^2 \left(\frac{\partial P'}{\partial t} + V' \nabla \rho_M \right) \tag{23}$$

where

$$a_M^2 = \left(\frac{\partial P}{\partial \rho}\right)_{S = S_M} \tag{24}$$

is the variable sound speed which depends on the height z. Combining Equations (21) through (23) and eliminating the acoustic variables, with the exception of pressure, yields

$$\frac{1}{a_M^2} \frac{\partial^2 p'}{\partial t^2} - \nabla^2 p' - \frac{\nabla \rho_o \nabla p'}{\rho_o} = Q \quad . \tag{25}$$

Hereafter, the primes on P and V are deleted for simplicity. The first two terms in Equation (25) are of order $(\omega/a_\infty)^2$ and the third term, based on the temperature profile given by (1), is of order $(\alpha\omega/a_\infty)$. Here ω is the angular frequency of the sound source and α describes the temperature gradient at ground. Note that the term (ω/a_∞) is actually the reciprocal of wavelength and the third term is nondimensionialized by α. Thus, if the frequency is sufficiently high that the wave length is small compared to the scale of the variation α in temperature in the atmosphere, so that $\omega/(a_\infty\alpha) >> 1$, then the third term in Equation (25) is negligible compared to the previous two. Hence, if the assumption is made that the frequency is high along with small perturbations, the simple wave equation with variable sound speed results:

$$\frac{1}{a_M^2(z)} \frac{\partial^2 p}{\partial t^2} - \nabla^2 p = Q \tag{26}$$

where the source term Q is represented by

$$Q = q \frac{\delta(r)}{\pi r} \ell(z-s) e^{i\omega t} \tag{27}$$

a point source at $z = s$ and $r = 0$, and from Equation (3)

$$a_M^2(z) = a_\infty^2 \left(1 + \frac{\Delta T}{T\infty} \frac{1}{1 + \alpha z}\right) . \tag{3}$$

At the surface ($z=0$) the boundary condition is

$$- Z w = P \tag{28}$$

where w is the vertical component of the acoustic fluid velocity obtained from $\partial w/\partial t = - 1/\rho(\partial P/\partial z)$ and Z is the normal acoustical impedance of the surface. Also, as $z \to \infty$ a radiation condition requiring all waves to be propagating upward must be applied.

The solution is obtained by first separating out the time dependance by defining a function $\overline{G}(z,r)$ such that

$$P(z,r,t) = e^{i\omega t} \overline{G}(z,r) . \tag{29}$$

Taking the Hankel transformation (two-dimensional Fourier transform) of the resulting governing equation and boundary condition then yields

$$\frac{d^2G}{dz^2} + \left(\frac{\omega^2}{a_\infty^2} \frac{1 + \alpha z}{1 + \alpha z + \frac{\Delta \bar{T}}{T}} - \beta^2\right)G = - \frac{q}{2\pi} \delta(z-s) \tag{30}$$

and

$$G = \frac{iZ}{\omega \rho_0} \left.\frac{\partial G}{\partial z}\right|_{z = 0} \tag{31}$$

on $z = 0$. The function $G(z,\beta)$ is the Hankel transform of $\overline{G}(r,z)$ and is defined by

$$G(z,\beta) = \int_0^\infty \bar{G}(z,r)\, r\, J_0(\beta r)\, dr \quad . \tag{32}$$

The inverse Hankel transform yields $\bar{G}(r,z)$ and is given by

$$\bar{G}(z,r) = \int_0^\infty G(z,\beta)\, \beta\, J_0(\beta r)\, d\beta \quad . \tag{33}$$

Nayfeh [16] gives a method of obtaining an approximate solution of Equation (30) which is valid when $\lambda = \omega/(a_\infty \alpha) >> 1$. This requirement is the same as that found to be valid for Equation (26), so no new approximation is required. The approximate solutions can be expressed as

$$G = \frac{A}{\sqrt{g'(z)}}\, h_1(\eta(z)) + \frac{B}{\sqrt{g'(z)}}\, h_2(\eta(z)) \tag{34}$$

where

$$\eta(z) = \left(\frac{3}{2}\lambda\right)^{2/3} g(z) \tag{35}$$

$$h_1(\xi) = \left(\frac{2}{3}\right)^{1/3} \xi^{1/2}\, H^{(1)}_{1/3}\left(\frac{2}{3}\xi^{3/2}\right) \tag{36}$$

and

$$h_2(\xi) = \left(\frac{2}{3}\right)^{1/3} \xi^{1/2}\, H^{(2)}_{1/3}\left(\frac{2}{3}\xi^{3/2}\right) \quad . \tag{37}$$

Values of the modified one-third order Hankel functions, h_1 and h_2, are tabulated and their properties are discussed in Reference [17]. The function

$$g'(z) = \frac{2}{3}\alpha \sqrt{\frac{(1 - ((a_\infty/\omega\,\beta)^2)\,(1 + \alpha z + \Delta T/T)^2 - (\Delta T/T)}{g(z)\,(1 + \alpha z + \Delta T/T)}} \tag{38}$$

giving

$$g^{3/2}(z,\beta) = \sqrt{(1 - (\frac{a_\infty}{\omega}\beta)^2)(1 + \alpha z + \frac{\Delta T}{T})^2 - \frac{\Delta T}{T}\,(1 + \alpha z + \frac{\Delta T}{T})}$$

$$- \frac{1}{2}\,\frac{\Delta T}{T}\,\frac{1}{\sqrt{1 - ((a_\infty/\omega\,\beta)^2}}\,\ln\,(\frac{1 + \phi}{1 - \phi}) \tag{39}$$

where

$$\phi = \sqrt{\frac{(1 - (\frac{a_\infty}{\omega}\beta)^2)(1 + \alpha z + \frac{\Delta T}{T}) - \frac{\Delta T}{T}}{(1 - (\frac{a_\infty}{\omega}\beta)^2)(1 + \alpha z + \frac{\Delta T}{T})}} \tag{40}$$

This solution is the same as for the plane wave case [11] provided that cos θ in the plane wave case is replaced by $(a_\infty/\omega)\beta$. Here θ is the incidence angle of the plane wave at infinity and a is the speed of sound at infinity. This result, obtained from the Hankel transformation, shows that the point source problem in fact can be interpreted as a summation of the plane wave solutions. Before we can proceed to the final solution, it is necessary to examine the nature of the plane wave propagation associated with the point source problem.

In the plane wave problem all real incidence angles were possible, and cos θ could vary between zero and one. In the point source problem the range is more limited. First consider the waves propagating down-

ward from the source located at height s. Wave that are directed downward at a sufficient angle will reach the ground as in the plane wave case. Plane wave rays directed downward at an infinite height with incidence angles between 90° and some value θ_0, or $0 < \beta < \beta_0 = (\omega/a_\infty) \cos \theta_0 = (\omega/a_\infty) \sqrt{1/(1+\Delta T/T)}$ can pass through the source location and reach the ground where they are reflected (see Figure 2). The turning points of these waves are below the ground surface. The initial angle θ_0 characterizes the waves whose turning point is at the ground level, z = 0. Waves in this range of initial angle and their reflections from the ground constitute two groups of possible waves and one of the forms of the solution.

A second group of waves which is initially directed downward at the source are rays with angles at infinity in the range between θ_0 and θ_z or $\beta_0 < \beta < \beta_z = (\omega/a_\infty) \cos \theta_z = (\omega/a_\infty)\sqrt{((1+\alpha z)/(1 + \alpha z + \Delta T/T))}$. The angle θ_z characterizes the wave whose turning point is located at the observer height z. This range of angles or of betas then characterizes waves that pass through the source location and whose turning point is above the ground level but below the observer (see Figure 3). These waves, before passing through the turning point, and after passing through the turning point, contribute a second form to the solution.

A third group of waves propagating downward at the source has angles at infinity in the range between θ_z and θ_s or $\beta_z < \beta < \beta_s = (\omega/a_\infty) \cos \theta_s = (\omega/a_\infty)\sqrt{((1 + \alpha s)/(1 + \alpha s + \Delta T/T))}$. The value θ_s characterizes the wave with its turning point at the height s. It is the wave that leaves the source horizontally and is the limiting case of waves leaving the source and propagating downward. Waves in this

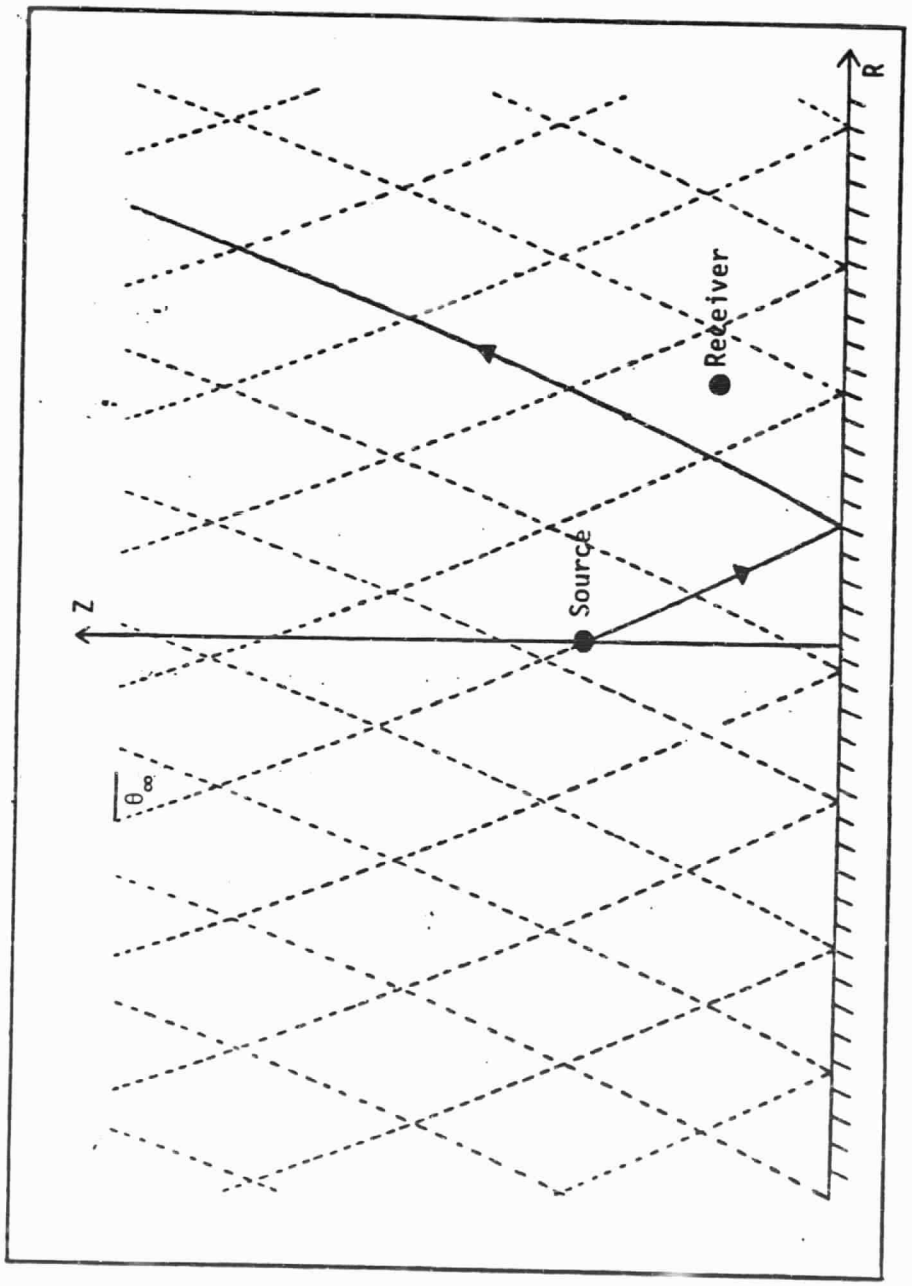

Figure 2. Ray diagram for a plane wave passing through the point source location and being reflected from the ground.

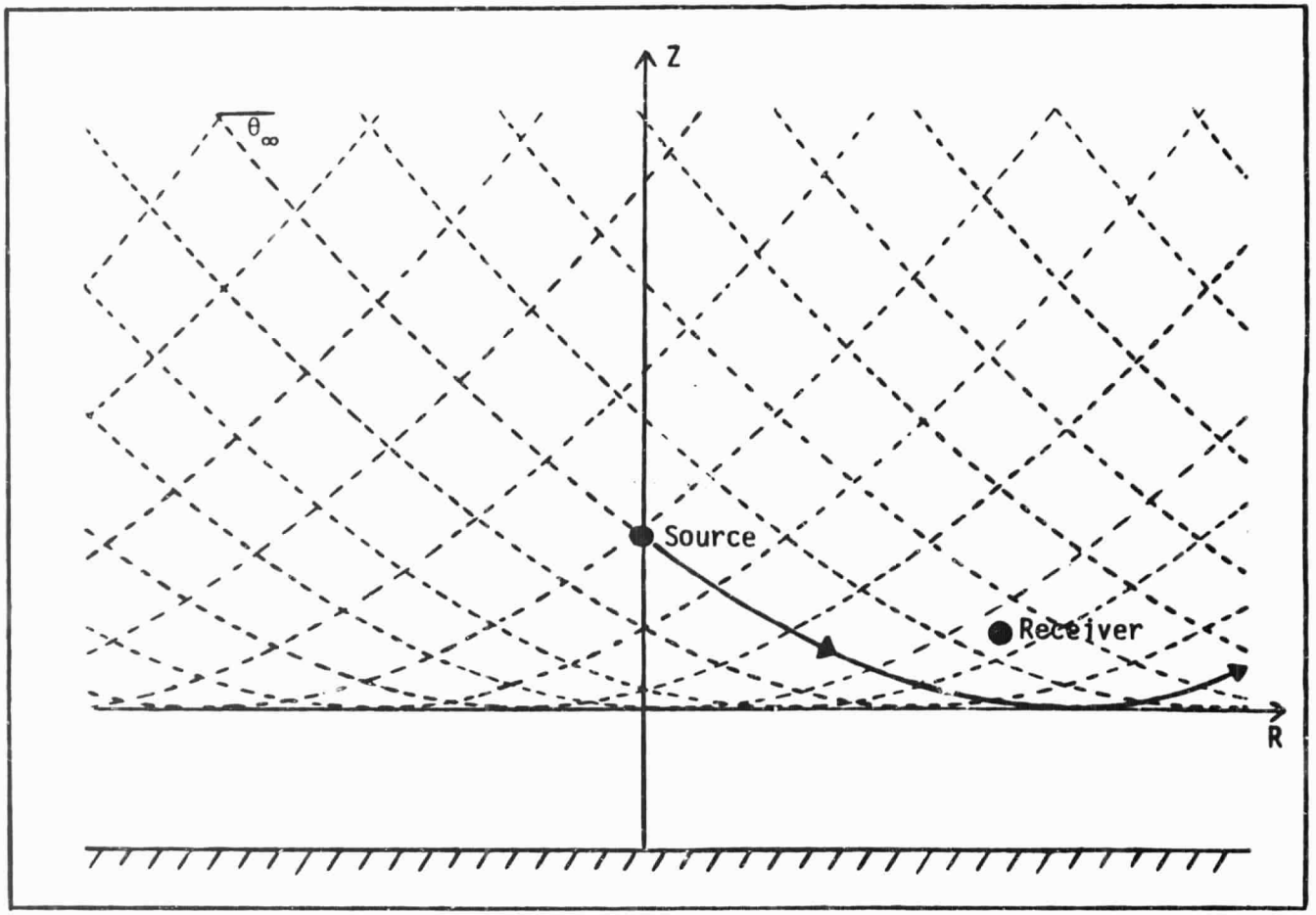

Figure 3. Ray diagram for a plane wave passing through the point source location and being refracted before reaching the ground but below the receiver.

group have their turning points above the observer (see Figure 4), and thus cannot contribute an oscillating term to the total solution but rather have an exponential behavior. This behavior is further discussed in connection to the Saddle Point method of evaluation. This group of waves and their continuation after being refracted upward constitute a third form of the solution.

The fourth form of the solution is due to waves which leave the source and propagate upward. These waves as shown in Figures 5 and 6 have $\theta_s < \theta \leq 90°$ or $0 \leq \beta < \beta_s$ but are not of the same form as described earlier as their amplitude must be corrected for waves leaving the source rather than waves reflected or refracted upward. These waves constitute a fourth form of the solution.

All of the waves of the four types described above can be seen in the ray diagram of the point source Figure 1, but a number of additional types of waves need to be included in the total solution which do not appear in the ray diagram. The fifth form of the solution has $\theta_s > \theta \geq 0°$ or $\beta_s < \beta \leq \omega/a_\infty$. These are waves with their turning points above the source and do not appear in the ray diagram but contribute to the full solution. In this case $g(s,\beta)$ is a complex number with phase of $\pi/3$ and the solution has an exponential behavior.

The actual forms of the solution are obtained by requiring Equation (30) to satisfy the surface boundary condition, (31), at $z = 0$: at $z = s$, the source height, the solution must satisfy the condition that

$$\lim_{z \to s_-} [G(\beta,z)] = \lim_{z \to s_+} [G(\beta,z)] \tag{41}$$

which requires continuity of pressure and the condition that

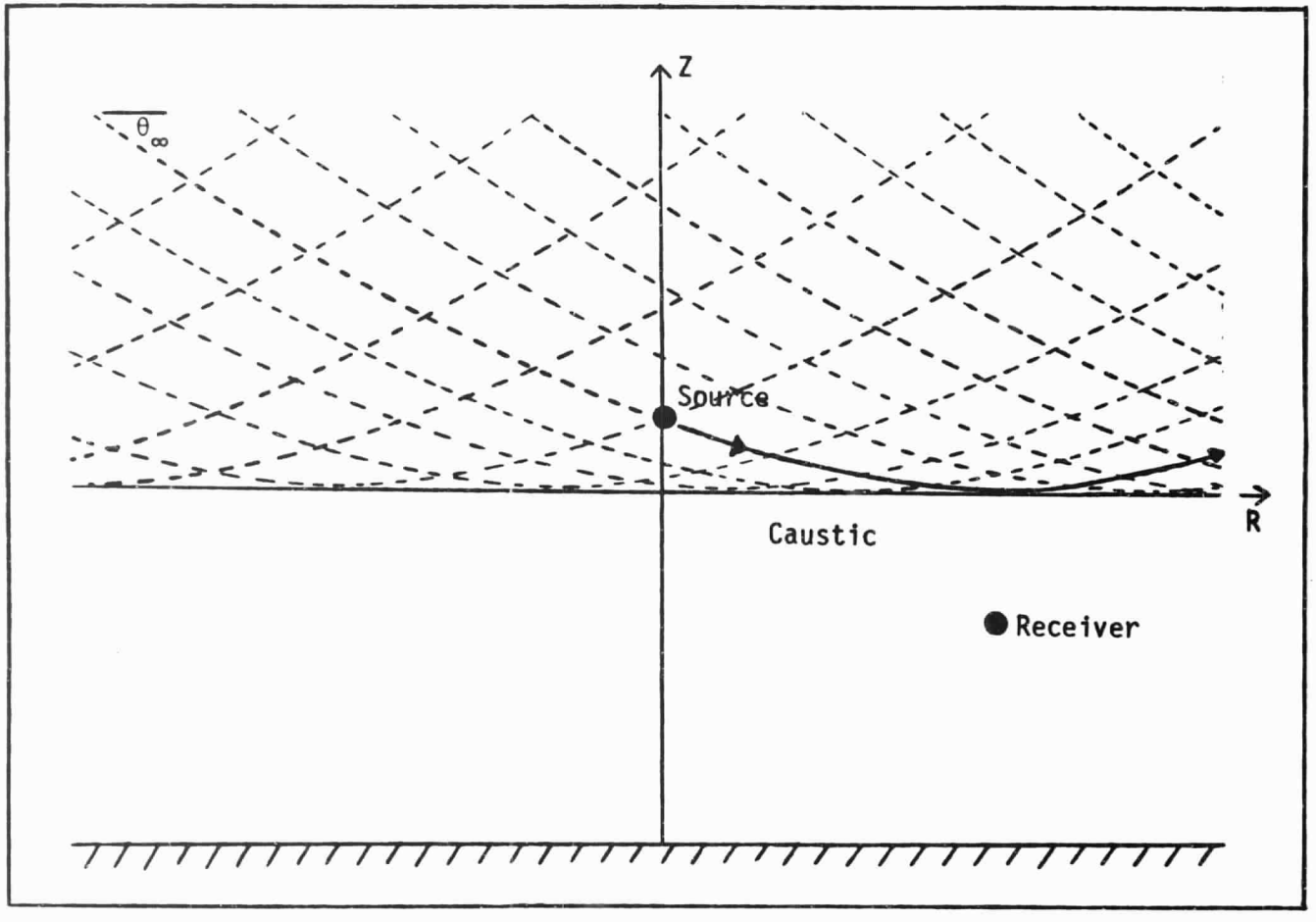

Figure 4. Ray diagram for a plane wave passing through the point souce location and being refracted before reaching the ground and above the receiver.

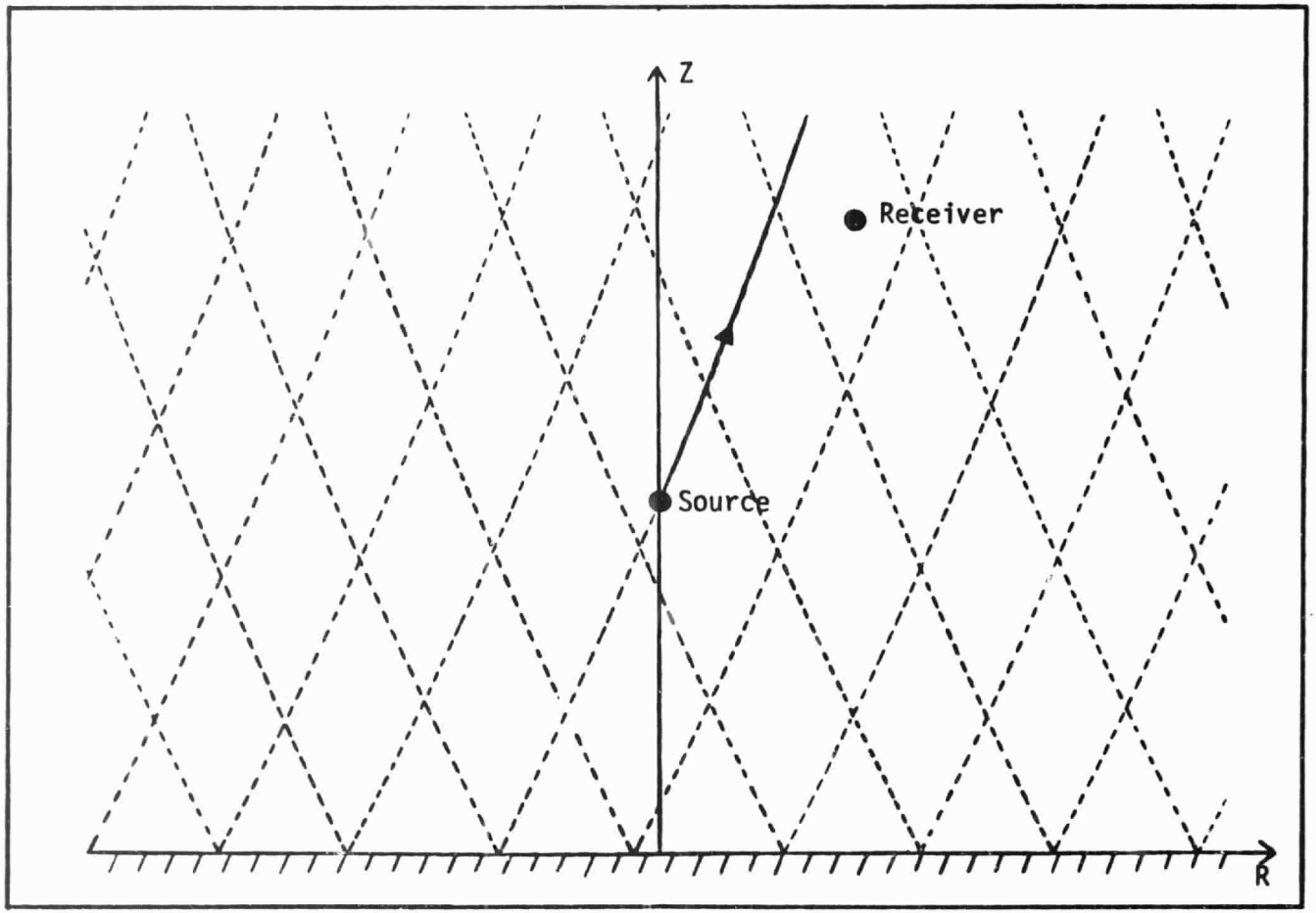

Figure 5. Ray diagram for a reflected plane wave passing through the point source and propagated upward.

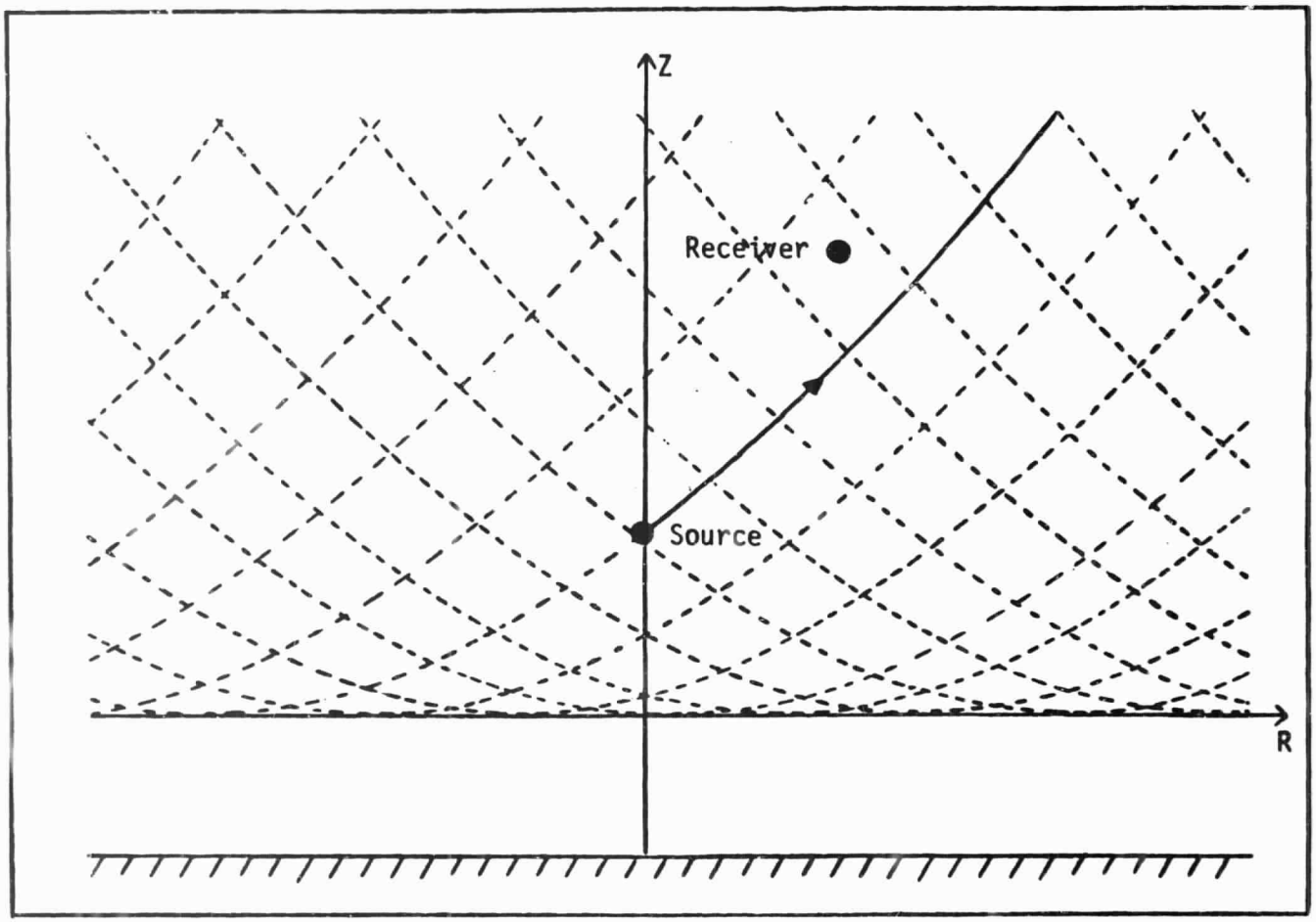

Figure 6. Ray diagram for a refracted wave passing through the point source and propagated upward.

$$\lim_{z \to s_-} \left[\frac{\partial G}{\partial z}\right] - \lim_{z \to s_+} \left[\frac{\partial G}{\partial z}\right] = \frac{q}{2\pi} \tag{42}$$

which is obtained by integrating Equation (30) from $z = s - \varepsilon$ to $z = s + \varepsilon$ and taking the limits of $\varepsilon \to 0$. At the turning point height the condition

$$\lim_{z \to z_{TP+}} [G(\beta,z)] = \lim_{z \to z_{TP-}} [G(\beta,z)] \tag{43}$$

is required if the turning point is above ground surface, $z = 0$. With some mathematical manipulation [11], the resulting solution can be written in the following form:

For $z > s$,

$$G = K\left\{h_2\,(\eta(\beta,z))\,[\,h_1\,(\eta(\beta,s)) + R_0\,(\eta(\beta,0))\,h_2\,(\eta(\beta,s))\,]\right\} \tag{44}$$

for $\omega/a_\infty > \beta_z > \beta_s > \beta_0 > \beta > 0$,

$$G = K\left\{h_2\,(\eta(\beta,z))\,[h_1\,(\eta(\beta,s)) + R_0\,(\eta(\beta,0)e^{i\frac{2\pi}{3}})\;h_2\,(\eta(\beta,s))]\right\} \tag{45}$$

for $\omega/a_\infty > \beta_z > \beta_s > \beta > \beta_0 > 0$,

$$G = K\left\{h_2\,(\eta(\beta,z))\,[h_1\,(\eta(\beta,s)e^{i\frac{2\pi}{3}}) + R_0\,(\eta(\beta,0)e^{i\frac{2\pi}{3}})\;h_2\,(\eta(\beta,s)e^{i\frac{2\pi}{3}})]\right\} \tag{46}$$

for $\omega/a_\infty > \beta_z > \beta > \beta_s > \beta_0 > 0$ and

$$G = K\left\{h_2\,(\eta(\beta,z)e^{i\frac{2\pi}{3}})\,[h_1\,(\eta(\beta,s)e^{i\frac{2\pi}{3}}) + R_0\,(\eta(\beta,0)e^{i\frac{2\pi}{3}})\;h_2\,(\eta(\beta,s)e^{i\frac{2\pi}{3}})]\right\} \tag{47}$$

for $\omega/a_\infty > \beta > \beta_z > \beta_s > \beta_0 > 0$. For $z < s$

$$G = K\left\{h_2\,(\eta(\beta,s))\,[h_1\,(\eta(\beta,z)) + R_0\,(\eta(\beta,0))\,h_2\,(\eta(\beta,z))]\right\} \tag{48}$$

for $\omega/a_\infty > \beta_s > \beta_z > \beta_0 > \beta > 0$,

$$G = K\left\{h_2\,(\eta(\beta,s))\,[h_1\,(\eta(\beta,z)) + R_0\,(\eta(\beta,o)e^{i\frac{2\pi}{3}})\,h_2\,(\eta(\beta,z))]\right\} \tag{49}$$

for $\omega/a_\infty > \beta_s > \beta_z > \beta > \beta_0 > 0$,

$$G = K\left\{h_2\,(\eta(\beta,s))\,[h_1\,(\eta(\beta,z)e^{i\frac{2\pi}{3}}) + R_0\,(\eta(\beta,0)e^{i\frac{2\pi}{3}})\;h_2\,(\eta(\beta,z)e^{i\frac{2\pi}{3}})]\right\} \tag{50}$$

for $\omega/a_\infty > \beta_s > \beta > \beta_z > \beta_0 > 0$ and

$$G = K\left\{h_2\,(\eta(\beta,s)e^{i\frac{2\pi}{3}})\,[h_1\,(\eta(\beta,z)e^{i\frac{2\pi}{3}}) + R_0\,(\eta(\beta,o)e^{i\frac{2\pi}{3}})\,h_2\,(\eta(\beta,z)e^{i\frac{2\pi}{3}})]\right\} \tag{51}$$

for $\omega/a_\infty > \beta > \beta_s > \beta_z > \beta_0 > 0$, where

$$K = \frac{q}{12i\lambda^{2/3}}\,\frac{1}{\sqrt{g_z(\beta,s)}}\,\frac{1}{\sqrt{g_z(\beta,z)}} \tag{52}$$

$$R_0 = -\,\frac{\tau\,h_1\,(\eta(\beta,0)) + i\,\psi\,h_1'\,(\eta(\beta,0))}{\tau\,h_2\,(\eta(\beta,0)) + i\,\psi\,h_2'\,(\eta(\beta,0))} \tag{53}$$

$$\tau = \alpha\,\lambda - \frac{i}{2}\,\frac{Z}{\rho a_\infty}\,\frac{g_{zz}(\beta,0)}{g_z\,(\beta,0)} \tag{54}$$

$$\psi = \frac{Z}{\rho a_\infty}\,\lambda^{2/3}\,g_z\,(\beta,0)\left(\frac{3}{2}\right)^{2/3} \tag{55}$$

Note that g_z (z) here denotes the derivative is taken with respect of αz rather than z as in g' (z). These eight forms account for the five physical situations described above since some forms are repeated. These forms of solutions are useful in the way that the first term always represents the direct wave and the second the reflected or refracted wave. This then completes the formal solution to the problem with the solution given in the form of an integral, Equation (33), the inverse transformation of the function $G(\beta,z)$ given by Equation (44) through (51). This is a very complex integral and approximations are necessary to proceed toward its numerical evaluation.

CHAPTER IV

EVALUATION OF THE FORMAL SOLUTION

As we have seen in Chapter III, the problem that needs to be solved is the inverse Hankel transformation of the functions defined by

$$\bar{G}(r,z) = \int_0^\infty G(\beta,z)\, \beta\, J_0(\beta r)\, d\beta \tag{56}$$

where $G(\beta,z)$ is given in Equations (44) through (51) depending on the location of the receiver. Because of the complexity of the functions involved, it is unlikely that an exact solution can be obtained through an analytical approach. The second alternative that came into consideration was the direct numerical integration. However, in doing so, it would require the integral in the inverse Hankel transform to be evaluated at each point of interest. Of course, this could be done except that it requires a tremendous amount of computing time and, also, the understanding of the physical nature of the solution is reduced. The most satisfying remedy to this problem is to employ an approximate integration. The Saddle Point method, or the method of steepest descent, has been used successfully in the isothermal problem and appears to be useful here.

The Saddle point method is a method of approximately integrating expressions of the form

$$\int_{-\infty}^{\infty} F(\beta)e^{\xi f(\beta)}d\beta \tag{57}$$

where ξ is a large parameter. If we interpret this integral as an integral in complex β space, the path of integration can be modified according to the rules of contour integration in the complex plane. What would appear to be desired, then, is to find a point (or points) in the complex β plane where the integrand of Equation (57) is a maximum and to distort the path of integration to pass through this point in such a way that the exponential term in Equation (57) decreases rapidly as one moves along the modified path of integration away from the point of maximum integrand. In the complex plane, however, a regular function does not have a maximum: but rather a point where

$$\left.\frac{\partial f}{\partial \beta}\right|_{\beta = \beta_{sp}} = 0 \tag{58}$$

is a saddle point of the function, a point where the function surface looks like a mountain pass, col, or saddle. This point is found to give the major contribution to the integral when the path is modified to give a rapidly decreasing integrand as one moves away from it. Approximately integrating Equation (57) then can be shown to give

$$\sqrt{-\frac{2\pi}{\xi f''(\beta_{sp})}}\, f(\beta_{sp})e^{\xi f(\beta_{sp}) + i\sigma} \tag{59}$$

where σ is the angle at which the path of integration crosses through the saddle point. This method is described in more detail and with

more rigor in most texts on advanced mathematical methods, Reference [13], for example. This method is not a fool-proof one however, as the modified path of integration may intersect branch lines, pass around poles, or lead into other difficulties. Keller [18], however, asserts that the major part of the solution is obtained. Also if no saddle point occurs then the integral can be approximated as zero. Using this rather crude approach the integrals can be approximated relatively easily.

In order to ultilize the Saddle Point method, some modifications of the integral are necessary. The method requires an integral involving an exponential term to be evaluated from negative infinity to positive infinity. This can be achieved by first noting that the Bessel function $J_0(\beta r)$ in Equation (56) can be written [19] as

$$J_0(\beta r) = \frac{1}{2}\left[H_0^{(1)}(\beta r) + H_0^{(2)}(\beta r) \right] \tag{60}$$

also

$$H_0^{(1)}(-\beta r) = -H_0^{(2)}(\beta r) \tag{61}$$

and $G(\beta,z)$ is an even function of β. Thus Equation (56) can be written as

$$\bar{G}(\beta,z) = \frac{1}{2}\int_{-\infty}^{\infty} G(\beta,z)\, H_0^{(2)}(\beta r)\, d\beta \quad . \tag{62}$$

The exponential forms are obtained by then assuming the arguments of

all the Hankel functions involved are sufficiently large to allow replacement by their asymptotic forms [19]; carrying out this asymptotic expansion process the resulting expressions are of the form (59) with the integrand of each integral consisting of two terms: one will be seen to represent the direct waves, and the second the reflected and/or refracted waves. This becomes clear when the derivative with respect to β is taken of the argument of the exponential terms to find the saddle points. It is found that

$$\frac{\partial(\lambda\, g^{3/2}(\beta,z))}{\partial\beta} = -\, F(\beta,z) \tag{63}$$

where $F(\beta,z)$ is the same function that occures in the ray tracing proded that $\cos\theta$ is replaced by $(a_\infty/\omega)\beta$ where θ is the incidence angle of the plane wave at infinity. Thus, the finding of the saddle points, which could be numerically quite difficult, has a clear physical interpretation in terms of the rays of the point source. For an observer located at a point in physical, (r,z), space which is "illuminated" by the point source, the saddle points of the approximate integrals found for the solution correspond to the β values of the two rays passing through that point as shown in Figure 1. Physically this is interpreted as indicating that the wave front travelling along the ray that passes through the source and receiver location is the major contributor to the sound level that is experienced.

At any point in the "illuminated" region of physical space the solution is then approximated, as described above, by two of the terms listed below. For direct waves, with $z > s$, region 1 and 2 of Figure 1,

$$\bar{G}_D = \frac{\sqrt{2\pi}\, K_2\, e^{-i(\beta_{sp} r + \phi_1)}}{\sqrt{-\phi_1''(\beta_{sp})}} \tag{64}$$

where

$$\phi_1(\beta) = -\lambda\, g^{2/3}\,(\beta, s) + \lambda\, g^{3/2}\,(\beta, z) - \frac{\pi}{2} \tag{65}$$

and β_{sp} is the root of

$$r + \phi_1'(\beta_{sp}) = 0 \ . \tag{66}$$

For direct waves with $0 < z < s$, regions 3 and 4 of Figure 1

$$\bar{G}_D = \frac{2\pi\, K_2\, e^{-i(\beta_{sp} + \phi_2)}}{\sqrt{-\phi_2''(\beta_{sp})}} \tag{67}$$

where

$$\phi_2(\beta) = \lambda\, g^{3/2}\,(\beta, s) - \lambda\, g^{3/2}\,(\beta, z) - \frac{\pi}{2} \tag{68}$$

and β_{sp} is the root of

$$r + \phi_2'(\beta_{sp}) = 0 \ . \tag{69}$$

For reflected waves, regions 1,3, and 5 of Figure 1

$$\bar{G}_R = \frac{2\pi K_2 R_2(\beta_{sp}) e^{-i(\beta_{sp} r+\phi_3)}}{\sqrt{\phi_3''(\beta_{sp})}} \tag{70}$$

where

$$\phi_3(\beta) = \lambda g^{3/2}(\beta,s) + \lambda g^{3/2}(\beta,z) - 2\lambda g^{3/2}(\beta_{sp},0) - \frac{\pi}{2} \tag{71}$$

and β_{sp} is the root of

$$r + \phi_3'(\beta_{sp}) = 0 \quad . \tag{72}$$

For refracted waves which have not contacted the caustic, Regions 4,5, and 6 of Figure 1

$$\bar{G}_R = \frac{\sqrt{2\pi} K_2 e^{-i(\beta_{sp} r+\phi_3)}}{\sqrt{\phi_4''(\beta_{sp})}} R_1(\beta_{sp})) \tag{73}$$

where

$$\phi_4(\beta) = \lambda g^{3/2}(\beta,s) + \lambda g^{3/2}(\beta,z) + \frac{11\pi}{6} \tag{74}$$

and β_{sp} is the root of

$$r + \phi_4'(\beta_{sp}) = 0 \quad . \tag{75}$$

For refracted waves that have contacted the caustic, regions 2,4, and 6 of Figure 1

$$\bar{G}_R = \frac{2\pi\, k_2\, e^{-i(\beta_{sp} r + \phi_5)}}{\sqrt{-\phi_5''(\beta_{sp})}} \tag{76}$$

where

$$\phi_5 = \phi_4 - \frac{\pi}{2} \tag{77}$$

and β_{sp} is also a root (the smaller of the two roots for region 6) of Equation (75).

The derivative of $g^{3/2}(z,\beta)$ is defined by Equation (39).

$$K_2(\beta_{sp}) = -\frac{q}{12\pi i}\sqrt{\frac{2\beta_{sp}}{\pi}}\,\frac{1}{\sqrt{g_z(\beta_{sp},z)}}\,\frac{1}{\sqrt{g_z(\beta_{sp},s)}}\,\frac{1}{g^{1/4}(\beta_{sp},z)}\,\frac{1}{g^{1/4}(\beta_{sp},s)} \tag{78}$$

$$R_1 = \frac{e^{-i\frac{\pi}{6}}}{\left(e^{i\frac{\pi}{6}} - i\,R_o\right)} \tag{79}$$

and

$$R_2 = \frac{\tau + \psi\, i\,(\frac{3}{2}\lambda)^{1/3}\sqrt{g(\beta,0)}}{\tau - \psi\, i\,(\frac{3}{2}\lambda)^{1/3}\sqrt{g(\beta,0)}} \tag{80}$$

where R_o, τ and ψ are defined in Equations (53), (54) and (55). Thus, the problem has resolved itself into a relatively simple expression, but two difficulties remain. First, the expressions given above are not continuous as the receiver is moved from region to region in physical space. Secondly, no expression has been obtained that is valid in the shadow, region 7 in Figure 1. The first difficulty is easily

resolved by an ad hoc approach. The discontinuity results from the fact that on the boundary between regions the arguments of one of the modified Hankel functions is zero and it has been assumed that all of the arguments are large enough to allow use of the asymptotic forms. The actual integrals are continuous at these boundaries but the asymptotic forms are not. Thus, by replacing the asymptotic forms of the modified Hankel functions in Equations (64), (67), (70), (73) and (76) by the modified Hankel functions themselves one obtains: in place of Equation (64)

$$\bar{G}_D = \frac{\sqrt{2\pi}\, K_3}{\sqrt{\frac{\partial^2}{\partial \beta^2}(\phi_1)}} e^{-i(\beta_{sp} r - \pi/2)} h_2(\eta(\beta_{sp},z))\, h_1(\eta(\beta_{sp},s)) \qquad (81)$$

for direct wave at $z < s$: in place of Equation (67)

$$G_D = \frac{\sqrt{2\pi}\, K_3}{\sqrt{\frac{\partial^2}{\partial \beta^2}(\phi_2)}} e^{-i(\beta_{sp} r - \pi/2)} h_1(\eta(\beta_{sp},z))\, h_2(\eta(\beta_{sp},s)) \qquad (82)$$

for direct waves at $z > s$: in place of Equation (70)

$$G_R = \frac{\sqrt{2\pi}\, K_3\, R_o(\beta_{sp})}{\sqrt{-\frac{\partial^2}{\partial \beta^2}(\phi_3)}} e^{-i(\beta_{sp} r - \pi/2)} h_2(\eta(\beta_{sp},z))\, h_2(\eta(\beta_{sp},s)) \qquad (83)$$

for reflected wave; in place of Equation (73)

$$G_R = \frac{\sqrt{2\pi}\, K_3\, R_1(\beta_{sp})}{\sqrt{\frac{\partial^2}{\partial \beta^2}(\phi_4)}} e^{-i(\beta_{sp} r - \pi)} h_2(\eta(\beta_{sp},z))\, h_2(\eta(\beta_{sp},s)) \qquad (84)$$

for refracted waves that have contacted the caustic; and, in place of

Equation (76)

$$G_R = \frac{\sqrt{2\pi}\, K_3\, R_1\,(\beta_{sp})}{\sqrt{\frac{\partial^2}{\partial\beta^2}(\phi_5)}}\, e^{-i(\beta_{sp} r - \pi/2)}\, h_2\,(n(\beta_{sp},z))\, h_2\,(n(\beta_{sp},s)) \tag{85}$$

for refracted wave that have contacted the caustic. Here

$$K_3 = \frac{q}{24\, i\, \lambda^{2/3}}\, \frac{1}{\sqrt{g_z(\beta_{sp},z)}}\, \frac{1}{\sqrt{g_z(\beta_{sp},s)}}\, \frac{2\beta_{sp}}{\pi r} \quad . \tag{86}$$

The second problem, an expression valid in region 7, the shadow, can also be circumvented. Examination of Equations (84) and (85) the expressions valid in region 6 shows that these expression become in finite at the caustic, where

$$\frac{\partial^2\phi_4}{\partial\beta^2} = \frac{\partial^2\phi_5}{\partial\beta^2} = 0 \quad . \tag{87}$$

This result is easily understood by realizing that the refracted rays are given by $r = F(s,\beta) + F(z,\beta)$, the same as Equation (75) expressed in F. Recall that the caustic is defined by the largest radius that can be obtained for fixed observer height, z, and source height, s, or where $\partial r/\partial\beta = 0$, thus yielding the above expression. This singularity, in the mathematical sense, results from expanding the argument of the exponential terms in the saddle point method in a Taylor series but retaining only second terms, which are zero in this case. In the physical sense it arises from the ray tube area going to zero and conservation of energy. A result valid near the caustic has been obtained by Sachs and Silbiger [20]. Using their approach, which essentially

involves expanding the exponential terms about the ray tangent to the caustic rather than the saddle point, yields the expression

$$G_R = 2\ K_3(\beta_c)\ \left(\frac{2}{\phi'''(\beta_c)}\right)^{1/2} e^{-i(\ c^r - \frac{\pi}{4})}\ \mathrm{Ai}\ \left(\left(\frac{2}{\phi'''(\beta_c)}\right)^{1/3} \Delta r\right) \cdot$$

$$h_2\ (n(\beta_c,z))\ h_2\ (n(\beta_c,s)) \tag{88}$$

where β_c is the root of

$$\phi_4''\ (\beta_c) = 0 \tag{89}$$

which is valid near the caustic and on both the "illuminated" and the shadow side of it. Here

$$\Delta r = r - r_c \tag{90}$$

where the caustic radius

$$r_c = -\ \phi'\ (\beta_c)\ . \tag{91}$$

The applicability of Equation (88) is restricted not only to large frequencies, as we pointed out in the beginning of the discussion, but also to the vicinity of the caustic. Above the caustic, the range where Equation (88) is applicable is determined by a numerical matching between Equation (88) and the governing equations for the adjacent regions. In the shadow region, the criteria of the range of validity are not quite clear at the present time and will be left as a subject for the future study.

CHAPTER V

PROGRAM CONTENT

With the results developed in the previous sections, we can now proceed to implement them with a computer program. It is hoped that this will enable us to examine thoroughly the behavior of sound intensity under the effect of thermal inhomogeneity, and as a result provide a better prediction scheme in the future. This program carries out the necessary procedures in the appropriate order, and its contents are described in the following.

The first step is to determine at which region the acoustic receiver resides. This is done by first evaluating the corresponding boundaries at the height of the receiver. There are four boundaries that separate the physical space into seven different regions, with each region characterized by two different rays as shown in Figure 1. Their governing equations are given as follows:

$$\text{Boundary I:} \quad B_I = F(z,0) \ . \tag{92}$$

This is the ray whose initial angle is zero, or at an angle parallel to the horizontal.

$$\text{Boundary II:} \quad B_{II} = F(z,\theta_{S_I}) + F(s,\theta_{S_{II}}) \ . \tag{93}$$

This is the ray with its turning point at the ground ($z = 0$). Here θ_S corresponds to the initial angle at the source. $\theta_{S_{II}}$ is obtained

from the fact that at the turning point

$$Az + B = 0 \tag{94}$$

or

$$B = 0 \tag{95}$$

where A and B are defined as before in Equation (10). Carrying out the mathematics we find that the angle

$$\text{Cos } \theta_{S_{II}} = \sqrt{\frac{1 + \alpha s + \Delta T/T}{(1 + \Delta T/T)(1 + \alpha s)}} \tag{96}$$

or in terms of β

$$\beta_{II} = \frac{\omega}{a_\infty}\sqrt{\frac{1}{1 + \Delta T/T}} \quad . \tag{97}$$

$$\text{Boundary III: } B_{III} = F(s, \theta_{S_{III}}(z)) \quad . \tag{98}$$

This boundary does not represent one single sound ray but rather the locus of all the turning points between the source and the ground. This is determined by the same equation that governs boundary II

$$Az + B = 0 \tag{94}$$

except that z now is varied depending upon the height in interest. Carrying out the appropriate steps gives

$$\text{Cos } \theta_{S_{III}}(z) = \sqrt{\frac{1 + \alpha z}{1 + \alpha z + \Delta T/T} \cdot \frac{1 + \alpha s + \Delta T/T}{1 + \alpha s}} \tag{99}$$

the wave, having a turning point above the receiver which we have ignored. Nevertheless, because of the reflective index $R_0(\beta)$, which involves complex value $g^{3/2}(z,\beta)$, its derivatives have to be evaluated properly. Besides, it is very likely that this will be found to be useful if any further study of the approximation scheme is desired. As a result of choosing this particular branch cut, $\sqrt{-1}$ is now being taken as -i and $\ln(-1)$ is equal to -1π instead of $i\pi$. In terms of Cartesian coordinates, the branch cut has shifted from the negative X-axis to the positive Y-axis for this purpose. All these modifications have to be taken into consideration in the programming process.

Table 1 summarizes all the subroutine and functions being facilitated in this program.

TABLE 1

Subroutines and Functions

SUBROUTINES	
Name	Function
FINREG	Finding the region at which the receiver locates.
FINDIR	Finding the saddle point that corresponds to the direct wave.
FINRFL	Finding the saddle point that correspond to the reflected wave.
FINRFC	Finding the saddle point that corresponds to the refracted wave.
INTEG	Evaluating the pressure at the receiver's location.
EVALB4	Evaluating the location of boundary.
ROOT	Root finding routine using the secant method.
HKFCT	Evaluating the modified Hankel functions.

FUNCTIONS	
Name	Function
FNRAY	Evaluating the $F(z,\theta_s)$ function.
G32	Evaluating the $g^{3/2}(z,\beta)$ function.
G32PI	Evaluating the first derivative of $g^{3/2}(z,\beta)$ with respect to β.
G32PI2	Evaluating the second derivative of $g^{3/2}(z,\beta)$ with respect to β.
G32PI3	Evaluating the third derivative of $g^{3/2}(z,\beta)$ with respect to β.
GPIZ	Evaluating the first derivative of $g^{3/2}(z,\beta)$ with respect to α.
GPIZ2	Evaluating the second derivative of $g^{3/2}(z,\beta)$ with respect to αz.
CG32	Complex version of G32.
CGPIZ	Complex version of GPIZ.

CHAPTER VI

DISCUSSION OF RESULTS

Numerical evaluation of the solution for the propagation of sound waves in a thermally stratified medium has been performed on a digitial computer. Plots of results can be found at the end of this section. Surface impedance values given by Chessel's relationship [5] for grass have been used, with specific flow resistance chosen as 300 cgs units. Speed of sound high above the ground ($z \to \infty$) is chosen as 340 m/s, the standard atmospheric condition. The sound source has been chosen to be 3 meters above the surface with an arbitrary strength of unity for simplicity. These values remain constant throughout the entire calculation. The various parameters considered for examination of their effects on sound propagation are the angular frequency ω, the temperature parameters α and $\Delta T/T$, which correspond to the vertical scale of temperature, respectively. ω is chosen to be in the range between 10,000 and 15,000 rad/sec. Using data obtained by NASA [21] and by Butterworth [22] and fitting these data to the temperature profile described in Equation (1), typical values of α are found to range from 1.2 to 5.9 m^{-1} and $\Delta T/T$ from 0.0032 to 0.342 for the lapse conditions. The values used for examinations are based on the above range of variation.

Figure 1 depicts the formation of regions in physical space with $\alpha = 2.5\ m^{-1}$, $\Delta T/T = 0.025$, and $S = 3$ m. With this figure as the refer-

ent, we can see from Figures 7 through 10 that the variation of the temperature parameters α and $\Delta T/T$ resulted in shifting the relative locations of the regions. This may result in switching from one governing equation to another as discussed in Chapter III but appears to have little effect on the general nature of the solution.

Figure 10 through 20 are plots of sound pressure level (with an arbitrary reference) versus elevation at radii of 20, 40 and 80 m. Figures 10 to 12 are intended as the referent as parameters are varied in other drawings; they are for values of $\Delta T/T = 0.25$, $\alpha = 2.5\ m^{-1}$, S = 3 m, the same conditions as the ray diagram of Figure 1, and frequency of about 1600 Hz (w = 10,000 rad/sec.)

At r 20 m, Figure 10 shows a rather normal looking interference pattern with a mean sound level of about 32 dB. This radius is sufficiently close to the source that most of the acoustic energy is contributed from the direct and reflected waves; only waves leaving the source at very shallow angles are refracted upward before reaching the ground (see Figure 1). The regions of Figure 1 are indicated on Figure 10 for reference. The oscillations, in this interference pattern, slowly increase in amplitude as it moves away from the source height. This is due to the behavior of the strength of the reflected wave as shown in Figure 21. One conspicuous feature noticed in Figure 10 is the dramatic drop of sound level occurs at location near the source height S = 3 m; this violates our intuition that a higher sound level at that location should be experienced instead. This peculiar behavior near the source height and at small radii turned out to be the characteristic of the solution. Carefully examining the ray diagram in Figure 22, which is plotted with the rays emitted in equal angular interval,

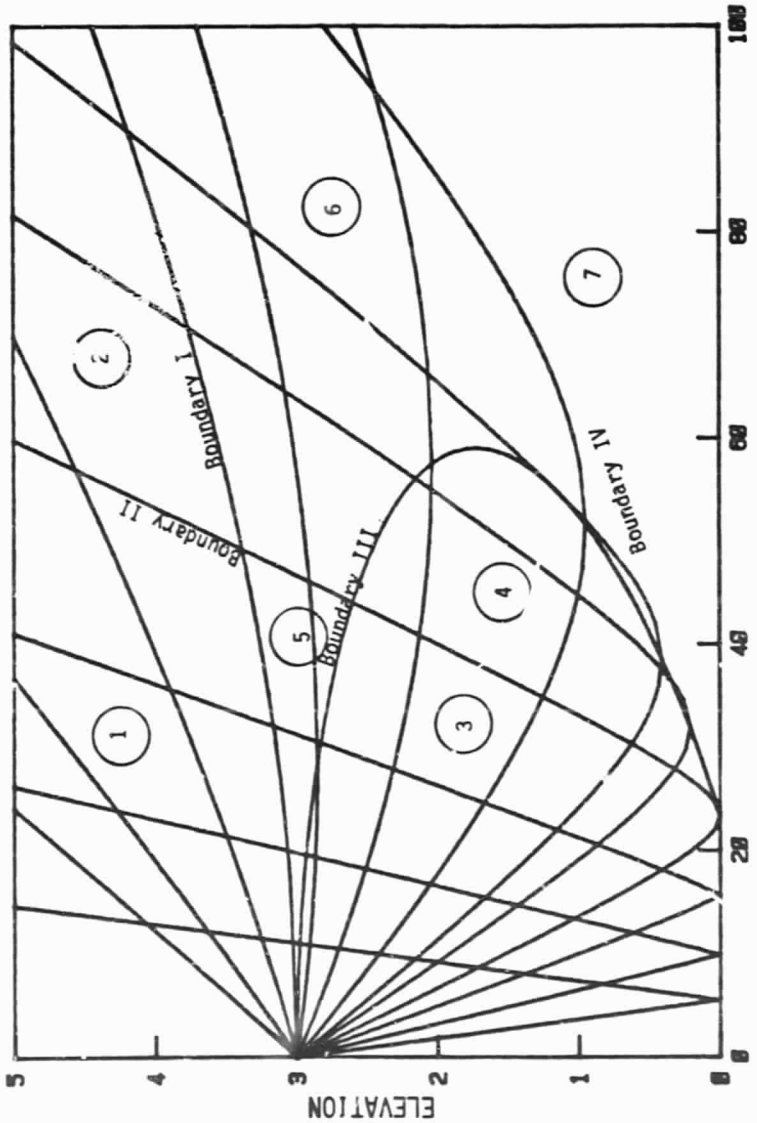

Figure 7. Ray tracing diagram for s = 3 m, α = 3.5 m^{-1} and $\Delta T/T$ = 0.025.

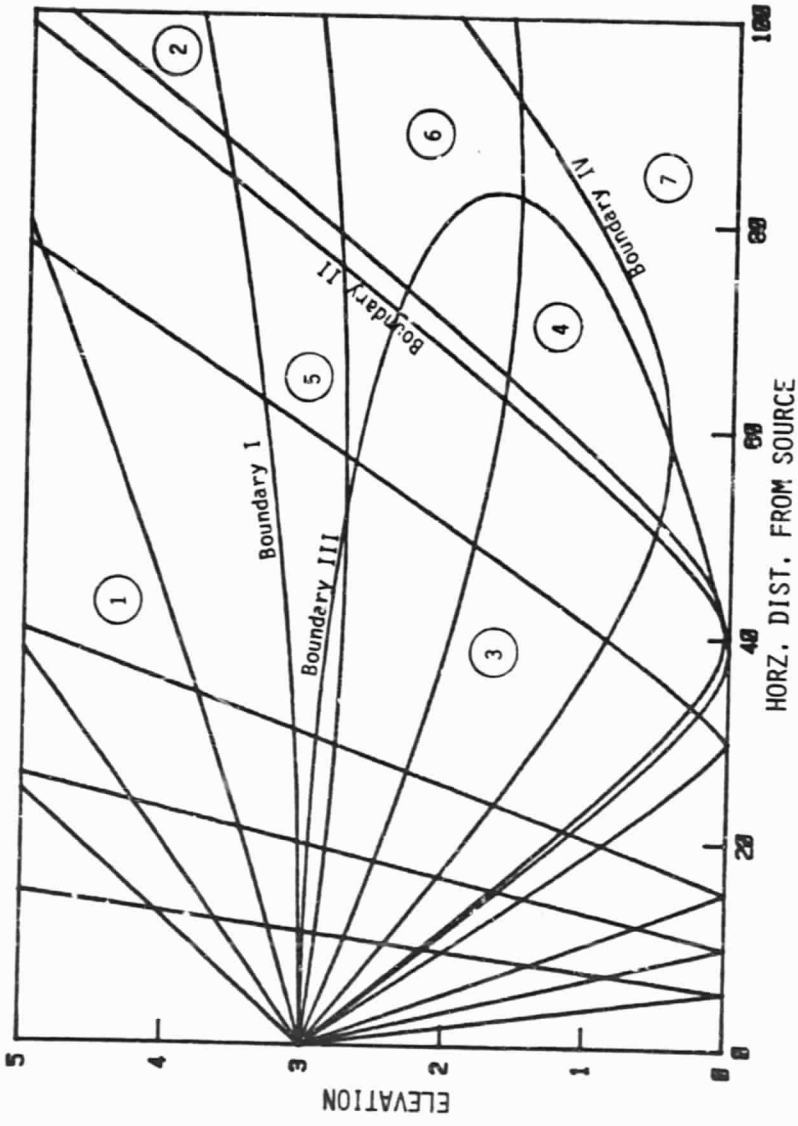

Figure 8. Ray tracing diagram for s = 3 m, α = 2.5 m^{-1} and $\Delta T/T$ = 0.01.

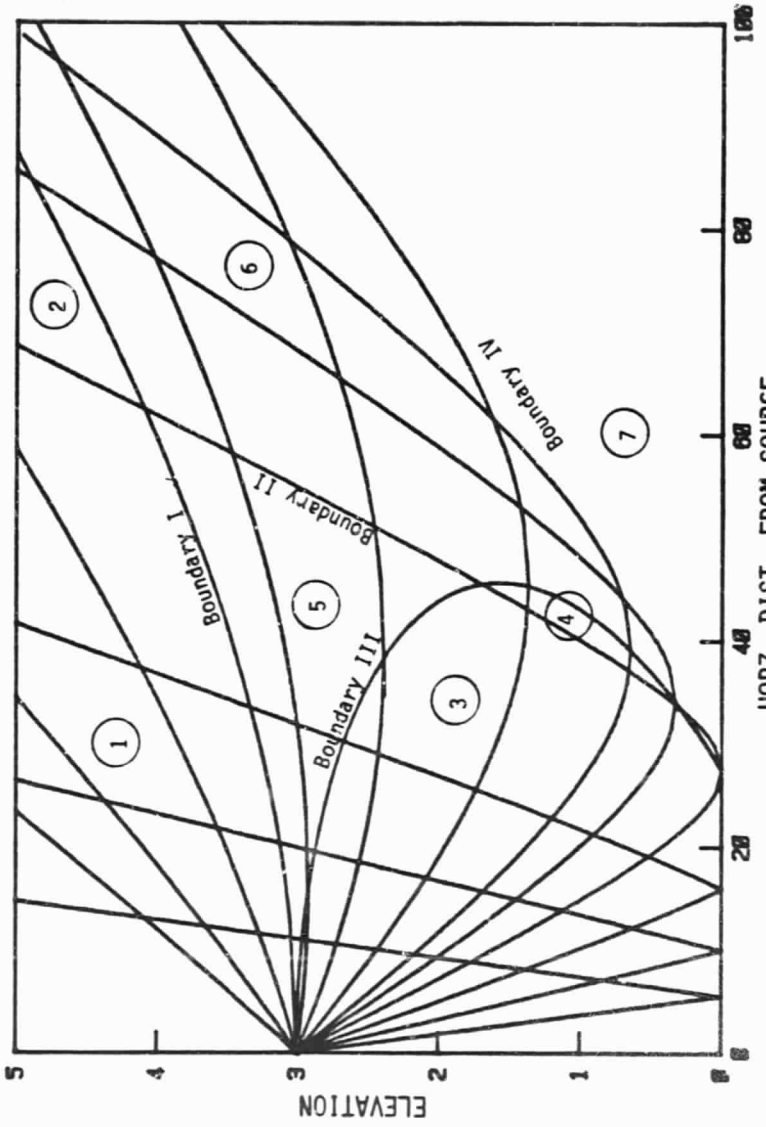

Figure 9. Ray tracing diagram for s = 3 m, α = 1.5 m^{-1} and $\Delta T/T$ = 0.025.

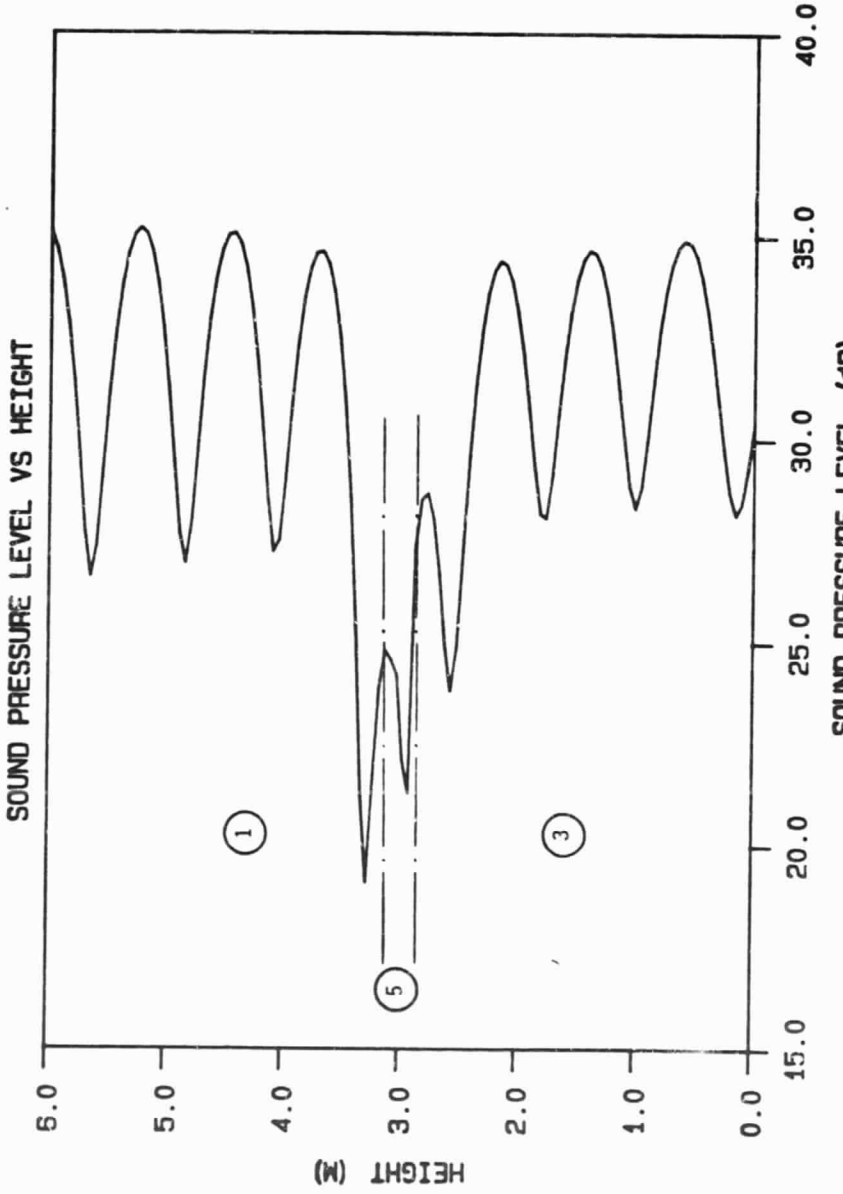

Figure 10. SPL vs HEIGHT at r = 20 m, α = 1.5 m^{-1} $\Delta T/T$ = 0.025, and ω = 10,000 rad/sec.

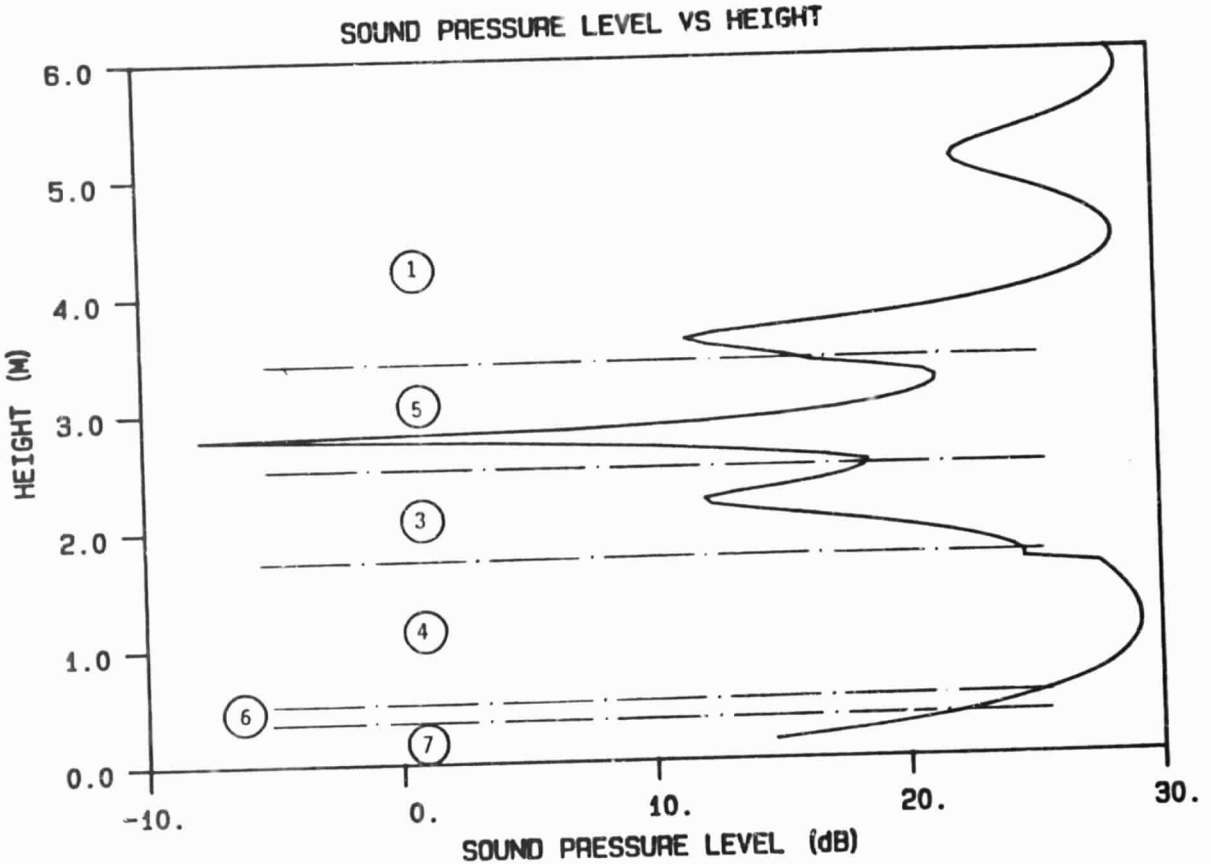

Figure 11. SPL vs HEIGHT at r = 40 m, α = 1.5 m^{-1} $\Delta T/T$ = 0.025, and ω = 10,000 rad/sec.

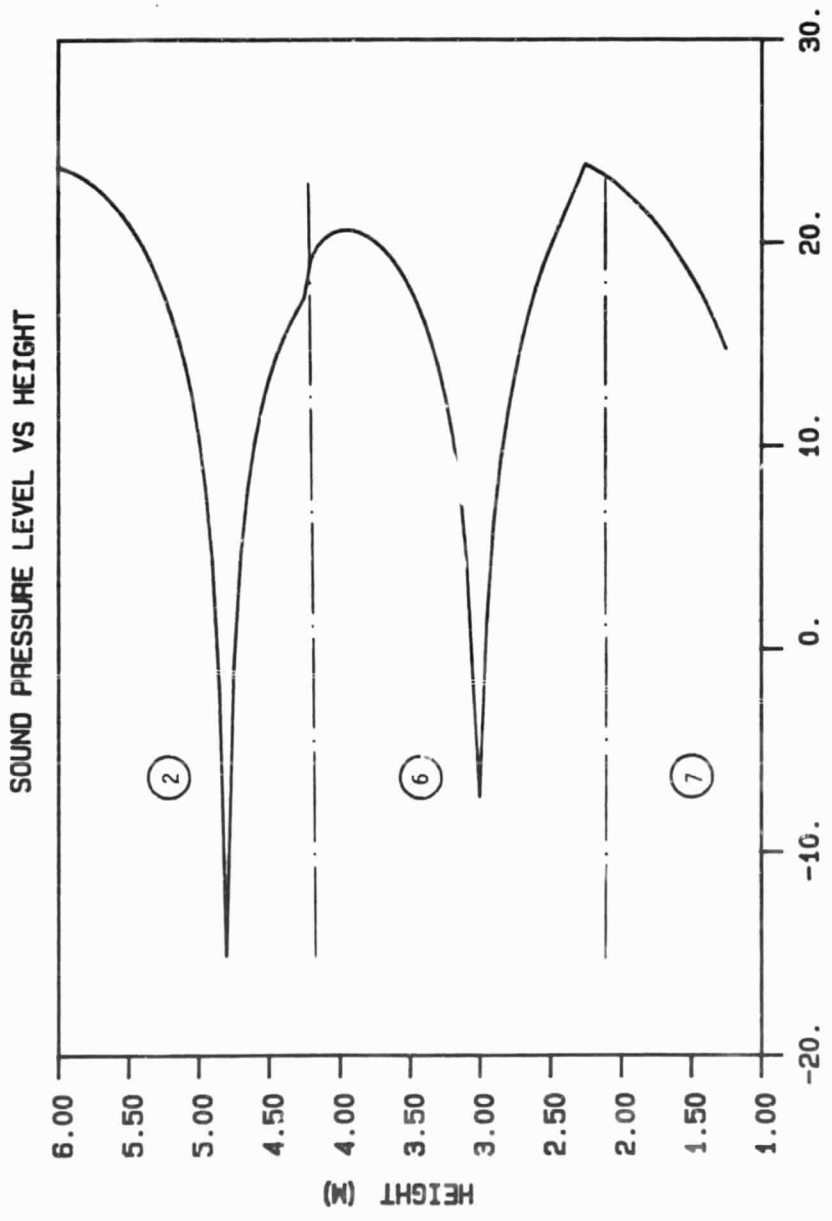

Figure 12. SPL vs HEIGHT at $r = 80$ m, $\alpha = 2.5$ m^{-1}
$\Delta T/T = 0.025$, and $\omega = 10,000$ rad/sec.

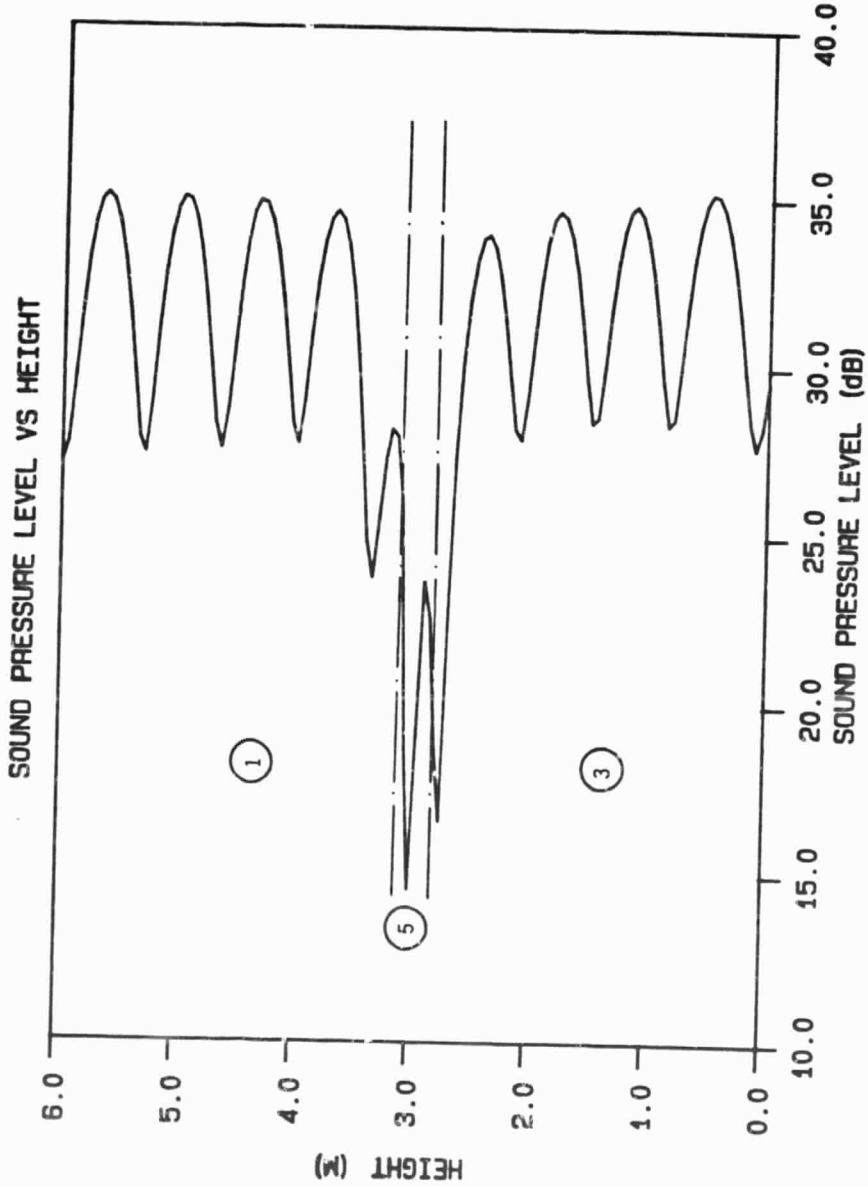

Figure 13. SPL vs HEIGHT at r = 20 m, α = 2.5 m^{-1}
$\Delta T/T$ = 0.025, and ω = 12,000 rad/sec.

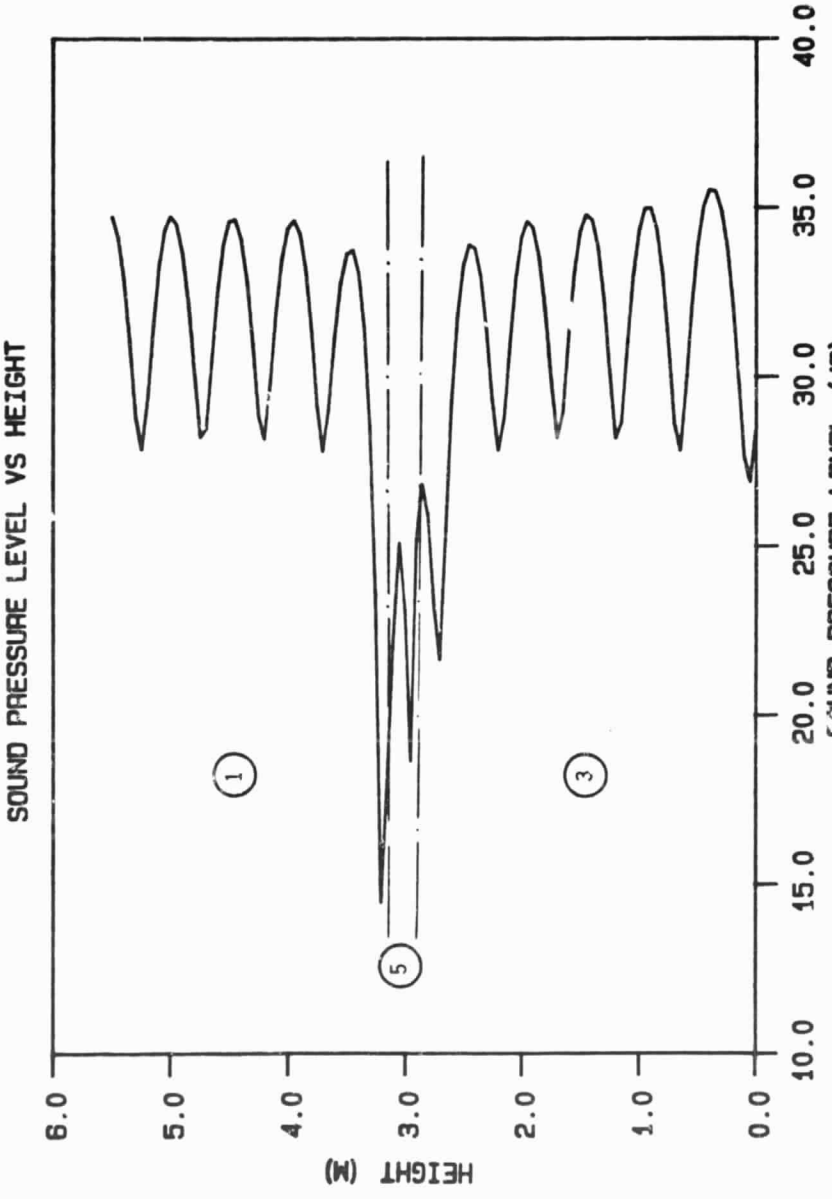

Figure 14. SPL vs HEIGHT at r = 20 m, α = 2.5 m^{-1}
$\Delta T/T$ = 0.025, and ω = 15,000 rad/sec.

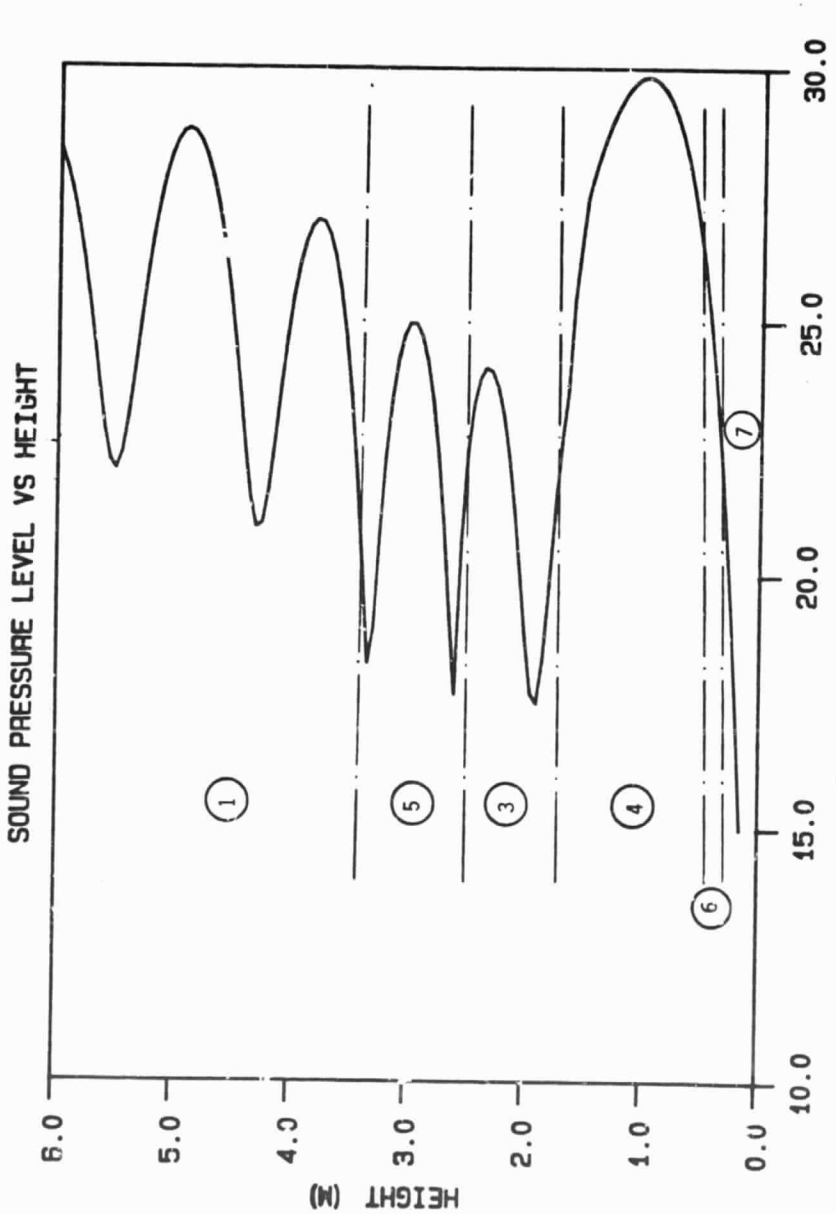

Figure 15. SPL vs HEIGHT at $r = 40$ m, $\alpha = 2.5$ m^{-1}
$\Delta T/T = 0.025$, and $\omega = 12{,}000$ rad/sec.

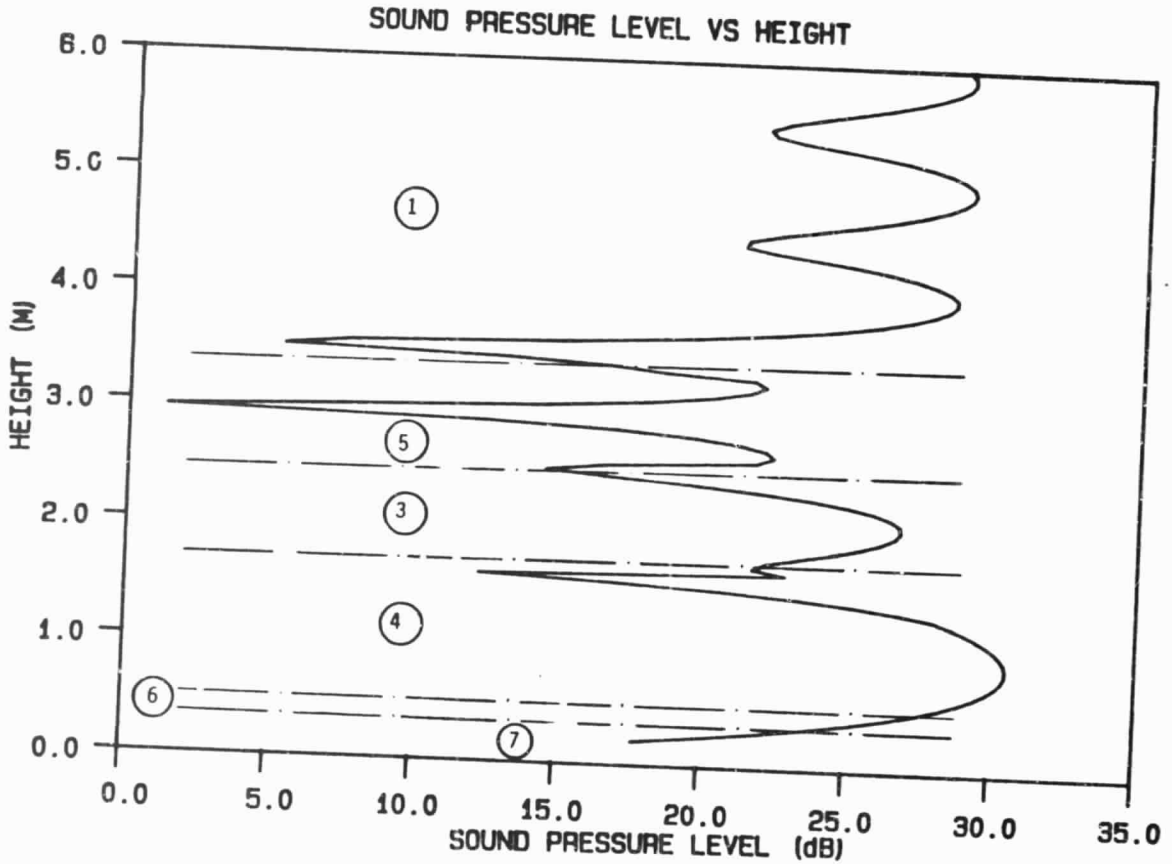

Figure 16. SPL vs HEIGHT at r = 40 m, α = 2.5 m^{-1} $\Delta T/T$ = 0.025, and ω = 15,000 rad/sec.

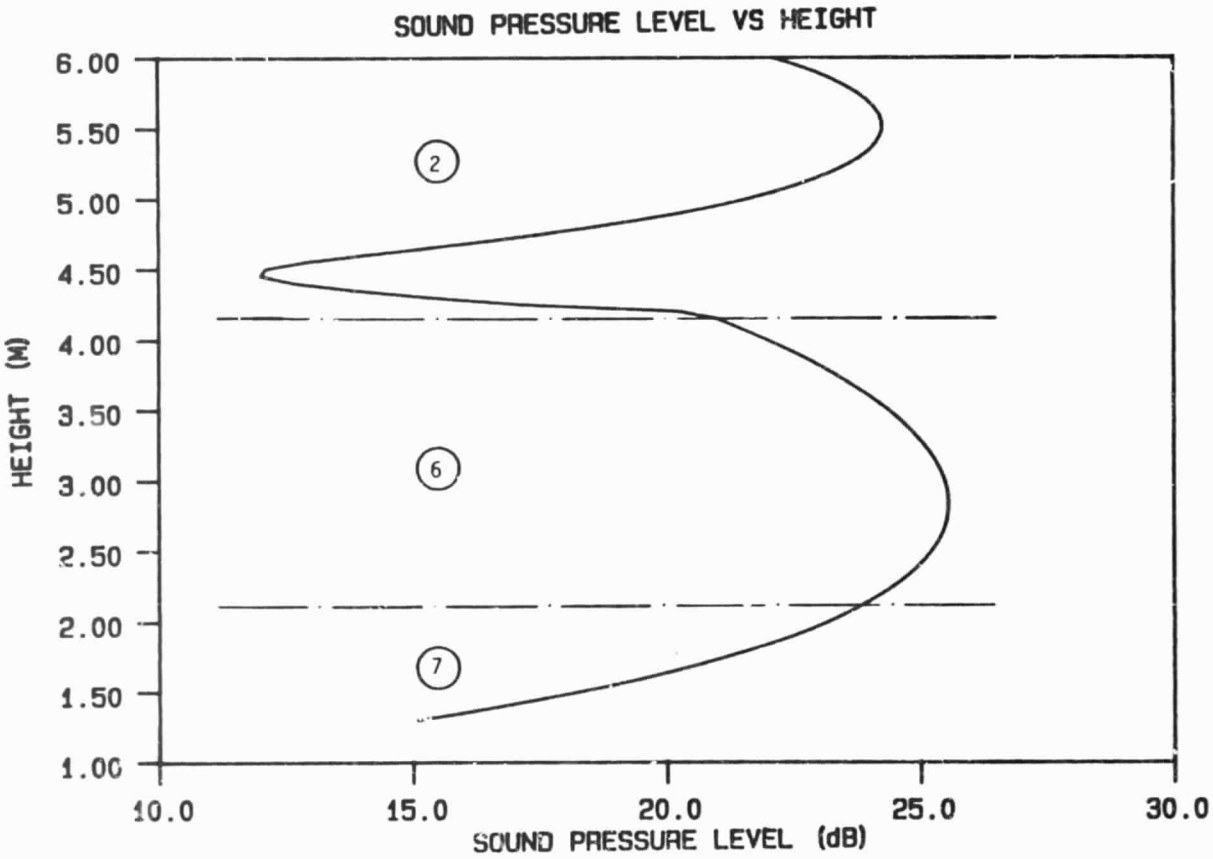

Figure 17. SPL vs HEIGHT at r = 80 m, α = 2.5 m^{-1} $\Delta T/T$ = 0.025, and ω = 12,000 rad/sec.

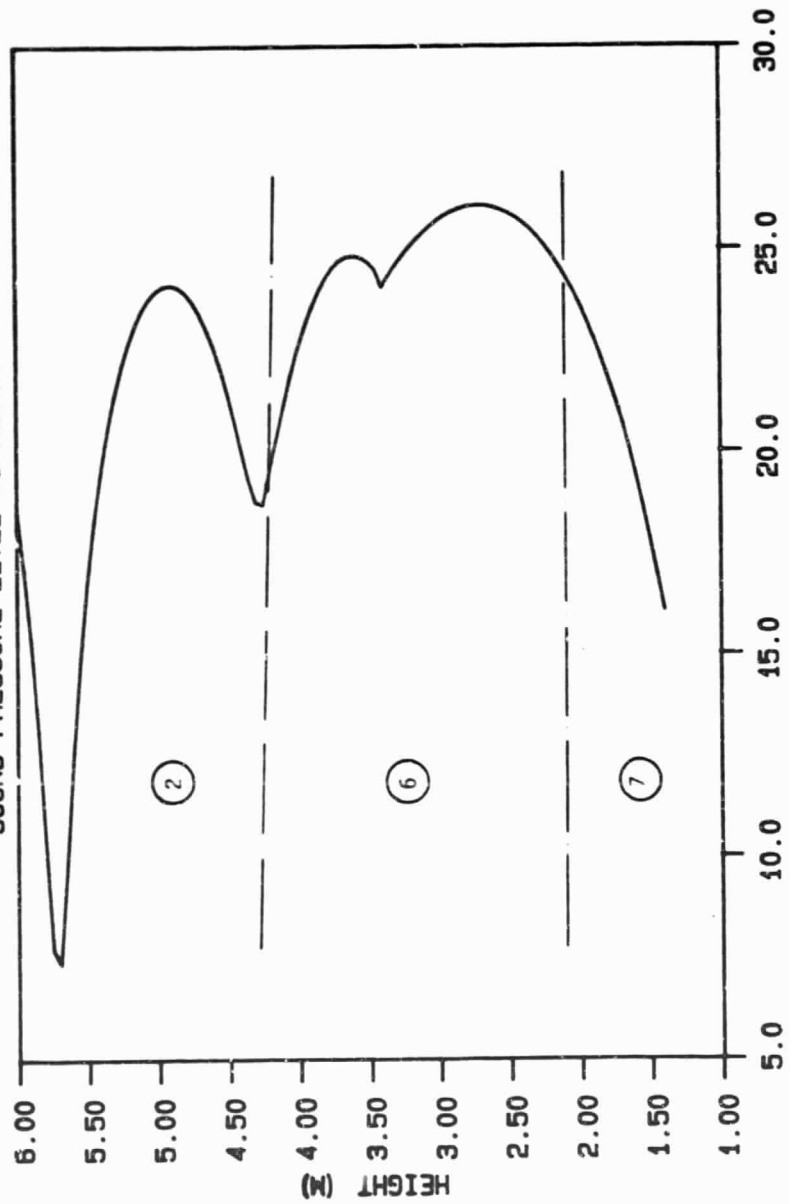

Figure 18. SPL vs HEIGHT at r = 80 m. α = 2.5 m^{-1}
$\Delta T/T$ = 0.025, and ω = 15,000 rad/sec.

C - 2

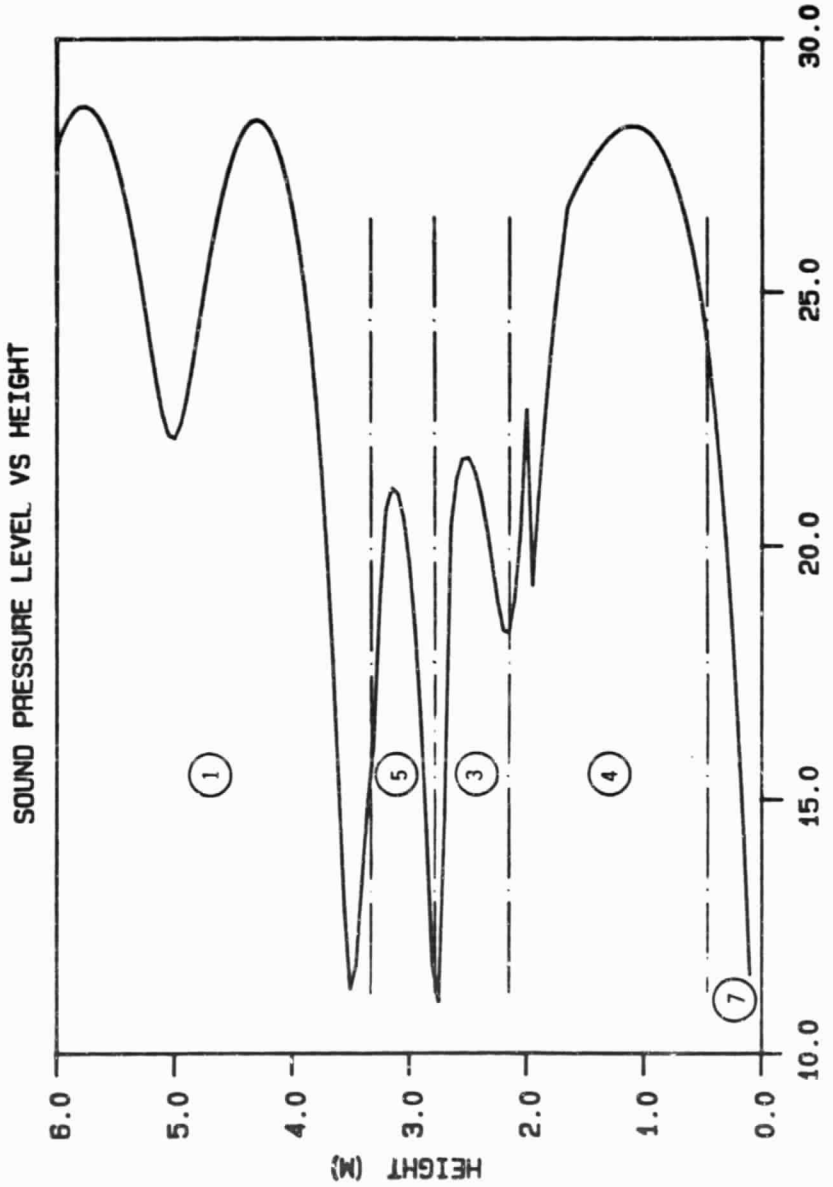

Figure 19. SPL vs HEIGHT at $r = 40$ m, $\alpha = 3.5\ m^{-1}$
$\Delta T/T = 0.025$, and $\omega = 10{,}000$ rad/sec.

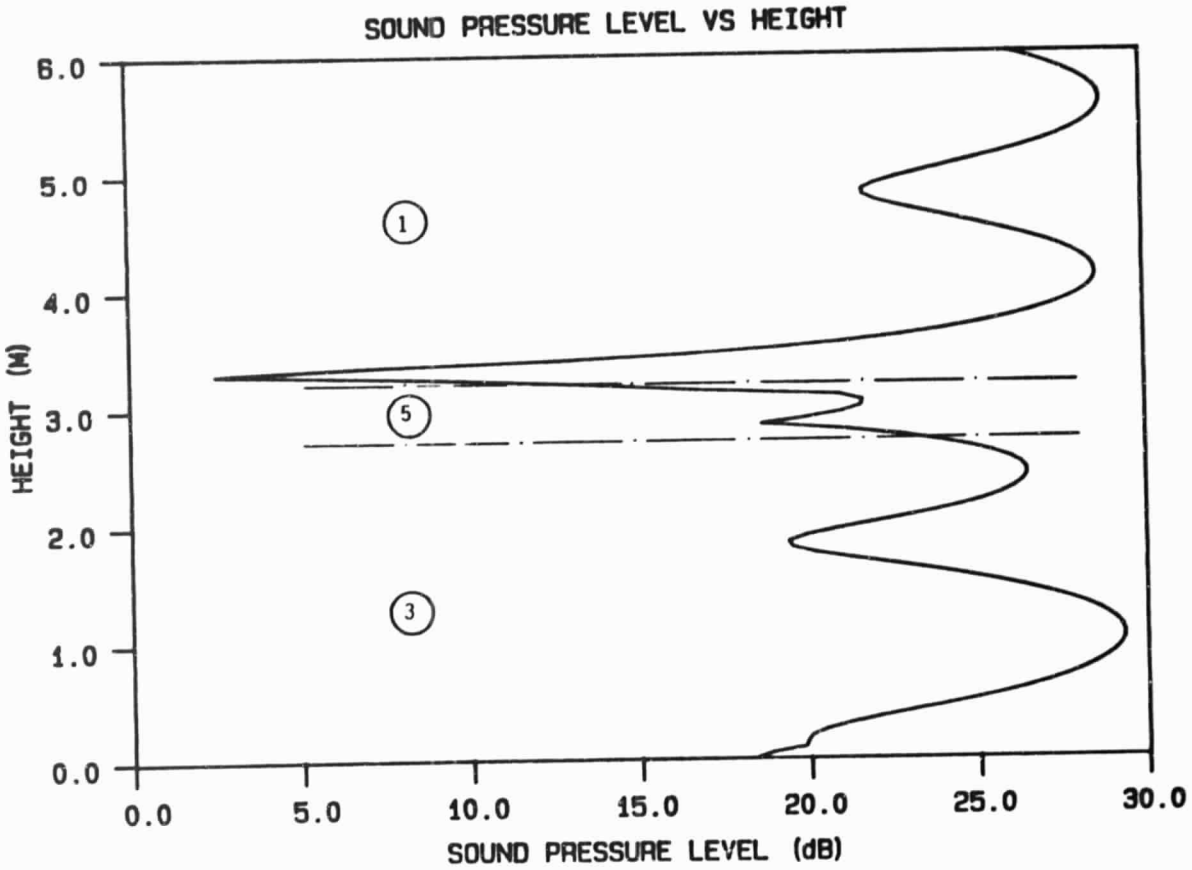

Figure 20. SPL vs HEIGHT at r = 40 m, α = 2.5 m^{-1} $\Delta T/T$ = 0.01, and ω = 10,000 rad/sec.

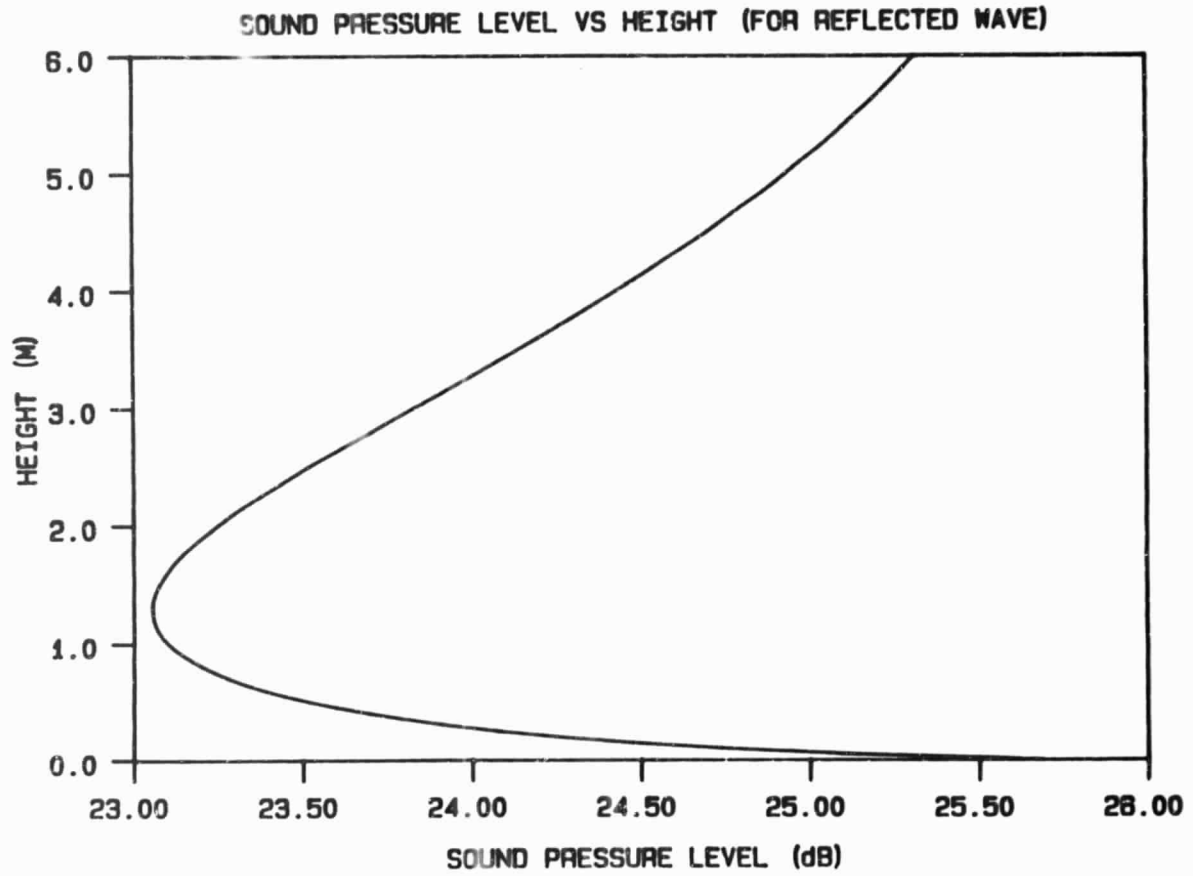

Figure 21. Sound pressure level vs height for reflected wave.

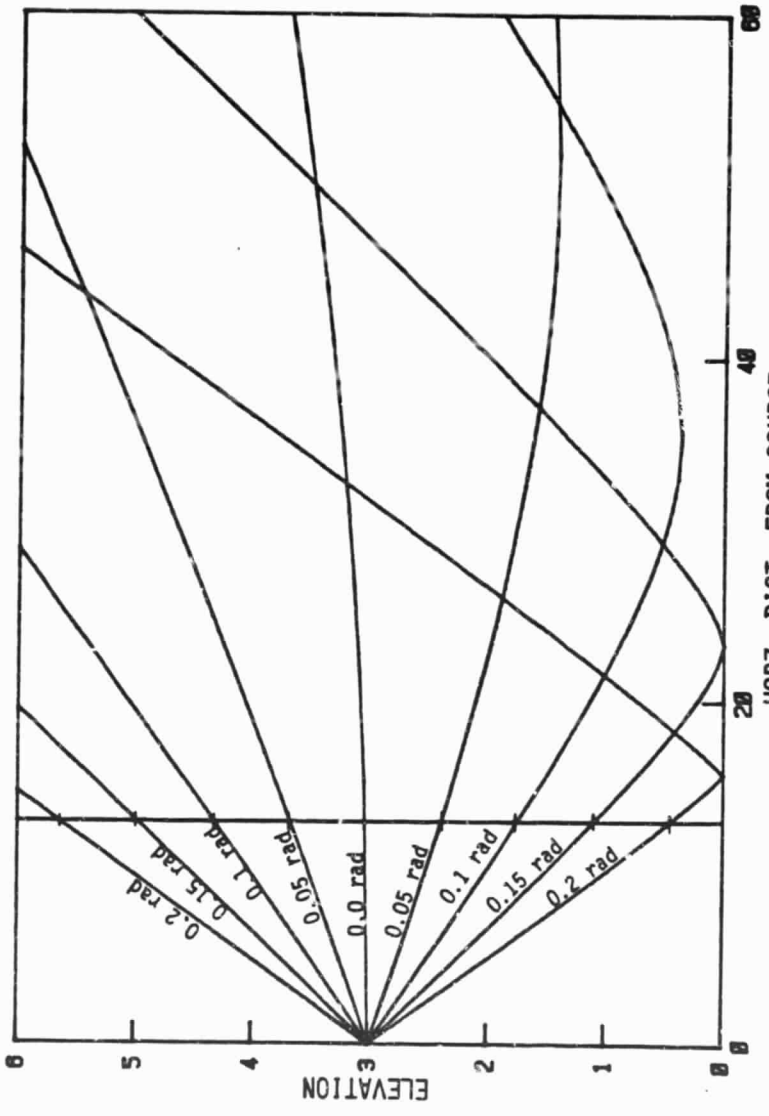

Figure 22. Ray diagram with rays emitted in equal angular intervals.

we noticed that the perpendicular distance between rays is further apart at this location than anywhere else at the same radius. If the equal acoustic energy is assumed to be present between rays, a location with a large distance between rays should be a region of low acoustic pressure. With this argument, the low sound level which occurs in the locations near the source height can then be accounted for.

Figure 11 is a similar plot at r = 40 m. At this radius, the receiver has traversed a number of different regions and this accounts for the irregular interference pattern in the result. The mean sound level in this interference is about 26 dB, 6 dB less than the mean on the previous plot, as is expected. Near the source height a large drop of pressure takes place due to the ray spreading discussed above. One interesting feature observed from this plot is that the peak pressure occurs not on the caustic itself, as would be expected from the ray acoustics, but rather at some distance above it. In the shadow zone, the field is decaying exponentially with increasing distance from the caustic boundary. This is due to the diffraction effects which occur anytime a wavefront cross section is limited in some manner. In this case it is limited by an inability to penetrate the caustic boundary. This phenomenon is explained by the Huygen's principle discussed in some acoustic texts, Reference [15], for example. This particular location of the peak pressure and the decaying behavior can be seen in all the plots where there is a shadow region. At a height of about 1.6 m a discontinuity occurs in the sound for the integral level. This results from the higher approximation we used in the vicinity of the caustic boundary than the one for other locations.

Figure 12 is plotted at r = 80 m. Note that the height scale

does not continue to the ground at z = 0. It is because the approximation, Equation (88), we use in the vicinity of the causic is not valid for the entire shadow region as discussed in Chapter IV. Again the regions of Figure 1 are shown on the plot. Here, discontinuities in slope occur at about 4.2 and 2.2 m. The first is at the boundary between the direct and the refracted waves, resulting from the approximation error, and the second is accounted for by the numerical matching which has deliberately forced the solutions to be continuous in magnitude but not in slope. Again the mean sound level has decreased about 6 dB to near 20 dB with the doubling of the distance from the source as compared to the previous figure.

Figures 13 to 18 are plotted with the same parameters as the referent figures except that higher frequencies at ω = 12,000 rad/sec (f = 1,910 Hz) and ω = 15,000 rad/sec (f = 2,390 Hz) have been used. From these results, we found the increases in the frequency of the sound source have little effect on the general behavior of the sound level rather than an increased oscillation in the interference pattern. Plots with different temperature parameters α and $\Delta T/T$ can also be found in Figures 19 and 20.

Figure 23 is a plot of sound level versus horizontal distance from the source. Again the regions of Figure 1 are shown along with the empirical model of Wiener and Keast [23]. The Wiener and Keast model suggests that a simple source model (corrected for atmospheric absorption which is not present here) yields the sound level between the source and shadow boundary. A simple source model represents a direct wave propagating out from the source in a homogenous medium with its attenuation accouting only for the geometrical spreading.

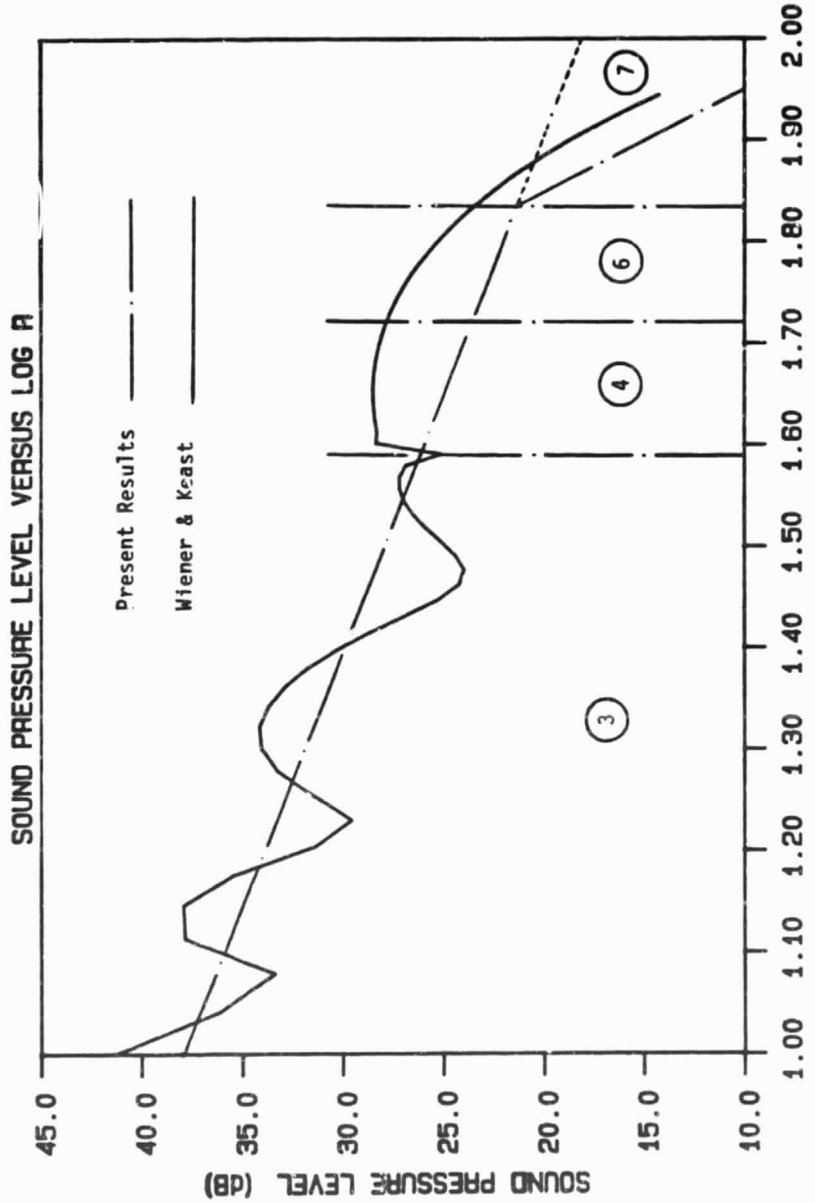

Figure 23. Sound pressure level vs log (R).

Thus, no interference pattern can be produced in this model but only the local mean sound level. Beyond the shadow boundary an empirically obtained excess attentuation is applied to the simple source model. This empirical model, based on the experimental data collected by Wiener and Keast, shows a good agreement with the local mean sound level in the interference region and good agreement with the slope of the decay of the sound level in the shadow region. The Wiener and Keast model would be in better agreement with the present model in the shadow region if we applied the excess attenuation at the radial location where the sound level starts falling below the simple source value rather than at the actual shadow boundary where the sound level is always greater than the simple source. Figure 24 compares the excess attenuation seen in this case with the model of Wiener and Keast. Note that if Wiener and Keast did not correctly determine the shadow location the "constant" difference between their model and the present model would be accounted for. Thus, the best experimental data currently available, which are summarized in the Wiener and Keast model, appear to be in good agreement with the present model.

There are some mathematical difficulties in the present model even though it gives remarkable results. These results arise from the asymptotic behavior of the Hankel functions which restrict their arguments from being too large or when overflow occurs during calculation. In the present case, the arguments of the Hankel functions involve the $g^{3/2}(z,\beta,)$ and λ, or $(\omega/a\alpha)$, terms; thus variation of any of these variables z, β, ω, a, and α can result in too big a value for the Hankel function subroutine to handle, which in turn will appear as an overflow error in the computer program. As far as this program is concerned, the

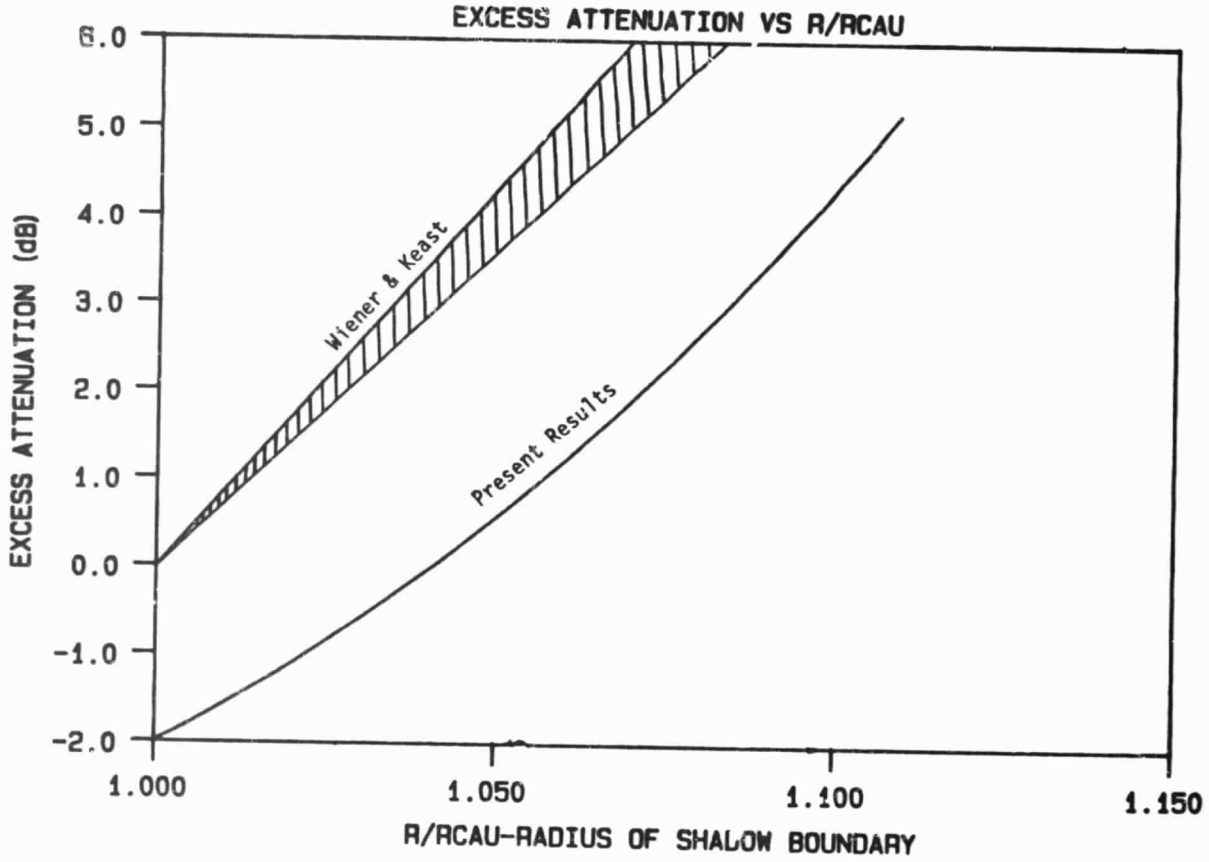

Figure 24. Comparison between the Wiener and Keast model and the present model for the excess attentuation in the shadow region.

upper limit for the argument of the Hankel function is a magnitude of about 27. The range of ω and α has been discussed in a previous paragraph; and since a in practice does not vary significantly, the question remains on finding the range of the variables z and β for which the Hankel function can be evaluated properly. In doing so, it is necessary to first examine the behavior of the $g^{3/2}(z,\beta)$ function with respect to its arguments z and β. It is found that this function increases with increasing z and decreasing β and vice versa. Since z and β represent the height of receiver and the initial angle of the sound ray ($\beta_s = (\omega/a_\infty)\sqrt{(1 + \alpha s)/(1 + \alpha s + \Delta T/T)\cos\theta_s}$) that reaches the receiver, respectively, their limits actually form a boundary in the physical space beyond that which the Hankel function cannot be evaluated. For example, with λ set equal to 11.8 rad and a height of 5 meters above the ground, the minimum horizontal distance r from the sound source is around 10 meters. At radii below this the problem will occur. The limit of r rather than β is used because the saddle point β is totally depended on the location of the receiver specified by z and r, which are the input data for the computer program. On the other hand, in tracing the height along a constant radius of 40 meters, we found the maximum value of z is about 10 meters. Beyond that, an error will occur. Fortuitously, the locations corresponding to these large arguments are usually of no significant interet; they are places either in the close vicinity of the sound source or very high above it.

CHAPTER VII

CONCLUSION

A model of acoustic propagation in a thermally inhomogeneous medium has been developed by Van Moorhem and numerically implemented on a Vax computer at the University of Utah. The temperature profile considered is a lapse condition, with temperature decreases in height, along with a finite impedance ground surface using Chessel's model. The results appear to be in good agreement with the empirical model of Wiener and Keast, which by far, has the most reliable experimental data available. Yet further improvement is necessary for the present model. Poles that may occur in the integration process which are believed to lead to a surface wave term have not been considered here. Also the behavior of sound propagation in the shadow region far away from the caustic is yet to be examined. Investigation of these two subjects has been undertaken by Yiping Ma [24] and their resolutions are expected to be available in the near future.

APPENDIX

PROGRAM ACOUSTICS AND ITS USAGE

This FORTRAN program carries out the numerical calculations as discussed in the preceding sections. It was written on the VAX/VMS system at the Mechanical Engineering Department of the University of Utah. With the input of the receiver's location along with the appropriate parameters, the program will evaluate the corresponding sound pressure level. Except for the location of the receiver, all the other parameters are assigned with default values which are commonly used. The command 'namelist' is used to provide a convenient way to specify changes in the parameters of concern. The default values are assigned as follows

Mathematical Variable	FORTRAN Variable	Default Value
a	SPEED	340 m/s
$\Delta T/T$	DTOT	0.025
ω	OMEGA	10,000 Hz
α	ALPHA	2.5 m^{-1}

In order to execute the program, simply type in 'RUN ACOUSTIC' followed by the changes of defaulted parameters if desired.

Example:
```
$RUN ACOUSTIC
 $VALUES
 $END
```

The above commands will initiate the execution of the program using the default values since no changes are specified.

Example 2:

```
$RUN ACOUSTIC
 $VALUES
 OMEGA = 15000.
 ALPHA = 2.5
 $END
```

The above commands will initiate the execution of the program substituting OMEGA = 15,000.0 and ALPHA = 3.0 for their default values. The program will then ask for the location of the receiver and the number of points that need to be evaluated. Here 'ELEV' is the height and 'HDIST' is the horizontal distance of the receiver's location. 'RLOW' is the lower limit of the height to be evaluated and 'NO' is the number of values calculated between 'ELEV' and 'RLOW.'

Example 3.

```
ENTER  INPUT  ELEV.  HDIST:
5.0, 20.0

ENTER  INPUT  RLOW, NO:
0.0, 100
```

These input values will enable the program to evaluate the receiver's location from 5.0 meters to ground (0.0 meter) along a constant radius of 20.0 meters with intervals of 5.0/100 or 0.02 meters. If only one point in space is being evaluated, 'RLOW' will be the same as 'ELEV' and NO will be 1.

All calculations are performed in double precision arithmetic.

After the program has carried out the entire calculation, a result of sound pressure level versus height will store in a data file named 'FOR026.' A program named 'MGRAPH' is available and recommended for a quick view of the plot of the result if the user runs this program

on the same system as it the program was written. A copy of program ACOUSTIC can be found in the remainder of this appendix.

```
      PROGRAM ACOUSTIC
C
C
C     ***  THIS PROGRAM DETERMINES THE SOUND PRESSURE AT ANY  ***
C     ***  GIVEN LOCATION IN A THERMALLY STRATIFIED MEDIUM    ***
C     ***  WITH THE TEMPERATURE PROFILE DISCUSSED IN CHAPTER  ***
C     ***  II.  A NUMBER OF LOCATIONS CAN ALSO BE EVALUATED   ***
C     ***  IN THE EVENT THAT A PLOT OF SOUND PRESSURE LEVEL   ***
C     ***  VERSUS HEIGHT IS DESIRED.                          ***
C
C
      IMPLICIT DOUBLE PRECISION (A-H,O-Z)
      COMPLEX*16 PDIR,PRFL,PRFC1,PRFC2,PCAU,PD(300),PR(300),
     1           RG1(300),RG2(300),PCU(300)
      DIMENSION A(300),SADRFC(2)
      REAL*8 MAG(300)
      INTEGER REGION
      COMMON /ONE/SPEED,OMEGA,ALPHA,DTOT/TWO/S
      NAMELIST /VALUES/SPEED,OMEGA,ALPHA,DTOT,S
C
C
C     ***  VARIABLE USAGES:                                   ***
C     ***                                                     ***
C     ***     S = HEIGHT OF THE SOUND SOURCE'S LOCATION       ***
C     ***     SPEED = SPEED OF SOUND OUTSIDE THE THERMALLY    ***
C     ***             STRATIFIED REGION (AT INFINITE HEIGHT)  ***
C     ***     OMEGA = ANGULAR FREQUENCY                       ***
C     ***     ALPHA = A TEMPERATURE PROFILE PARAMETER         ***
C     ***     DTOT = (DELTA-T)/(T-INFINITY)                   ***
C     ***     ELEV = HEIGHT OF THE RECEIVER'S LOCATION        ***
C     ***     HDIST = HORIZONTAL DISTANCE BETWEEN RECEIVER    ***
C     ***             AND THE POINT SOURCE                    ***
C
C
      S=3.0D+00
      SPEED=3.4D+02
      OMEGA=1.0D+04
      ALPHA=2.5D+00
      DTOT=2.5D-02
      PI=4.0D+00*DATAN(1.0D+00)
C
      READ (5,VALUES)
      PRINT*,'ENTER INPUT ELEV,HDIST:'
      READ*,ELEV,HDIST
C
C     ***  RLOW IS THE LOWER LIMIT OF THE HEIGHT TO BE  ***
C     ***  EVALUATED. (FOR THE CASE THAT A NUMBER OF    ***
C     ***  LOCATIONS NEED TO BE CALCULATED).            ***
C     ***  NO IS THE NUMBER OF VALUES CALCULATED        ***
C     ***  BETWEEN ELEV AND RLOW.                       ***
C
      PRINT*,'ENTER INPUT RLOW,NO:'
      READ*,RLOW,NO
```

```
      PRINT 1
 1    FORMAT ('1')
      IF (NO .EQ. 1)THEN
          RINC=0.0
          GO TO 3
        ENDIF
C
C     ***  RINC IS THE INCREMENT  ***
C
      RINC=(ELEV-RLOW)/(NO-1)
      ELEV=ELEV+RINC
C
C     ***  ICOMP IS A CONTROL STATEMENT FOR THE  ***
C     ***  NUMERICAL MATCHING.                   ***
C
      ICOMP=0
C
 3    DO 200, K=1,NO
C
      ELEV=ELEV-RINC
      PRINT 5, ELEV,HDIST
 5    FORMAT('0','ELEV = ',F7.3,2X,'HDIST = ',F7.3)
      IF (ELEV .LT. 1.E-10)ELEV=0.000001
C
C     ***  FINDING THE REGION AT WHICH THE RECIVER LOCATES  ***
C
      CALL FINREG(S,ELEV,HDIST,REGION)
C
      GO TO (10,20,30,55,50,55,55),REGION
C
C     ***  THE SUBROUTINES ARE NAMED AS FOLLOWS:       ***
C     ***                                              ***
C     ***  FINDIR - FINDING THE SADDLE POINT FOR THE   ***
C     ***           DIRECT WAVE                        ***
C     ***  FINRFL - FINDING THE SADDLE POINT FOR THE   ***
C     ***           REFLECTED WAVE                     ***
C     ***  FINRFC - FINDING THE SADDLE POINT FOR THE   ***
C     ***           REFRACTED WAVE                     ***
C     ***  INTEG - EVALUATING THE SOUND PRESSURE WITH  ***
C     ***          THE EQUATIONS DEVELOPED IN CH. III  ***
C
 10   CALL FINDIR(S,ELEV,HDIST,SADDIR)
      IDEC=1
      CALL INTEG(S,ELEV,HDIST,REGION,SADDIR,PDIR,IDEC)
      PRINT*
      CALL FINRFL(S,ELEV,HDIST,SADRFL)
      IDEC=2
      CALL INTEG(S,ELEV,HDIST,REGION,SADRFL,PRFL,IDEC)
      GO TO 100
C
 20   CALL FINDIR(S,ELEV,HDIST,SADDIR)
      IDEC=1
      CALL INTEG(S,ELEV,HDIST,REGION,SADDIR,PDIR,IDEC)
```

```
      PRINT*
      CALL FINRFC(S,ELEV,HDIST,REGION,SADRFC)
      IDEC=2
      CALL INTEG(S,ELEV,HDIST,REGION,SADRFC(1),PRFC1,IDEC)
C
C     ***  NUMERICAL MATCHING FOR THE APPROXIMATED SOLUTIONS  ***
C     ***  BETWEEN REGION 2 AND THE SHADOW REGION             ***
C
      IF (REGION .EQ. 4) THEN
      ORIG=DSQRT(DREAL(PDIR+PRFC1)**2+DIMAG(PDIR+PRFC1)**2)
      RMOD=DSQRT(DREAL(PCAU)**2+DIMAG(PCAU)**2)
      ERPCT=ABS(ORIG-RMOD)/ORIG
      IF (ERPCT .LT. 0.02) THEN
          IDEC=3
          ICOMP=1
        ENDIF
      ENDIF
      GO TO 100
C
 30   GO TO 10
C
 40   GO TO 55
C
 50   CALL FINRFL(S,ELEV,HDIST,SADRFL)
      IDEC=1
      CALL INTEG(S,ELEV,HDIST,REGION,SADRFL,PRFL,IDEC)
      PRINT*
      CALL FINRFC(S,ELEV,HDIST,REGION,SADRFC)
      IDEC=2
      CALL INTEG(S,ELEV,HDIST,REGION,SADRFC(1),PRFC1,IDEC)
      GO TO 100
C
C     ***  EVALB4 - EVALUATING BOUNDARY IV  ***
C
 55   CALL EVALB4(S,ELEV,ANGLE4,BOUND4)
      SADCAU=(OMEGA/SPEED)*DSQRT((1.+ALPHA*S)/(1.+ALPHA*S+DTOT))*
     1       DCOS(ANGLE4)
      PRTA=G32PI3(S,SADCAU)
      PRTB=G32PI3(ELEV,SADCAU)
      ZETA=(2./(PRTA+PRTB))**(1./3.)
      DELR=HDIST-BOUND4
      ARGU=ABS(ZETA*DELR)**(3./2.)
      GO TO 70
C
 60   CALL FINRFC(S,ELEV,HDIST,REGION,SADRFC)
      IDEC=1
      CALL INTEG(S,ELEV,HDIST,REGION,SADRFC(2),PRFC1,IDEC)
      IDEC=2
      CALL INTEG(S,ELEV,HDIST,REGION,SADRFC(1),PRFC2,IDEC)
C
C     ***  NUMERICAL MATCHING FOR THE APPROXIMATED SOLUTIONS  ***
C     ***  BETWEEN REGION 6 AND THE SHADOW REGION             ***
C
```

```
      ORIG=DSQRT(DREAL(PRFC1+PRFC2)**2+DIMAG(PRFC1+PRFC2)**2)
      RMOD=DSQRT(DREAL(PCAU)**2+DIMAG(PCAU)**2)
      ERPCT=ABS(ORIG-RMOD)/ORIG
      IF (ERPCT .LT. 0.02) THEN
          IDEC=3
          ICOMP=1
        ENDIF
      GO TO 100
C
 70   IF ((REGION .EQ. 7) .AND. (ARGU .GT. 1.0)) THEN
          GO TO 350
        ELSE
          IDEC=3
          CALL INTEG(S,ELEV,HDIST,REGION,SADCAU,PCAU,IDEC)
        ENDIF
      IF (ICOMP .EQ. 1)GO TO 100
      IF (REGION .EQ. 4)GO TO 20
      IF (REGION .EQ. 6)GO TO 60
C
C
 100  A(K)=ELEV
      CT=10000.
      PD(K)=PDIR*CT
      PR(K)=PRFL*CT
      RG1(K)=PRFC1*CT
      RG2(K)=PRFC2*CT
      PCU(K)=PCAU*CT
C
C     ***  WRITING THE VALUES OF THE HEIGHT AND ITS  ***
C     ***  CORRESPONDING SOUND PRESSURE LEVEL INTO   ***
C     ***  THE DATA FILE.                            ***
C
      GO TO (11,21,11,21,51,61,71),REGION
 11   MAG(K)=DSQRT(DREAL(PD(K)+PR(K))**2+DIMAG(PD(K)+PR(K))
     1       **2)
      GO TO 81
 21   IF (IDEC .EQ. 3)GO TO 71
      MAG(K)=DSQRT(DREAL(PD(K)+RG1(K))**2+DIMAG(PD(K)+RG1(K))
     1       **2)
      GO TO 81
 51   MAG(K)=DSQRT(DREAL(PR(K)+RG1(K))**2+DIMAG(PR(K)+RG1(K))
     1       **2)
      GO TO 81
 61   IF (IDEC .EQ. 3)GO TO 71
      MAG(K)=DSQRT(DREAL(RG1(K)+RG2(K))**2+DIMAG(RG1(K)+RG2(K))
     1       **2)
      GO TO 81
 71   MAG(K)=DSQRT(DREAL(PCU(K))**2+DIMAG(PCU(K))**2)
 81   WRITE (26,91) 20*DLOG10(MAG(K)),A(K)
 91   FORMAT(1X,F10.5,2X,F7.3)
C
 200  CONTINUE
C
```

```
 350   STOP
       END
C
C
C      ************************************************
C
C
       SUBROUTINE FINREG(S,ELEV,HDIST,REGION)
C
C      ***  FINDING THE REGION AT WHICH THE RECEIVER LOCATES  ***
C
       IMPLICIT DOUBLE PRECISION (A-H,O-Z)
       INTEGER REGION
       COMMON /ONE/SPEED,OMEGA,ALPHA,DTOT
C
C      THE FOLLOWING STATEMENT IS USED BECAUSE OF THE
C      PROBLEM ARISED FROM THE DOUBLE PRECISION.
       IF (ABS(ELEV-S) .LT. 0.1E-10)GO TO 5
C
       IF (ELEV .LE. S) THEN
C
C
           IF (ELEV .LT. 1E-5)GO TO 8
C
C      ***  ANGLE2 - THE INITIAL ANGLE OF THE RAY WHICH HAS  ***
C      ***           THE TURNING POINT AT GROUND (Z=0)
C      ***  BOUND2 - BOUNDARY II
C
 5         ANGLE2=DACOS(DSQRT((1.+ALPHA*S+DTOT)/((1.+DTOT)
     1           *(1.+ALPHA*S))))
           BOUND2=FNRAY(ELEV,ANGLE2)+FNRAY(S,ANGLE2)
C
 8         IF ((ELEV .GT. 2.99999) .AND. (ELEV .LT. 3.00001))THEN
             BOUND3=0.0
             GO TO 10
           ENDIF
C
C      ***  ANGLE3 - THE INITAL ANGLE OF THE RAY WHICH HAS  ***
C      ***           THE TURNING POINT AT THE RECEIVER'S    ***
C      ***           HEIGHT                                 ***
C      ***  BOUND3 - BOUNDARY III                          ***
C
           ANGLE3=DACOS(DSQRT((1.+ALPHA*S+DTOT)*(1.+ALPHA*
     1           ELEV)/((1.+ALPHA*ELEV+DTOT)*(1.+ALPHA*S))))
           BOUND3=FNRAY(S,ANGLE3)
           IF (ELEV .LT. 1E-5)BOUND2=BOUND3
C
 10        IF ((HDIST .GT. BOUND2) .AND. (HDIST .GT. BOUND3)) THEN
             IF (ELEV .GT. 1E-5)THEN
               CALL EVALB4(S,ELEV,ANGLE4,BOUND4)
             ELSE
               BOUND4=BOUND2
             ENDIF
```

```
            IF (HDIST .LE. BOUND4) THEN
                REGION=6
              ELSE
                REGION=7
              ENDIF
            ELSE
              IF ((HDIST .GT. BOUND2) .AND. (HDIST .LT. BOUND3)) THEN
                REGION=4
              ELSEIF ((HDIST .GT. BOUND3) .AND. (HDIST .LT.
     1                BOUND2)) THEN
                REGION=5
              ELSE
                REGION=3
              ENDIF
            ENDIF
C
C
          ELSE
C
C
            ZERO=0.0
C
C       ***  BOUND1 - BOUNDARY I  ***
C
            BOUND1=FNRAY(ELEV,ZERO)
C
C       ***  ANGLE2 - THE INITIAL ANGLE OF THE RAY WHICH HAS THE  ***
C       ***           TURNING POINT AT GROUND (Z=0)               ***
C       ***  BOUND2 - BOUNDARY II                                 ***
C
            ANGLE2=DACOS(DSQRT((1.+ALPHA*S+DTOT)/((1.+DTOT)
     1           *(1.+ALPHA*S))))
            BOUND2=FNRAY(ELEV,ANGLE2)+FNRAY(S,ANGLE2)
C
            IF ((HDIST .LT. BOUND2) .AND. (HDIST .LT. BOUND1)) THEN
                REGION=1
              ELSEIF ((HDIST .LT. BOUND1) .AND. (HDIST .GT. BOUND2)) THEN
                REGION=2
              ELSEIF ((HDIST .LT. BOUND2) .AND. (HDIST .GT. BOUND1)) THEN
                REGION=5
              ELSE
C
C       ***  EVALB4 - EVALUATING THE BOUNDARY IV(THE CAUSTIC)  ***
C
                CALL EVALB4(S,ELEV,ANGLE4,BOUND4)
                IF (HDIST .LT. BOUND4) THEN
                    REGION=6
                    GO TO 20
                  ENDIF
                REGION=7
              ENDIF
C
C
```

```
        ENDIF
C
 20     PRINT 25,REGION
 25     FORMAT(1X,'IT LOCATES AT REGION',I2)
C
        RETURN
        END
C
C
C       ***************************************************
C
C
        SUBROUTINE FINDIR(S,ELEV,HDIST,SADDIR)
C
C       ***  FINDING THE SADDLE POINT FOR THE DIRECT WAVE  ***
C
        IMPLICIT DOUBLE PRECISION (A-H,O-Z)
        COMMON /ONE/SPEED,OMEGA,ALPHA,DTOT
C
        THETA=DATAN(ABS(ELEV-S)/HDIST)
        IF (ELEV .LT. S) THEN
            ANGLE3=DACOS(DSQRT((1.+ALPHA*S+DTOT)*(1.+ALPHA*ELEV)/
     1             ((1.+ALPHA*ELEV+DTOT)*(1.+ALPHA*S))))
          ENDIF
        QUAN=(OMEGA/SPEED)*DSQRT((1.+ALPHA*S)/
     1       (1.+ALPHA*S+DTOT))
        XL=QUAN*DCOS(THETA)
C
        IF (ELEV .GT. S) THEN
            XR=QUAN
          ELSEIF (THETA .GT. ANGLE3) THEN
            XR=XL-0.02
          ELSE
            XL=QUAN*DCOS(ANGLE3)
            XR=XL-0.001
          ENDIF
C
        ICOUNT=0
        IF (ELEV .GT. S) THEN
            SI=-1.0
          ELSE
            SI=1.0
          ENDIF
C
 10     ICOUNT=ICOUNT+1
        IF (ICOUNT .GT. 100) THEN
            PRINT*,'SOMETHING WRONG WITH FINDIR!!!'
            GO TO 20
          ENDIF
        FXL=HDIST+SI*(G32PI(S,XL)-G32PI(ELEV,XL))
        FXR=HDIST+SI*(G32PI(S,XR)-G32PI(ELEV,XR))
        CALL ROOT(XL,XR,FXL,FXR,SADDIR)
        IF (SADDIR .EQ. 0.0)GO TO 10
```

```
C
      PRINT 30,SADDIR
 30   FORMAT(1X,'SADDLE POINT FOR THE DIRECT WAVE IS ',F7.4)
      PI=4.0D+00*DATAN(1.0D+00)
      OA=OMEGA/SPEED
      ANGLE=DACOS(SADDIR/(OA*DSQRT((1.+ALPHA*S)/(1.+ALPHA*S+DTOT))))
     1      *180./PI
      PRINT 40, ANGLE
 40   FORMAT(1X,'INITIAL ANGLE FROM THE SOURCE IS',F5.2,' DEG')
      CDIST=SI*(G32PI(ELEV,SADDIR)-G32PI(S,SADDIR))
      PRINT 50, CDIST
 50   FORMAT(1X,'CHECK: HDIST FOR THE DIRECT WAVE IS ',F7.4)
C
 20   RETURN
      END
C
C
C     ************************************************
C
C
      SUBROUTINE FINRFL(S,ELEV,HDIST,SADRFL)
C
C     ***  FINDING THE SADDLE POINT FOR THE REFLECTED WAVE  ***
C
      IMPLICIT DOUBLE PRECISION (A-H,O-Z)
      COMMON /ONE/SPEED,OMEGA,ALPHA,DTOT
C
      PI=4.0D+00*DATAN(1.0D+00)
      ANGLE2=DACOS(DSQRT((1.+ALPHA*S+DTOT)/((1.+DTOT)*
     1       (1.+ALPHA*S))))
C
      GUESS1=ANGLE2
      GUESS2=PI/2.
      ICOUNT=0
      ZERO=0.0
 10   ICOUNT=ICOUNT+1
      IF (ICOUNT .GT. 500) THEN
          PRINT*,'SOMETHING WRONG WITH FINRFL!'
          GO TO 40
        ENDIF
      REFL1=HDIST-FNRAY(ELEV,GUESS1)-FNRAY(S,GUESS1)
     1      +2.*FNRAY(ZERO,GUESS1)
      REFL2=HDIST-FNRAY(ELEV,GUESS2)-FNRAY(S,GUESS2)
     1      +2*FNRAY(ZERO,GUESS2)
      CALL ROOT(GUESS1,GUESS2,REFL1,REFL2,SADDLE)
      IF (SADDLE .EQ. 0.0)GO TO 10
      SADRFL=(OMEGA/SPEED)*DSQRT((1.+ALPHA*S)/(1.+ALPHA*S+
     1       DTOT))*DCOS(SADDLE)
C
      PRINT 20,SADRFL
 20   FORMAT(1X,'SADDLE POINT FOR THE REFLECTED WAVE IS ',F7.4)
      PRINT 30,SADDLE*180./PI
 30   FORMAT(1X,'INITIAL ANGLE FROM THE SOURCE IS ',F5.2,' DEG')
```

```
      CDIST=FNRAY(ELEV,SADDLE)+FNRAY(S,SADDLE)-2.*FNRAY(ZERO,SADDLE)
      PRINT 35,CDIST
 35   FORMAT(1X,'CHECK: CDIST FOR THE REFLECTED WAVE IS ',F8.4)
C
 40   RETURN
      END
C
C
C     ************************************************
C
C
      SUBROUTINE FINRFC(S,ELEV,HDIST,REGION,SADRFC)
C
C     ***  FINDING THE SADDLE POINT FOR THE REFRACTED WAVE  ***
C
      IMPLICIT DOUBLE PRECISION (A-H,O-Z)
      INTEGER REGION
      DIMENSION SADRFC(2),RFC(2)
      COMMON /ONE/SPEED,OMEGA,ALPHA,DTOT
C
      ANGLE2=DACOS(DSQRT((1.+ALPHA*S+DTOT)/((1.+DTOT)*
     1       (1.+ALPHA*S))))
      IF (ELEV .LT. S) THEN
          ANGLE3=DACOS(DSQRT((1.+ALPHA*S+DTOT)*(1.+ALPHA*ELEV)/
     1           ((1.+ALPHA*ELEV+DTOT)*(1.+ALPHA*S))))
        ENDIF
C
      NUM=1
      IF (REGION .EQ. 5) THEN
          GUESS1=0.0000001
          IF (ELEV .LT. S) GUESS1=ANGLE3+.0000001
          GUESS2=0.05
 10       REFL2=HDIST-FNRAY(ELEV,GUESS2)-FNRAY(S,GUESS2)
          IF (REFL2 .GT. 0.0) THEN
              GUESS2=GUESS2+0.02
              GO TO 10
            ENDIF
      ELSEIF (REGION .EQ. 4) THEN
          GUESS1=ANGLE2
          GUESS2=ANGLE3+.000001
      ELSEIF (REGION .EQ. 2) THEN
          GUESS1=ANGLE2
          GUESS2=0.0000001
      ELSEIF (REGION .EQ. 6) THEN
          CALL EVALB4(S,ELEV,ANGLE4,BOUND4)
          NUM=2
      ENDIF
C
      DO 40,J=1,NUM
C
      IF ((REGION .EQ. 6) .AND. (J .EQ. 1)) THEN
           GUESS1=0.0000001
           IF (ELEV .LT. S) GUESS1=ANGLE3+0.00000001
```

```
            GUESS2=ANGLE4
          ELSEIF ((REGION .EQ. 6) .AND. (J .EQ. NUM)) THEN
            GUESS1=ANGLE4
            GUESS2=ANGLE2
          ENDIF
C
      ICOUNT=0
C
 30   ICOUNT=ICOUNT+1
      IF (ICOUNT .GT. 100) THEN
          PRINT*,'SOMETHING WRONG WITH FINRFC!'
          GO TO 50
        ENDIF
C
      FXL=HDIST-FNRAY(ELEV,GUESS1)-FNRAY(S,GUESS1)
      FXR=HDIST-FNRAY(ELEV,GUESS2)-FNRAY(S,GUESS2)
      CALL ROOT(GUESS1,GUESS2,FXL,FXR,RFC(J))
      IF (RFC(J) .EQ. 0.0)GO TO 30
C
      SADRFC(J)=(OMEGA/SPEED)*DSQRT((1.+ALPHA*S)/(1.+ALPHA*
     1          S+DTOT))*DCOS(RFC(J))
C
      PRINT 35,SADRFC(J)
 35   FORMAT(1X,'SADDLE POINT FOR THE REFRACTED WAVE IS ',F7.4)
      ANGLE=RFC(J)*180./3.141592654
      PRINT 37,ANGLE
 37   FORMAT(1X,'INITIAL ANGLE FROM THE SOURCE IS ',F5.2,'DEG')
      CHK=FNRAY(ELEV,RFC(J))+FNRAY(S,RFC(J))
      PRINT 38,CHK
 38   FORMAT(1X,'CHECK: HDIST FOR THE REFRACTED WAVE IS ',F8.4)

C
 40   CONTINUE
 50   RETURN
      END
C
C
C     ************************************************
C
C
      SUBROUTINE INTEG(S,ELEV,HDIST,REGION,SADDLE,PINT,IDEC)
C
C     ***  EVALUATING THE SOUND PRESSURE WITH EQUATIONS  ***
C     ***  GIVEN IN SECTION
C
      IMPLICIT DOUBLE PRECISION (A-H,O-Z)
      COMPLEX*16 ZI,PRT1,K1,ARG1,ARG2,H1,H2,H1P,H2P,PRT4A,
     1           PRT4B,PRT5A,PRT5B,PRT6,ARG3,T1,T2,R,PRT8,
     2           PRT6A,PRT6B,PINT,G32C,CMPSAD,CGPIZ,CGPIZ2,
     3           ARG,AI,BI,AIP,BIP,PINT1
      REAL*8 LANDA,IMI
      INTEGER REGION
      COMMON /ONE/SPEED,OMEGA,ALPHA,DTOT
```

```
C
      PI=4.0D+00*DATAN(1.0D+00)
      SIGMA=300.
C
C     ***  ZI IS THE NORMAL IMPEDANCE FROM CHESSEL'S MODEL  ***
C
      REI=1.+9.08*(2.*PI*300./OMEGA)**0.75
      IMI=-11.9*(2.*PI*300./OMEGA)**0.73
      ZI=DCMPLX(REI,IMI)
      LANDA=OMEGA/(SPEED*ALPHA)
      ZERO=0.0
      CMPSAD=SADDLE*DCMPLX(1.,0.0)
C
      PRT1=DCMPLX(0.0,1.0)*24.*LANDA**(2./3.)
      PRT2=DSQRT(GPIZ(ELEV,SADDLE)*GPIZ(S,SADDLE))
      PRT3=DSQRT((2.*SADDLE)/(PI*HDIST))
      K1=PRT3/(PRT1*PRT2)
      ARG1=(3.*LANDA/2.*G32(S,SADDLE))**(2./3.)
      ARG2=(3.*LANDA/2.*G32(ELEV,SADDLE))**(2./3.)
      CALL H(ARG1,H1,H2,H1P,H2P)
      PRT4A=H1
      PRT4B=H2
      CALL H(ARG2,H1,H2,H1P,H2P)
      PRT5A=H1
      PRT5B=H2
      PRT6=CDEXP(DCMPLX(0.0,-1.0)*(SADDLE*HDIST-PI/2.))
      PRT7A=G32PI2(S,SADDLE)
      PRT7B=G32PI2(ELEV,SADDLE)
C
      IF ((IDEC .EQ. 2) .OR. (IDEC .EQ. 3)) GO TO 100
      GO TO (10,10,10,10,100,100) REGION
C
 10   IF (ELEV .GT. S) THEN
C
C     ***  EQ. (81)  ***
C
        PINT=DSQRT(2.*PI)*K1*PRT6*PRT4A*PRT5B/
     1       DSQRT(PRT7A-PRT7B)
      ELSE
C
C     ***  EQ. (82)  ***
C
        PINT=DSQRT(2.*PI)*K1*PRT6*PRT4B*PRT5A/
     1       DSQRT(PRT7B-PRT7A)
      ENDIF
      PRINT 15, ' INTEGRAL FOR THE DIRECT WAVE IS',PINT
 15   FORMAT(A,2F12.6)
      GO TO 200
C
 100  ARG3=(3.*LANDA/2.*G32C(ZERO,CMPSAD))**(2./3.)
      CALL H(ARG3,H1,H2,H1P,H2P)
      T1=1.-DCMPLX(0.0,1.0)/2.*(SPEED/OMEGA)*ZI*
     1   CGPIZ2(ZERO,CMPSAD)/CGPIZ(ZERO,CMPSAD)
```

```
      T2=DCMPLX(0.0,1.0)*(SPEED/OMEGA)*ZI*(3.*LANDA/2.)**
     1    (2./3.)*CGPIZ(ZERO,CMPSAD)
      R=-(T1*H1+T2*H1P)/(T1*H2+T2*H2P)
      PRT8=CDEXP(PI/6.*DCMPLX(0.0,-1.))/(CDEXP(DCMPLX(0.0,1.)*PI/6.)-
     1     DCMPLX(0.0,1.0)*R)
      IF (IDEC .EQ. 3)GO TO 60
      IF (IDEC .EQ. 2) THEN
          GO TO (30,40,30,40,50,50) REGION
        ENDIF
      IF (REGION .EQ. 5) GO TO 30
      IF (REGION .EQ. 6) GO TO 40
C
 30   PRT7C=2.*G32PI2(ZERO,SADDLE)
C
C     *** EQ. (83) ***
C
      PINT=DSQRT(2.*PI)*K1*R*PRT6*PRT4B*PRT5B/
     1     DSQRT(PRT7C-PRT7B-PRT7A)
      PRINT 15, ' INTEGRAL FOR THE REFLECTED WAVE IS',PINT
      GO TO 200
C
C     *** EQ. (85) ***
C
40    PINT=DSQRT(2.*PI)*K1*PRT6*PRT4B*PRT5B/DSQRT(-PRT7A-
     1     PRT7B)*PRT8
      PRINT 15, ' INTEGRAL FOR THE REFRACTED WAVE IS',PINT
      GO TO 200
C
 50   PRT6A=CDEXP(DCMPLX(0.0,-1.0)*SADDLE*HDIST)
C
C     *** EQ. (84) ***
C
      PINT=DSQRT(2.*PI)*K1*PRT6A*PRT4B*PRT5B/DSQRT(PRT7A+
     1     PRT7B)*PRT8
      PRINT 15, ' INTEGRAL FOR THE REFRACTED WAVE IS',PINT
      GO TO 200
C
 60   PRT6B=CDEXP(DCMPLX(0.0,-1.0)*(SADDLE*HDIST-PI/4.))
      PRT7C=G32PI3(S,SADDLE)
      PRT7D=G32PI3(ELEV,SADDLE)
      FPI3=(2./(PRT7C+PRT7D))**(1./3.)
      CALL EVALB4(S,ELEV,ANGLE,BOUND4)
      DELR=HDIST-BOUND4
      IF ((REGION .EQ. 6) .OR. (REGION .EQ. 4)) THEN
          ARG=-ABS(FPI3*DELR)
        ELSE
          ARG=ABS(FPI3*DELR)
        ENDIF
      CALL CGBAIR(ARG,AI,BI,AIP,BIP)
C
C     *** EQ. (89) ***
C
      PINT=2.*PI*K1*PRT6B*PRT4B*PRT5B*FPI3*AI*PRT8
```

```
      PRINT 15, ' INTEGRAL FOR THE WAVE BY CAUSTICS IS',PINT
C
 200  RETURN
      END
C
C
C     ************************************************
C
C
      SUBROUTINE EVALB4(S,ELEV,ANGLE4,BOUND4)
C
C     ***  THIS SUBROUTINE EVALUATES THE LOCATION OF  ***
C     ***  BOUNDARY IV                                ***
C
      IMPLICIT DOUBLE PRECISION (A-H,O-Z)
      COMMON /ONE/SPEED,OMEGA,ALPHA,DTOT
C
      GUESS2=(OMEGA/SPEED)*DSQRT(1./(1.+DTOT))
      IF (ELEV .LT. 1.E-5) THEN
          ANGLE4=DACOS(DSQRT((1.+ALPHA*S+DTOT)/((1.+DTOT)
     1           *(1.+ALPHA*S))))
          BOUND4=FNRAY(ELEV,ANGLE4)+FNRAY(S,ANGLE4)
          GO TO 50
        ENDIF
      IF (ELEV .GT. S) THEN
          GUESS1=(OMEGA/SPEED)*DSQRT((1.+ALPHA*S)/
     1     (1.+ALPHA*S+DTOT))-0.0000001
        ELSE
          GUESS1=(OMEGA/SPEED)*DSQRT((1.+ALPHA*ELEV)/
     1     (1.+ALPHA*ELEV+DTOT))-0.0000001
        END IF
      ICOUNT=0
10    ICOUNT=ICOUNT+1
      IF (ICOUNT .GT. 100)THEN
          PRINT*,'SOMETHING WRONG WITH EVALB4!!!'
          GO TO 50
        ENDIF
      Y1=G32PI2(ELEV,GUESS1)+G32PI2(S,GUESS1)
      Y2=G32PI2(ELEV,GUESS2)+G32PI2(S,GUESS2)
      CALL ROOT(GUESS1,GUESS2,Y1,Y2,BETA)
      IF (BETA .EQ. 0.0)GO TO 10
      ANGLE4=DACOS((BETA*SPEED)/(OMEGA*DSQRT((1.+
     1 ALPHA*S)/(1.+ALPHA*S+DTOT))))
      BOUND4=FNRAY(ELEV,ANGLE4)+FNRAY(S,ANGLE4)
C
 50   RETURN
      END
C
C
C     ************************************************
C
C
      SUBROUTINE ROOT(XL,XR,FXL,FXR,SOLN)
```

```
C
C       ***  THIS SUBROUTINE UTILIZES THE BISECTION  ***
C       ***  METHOD FOR ROOT FINDING                 ***
C
        IMPLICIT DOUBLE PRECISION (A-H,O-Z)
        SOLN=0.0
        IF ((FXL*FXR) .GT. 0.0)THEN
            XR=XL
            XL=TEMP
            XL=(XL+XR)/2.0
            GO TO 10
          ENDIF
        IF (ABS(XR-XL) .GT. 1.E-10)THEN
            TEMP=XL
            XL=(XL+XR)/2.0
            GO TO 10
          ENDIF
C
        SOLN=(XL+XR)/2.0
C
 10     RETURN
        END
C
C
C       ****************************************************
C
C
        SUBROUTINE H(Z,H1,H2,H1P,H2P)
C
C       ***  H USES SUBROUTINE CGBAIR TO CALCULATE 1/3 ORDER HANKLE  ***
C       ***  FUNCTIONS FROM AIRY FUNCTIONS.                          ***
C
        IMPLICIT REAL*8 (A-H,O-Z)
        COMPLEX*16 Z,AI,BI,AIP,BIP,K,KS,H1,H2,H1P,H2P,ARG,CI
        CI= DCMPLX(0.DO,1.DO)
        PI= 3.141592654DO
        ARG= DCMPLX(0.DO,-PI/6.DO)
        K= (12.DO)**(1.DO/6.DO)*CDEXP(ARG)
        KS= DCONJG(K)
        CALL CGBAIR(-Z,AI,BI,AIP,BIP)
        H1= K*(AI-CI*BI)
        H2= KS*(AI+CI*BI)
        H1P= -K*(AIP-CI*BIP)
        H2P= -KS*(AIP+CI*BIP)
        RETURN
        END
        SUBROUTINE CGBAIR(Z,AI,BI,AIP,BIP)
        IMPLICIT REAL*8 (A-H,O-Z)
C
C       CALCULATE AIRY FUNCTIONS FOR COMPLEX*16 ARGUMENT
C       REF. HANDBOOK OF MATHEMATICAL FUNCTIONS, ABRAMOWITZ AND STEGUN.
C
C
```

```
C       ENTRY
C       CALCULATE ARGUMENT(Z) AND ABSOLUTE VALUE(Z)
C   4   IF /Z/ LT 5
C       THEN USE EQS. 10.4.2 THRU 10.4.5 FOR AI,BI,AIP,BIP
C  10   ELSE IF ARG(Z) LT PI/3
C            THEN CALCULATE ZETA(Z)
C            USE EQS. 10.4.59, 10.4.61, 10.4.63, 10.4.66 FOR AI,BI,AIP,BIP
C  20        ELSE CALCULATE ZETA(-Z)
C            USE EQS. 10.4.60, 10.4.62, 10.4.64, 10.4.67 FOR AI,BI,AIP,BIP
C            ENDIF
C       ENDIF
C       EXIT
C       END
C
        COMPLEX*16 Z,AI,BI,AIP,BIP,ZETA,CZETA,Z14,SUM1,SUM2,SUM3,SUM4,
     1  ZETAP,FACT1,FACT2,SN,CS,FTERM,FPTERM,GTERM,GPTERM,F,FP,G,GP,Z3
        DIMENSION C(21),D(21)
        DATA C1,C2,PIRT,PI4/.3550280539D0,.2588194038D0,1.772453851D0,
     + .7853981635D0/
        DATA C/1.D0,.069444444444444D0,
     + .037133487654321D0,.0379930591278OOD0,
     1 .0576491904126690,.11609906402551D0,
     + .291591399230740,.87766696950998D0,
     2 3.0794530301731D0,12.341573332345D0,
     + 55.622785365914D0,278.46508077759D0,
     3 1533.1694320127D0,9207.2065997258D0,
     + 59892.513565875D0,419524.87511653D0,
     4 3148257.4178666D0,25198919.871601D0,
     + 214288036.96366D0,1929375549.1823D0,
     5 18335766937.889D0/
        DATA D/1.D0,
     + -.097222222222221D0,-.043885030864197D0,-.042462830789894D0,
     1 -.062662163492031D0,-.12410589602727D0,-.30825376490107D0,
     2 -.92047999241291D0,-3.2104935846485D0,-12.807293080735D0,
     3 -57.508303513911D0,-287.03323710920D0,-1576.35730333700,
     4 -9446.3548230953D0,-61335.706663847D0,-428952.40040004D0,
     5 -3214536.5214006D0,-25697908.383909D0,-218293420.83214D0,
     6 -1963523788.9909D0,-18643931088.105D0/
        ABSZ=ABS(Z)
        IF(ABSZ.EQ.0) GO TO 3
        IF(ABS(DIMAG(Z)).LE.1.D-12.AND.DREAL(Z).LT.0.D0) GO TO 5
        ARGZ=ATAN2(DIMAG(Z),DREAL(Z))
        GO TO 4
    3   ARGZ=0.D0
        GO TO 4
    5   ARGZ=3.1415926535898D0
    4   CONTINUE
        IF(ABSZ.GT.4.5D0) GO TO 10
C
C       ASCENDING SERIES
C       EQS. 10.4.2,10.4.3
C
```

```
      Z3=Z**3
      FTERM=1.D0
      FPTERM=Z*Z/2.D0
      GTERM=Z
      GPTERM=1.D0
      GLIM=1.D-13*ABSZ
      F=FTERM
      FP=FPTERM
      G=GTERM
      GP=GPTERM
      DO 1 I=1,100
      I3=3*I
      FTERM=FTERM*Z3/((I3-1.D0)*I3)
      FPTERM=FPTERM*Z3/(I3*(I3+2.D0))
      GTERM=GTERM*Z3/(I3*(I3+1.D0))
      GPTERM=GPTERM*Z3/((I3-2.D0)*I3)
      F=F+FTERM
      FP=FP+FPTERM
      G=G+GTERM
      GP=GP+GPTERM
      IF(ABS(GTERM).LE.GLIM) GO TO 2
    1 CONTINUE
      PRINT 6000, Z
 6000 FORMAT(/' Z='2E14.5,' ERROR IN CGBAIR, NONCONVERGENCE')
    2 AI=C1*F-C2*G
      AIP=C1*FP-C2*GP
      BI=1.732050808D0*(C1*F+C2*G)
      BIP=1.732050808D0*(C1*FP+C2*GP)
      GO TO 9999
C     ASYMPTOTIC EXPANSIONS FOR /Z/ LARGE
   10 SIGN=1.D0
      SUM1=0.D0
      SUM2=0.D0
      SUM3=0.D0
      SUM4=0.D0
C     PI/3 = 1.047197551
      IF(ABS(ARGZ).GE.1.3D0) GO TO 20
C
C     /ARG(Z)/ LE PI/3
C     EQS. 10.4.59, 10.4.61, 10.4.63, 10.4.66
C
      ZETA=CZETA(ABSZ,ARGZ)
      DO 11 I=1,12
      K=I-1
      ZETAP=ZETA**K
      SUM1=SUM1+SIGN*C(I)/ZETAP
      SUM2=SUM2+SIGN*D(I)/ZETAP
      SUM3=SUM3+C(I)/ZETAP
      SUM4=SUM4+D(I)/ZETAP
   11 SIGN=-SIGN
      Z14=ABSZ**.25D0*DCMPLX(COS(ARGZ/4.D0),SIN(ARGZ/4.D0))
      FACT1=.5D0*EXP(-ZETA)/(PIRT*Z14)
      FACT2=.5D0*EXP(-ZETA)*Z14/PIRT
```

```
      AI=FACT1*SUM1
      AIP=-FACT2*SUM2
      FACT1=EXP(ZETA)/(PIRT*Z14)
      FACT2=EXP(ZETA)*Z14/PIRT
      BI=FACT1*SUM3
      BIP=FACT2*SUM4
      GO TO 9999
C
C     /ARG(Z)/ GT PI/3
C     EQS. 10.4.60, 10.4.62, 10.4.64, 10.4.67
C
   20 ARGZ=ATAN2(-DIMAG(Z),-DREAL(Z))
      ZETA=CZETA(ABSZ,ARGZ)
      DO 21 I=1,10
      K2=(I-1)*2
      J=K2+1
      ZETAP=ZETA**K2
      SUM1=SUM1+SIGN*C(J)/ZETAP
      SUM2=SUM2+SIGN*C(J+1)/(ZETAP*ZETA)
      SUM3=SUM3+SIGN*D(J)/ZETAP
      SUM4=SUM4+SIGN*D(J+1)/(ZETAP*ZETA)
   21 SIGN=-SIGN
      Z14=ABSZ**.25DO*DCMPLX(COS(ARGZ/4.DO),SIN(ARGZ/4.DO))
      FACT1=1.DO/(PIRT*Z14)
      FACT2=Z14/PIRT
      SN=SIN(ZETA+PI4)
      CS=COS(ZETA+PI4)
      AI=FACT1*(SN*SUM1-CS*SUM2)
      AIP=-FACT2*(CS*SUM3+SN*SUM4)
      BI=FACT1*(CS*SUM1+SN*SUM2)
      BIP=FACT2*(SN*SUM3-CS*SUM4)
 9999 RETURN
      END
C
C
C     ***************************************************
C
C
      FUNCTION CZETA(ABSZ,ARGZ)
      IMPLICIT REAL*8 (A-H,O-Z)
      COMPLEX*16 CZETA
      ARG=ARGZ*1.5DO
      CZETA=(ABSZ**1.5DO)*DCMPLX(COS(ARG),SIN(ARG))*.66666666666667DO
      RETURN
      END
C
C
C     ***************************************************
C
C
      FUNCTION FNRAY (Z,THETA)
      IMPLICIT DOUBLE PRECISION (A-H,O-Z)
      COMMON /ONE/SPEED,OMEGA,ALPHA,DTOT/TWO/S
```

```
      A=ALPHA*(1.+ALPHA*S+DTOT-DCOS(THETA)**2*(1.+ALPHA*S))
      B=1.+ALPHA*S+DTOT-DCOS(THETA)**2*(1.+DTOT)*(1.+ALPHA*S)
      IF (ABS(B) .LT. 1E-15)B=0.0
      C=DCOS(THETA)**2*(1.+ALPHA*S)*ALPHA
      D=(1.+DTOT)*(1.+ALPHA*S)*DCOS(THETA)**2
      E=C*(A*Z+B)/(A*(C*Z+D))
      P=DSQRT(C*(A*Z+B)/(A*(C*Z+D)))
      FNRAY=DSQRT((A*Z+B)*(C*Z+D))/A+(A*D-B*C)*DLOG((1+P)/
     1 (1-P))/(A*DSQRT(A*C)*2.)
      RETURN
 10   END
C
C
C     ************************************************
C
C
      FUNCTION G32(Z,BETA)
      IMPLICIT DOUBLE PRECISION (A-H,O-Z)
      COMMON /ONE/SPEED,OMEGA,ALPHA,DTOT
      AA=1.+ALPHA*Z+DTOT
      BB=1.-(SPEED*BETA/OMEGA)**2
      ROOTBB=DSQRT(BB)
      PHI=DSQRT((BB*AA-DTOT)/(BB*AA))
      FOO=DLOG((1.+PHI)/(1.-PHI))
      G32=DSQRT(BB*AA**2-DTOT*AA)-0.5*DTOT/ROOTBB*FOO
      RETURN
      END
C
C
C     ************************************************
C
C
      FUNCTION G32PI(Z,BETA)
      IMPLICIT DOUBLE PRECISION (A-H,O-Z)
      COMMON /ONE/SPEED,OMEGA,ALPHA,DTOT
      AA=1.+ALPHA*Z+DTOT
      BB=1.-(SPEED*BETA/OMEGA)**2
      ROOTBB=DSQRT(BB)
      QUAN=BB*AA-DTOT
      IF (QUAN .LT. 1.E-15) THEN
          PHI=0.0
          CC=0.0
        ELSE
          PHI=DSQRT(QUAN/(BB*AA))
          CC=DSQRT(BB*AA**2-DTOT*AA)
        ENDIF
      FOO=DLOG((1.+PHI)/(1.-PHI))
      DD=0.5*DTOT/ROOTBB*FOO
      G32PI=((-SPEED*BETA)/(ALPHA*OMEGA*BB))*(CC+DD)
      RETURN
      END
C
C
```

```
C     ***************************************************
C
C
C
      FUNCTION G32PI2(Z,BETA)
      IMPLICIT DOUBLE PRECISION (A-H,O-Z)
      COMMON /ONE/SPEED,OMEGA,ALPHA,DTOT
      AA=1.+ALPHA*Z+DTOT
      BB=1.-(SPEED*BETA/OMEGA)**2
      CC=1.+2.*(SPEED*BETA/OMEGA)**2
      ROOTBB=DSQRT(BB)
      PHI=DSQRT((BB*AA-DTOT)/(BB*AA))
      FOO=DLOG((1.+PHI)/(1.-PHI))
      G32PI2=(-SPEED/(ALPHA*OMEGA*BB**2))*
     1 (((BB*AA**2-CC*DTOT*AA)/DSQRT(BB*AA**2-DTOT*AA))+
     1 ((CC*DTOT)/(2.*ROOTBB))*FOO)
      RETURN
      END
C
C
C     ***************************************************
C
C
      FUNCTION G32PI3(Z,BETA)
      IMPLICIT DOUBLE PRECISION (A-H,O-Z)
      COMMON /ONE/SPEED,OMEGA,ALPHA,DTOT
      A=(SPEED*BETA/OMEGA)**2
      AO=A/BETA
      A1=1.-A
      A2=1.+2.*A
      A3=5.-2.*A
      B=1.+ALPHA*Z+DTOT
      P=DSQRT((A1*B-DTOT)/(A1*B))
      F=DLOG((1.+P)/(1.-P))
      PRTO=-(SPEED/(ALPHA*OMEGA))/A1**2
      PRT1=AO*B**2*(2.*A*DTOT*B+4.*DTOT**2-A1*B**2-3.*DTOT*B)
      PRT2=(A1*B**2-DTOT*B)**(3./2.)
      PRT3=F*AO*A3/A1**(3./2.)-2.*AO*A2*DSQRT(B)/
     1      (A1*DSQRT(A1*B-DTOT))
      PRT4=4.*AO/A1*G32PI2(Z,BETA)
      G32PI3=PRTO*(PRT1/PRT2+0.5*DTOT*PRT3)+PRT4
      RETURN
      END
C
C
C     ***************************************************
C
C
      FUNCTION G32C(Z,BETA)
      IMPLICIT REAL*8 (A-H,O-Z)
      COMPLEX*16 BETA,PHI,SQRT1,SQRT2,FOO,G32C,MODLOG
      COMMON /ONE/SPEED,OMEGA,ALPHA,DTOT
      AA=1.+ALPHA*Z+DTOT
      PHI=SQRT1(BETA,Z)/(SQRT2(BETA)*DSQRT(AA))
```

```
      FOO=MODLOG((1.+PHI)/(1.-PHI))
      G32C=SQRT(AA)*SQRT1(BETA,Z)-.5*DTOT*FOO/SQRT2(BETA)
      RETURN
      END
C
C
C     ************************************************
C
C
      FUNCTION SQRT1(BETA,Z)
      IMPLICIT REAL*8 (A-H,O-Z)
      COMPLEX*16 BETA,AA,SQRT1
      COMMON /ONE/SPEED,OMEGA,ALPHA,DTOT
      AA=1.-((SPEED/OMEGA)*BETA)**2.
      BB=1.+ALPHA*Z+DTOT
      BRAN1=(OMEGA/SPEED)*DSQRT((1.+ALPHA*Z)/(1.+ALPHA*Z+DTOT))
      IF ((DREAL(BETA) .GT. BRAN1) .AND.
     1 (DIMAG(BETA) .LE. 0.0)) THEN
          SQRT1=-CDSQRT(AA*BB-DTOT)
        ELSE
          SQRT1=CDSQRT(AA*BB-DTOT)
        END IF
      RETURN
      END
C
C
C     ************************************************
C
C
      FUNCTION SQRT2(BETA)
      IMPLICIT REAL*8 (A-H,O-Z)
      COMPLEX*16 BETA,AA,SQRT2
      COMMON /ONE/SPEED,OMEGA,ALPHA,DTOT
      A=ALPHA+DTOT
      AA=1.-((SPEED/OMEGA)*BETA)**2.
      BRAN2=OMEGA/SPEED
      IF ((DREAL(BETA) .GT. BRAN2) .AND.
     1 (DIMAG(BETA) .LE. 0.0)) THEN
          SQRT2=-CDSQRT(AA)
        ELSE
          SQRT2=CDSQRT(AA)
        END IF
      RETURN
      END
C
C
C     ************************************************
C
C
      FUNCTION MODLOG(QUAN)
      IMPLICIT REAL*8 (A-H,O-Z)
      COMPLEX*16 QUAN,MODLOG
      IF ((DREAL(QUAN) .LT. 0.0) .AND. (DIMAG(QUAN)
```

```
     1  .GE. 0.0)) THEN
          MODLOG=LOG(QUAN)+DCMPLX(0.0,-2.*3.1415927)
        ELSE
          MODLOG=LOG(QUAN)
        END IF
        RETURN
        END
C
C
C       ***************************************************
C
C
C
        FUNCTION GPIZ(Z,BETA)
        IMPLICIT DOUBLE PRECISION (A-H,O-Z)
        COMMON /ONE/SPEED,OMEGA,ALPHA,DTOT
        A=1.-(SPEED*BETA/OMEGA)**2
        B=1.+ALPHA*Z+DTOT
        C=G32(Z,BETA)**(2./3.)
        GPIZ=(2.*ALPHA/3.)*DSQRT((A*B-DTOT)/(C*B))
        RETURN
        END
C
C
C       ***************************************************
C
C
C
        FUNCTION GPIZ2(Z,BETA)
        IMPLICIT DOUBLE PRECISION (A-H,O-Z)
        COMMON /ONE/SPEED,OMEGA,ALPHA,DTOT
        A=1.-(SPEED*BETA/OMEGA)**2
        B=1.+ALPHA*Z+DTOT
        C=G32(Z,BETA)**(2./3.)
        GPIZ2=(ALPHA**2./3.)/DSQRT(C*(B**2*A-DTOT*B))*
     1  (DTOT/B-(A*B-DTOT)*(GPIZ(Z,BETA)/(ALPHA*C)))
        RETURN
        END
C
C
C       ***************************************************
C
C
C
        FUNCTION CGPIZ(Z,CBETA)
        IMPLICIT DOUBLE PRECISION (A-H,O-Z)
        COMMON /ONE/SPEED,OMEGA,ALPHA,DTOT
        COMPLEX*16 CBETA,A,C,G32C,CGPIZ
        A=1.-(SPEED*CBETA/OMEGA)**2
        B=1.+ALPHA*Z+DTOT
        C=G32C(Z,CBETA)**(2./3.)
        IF (DIMAG(C) .EQ. 0.0) THEN
            SI=1.0
          ELSE
            SI=-1.0
          ENDIF
```

```
      CGPIZ=SI*(2.*ALPHA/3.)*SQRT((A*B-DTOT)/(C*B))
      RETURN
      END
C
C
C     ***************************************************
C
C
      FUNCTION CGPIZ2(Z,CBETA)
      IMPLICIT DOUBLE PRECISION (A-H,O-Z)
      COMMON /ONE/SPEED,OMEGA,ALPHA,DTOT
      COMPLEX*16 CBETA,A,C,G32C,CGPIZ,CGPIZ2
      A=1.-(SPEED*CBETA/OMEGA)**2
      B=1.+ALPHA*Z+DTOT
      C=G32C(Z,CBETA)**(2./3.)
      CGPIZ2=(ALPHA**2./3.)/CDSQRT(C*(B**2*A-DTOT*B))*
     1 (DTOT/B-(A*B-DTOT)*(CGPIZ(Z,CBETA)/(ALPHA*C)))
      RETURN
      END
```

REFERENCES

1. Herzveld, K.F. and Lifouitz, T.A., Absorption and Dispersion of Ultrasonic Waves, Academic Press, New York, 1959.

2. Evans, L.B, and Bess, H.E., Tables of Absorption and Velocity of Sound in Still Air at 68°F, Wyle Laboratory Report WR 72-2, 1972.

3. Wenze, A.R. "Propagation of Waves Along an Impedance Boundary," J. Acoust. Soc. Am., Vol.55, 1974, pp. 956-963.

4. Lawhead, R.B. and Rudnick, I, "Acoustic Ware Propagation Along a Constant Normal Impedance Boundary," J. Acoust. Soc. Am., Vol.23, 1951, pp. 546-549.

5. Chessel, C.I., "Propagation of Noise Along a Finite Impedance Boundary," J. Acoust. Soc. Am., Vol. 62, 1977, pp. 825-834.

6. Parkin, P.H. and Scholes, W.E., "The Horizontal Propagation of Sound from a Jet Engine Close to the Ground at Hatfield," J. Sound Vib., Vol. 2, 1965, pp. 353-374.

7. Albers, V. M., Underwater Sound, Dowden, Hutchinson and Ross, Inc., New York, 1972.

8. Pekeris, C.L., "Theory of Propagation of Sound in a Half-Space of Variable Sound Velocity under Conditions of Formation of a Shadow Zone," J. Acoust. Soc. America, Vol. 18, No. 2, 1946, pp. 295-315.

9. Pridmore-Brown, D. C., and Ingard U., "Sound Propagation into the Shadow Zone in a Temperature Stratified Atmosphere Above a Plane Boundary," J. Acoust. Soc. America, Vol. 27, No. 1, 1955.

10. Tolstoy, I., "Energy Transmission into Shadow Zone by Rough Surface Boundary Wave," J. Acoust. Soc. America, Vol. 69, No. 5, 1981.

11. Van Moorhem, W.K., "Fourth Semiannual Report to the National Aeronautics and Space Agency on Grant NAg-1-283: Acoustic Propagation in a Thermally Stratified Atmosphere," UTEC ME 83-050, Mechanical and Industrial Engineering Department, University of Utah, Salt Lake City, 1983.

12. G.K. Landheim, The Propagation of Plane Waves in A Thermally Stratified Atmosphere, M.E. Report, University of Utah, 1983.

13. Mathews, J. and Walker, R.L., Mathematical Methods of Physics, Benjamin/Cummings Publishing Co., Inc., Menlo Park, Calif., 1961.

14. Halliday, D. and Resnick, R., Fundamentals of Physics, John Wiley and Sons, Inc., New York, 1974.

15. Pierce, A.P., Acoustics--An Introduction to its Physical Principles and Applications, McGraw-Hill, Inc., New York, 1981.

16. Nayfeh, A.H., Perturbation Methods, John Wiley and Sons, Inc., New York, 1973.

17. Tables of the Modified Hankel Functions of Order One-Third and of their Derivatives, by the Staff of the Computation Lab, Harvard University Press, Cambridge, MA, 1945.

18. Keller, J.B. and Ahluwalia, D.S., "Exact and Asymptotic Representation of the Sound Field in a Stratified Ocean," Wave Propagation and Underwater Acoustics, J.B. Keller and J.S. Papadakis, Eds., Springer-Verlag, New York, 1977.

19. Abramowitz, M. and Stegun, I., Handbook of Mathematical Functions, Dover Publications, Inc., New York, 1965.

20. Sachs, D.A. and Silbiger, A., "Focusing and Refraction of Harmonic Sound and Transient Pulses in Stratified Media," J. Acoustical Soc., America, Vol. 49, No.3, 1971, p. 824.

21. Private Communication from W.L. Wilshire, NASA, Langley Research Center, Hampton, Virginia, 1979.

22. Butterworth, J., An Investigation of Sound Pressure Levels in an Acoustic Shadow, Master's Thesis, Mechanical and Industrial Engineering Department, University of Utah, 1979.

23. Wiener, F.M. and Keast, D. N., "Experimental Study of the Propagation of Sound over Ground," J. Acoust. Soc. America, Vol. 31, No. 6, 1959, p. 724.

24. Ma, Y., Master's Thesis, Mechanical and Industrial Engineering Department, University of Utah, 1984.

APPENDIX B

WAVE PROPAGATION ALONG A FINITE IMPEDANCE GROUND UNDER A TEMPERATURE LAPSE CONDITION

by

Yiping Ma

A thesis submitted to the faculty of
The University of Utah
in partial fulfillment of the requirements for the degree of

Master of Science

in

Mechanical Engineering

Department of Mechanical and Industrial Engineering

The University of Utah

December 1984

ABSTRACT

In this study, the wave propagation over a finite impedance ground under a temperature lapse condition is analyzed. The solution is expressed in terms of an integral. A surface wave term is found as a result of a pole occurring in the integration. The behaviors of the surface wave for different temperature gradients and ground impedance values are studied. This surface wave is seen to be important at low source frequencies. A ground wave-like term is also seen in the total pressure field, which is the dominant term well inside the shadow region. The calculated results of the pressure field show a very good agreement with the empirical model developed.

TABLE OF CONTENTS

NOMENCLATURE

a	Sound speed
a_∞	Sound speed at $z = \infty$
T	Temperature
T_∞	Temperature at $z = \infty$
ΔT	Temperature change between $z = 0$ and $z = \infty$
$\bar{G}$	Function defined by (5)
G	Hankel transform of $\bar{G}$
g	Function defined by (23)
h_1, h_2	Modified Harkel functions
i	$\sqrt{-1}$
P	Pressure
q	A constant giving the source strength
s	Source height
t	Time
R_0, R_1	Reflection and/or refraction coefficient defined by (18) and (19)
T_1, T_2	Constants defined by (20) and (21)
ω	Circular frequency
K, K_3	Constants defined (17) and (45)
β	Hankel transform variable
Z	Ground impedance
η	Function defined by (22)
z	Receiver height

r	Receiver radius
α	Parameter defined in (1)

ACKNOWLEDGEMENTS

I wish to express my sincere appreciation to my advisor, Dr. William K. Van Moorhem, for his help and understanding in the preparation of this thesis. I also wish to extend thanks to Dr. Gary A. Flandro and Dr. Kuan Chen for being members on my supervisory committee.

1. INTRODUCTION

The prediction of acoustic noise is of increasing interest, since the control and reduction of noise in the community has become a major social and technical problem. It is particularly true for the area around an airport. An airplane which is taking off or landing is one of the most significant noise sources in the community. For over three decades, people have been trying to understand the physics of the generation, propagation, and pe.ception of aircraft noise. This thesis is concerned with only the propagation.

The simplest physical model of outdoor sound propagation is a point source in free space which ignores the effect of ground, meteorological effects, and atmospheric absorption of sound. In the early 1950s Ingard [1] and Lawhead and Rundick [2, 3] each obtained an analytical solution of the sound propagation from a point source in a homogeneous atmosphere over a finite impedance ground. A finite impedance ground surface changes both the amplitude and phase of a sound wave being reflected from it. These solutions include the contributions of the direct and reflected waves plus a term now called the ground wave, and they describe an interference pattern above the ground surface. Although these solutions were accepted in this field little use was made of them for over twenty years. Because these models were really too simple, inconsistencies exist between them and the practical measurements made in laboratories and outdoors.

In 1972 Wenzel [4] showed that a term, the so-called surface wave,

was missing in the previous solutions. After solving the same problem as Ingard, and Lawhead and Rundick by a different approach, he suggested that some of these inconsistencies could be the result of a surface wave which appeared to be an essential component of the total sound pressure field generated by a point source above a finite impedance ground. He further pointed out that under certain limiting conditions his results differed from those of Ingard by just this surface wave term. Chien and Soroka [5] also obtained a similar kind of asymptotic solution for various limiting cases. However, their results applied to a more general case than that of Wenzel. They also found that in certain situations their solutions differed from Ingard by a surface wave term. This was also shown by Thomasson [6] and others. Tracing through the procedure used by Ingard, Thomasson found that Ingard, in the process of deforming the integration path while using the saddle-point method, failed to take proper account of a pole in the integrand. It is this pole which contributes the surface wave.

In 1973, Embleton, Piercy and Olson [7, 8] introduced the term ground wave to acoustic propagation. They showed that the ground wave term was the significant term in the sound field near the ground and far from the source. Since the ground wave decays as the square of the horizontal distance from the source, it decays more rapidly than the direct and reflected waves but dominates at large distance because of the cancellation of the direct and reflected waves. But the physical interpretations of the surface wave and ground wave are still not clear.

It should be noticed that all the solution models mentioned above are based on the assumption of homogeneous atmosphere. The refrac-

tion effects due to the inhomogeneity of the atmosphere had not been considered. On the other hand, most of the available experimental data showed a difference in the sound pressure level between the homogeneous and inhomogeneous atmosphere. For example, in 1959, Wiener and Keast [9] conducted a number of measurements of the difference between the simple source model and actual sound level, the so-called excess attenuation. They found that under the conditions producing an acoustic shadow zone the excess attenuation increased rapidly away from the shadow boundary and then leveled off to an approximately constant value well inside the shadow zone. This phenomenon could not be explained by the models used then. Parkin and Scholes [10, 11], after a series of experiments in two different locations, reported that the ground excess attenuation could sometimes be negative, which differs from the theory even more. Pao and Evans [12] showed similar evidence of the disagreement between theory and experiment. More recently, Jonasson [13], on the basis of a similar study, concluded that the agreement between theory used then and experiment was quite good for the case of soft boundary, but for the case of a harder boundary there was less agreement.

Therefore, it is necessary to study the wave propagation behaviors in an inhomogeneous atmosphere, especially the behaviors of surface wave and ground wave under the conditions creating acoustic shadow zone. This is the purpose of the present project.

The two major factors which may produce the shadow zone are the wind and temperature gradients. It is more difficult to find the solution in the presence of the wind since the problem is not symmetric. But the effect of wind vector on the acoustic sound field is similar

to that of temperature gradient (temperature lapse effect is similar to upwind propagation and temperature inversion effect similar to downwind propagation). Therefore, the only focus of this study is on the temperature gradient effect.

2. FORMATION OF THE SHADOW ZONE

A ray is defined as the line perpendicular to the wave front in the absence of wind. The idea of the ray is used here to examine the mechanism of shadow zone formation in the presence of a temperature gradient.

There are two kinds of temperature gradient conditions: inversion and lapse. For the case of a temperature inversion where the temperature and consequently, the acoustic speed increases with height, the sound rays from a source above a finite impedance ground are refracted downwards (Figure 1a). This downwards refraction results in an increase of acoustic energy near the ground, and no shadow zone is created near the ground surface. Temperature inversion usually occurs during the night, especially a clear summer night. This will not be the subject of the present study.

During the daytime when a temperature lapse commonly exists, the temperature and speed of sound decrease with an increase of height. Thus, the sound rays from a point source above the ground are refracted upwards (Figure 1b). As the result of this upward refraction, there exists a ray which just grazes the ground at a distance R_g from the source. Beyond that distance, an acoustic shadow zone, into which no ray can penetrate, is observed. From Figure 1, the wave pattern in the presence of a temperature gradient, is seen to be symmetrical around the sound source. This symmetry is also the reason why the three-dimensional wave propagation problem can be simplified as a two-

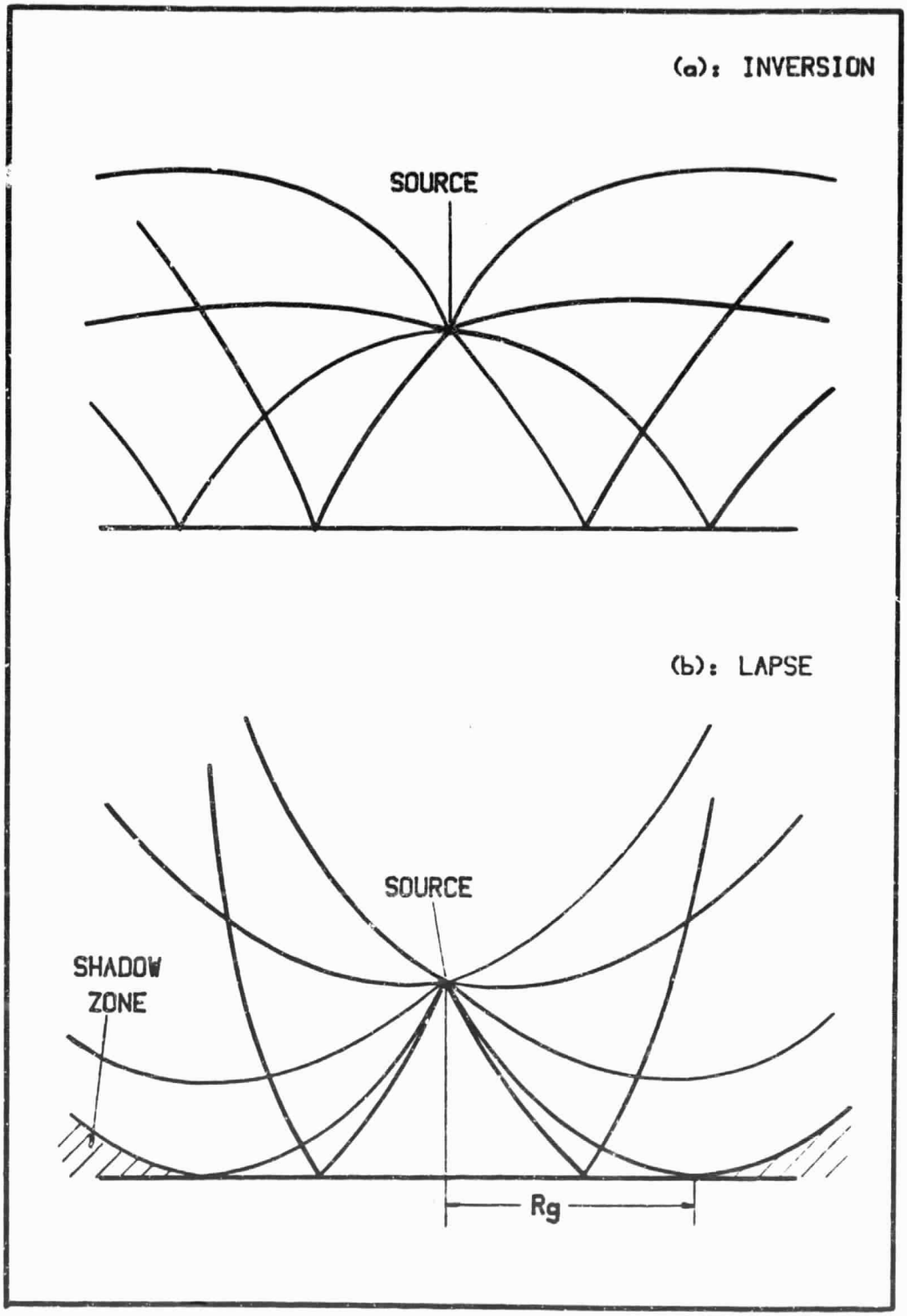

Figure 1. Sound rays in the presence of temperature.
(a) Inversion (b) Lapse

dimensional wave propagation problem.

A mathematical model of the ray pattern in the presence of a temperature lapse has been established in the previous study [14] by applying Snell's law, which shows that the physical space can be divided into seven regions (Figure 2). Each region is characterized by a different two-ray combination of direct, reflected and/or refracted rays, except for region seven which is the shadow region. It is also noticed that there are two kinds of refracted rays. To a receiver located at point A of Figure 3, refracted ray B has contacted caustic and ray C has not (Figure 3).

In this model, a temperature profile:

$$T = T_{\infty} + \frac{\Delta T}{1 + \alpha z} \tag{1}$$

is assumed, where $\Delta T > 0$ corresponds to lapse condition. This profile has been shown to fit the experimental data for a lapse condition very well [15].

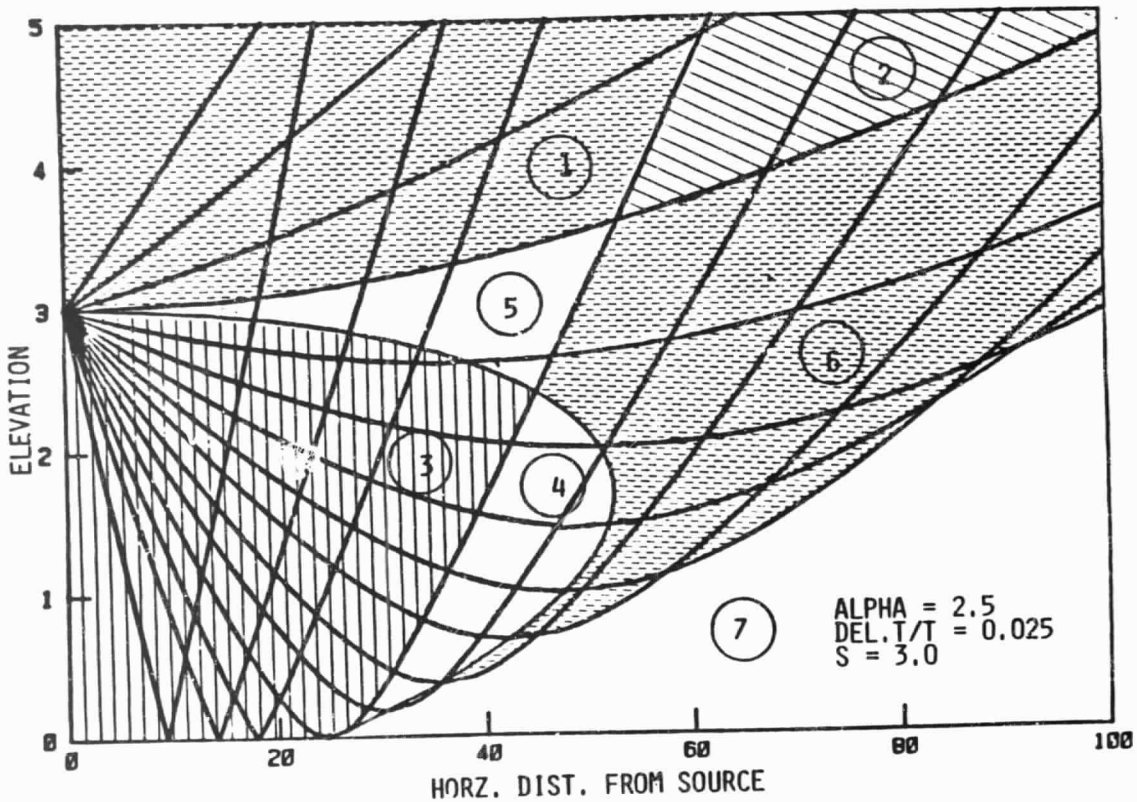

Figure 2. Ray diagram under a temperature lapse condition.

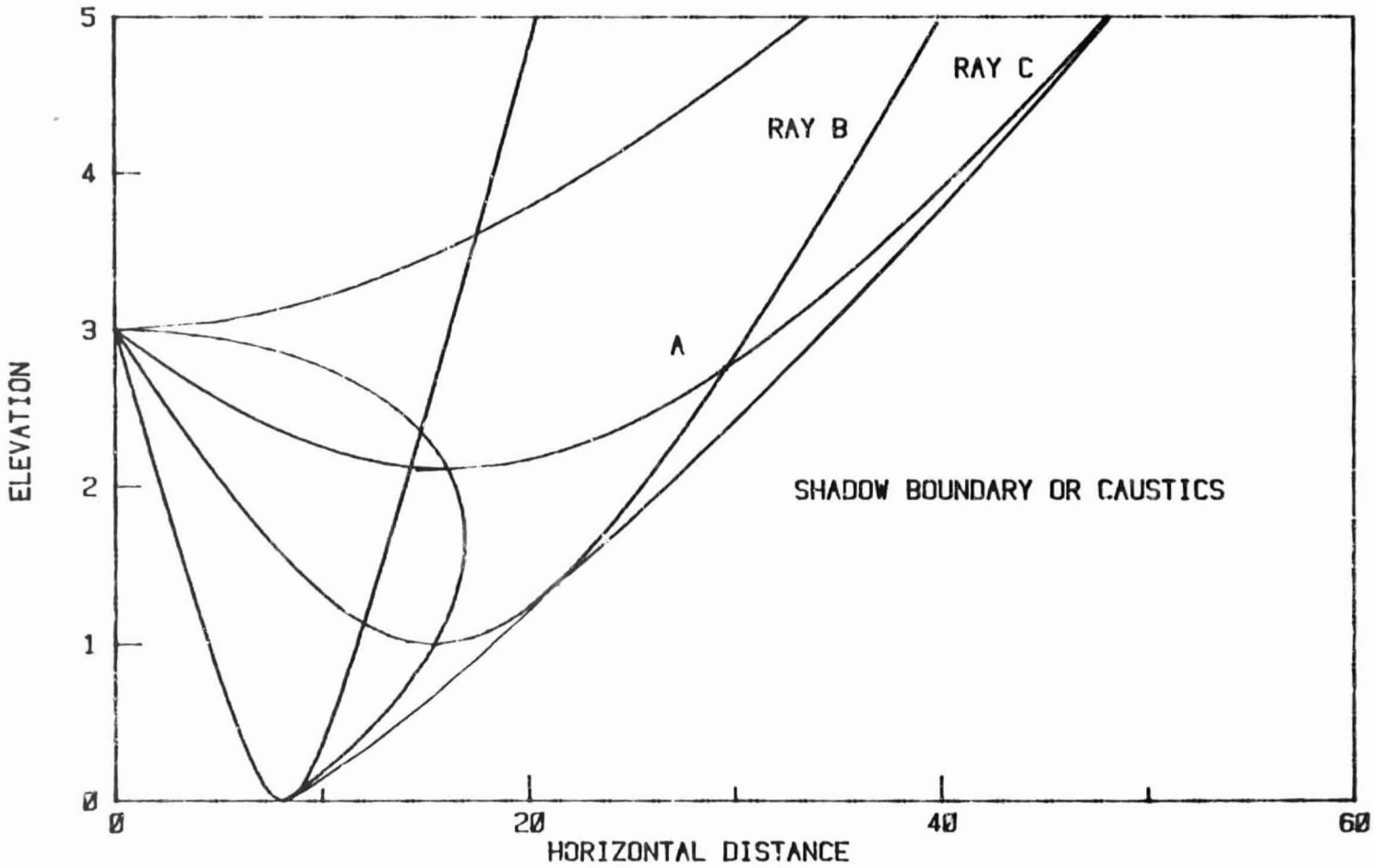

Figure 3. Ray pattern showing two kinds of refracted ray.

3. FORMAL SOLUTION

The problem of a point source over a finite impedance ground in the presence of a temperature lapse can be stated as follows. We are looking for a function $P(z,r,t)$ which satisfies the governing wave equation:

$$\frac{1}{a^2(z)} \frac{\partial^2 P}{\partial t^2} - \nabla^2 P = Q \tag{2}$$

where Q represents the source function:

$$Q = \frac{q}{\pi r} \delta(r) \delta(z - s) e^{i\omega t} \tag{3}$$

and $a(z)$ is sound speed profile:

$$a(z) = a_\infty \sqrt{1 + \frac{\Delta T}{T_\infty} \frac{1}{1 + \alpha z}} \tag{4}$$

which follows from the temperature profile (1). The solution must satisfy the boundary condition:

$$P = - W Z \tag{5}$$

at $z = 0$, where Z is the ground impedance, W is the vertical component of the acoustic velocity. A "radiation condition," which requires the waves to outgoing as either r or z tends to infinity, is also used. Due to the symmetry described in the previous section, this will be a

two-dimensional wave propagation problem, z represents elevation of the receiver and r is the horizontal distance from the source.

A solution developed by Van Moorhem [16] is used here. It gives:

$$P = e^{i\omega t}\,\bar{G}(r,z) \tag{6}$$

where $\bar{G}$ is the function of r and z only and is defined as the inverse Hankel transformation of a function G, i.e.:

$$G = \int_0^\infty \bar{G}(r,z)\; r\; J_0\,(\beta r)\; dr \tag{7}$$

$$\bar{G} = \int_0^\infty G(\beta,z)\;\beta\; J_0\,(\beta r)\; d\beta \quad . \tag{8}$$

G function in the complex plane is given as:

$$G = K\; h_2\,(\eta(\beta,z))\;[h_1(\eta(\beta,s)) + R_0\; h_2\,(\eta(\beta,s))] \tag{9}$$

in region A of the β plane (Figure 4a)

$$G = K\; h_2\,(\eta(\beta,z))\;[h_1(\eta(\beta,s)) + R_1\; h_2\,((\eta(\beta,s))] \tag{10}$$

in region B

$$G = K\; h_2\,(\eta(\beta,z))\;[h_1(\eta(\beta,s)e^{\frac{i2\pi}{3}}) + R_1\; h_2\,(\eta(\beta,s)e^{\frac{i2\pi}{3}})] \tag{11}$$

in region C

$$G = K\; h_2\,(\eta(\beta,z)e^{\frac{i2\pi}{3}})\;[h_1(\eta(\beta,s)e^{\frac{i2\pi}{3}}) + R_1\; h_2\,(\eta(\beta,s)e^{\frac{i2\pi}{3}})] \tag{12}$$

in region D for $z > s$ and

$$G = K\; h_2\,(\eta(\beta,s))\;[h_1(\eta(\beta,z)) + Ro\; h_2\,(\eta(\beta,z))] \tag{13}$$

in region E (Figure 4b)

$$G = K\, h_2\,(\eta(\beta,s))\,[h_1(\eta(\beta,z)) + R_1\, h_2\,(\eta(\beta,z))] \tag{14}$$

in region F

$$G = K\, h_2\,(\eta(\beta,s))\,[h_1(\eta(\beta,z)e^{\frac{i2\pi}{3}}) + R_1\, h_2\,(\eta(\beta,z)e^{\frac{i2\pi}{3}})] \tag{15}$$

in region G

$$G = K\, h_2\,(\eta(\beta,s)e^{\frac{i2\pi}{3}})\,[h_1(\eta(\beta,z)e^{\frac{i2\pi}{3}}) + R_1\, h_2\,(\eta(\beta,z)e^{\frac{i2\pi}{3}}) \tag{16}$$

in region H for $z < s$, where

$$K = \frac{q}{12i\ \lambda^{2/3}}\ \frac{1}{\sqrt{g_z(\beta,s)}}\ \frac{1}{\sqrt{g_z(\beta,z)}} \tag{17}$$

$$R_0 = \frac{T_1\, h_1\,(\eta(\beta.0)) + i\ T_2\, h_1'\,(\eta(\beta,0))}{T_1\, h_2\,(\eta(\beta.0)) + i\ T_2\, h_2'\,(\eta(\beta,0))} \tag{18}$$

$$R_1 = \frac{e^{-i\frac{\pi}{6}}}{e^{i\frac{\pi}{6}} - iR_0} \tag{19}$$

and

$$T_1 = \alpha\ \lambda - \frac{i}{2}\ \frac{Z}{\rho a_\infty}\ \frac{g_{zz}\,(\beta,0)}{g_z\,(\beta,0)} \tag{20}$$

$$T_2 = \frac{Z}{\rho a_\infty}\ (2/3\lambda)^{2/3}\ g_z\,(\beta,0) \tag{21}$$

$$\eta = (2/3\lambda)^{3/2}\ g(\beta,0) \quad . \tag{21}$$

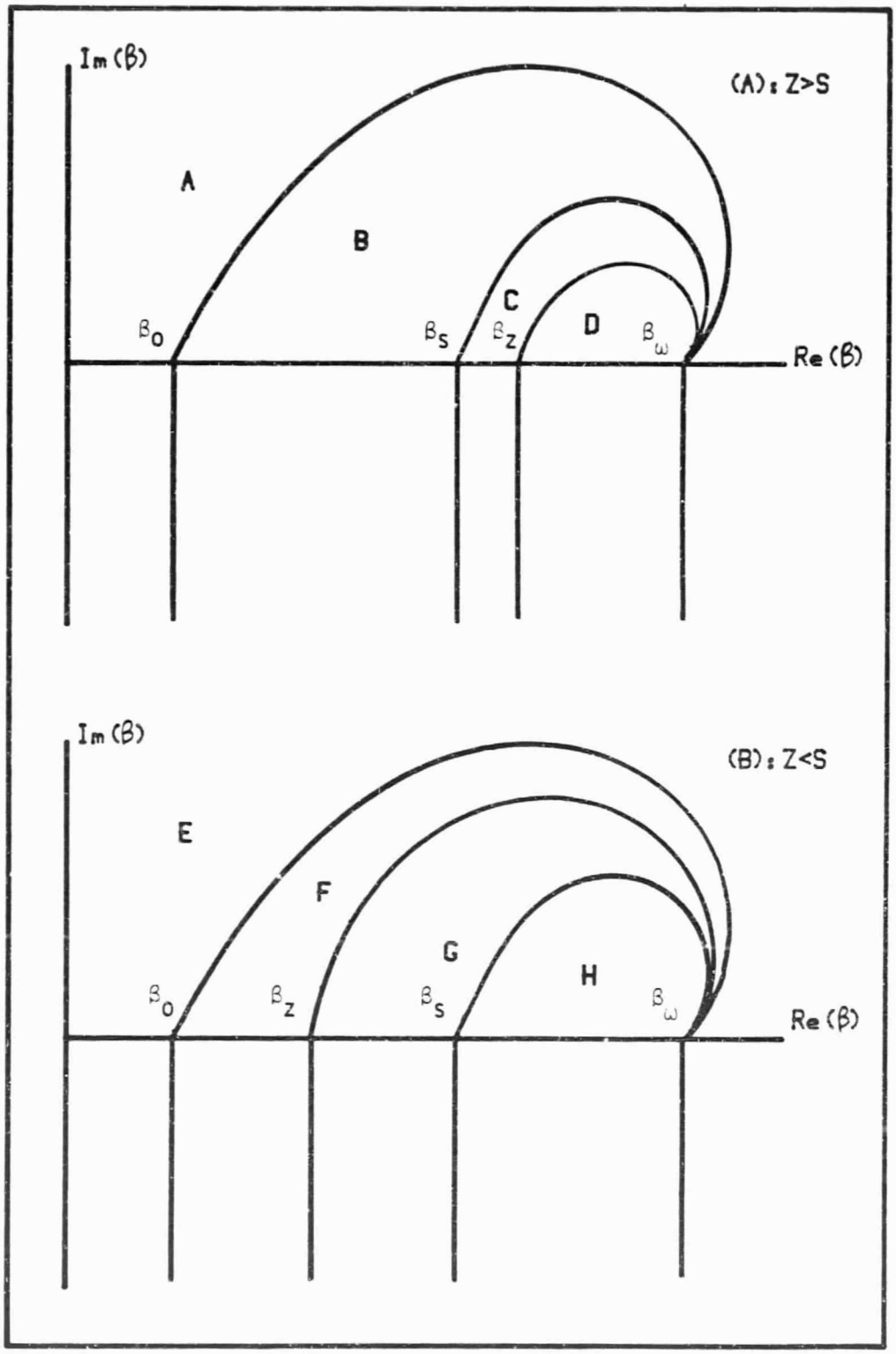

Figure 4. The valid regions of solutions in complex β plane.

The g function is defined by

$$g^{3/2}(\beta,z) = \sqrt{(1 + \alpha z + \frac{\Delta T}{T_\infty})\left((1 - \frac{a_\infty^2}{\omega^2}\beta^2)(1 + \alpha z + \frac{\Delta T}{T_\infty}) - \frac{\Delta T}{T_\infty}\right)}$$

$$- \frac{1}{2}\frac{\Delta T}{T_\infty} \frac{1}{\sqrt{1 - \frac{a_\infty^2}{\omega^2}\beta^2}} \ln\left(\frac{1 + \phi}{1 - \phi}\right) \tag{23}$$

$$\phi = \frac{(1 - \frac{a_\infty^2}{\omega^2}\beta^2)(1 + \alpha z + \frac{\Delta T}{T_\infty}) - \frac{\Delta T}{T_\infty}}{(1 - \frac{a_\infty^2}{\omega^2}\beta^2)(1 + \alpha z + \frac{\Delta T}{T_\infty})} . \tag{24}$$

The function $g(z,\beta)$ has two branch points, one at

$$\beta = \beta_z = \frac{\omega}{a_\infty}\sqrt{\frac{1 + \alpha z}{1 + \alpha z + \frac{\Delta T}{T_\infty}}} \tag{25}$$

and the other at $\beta = \beta\omega = \omega/a_\infty$. It is noticed that equations (11) to (18) contain the functions $g(0,\beta)$, $g(s,\beta)$ and $g(z,\beta)$. Thus these solutions involve four branch points β_0, β_s, β_z, and β_ω. These branch branch points form the boundaries of regions of different forms of the solution on the real β axis. The regions of validity of these solutions in the complex β plane are separated by the branch cuts of the different g functions. Each g function has two branch cuts. The first branch cut results from a square root in the g function and is chosen such that $\sqrt{-1} = -i$, which is required to produce the exponentially decay behavior of the pressure in the far field. The second branch line is the result of taking the 2/3 power to calculate g from $g^{3/2}$.

It is also noticed that every form of the solutions consists of two terms. The first term involves no ground impedance and represents the direct wave term. The other term which includes the effect of the ground is the reflected or refracted wave term. Physically the four branch points β_0, β_s, β_z, and β_ω represent the rays which have the turning points at height of zero, s, z and infinity, correspondingly. Thus, the second term in the solutions represents a ray which is reflected by the ground for real β, where $0 < \beta < \beta_0$, a refracted ray which has the turning point above the ground and below the altitude of the receiver for real β and $\beta_0 < \beta < \beta_z$ or a ray which has the turning point above the receiver and less than infinty for real β and $\beta_z < \beta < \beta_\omega$. Those rays which have the turning points above the source, or real β and $\beta_s < \beta < \beta_\omega$, are not seen in the ray diagram (Figure 3). For $\beta > \beta_\omega$ or $\mathrm{Im}(\beta) \neq 0$, the physical interpretation is not clear.

These solutions are very complicated to evaluate since the inverse Hankel transformation has to be carried out. Some approximating methods have to be adopted. The approximation used here is the saddle point method.

4. SADDLE POINT METHOD

The saddle point method has been frequently and successfully used in research on the wave propagation problems. It is an approximate integration method for integrals of the form [17, 18]:

$$I(\nu) = \int_C F(\beta) e^{\nu f(\beta)} d\beta \tag{26}$$

where ν is a large parameter and c is a contour in the complexe β plane. From complex variable theory, it is known that the integration path can be deformed while taking the proper account of the poles of the integrand. What then would be desirable is to deform the path so that there is very little contribution to the value of the integral over the whole path except in the immediate neighborhood of one or more points on the path, where practically the entire contribution takes place. These points are found to be the saddle points, where

$$\left.\frac{\partial f}{\partial \beta}\right|_{\beta = \beta_{sp}} = 0 \quad . \tag{27}$$

Around these points the function surface looks like a saddle or a mountain pass. If the path is chosen such that the exponential term in (26) decreases rapidly as one moves away from the saddle points, the objective is achieved. This path is call a steepest descent integration path and is defined by requiring

$$\mathrm{Im}\,(f(\beta)) = \text{const.} = \mathrm{Im}\,(f(\beta_{sp})) \tag{28}$$

to eliminate oscillations in the integral and allow only decay. This results in the approximate integration.

$$I(\nu) = \sqrt{\frac{2\pi}{-\lambda \dfrac{\partial^2 f}{\partial \beta^2}}}\; F(\beta_{sp}) e^{\nu f(\beta_{sp}) + i\theta} \tag{29}$$

where θ is the angle at which the path of the integration crosses the saddle point. If no saddle point has been found, the integral can be approximated as zero.

Applying the saddle point approach to the present problem, the inverse Hankel transform is first rewritten into the form

$$\bar{G}\,(r,z) = \frac{1}{2} \int_{-\infty}^{\infty} G(\beta,z)\; \beta\; H_0^{(2)}\,(\beta r)\; d\beta\;. \tag{30}$$

The exponential terms are obtained by assuming the argument of the Hankel functions are sufficiently large and the use of asympototic forms are valid. It then follows that for every point in the physical space, two saddle points occur, each corresponds to a specific ray which passes through that point, a direct, reflected or refracted ray. Extra caution has to be taken while tracing the integration path, since several branch cuts exist in the β plane. It will be possible for the integration path to run into a branch cut, which will require a term beyond the simple saddle point result.

A detailed examination of the integration path has been made. For the direct wave (Region 1, 2, 3, 4 of Figure 2), the integration path crosses the real β axis at the saddle point at an angle of $\pi/4$ and the

whole path will not interfere with any branch cuts (Figure 5). For a reflected wave (Region 1, 3, 5), the path of integration also crosses the real β axis at the saddle point at an angle of $\pi/4$. The path is also simple for most cases, but under certain conditions the path may run into the branch cut of the $g(0,\beta)$ function in the upper β plane, c_1 in Figure 6, and moves along this branch line, then reappears on the same side of the branch line (Figure 6). Note that Van Moorhem [16] has shown that although c_1 is a branch line for g function, the integral is continuous across it. For the refracted wave which has already contacted the caustic (Region 2, 4, 6), the path will run into both branch cuts of the $g(0,\beta)$ function, c_1 and c_2 in Figure 7. The path starts at $-\infty$, and runs into branch line c_2 first and reappears right at the other side of this branch cut. It then passes through the saddle point at an angle of $\pi/4$ and runs into the branch cut c_1. Two possibilities exist after this: it might move along the c1 line and reappear at the other side of c1 (Figure 7); or it might move along the c_1 line and run into the branch point β_ω. In the latter case, a modified path has to be chosen such that the path will not run into the branch point β_ω where the g function is infinite. This modified path is shown in Figure 8 and requires a constant phase of $\pi/4$ as the path moves away from the point β_ω.

For the refracted wave which has not contacted the caustic (Region 5, 6), the path of integration is quite different. This path will cross the saddle point at an angle of $3\pi/4$ rather than $\pi/4$ as in the other cases. The upper part of the path will turn right and merge into branch cut c1. The two situations discussed above then hold here. The lower part of the path will disappear into the branch line c_4 (Figure 9).

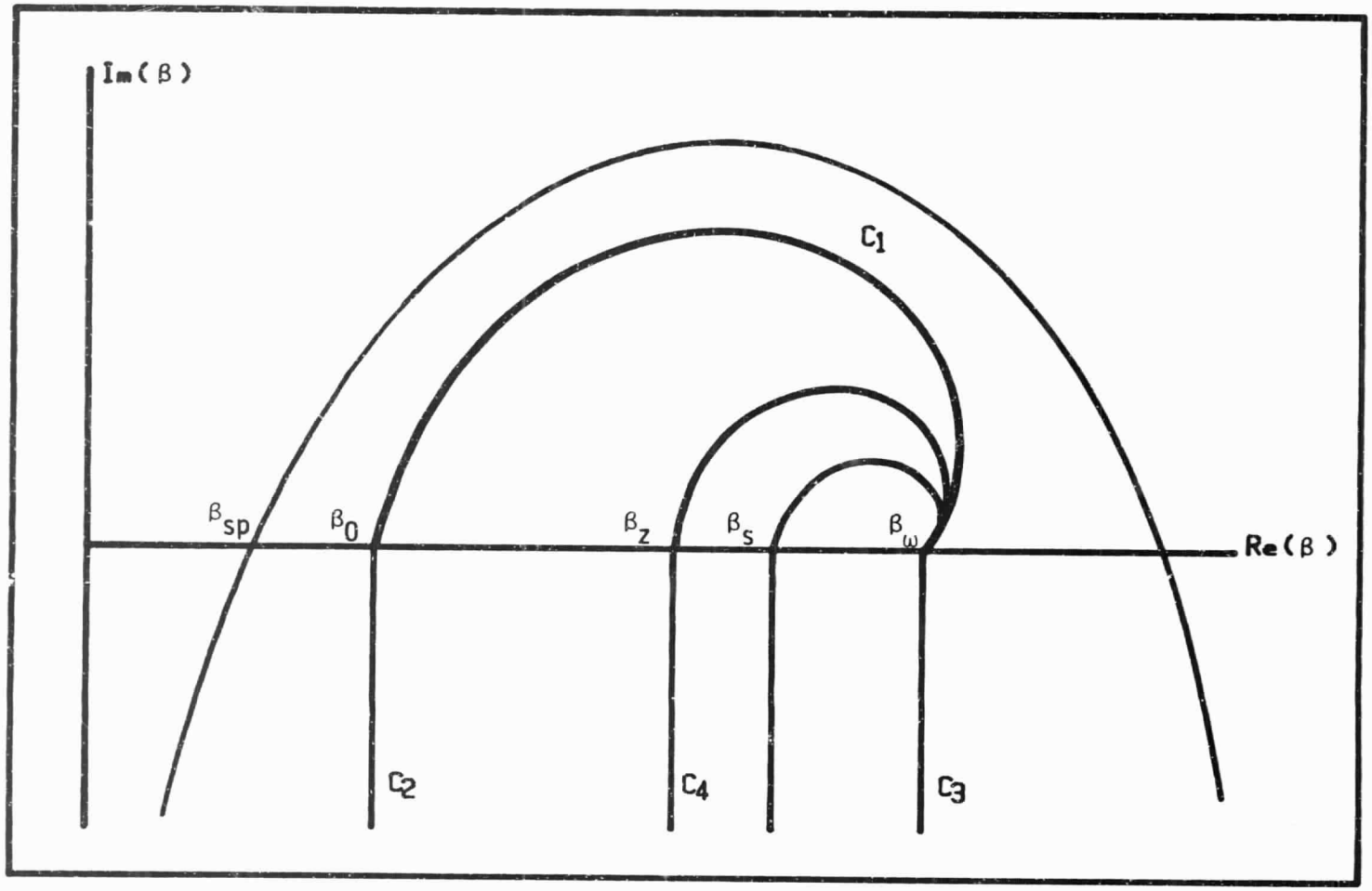

Figure 5. Integration path associated with direct and reflected waves.

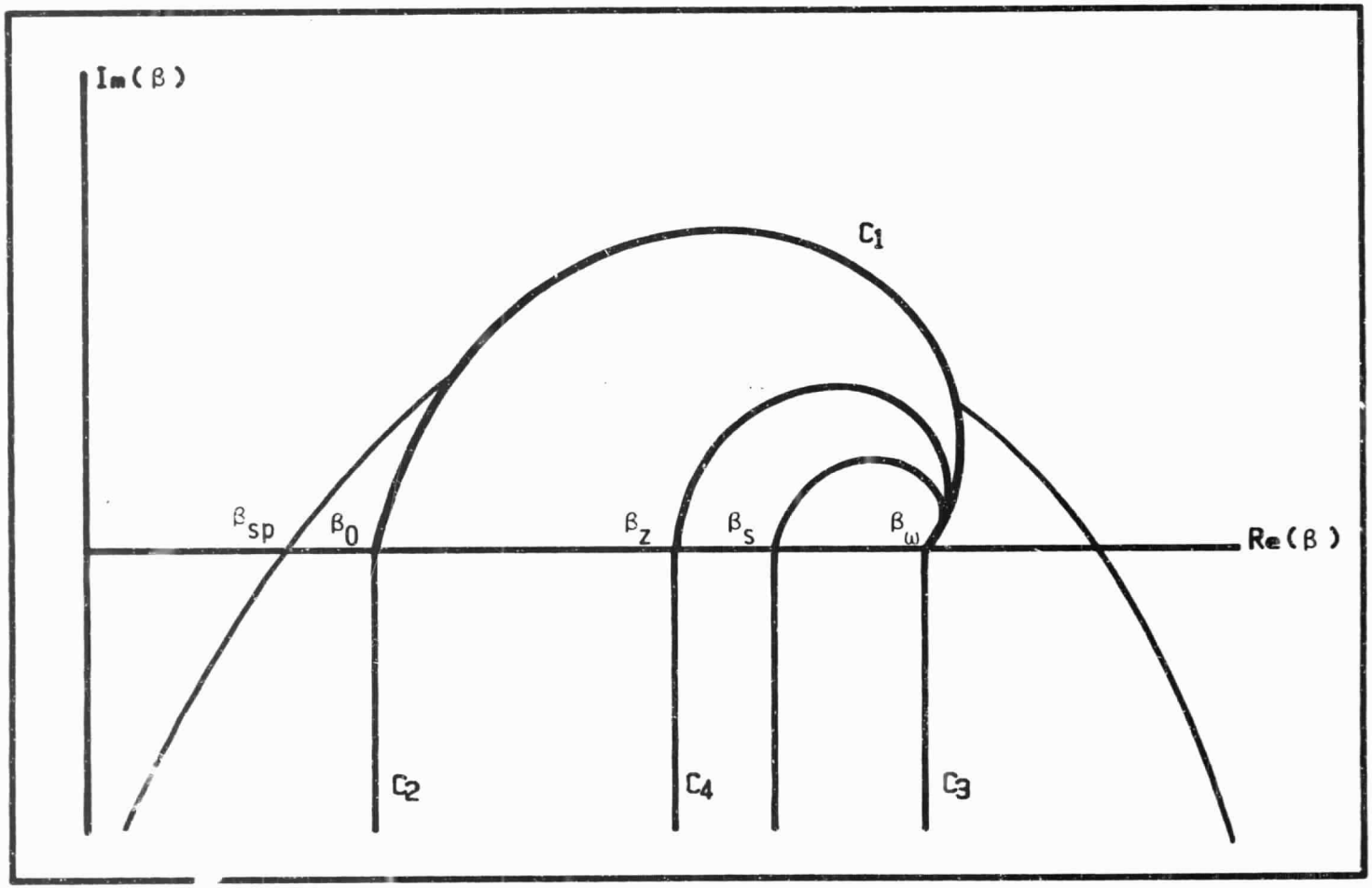

Figure 6. Integration path associated with reflected waves.

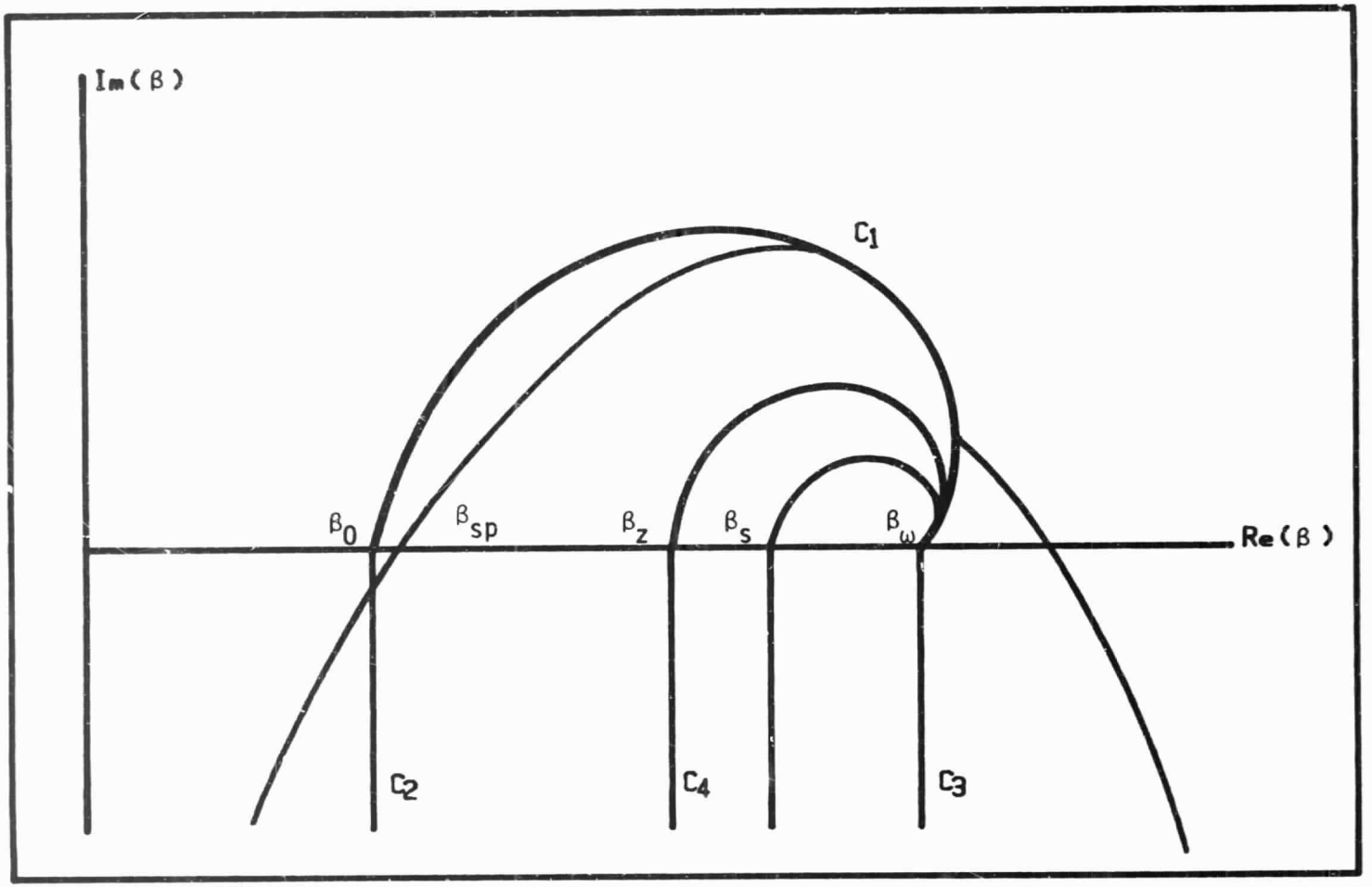

Figure 7. Integration path associated with refracted waves which could have contacted caustics.

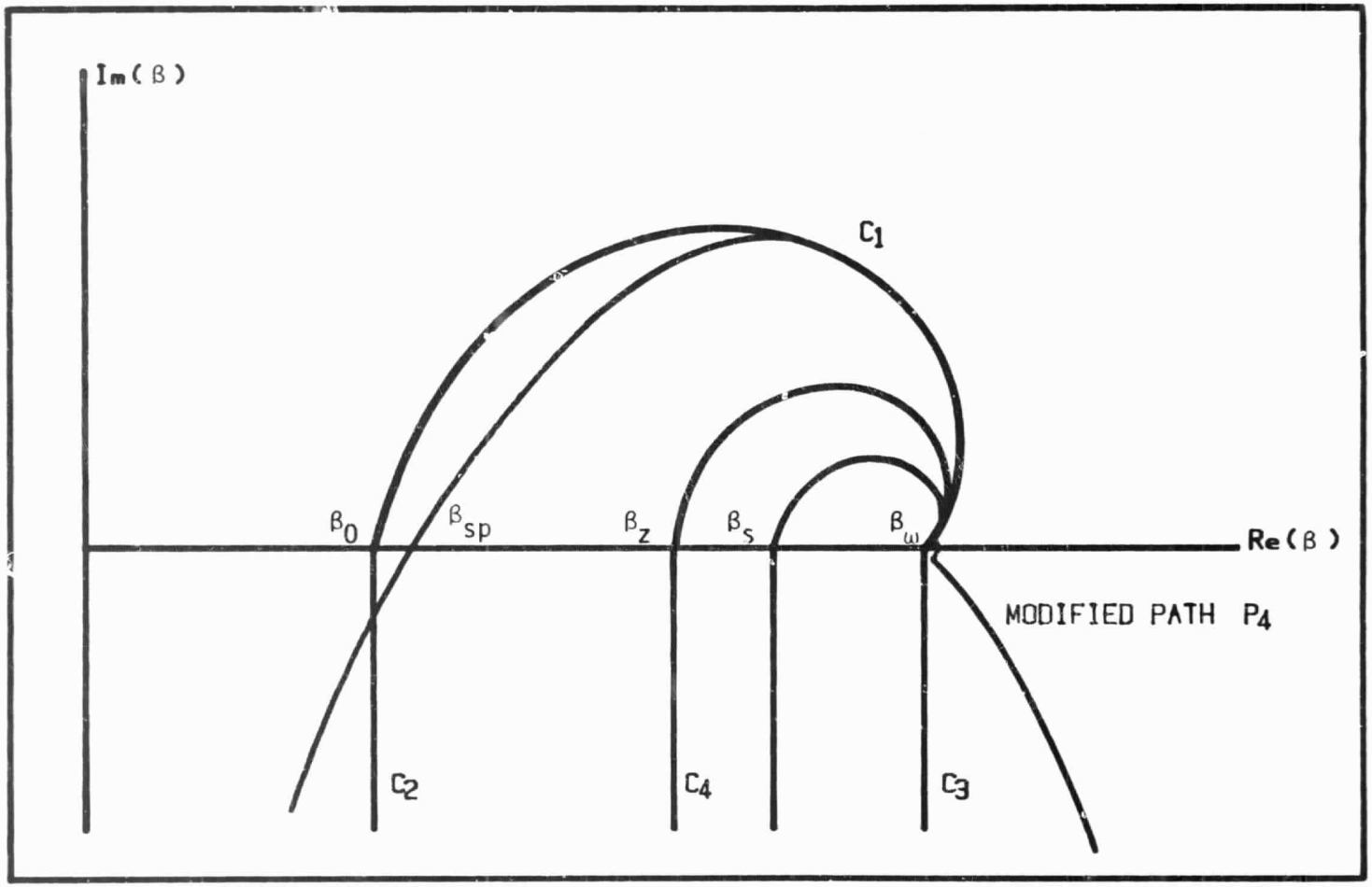

Figure 8. Integration path also associatd with refracted waves which have contacted caustics.

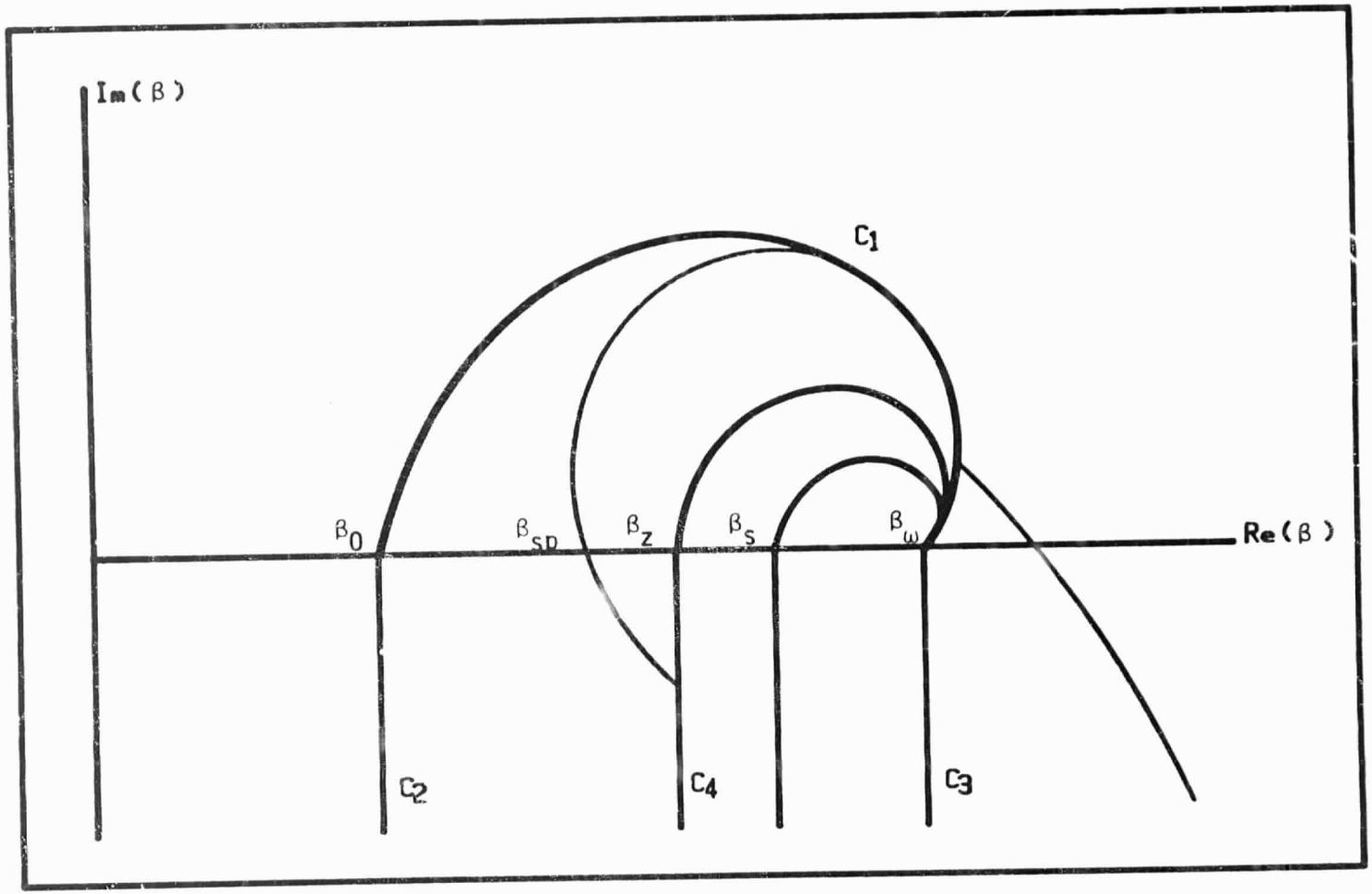

Figure 9. Integration path associated with refracted waves which have not contacted caustics.

But it is noticed that in Regions 5 and 6, both saddle points result from the second term of the solution. The integral for the first term, the direct wave term, will be approximated as zero since no saddle point has been found for this term. Furthermore, since the two saddle points come from the same term, a single path has to be found such that coincides with most parts of the integration paths of the two saddle points and passes through these two points. The simplest path which has all these properties is shown in Figure 10. It consists of four parts: p_1 coincides with part of the integration path of first saddle point; p_2 is a straight line which connects both saddle points; p_3 coincides with part of the integration path of the second saddle point; and p_4 is the modified steepest descent path. The integration along path p_2 can be done numerically. Physically, this integral represents the contribution of those rays radiated from an infinity height between the two rays represented by the two saddle points. Since these rays do not pass through the source, these contributions are practically small and are ignored in this study. The saddle point approximation still holds for the integration along p_1 and p_3. The integration along the p_4 is done by expanding the integrand around point β_ω and the result will be presented later in this section.

For a point in the shadow region, we can still find two saddle points. These saddle points are complex and represent rays with complex angles. Their physical meaning is not clear, but the path of integration for these saddle points have the same characteristics of the cases described above (Figure 11).

Thus, we come to the final solutions. For direct waves with $z > s$, Regions 1 and 2 of Figure 2, we get:

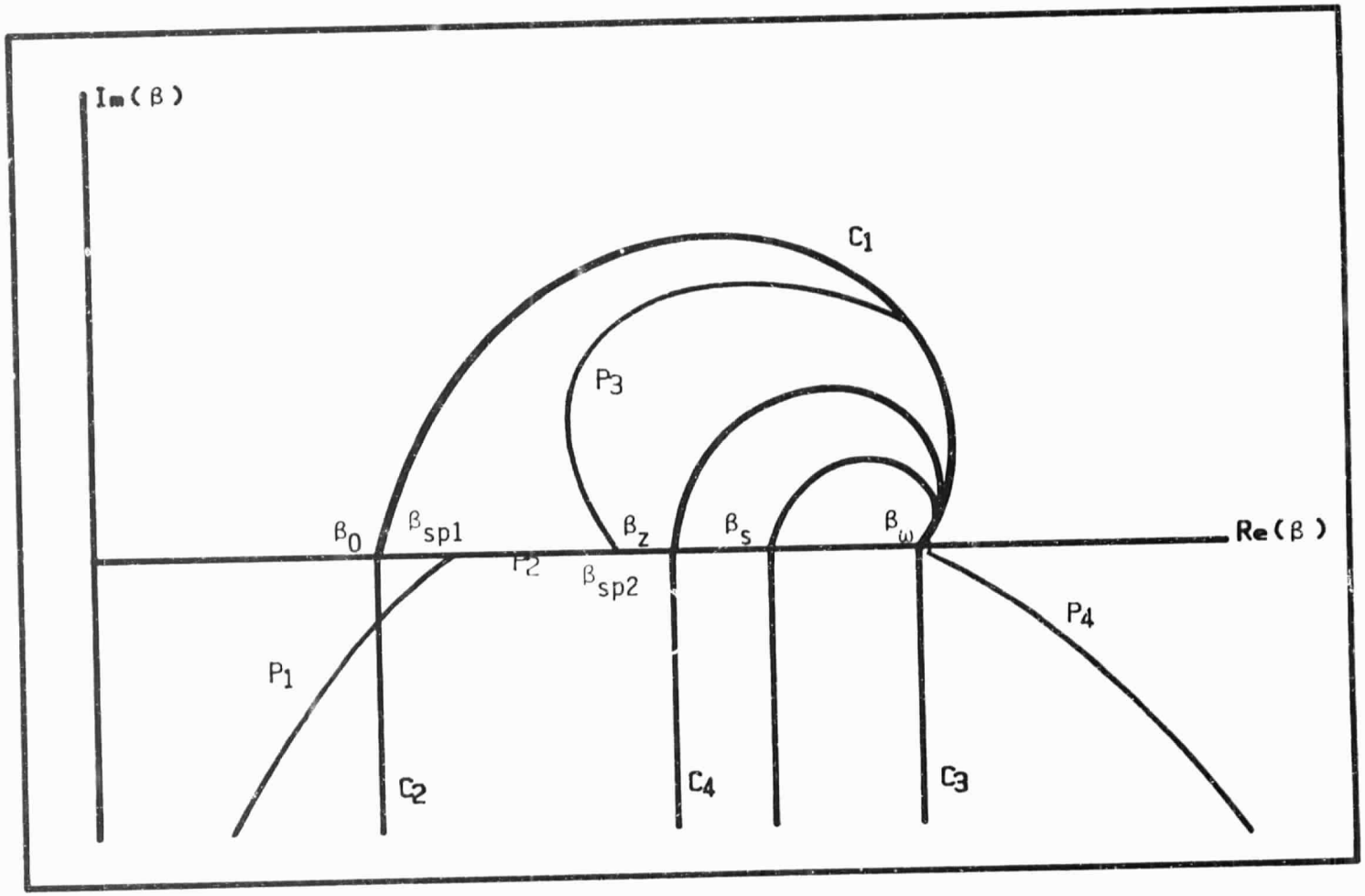

Figure 10. Integration path associated with two saddle points.

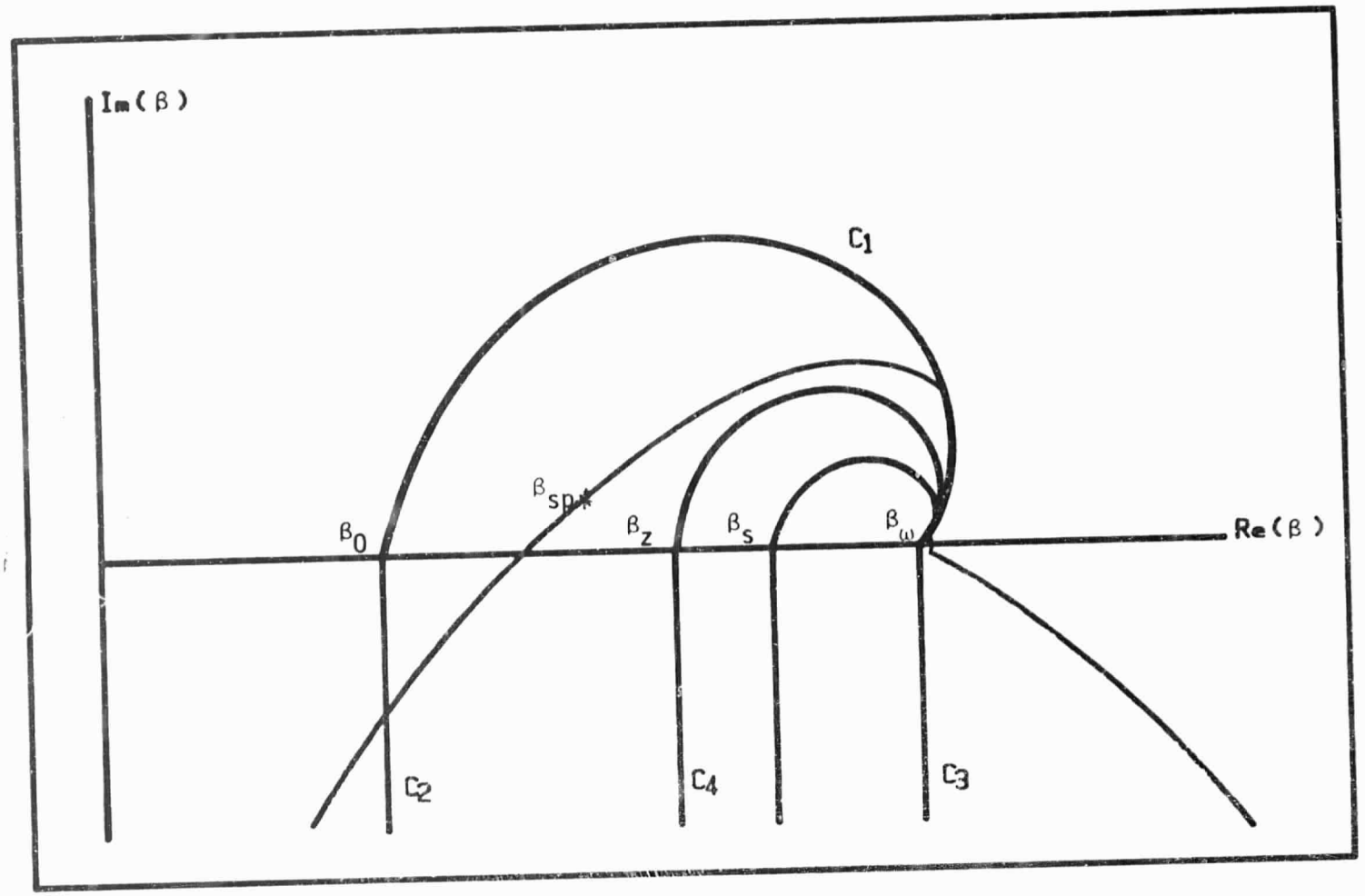

Figure 11. Integration path associated with complex saddle point.

$$\bar{G}_D = \frac{\sqrt{2\pi}\, K_3}{\sqrt{-\frac{\partial^2 \phi_1}{\partial \beta^2}}} \; e^{-i\left(\beta_{sp} r - \frac{\pi}{2}\right)} \; h_2\left(\eta(\beta_{sp}, z)\right) \; h_1\left(\eta(\beta_{sp}, s)\right) \qquad (31)$$

where

$$\phi_1 = -\lambda\, g^{2/3}(\beta, s) + \lambda\, g^{2/3}(\beta, z) - \frac{\pi}{2} \qquad (32)$$

and β_{sp} is the root of

$$r + \frac{\partial \phi_1}{\partial \beta} = 0 \quad . \qquad (33)$$

For direct waves with $z < s$, Region 3 and 4 of Figure 2, we get:

$$\bar{G}_D = \frac{\sqrt{2\pi}\, K_3}{\sqrt{-\frac{\partial^2 \phi_2}{\partial \beta^2}}} \; e^{-i\left(\beta_{sp} r - \frac{\pi}{2}\right)} \; h_1\left(\eta(\beta_{sp}, z)\right) \; h_2\left(\eta(\beta_{sp}, s)\right) \qquad (34)$$

where

$$\phi_2 = \lambda\, g^{3/2}(\beta, s) - \lambda\, g^{3/2}(\beta, z) - \frac{\pi}{2} \qquad (35)$$

and β_{sp} is the root of

$$r + \frac{\partial \phi_2}{\partial \beta} = 0 \, . \qquad (36)$$

For reflected waves, Regions 1, 3 and 5 of Figure 2, we get:

$$\bar{G}_R = \frac{\sqrt{2\pi}\, K_3}{\sqrt{-\frac{\partial^2 \phi_3}{\partial \beta^2}}}\, e^{-i(\beta_{sp} r - \frac{\pi}{2})} \left(h_2(\eta(\beta_{sp},z)) h_2(\eta(\beta_{sp},s))\right) \tag{37}$$

where

$$\phi_3 = \lambda\, g^{3/2}(\beta,s) + \lambda\, g^{3/2}(\beta,z) - 2\lambda\, g^{3/2}(\beta,o) - \frac{\pi}{2} \tag{38}$$

and β_{sp} is the root of

$$r + \frac{\partial \phi_3}{\partial \beta} = 0 \quad . \tag{39}$$

For refracted waves which have not contacted the caustic, Regions 4, 5 and 6 of Figure 2, we obtain

$$\bar{G}_R = \frac{\sqrt{2\pi}\, K_3\, R_1(\beta_{sp})}{\sqrt{-\frac{\partial^2 \phi_4}{\partial \beta^2}}}\, e^{-i(\beta_{sp} r - \pi)}\, h_2(\eta(\beta_{sp},z))\, h_2(\eta(\beta_{sp},s)) \tag{40}$$

where

$$\phi_4 = \lambda\, g^{3/2}(\beta,s) + \lambda\, g^{3/2}(\beta,z) + \frac{11}{6}\pi \tag{41}$$

and β_{sp} is the root of

$$r + \frac{\partial \phi_4}{\partial \beta} = 0 \quad . \tag{42}$$

For refracted waves which have contacted the caustic, Regions 2, 4 and 6 of Figure 2, we get:

$$G_R = \frac{\sqrt{2\pi}\ K_3\ R_1}{\sqrt{-\frac{\partial^2 \phi_5}{\partial \beta^2}}}\ e^{-i(\beta_{sp}\, r - \frac{\pi}{2})}\ h_2\ (n(\beta_{sp},z))\ h_2\ (n(\beta_{sp},s)) \tag{43}$$

where

$$\phi_5 = \phi_4 - \frac{\pi}{2} \tag{43}$$

and β_{sp} is also a root (and the smaller of the two roots for Region 6) of (42). And

$$K_3 = \frac{q}{24i\ \lambda^{2/3}} \sqrt{\frac{1}{g_z\ (\beta_{sp},z)}}\ \sqrt{\frac{1}{g_z\ (\beta_{sp},s)}} \sqrt{\frac{2\ \beta_{sp}}{\pi r}}\ . \tag{45}$$

If the modified path p4 is used, an extra term

$$\bar{G}_g = \frac{q}{8\ \alpha\lambda\pi} \sqrt{\frac{2\omega}{\pi r a_\infty}} \sqrt{\frac{T_\infty}{\Delta T}}$$

$$\frac{(1 + \alpha z + \frac{\Delta T}{T_\infty})^{1/4}\ \ (1 + \alpha s + \frac{\Delta T}{T_\infty})^{1/4}}{-ir - \frac{2}{3}\ \frac{a_\infty}{\omega} \sqrt{\frac{T_\infty}{\Delta T}} \left[(1 + \alpha z + \frac{\Delta T}{T_\infty})^{3/2} + (1 + \alpha s + \frac{\Delta T}{T_\infty})^{3/2} - 2\ (1 + \frac{\Delta T}{T_\infty})^{3/2}\right]}$$

$$\frac{(1 - \frac{i}{2}\frac{a_\infty}{\omega}\ \frac{Z}{\rho a_\infty}\ \frac{g_{zz}(0)}{g_z(0)}) - \frac{Z}{\rho a_\infty}\ \frac{a_\infty}{\omega}\ \frac{3}{2}\lambda\ \ g_z(0)\ g^{1/2}(0)}{(1 - \frac{i}{2}\frac{a_\infty}{\omega}\ \frac{Z}{\rho a_\infty}\ \frac{g_{zz}(0)}{g_z(0)}) - \frac{Z}{\pi a_\infty}\ \frac{a_\infty}{\omega}\ \frac{3}{2}\lambda\ \ g_z(0)\ g^{1/2}(0)} \tag{46}$$

$$e^{-i\frac{\omega}{a_\infty} r - 2\lambda\sqrt{\frac{\Delta T}{T_\infty}} \left(\sqrt{1 + \alpha z + \frac{\Delta T}{T_\infty}} + \sqrt{1 + \alpha z + \frac{\Delta T}{T_\infty}} - 2\sqrt{1 + \frac{\Delta T}{T_\infty}}\right) + \frac{\pi}{4} i}$$

has to be included. This term decays as -3/2 power of the horizontal distance but it will be the dominant term far into the shadow. Physically, this term represents a ground wave-like term but it is not exactly a ground wave since the ground wave decays as -2 power of the horizontal distance.

One problem with this approach is that at the shadow boundary we have

$$\frac{\partial^2 \phi_4}{\partial \beta^2} = \frac{\partial^2 \phi_5}{\partial \beta^2} = 0 \tag{47}$$

and a singularity occurs in (40) and (43). To avoid this singularity, a method presented by Saches and Silbiger [19] is used, which gives a nonuniform asymptotic solution valid around the shadow boundary. This approach gives

$$\bar{G}_R = 2\pi K_3(\beta_c) R_1(\beta_c) \left(\frac{\partial^3 \phi_4}{\partial \beta^3}\right)^{1/3} e^{-i(\beta_c r - \frac{\pi}{4})}$$

$$A_i\left(\left(\frac{\partial^3 \phi_4}{\partial \beta^3}\right)^{1/3} \Delta r\right) h_2(n(\beta_c, z)) \cdot h_2(n(\beta_c, s)) \tag{48}$$

where β_c is the root of

$$\frac{\partial^2}{\partial \beta^2}(\phi_4(\beta_c)) = 0 \tag{49}$$

and

$$\Delta r = r - r_c \tag{50}$$

where r_c is the caustic radius

$$r_c = - \frac{\partial}{\partial \beta} (\phi 4 \ (\beta_c)) \quad . \tag{51}$$

Reference 20 shows this solution is equivalent to the one-term series expansion of the uniform asymptotic formulation which can be approximately used in the shadow region.

5. SURFACE WAVE

A surface wave is a wave whose amplitude exponentially decays with the height above the ground and decreases with the distance from the source as the product of a -1/2 power and an exponential. Thus, for a certain range of distance r, if the exponential term is weak, this $r^{-1/2}$ decrease of the amplitude will make the surface wave dominant in the pressure field near the ground.

As suggested by most of the previous researchers, the surface wave is the result of the presence of the ground with complex impedance, and mathematically it results from the contribution of a pole which is located inside the path of integration.

Examining the solution forms, Equations (9) through (16), it is found that only two terms involve the ground impedance, R_0 and R_1. An effort has been made to find the poles of these two terms.

The method used here is called the modified Newton method which is valid to find the root of an equation of a complex variable

$$F(\beta) = 0 \tag{52}$$

where β is a complex variable. Since the terms R_0 and R_1 involve the ground impedance, either experimental data or a model must be used. The impedance model suggested by Chessell [21] is adapted here, which gives

$$Z = R + i\,X \tag{53}$$

where

$$\frac{R}{\rho a_\infty} = 1 + 9.08 \left(\frac{f}{\sigma}\right)^{-.75} \tag{54}$$

$$\frac{Z}{\rho a_\infty} = - 11.9 \left(\frac{f}{\sigma}\right)^{-.73} \tag{55}$$

where σ is the flow resistance and f is the frequency. This model has been shown to fit the experimental data very well. For the grass covered ground, such as one around an airport, the flow resistance σ is suggested to be between 150-300 c.g.s. unit by Piercy and Embleton [22].

Numerical calculation shows that the poles of R_1 are located inside the region A or E of the complex β plane in Figure 4 where the solution forms involving R_1 are not valid. Thus, these poles do not give any contribution to the total solution.

On the other hand, the poles of R_0 are of great interest. It is initially noticed that when temperature gradient is zero, an exact solution of the wave Equation (2) is obtainable. A set of poles of this exact solution for different ratios of σ/ω is then calculated, and so is a similar set of poles of R_0 for $\Delta T/T_\infty$ near zero. A comparison shows that these two sets of poles are located very close to each other as would be expected. Thus, it appears that these are related and it is the surface wave producing poles.

Pole of R_0 a ? also found for larger values of $\Delta T/T_\infty$. These poles are located at the right hand side of the branch cut c_3 (Figure 12). For certain combinations of $\Delta T/T_\infty$, σ, α and ω, the poles are found to be located inside the integration path. Therefore the residues of the poles

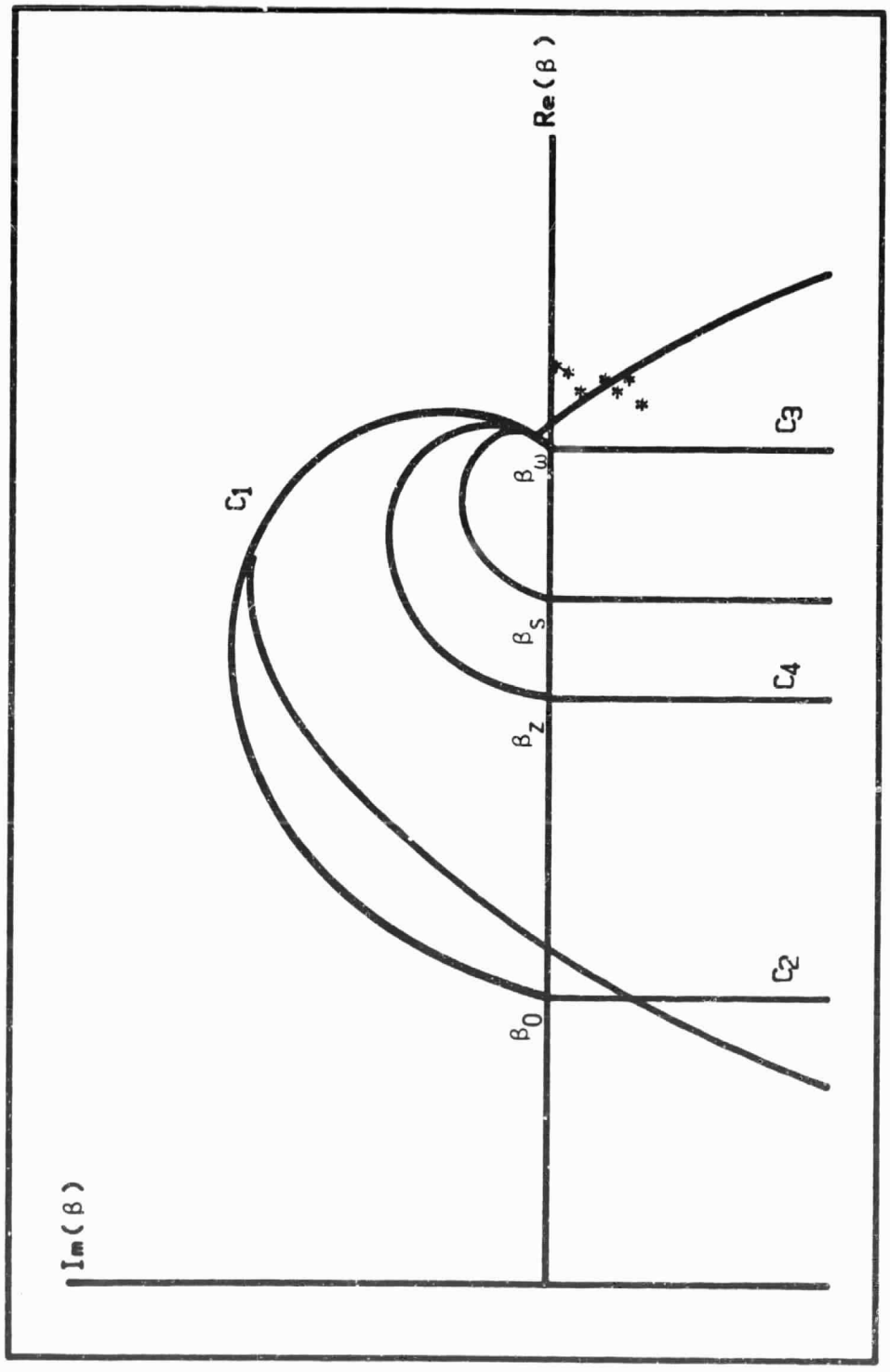

Figure 12. Locations of the poles.

have to be added into the total solution according to the Residue Theorem. The residue is given as

$$\bar{G}_s = -i\pi K\beta_p H_0^{(2)}(\beta_p r)\, h_2(\eta(\beta_p,z))\, h_2(\eta(\beta_p,s)) \cdot \frac{-T_1 h_1(\eta(\beta_p,0)) + i T_2 h_1'(\eta(\beta_p,0))}{\frac{\partial}{\partial\beta}(T_1 h_2(\eta(\beta_p,0)) + i T_2 h_2'(\eta(\beta_p,0)))} \tag{56}$$

or using the asymptotic form

$$\bar{G}_s = -i\pi K\sqrt{\frac{2\beta_p}{\pi r}}\, h_2(\eta(\beta_p,z))\, h_2(\eta(\beta_p,s))\, e^{-i\beta_p r + i\frac{\pi}{4}} \cdot \frac{-T_1 h_1(\eta(\beta_p,0)) + i T_2 h_1'(\eta(\beta_p,0))}{\frac{\partial}{\partial\beta}(T_1 h_2(\eta(\beta_p,0)) + i T_2 h_2'(\eta(\beta_p,0)))} . \tag{57}$$

This residue is found to describe a surface wave which exponentially decays with the height from the surface (Figure 13) and is the product of an exponentially decreasing term, since the pole locates at the lower β plane, and the reciprocal of the square root of distance from the source. It is also noticed that these poles which might be located inside the integration paths are very close to the real β axis, i.e.,

$$0 < -\mathrm{Im}(\beta_p) \ll 1 \quad . \tag{58}$$

Therefore, in the midrange of the horizontal distance, the exponential decay is quite weak which makes the surface wave a dominant component in the pressure field near the ground. But in the far field, the exponential decay behavior will quench the surface wave (Figure 14).

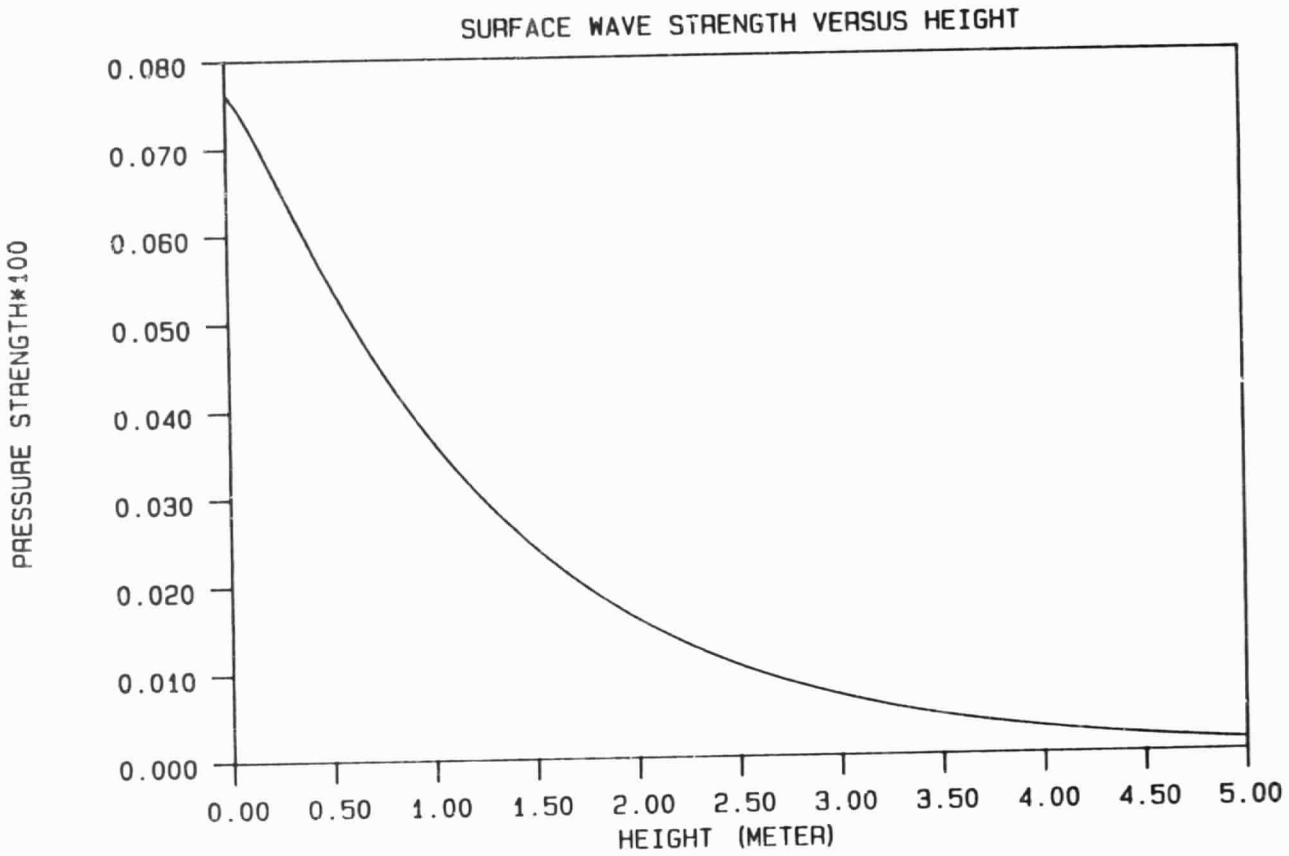

Figure 13. Surface wave versus elevation with $\Delta T/T_\infty = .01$, $\alpha = 6$, $\omega = 2000$, $s = 3m$, $r = 200m$.

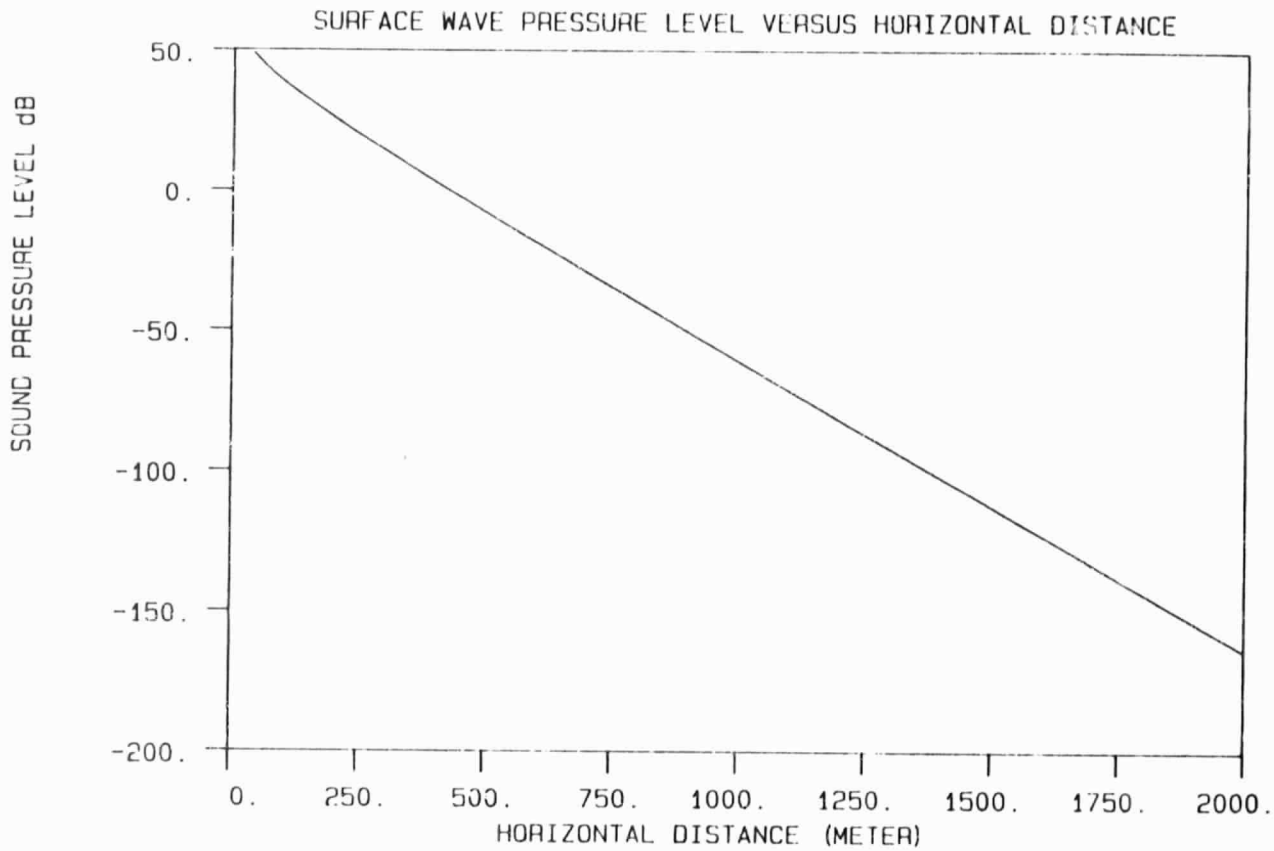

Figure 14. Surface wave versus horizontal distance with $\Delta T/T_\infty = .01$, $\alpha = 5$, $\omega = 2000$, $s = 3m$, $z = 1m$.

The effects of the temperature profile and the ground impedance on the surface wave are also analyzed. For a fixed α, σ and ω, the location of the pole will move closer to the branch cut c_3 with an increase of $\Delta T/T_\infty$, thus providing less chance to produce the surface wave. For a fixed $\Delta T/T_\infty$, σ and ω, the chance to see the surface wave increases with the value of α. These two facts show that the surface wave is more likely to be seen in the homogeneous atmosphere than in the inhomogeneous atmosphere. On the other hand, for a given temperature profile, the chance to see the surface wave and the magnitude of the surface wave increase with the ratio of σ/ω, which generally meets the criterion for the existence of a surface wave developed by Chien and Soraka in the homogeneous case, since the magnitude of the imaginary part of the ground impedance increases with the ratio of σ/ω faster than the real part of the ground impedance. Therefore, for a given ω, the harder the surface, the stronger the surface wave and the more the chance to see the surface wave: or, for a given flow resistance, the higher the angular frequency, the weaker the surface wave and the less the chance to see the surface wave. Figure 15 is a plot of surface wave versus frequency at flow resistance of 300 c.g.s. unit, which shows the magnitude of the surface wave decreases with an increase of frequency very fast and it becomes negligible when frequency > 500Hz. This result is similar to that of Piercy, Embleton and Sutherland (Figure 11 of reference 23).

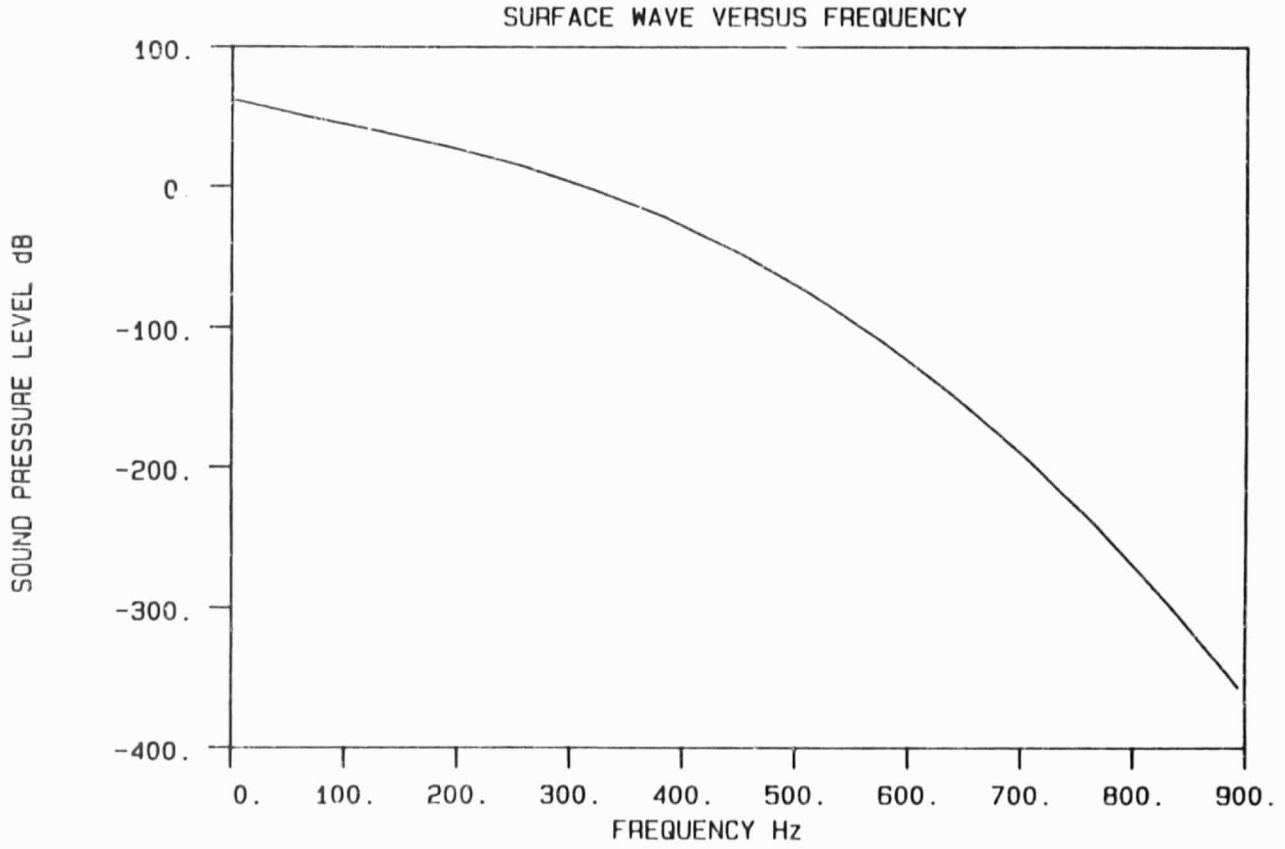

Figure 15. Surface wave versus frequency with $\Delta T/T_\infty$ = .001, α = 5, s = 3m, z = 1m, r = 260m.

6. RESULT OF CALCULATION

In this section, some results of calculation are presented and the flow resistance is assumed to be 300 c.g.s. units. First, it is noticed that the ray tracing model is based on the assumption of high frequency. But how high the frequency must be, so that this solution will be valid, is still a question. Figure 16 is a plot of sound pressure level versus frequency at z = 4m, r = 20m so that the receiver is located in region 3 of Figure 2, which shows that the sound pressure level oscillates about a mean level of 46 dB. From this plot, it is noticed that no strange behavior occurs at very low frequency of about 50 Hz.

Figure 17 is a similar plot but at r = 40m, it is noticed that a 6 db decay of the mean sound pressure level for doubling the distance is observed. The inteference pattern has a longer cycle than the previous plot, and no strange behavior is observed at low frequencies, too.

Figure 18 is another plot of sound pressure level versus frequency. The location of the receiver is chosen such that both the surface wave and the ground wave-like term are observed. This plot shows that the surface wave dominates the pressure field at low frequency. For frequency higher than about 500Hz, the surface wave has no effect on the sound pressure level at all. On the other hand, the ground wave-like term has less effect on the total sound pressure field at very low frequencies than the surface wave, but it shows a strong effect at fre-

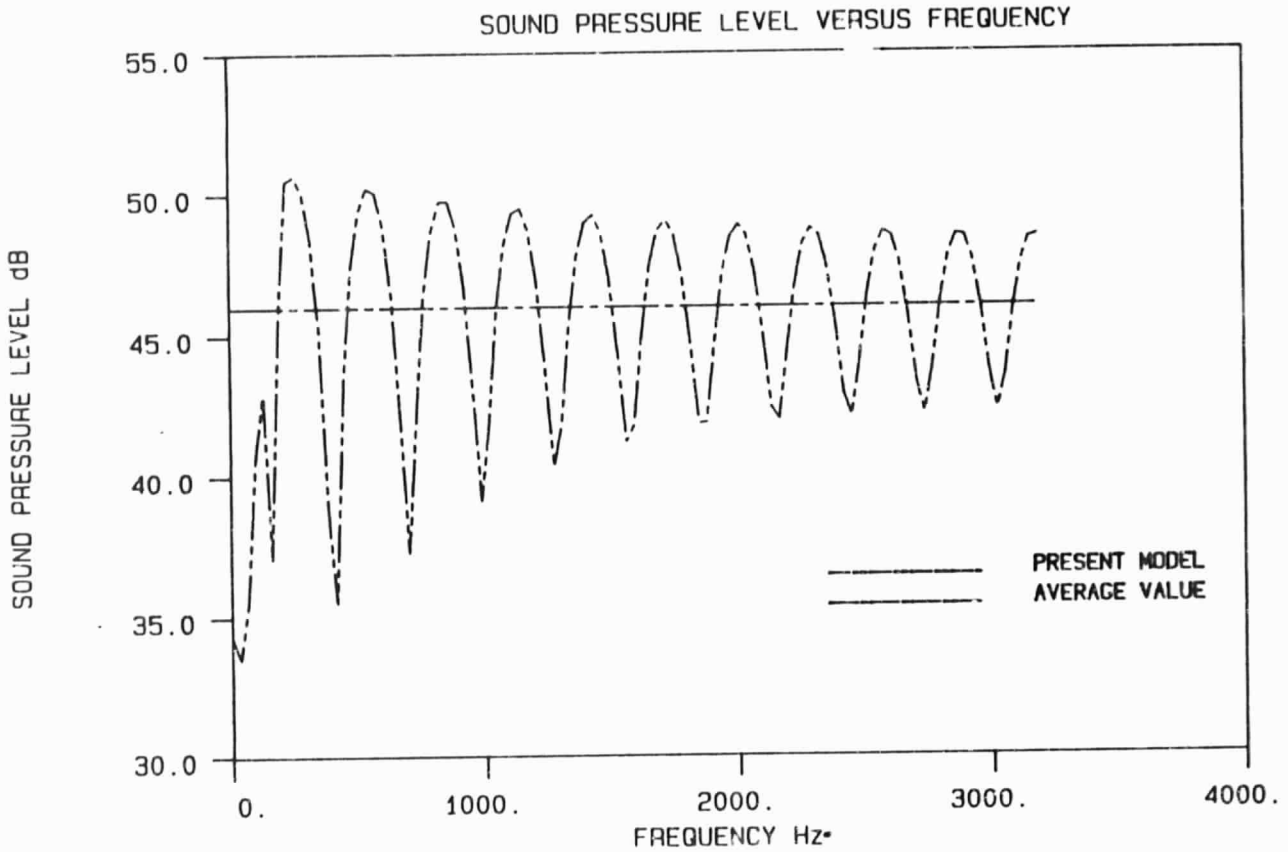

Figure 16. Sound pressure level versus frequency with $\Delta T/T_\infty = .01$, $\alpha = 6$, $s = 3m$, $z = 4m$, $r = 20m$.

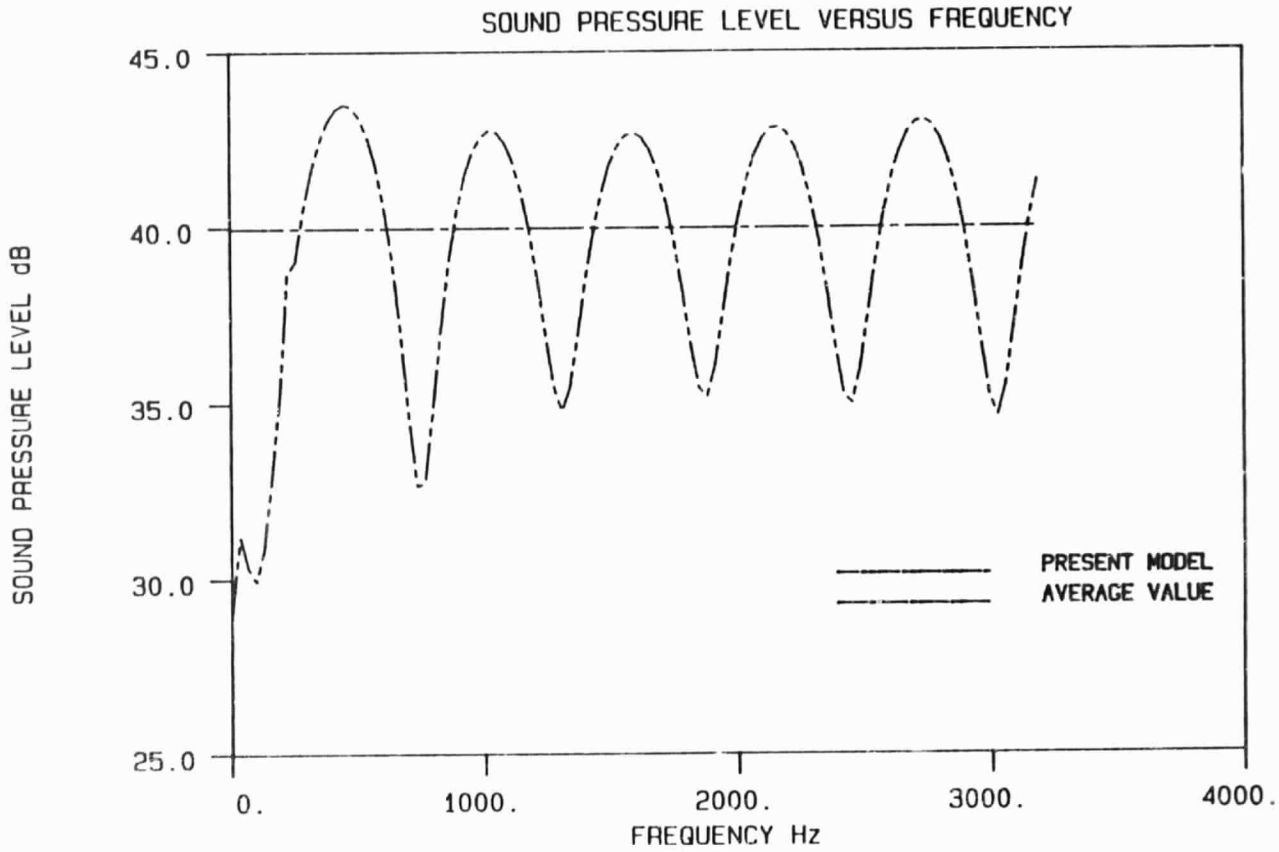

Figure 17. Sound pressure level versus frequency with $\Delta T/T_\infty = .01$, $\alpha = 6$, s = 3m, z = 4m, r = 40m.

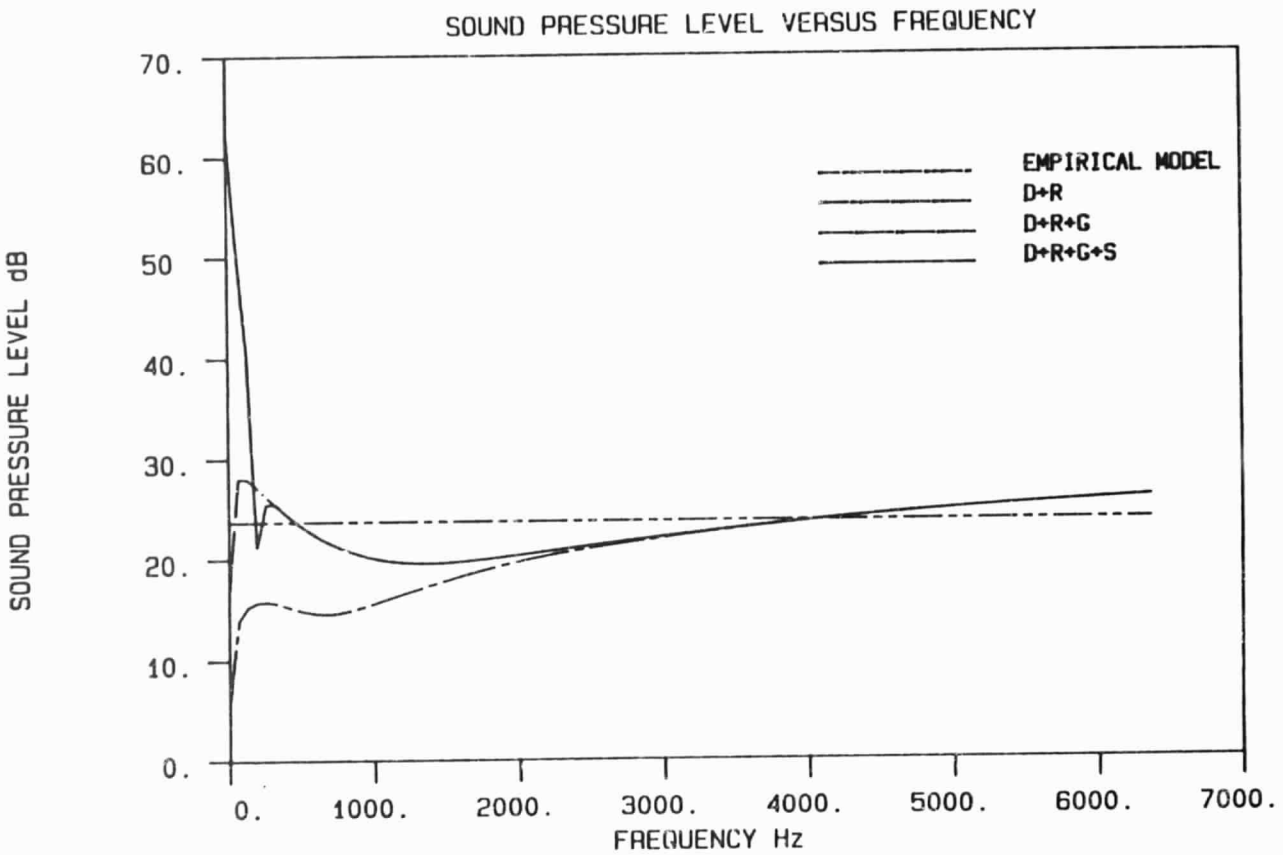

Figure 18. Sound pressure level versus frequency with $\Delta T/T_\infty = .001$, $\alpha = 5$, $s = 3m$, $z = 1m$, $r = 260m$.

quencies higher than 500 Hz and less than 3000 Hz.

Figure 19 is a plot of the ground wave-like term versus frequency. It shows that this term also decreases with the increase of the frequency, but a comparison between Figure 15 and Figure 19 indicates that the ground wave-like term decreases much slower with the increase of the frequency than the surface wave term.

Figure 20 is a plot of sound pressure level versus horizontal distance from the source. The regions in the physical space and the empirical model of Wiener and Keast [9] are also shown. The simple source model has been suggested by Wiener and Keast for the region between the source and the shadow boundary. Beyond the shadow boundary, a rapid increasing excess attentuation is applied to the simple source model and finally a large constant excess attentuation is applied to the simple source model when the receiver is well inside the shadow region. This empirical model is based on a number of experiments and summarizes the best experimental data collection available now. This plot shows a very good agreement between the present mathematical model and the empirical model. Since the simple source model only gives the mean sound pressure level, the oscillating behavior of the present model around the mean value is expected.

Figure 21 is a more detailed plot of the previous one which shows how each component of the pressure field add together to yield the total sound level. It is noticed that inside the shadow region there are three terms contributing to the total sound pressure level: the surface wave term; the nonuniform asymptotic term; and the ground wave-like term. The surface wave term has almost no effect on the total sound pressure field since it has decayed in an exponential manner and the

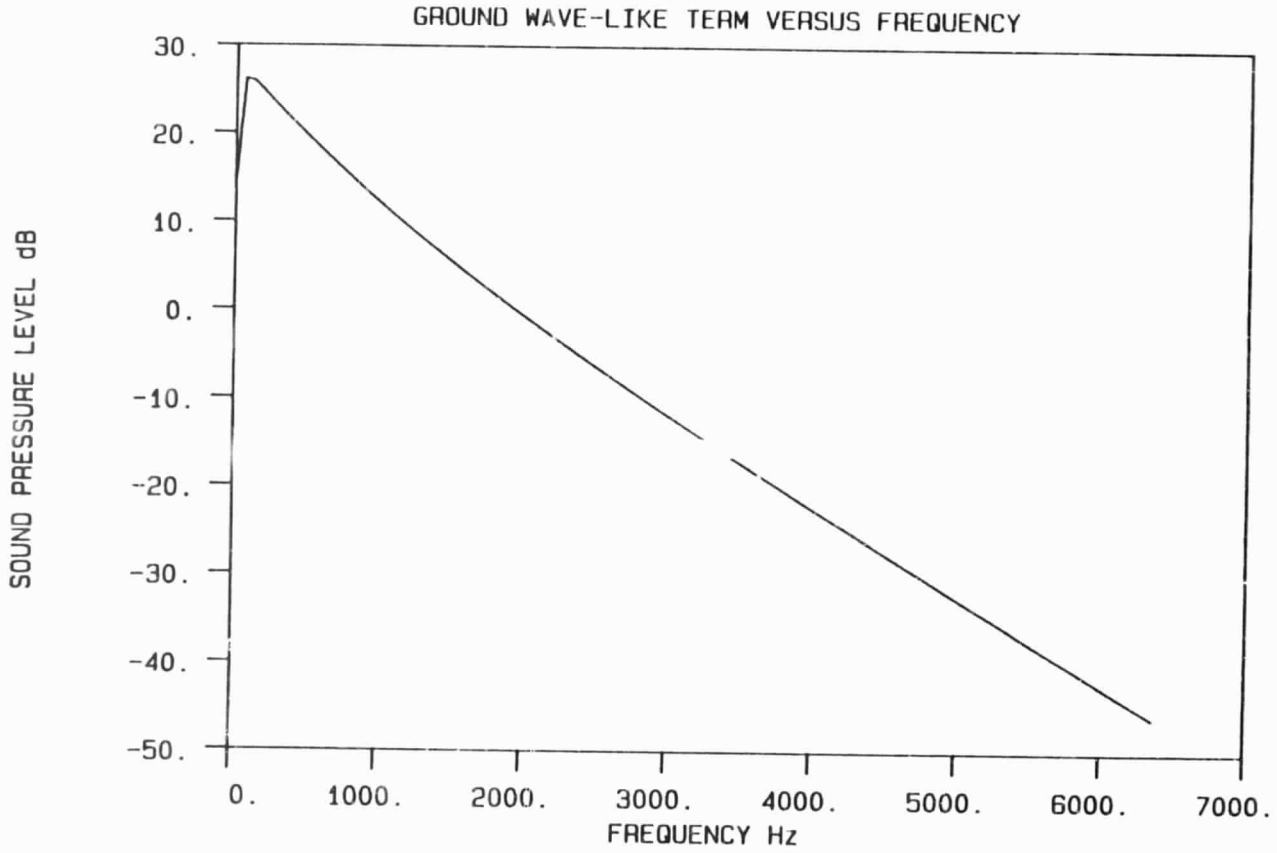

Figure 19. Ground wave-like term versus frequency with $\Delta T/T_\infty = .001$, $\alpha = 5$, $s = 3m$, $z = 1m$, $r = 260m$.

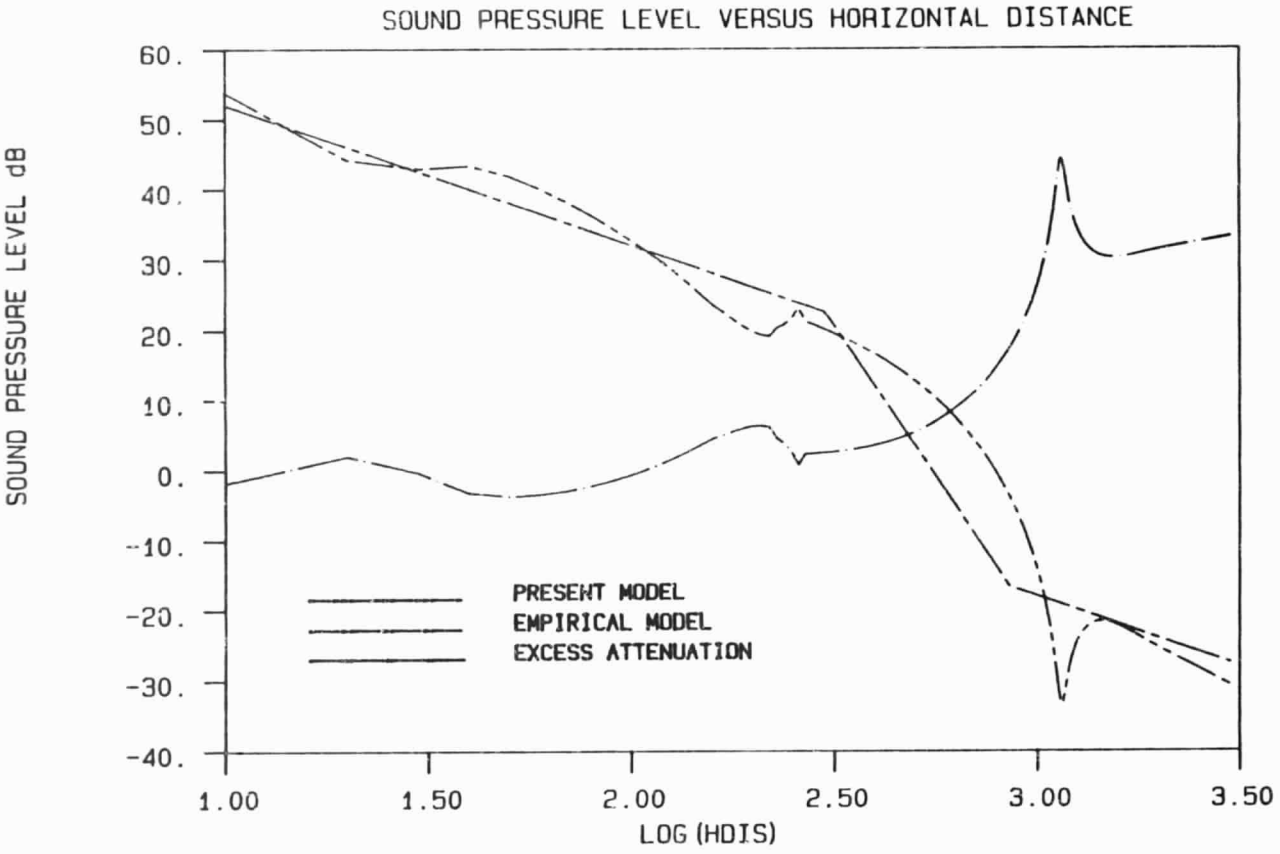

Figure 20. Sound pressure level versus horizontal distance with $\Delta T/T_\infty$ = .001, α = 3.5, ω = 10,000, s = 3m, z = 1m.

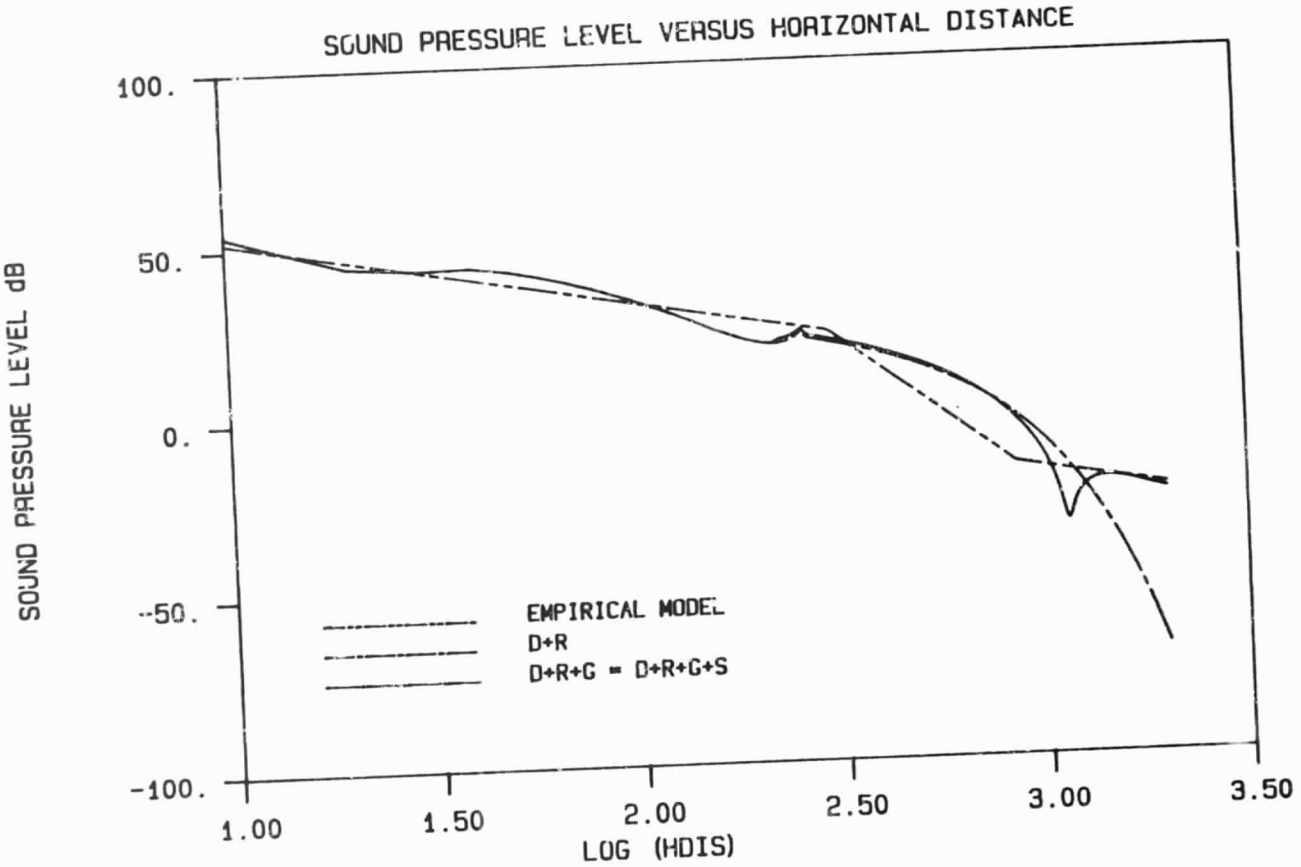

Figure 21. Sound pressure level versus horizontal distance with $\Delta T/T_\infty$ = .001, α = 3.5, ω = 10,000, s = 3m, z = 1m.

frequency of the source is relatively high. The nonuniform asymptotic term which physically represents the energy diffracted from those rays which pass close to the shadow boundary is also small when the receiver is well inside the shadow region because the exponential decay of the Airy function, Equation (48), inside the shadow region. The dominant term which gives the saturated behavior of the excess attenuation is the ground wave-like term. Again, this term is not exactly a ground wave term since it decays with the horizontal distance as a -3/2 power. The overshooting behavior of the sound pressure level just inside the shadow region results from the interference of the three terms and is actually observed, sometimes, in the practical measurements (Figure 2 of reference 9).

Figure 22 is also a detailed plot of the sound pressure level versus horizontal distance. It is observed that the surface wave has a strong effect on the pressure field for horizontal distance between 30m to 600m. Beyond that distance the exponential behavior actually makes the surface wave negligible.

Figure 23 is another plot of sound level versus horizontal distance. The heights of the source and the receiver are the same as in the experiments done by Wiener and Keast. The saturated value of 30 dB for excess attentuation far into the shadow suggested by them is observed. Figures 24 through 26 are also the plots of sound pressure level versus horizontal distance at different heights and under different temperature profiles, which show the similar kind of behavior to the previous plots. The saturated values of the excess attenuation are found to vary with the height of the receiver, the temperature profile and the source frequency. The dependancy of the ground wave-like

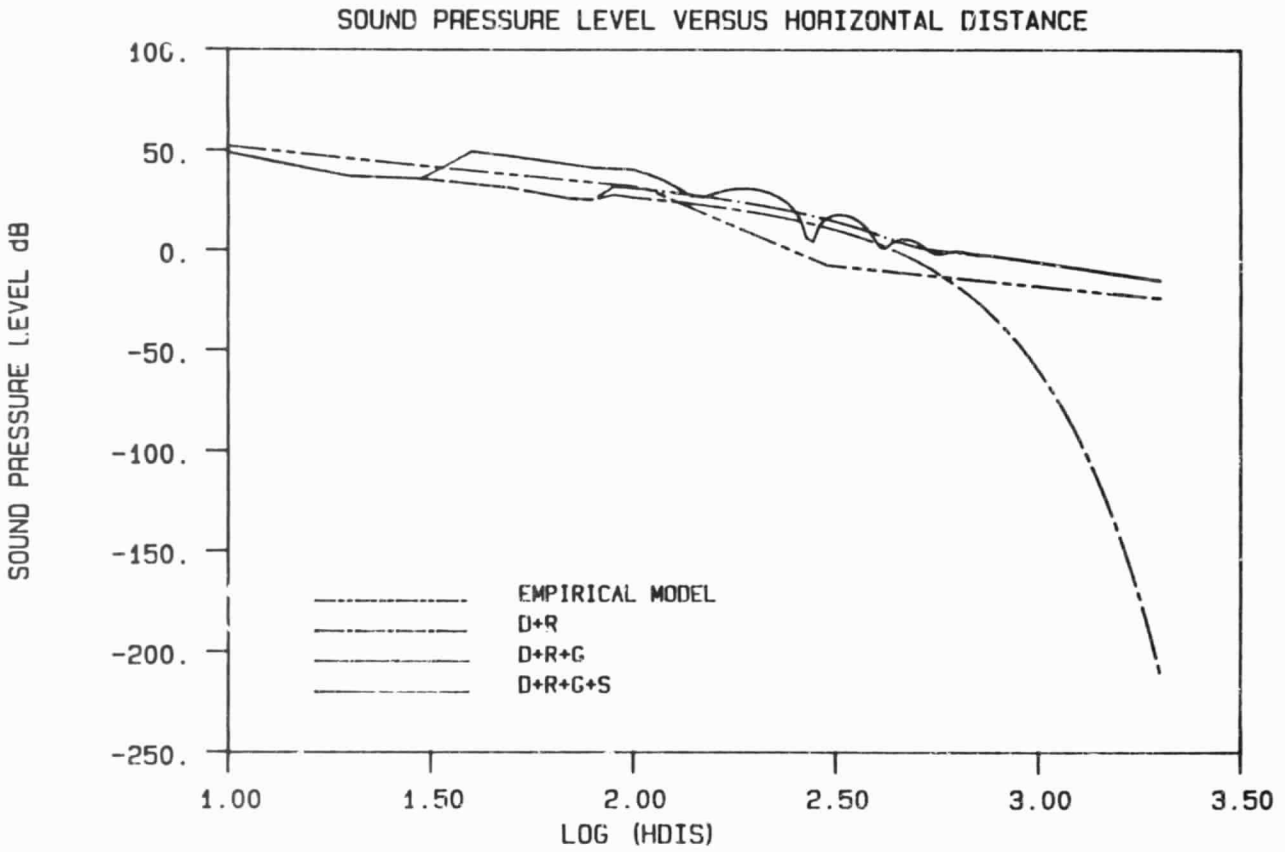

Figure 22. Sound pressure level versus horizonal distance with $\Delta T/T_\infty$ = .01, α = 5, ω = 2,000, s = 3m, z = 1m.

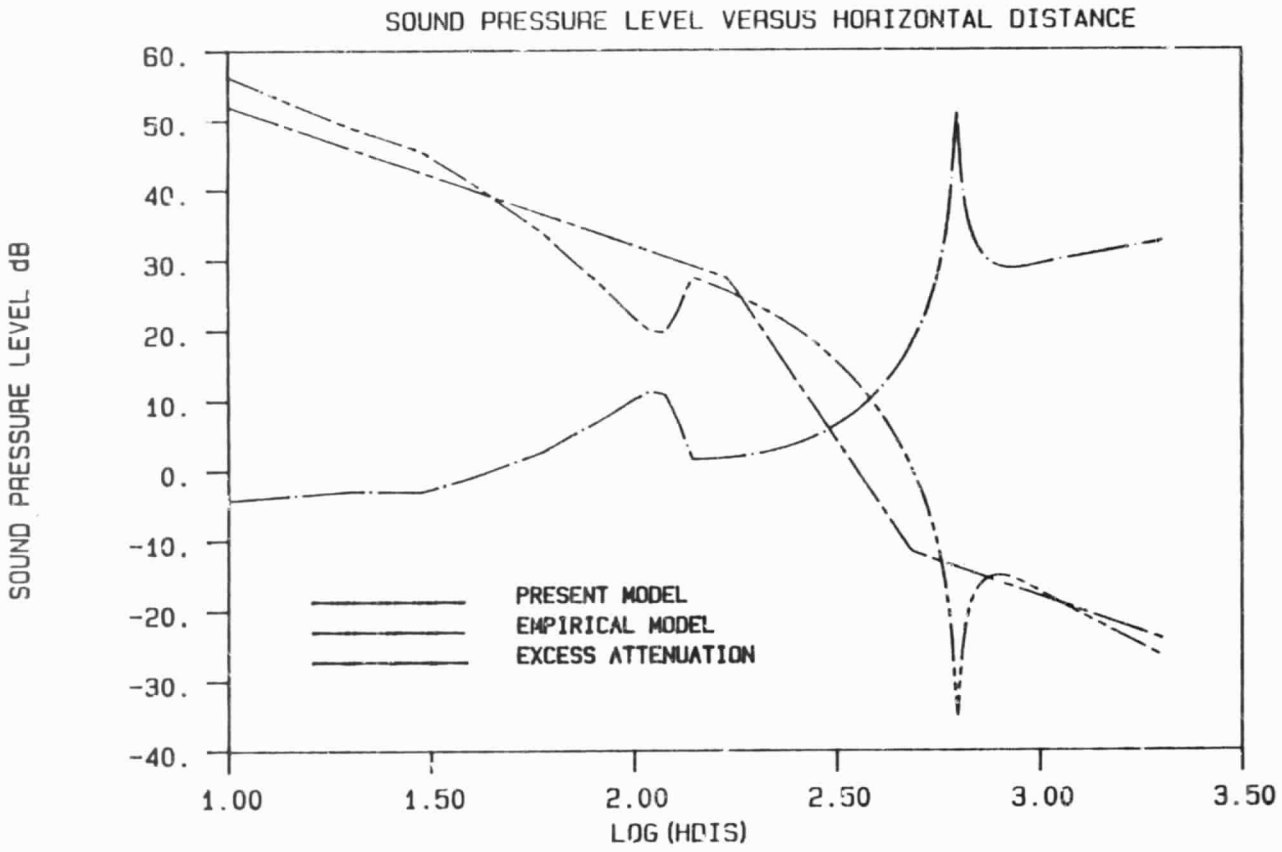

Figure 23. Sound pressure level versus horizontal distance with $\Delta T/T_\infty$ = .01, α = 5, ω = 4,000, s = 3.67m, z = 1.52m.

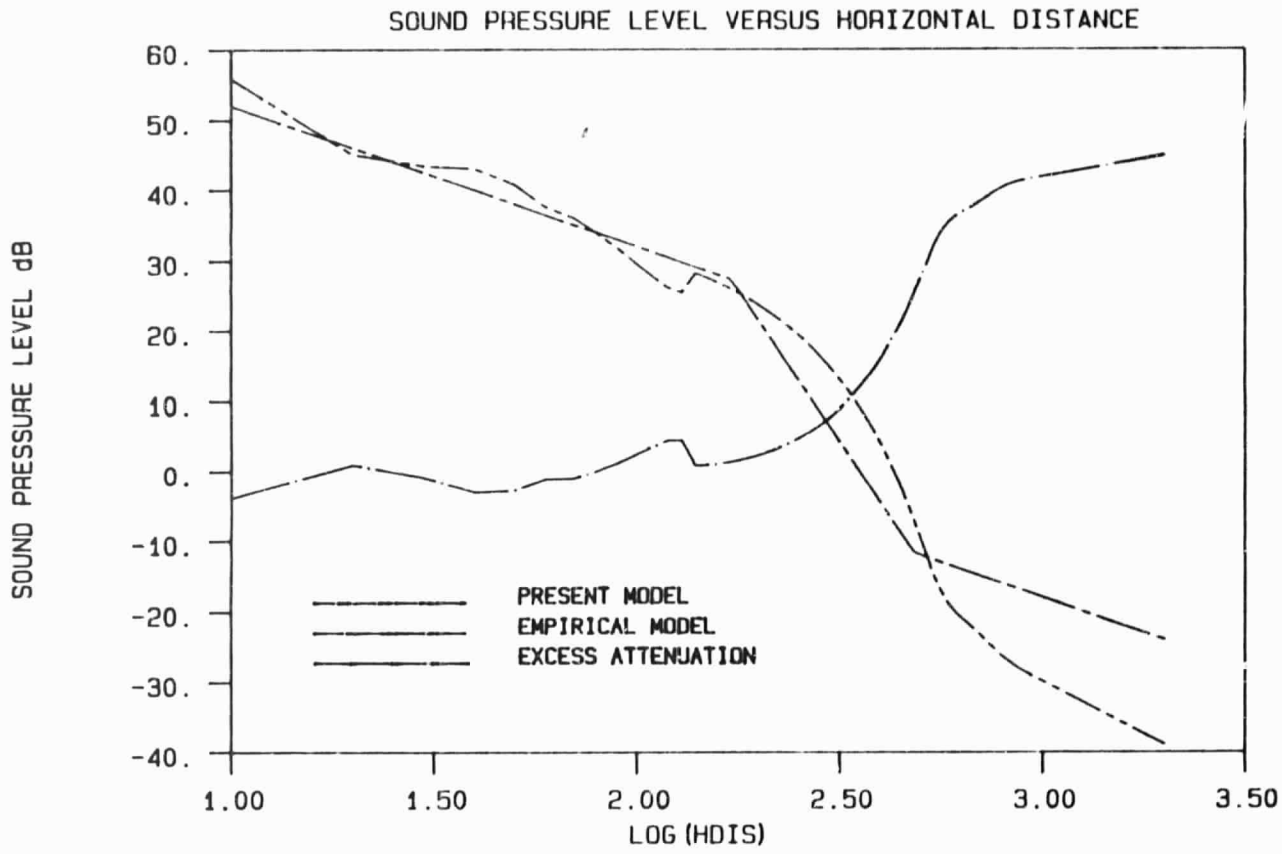

Figure 24. Sound pressure level versus horizontal distance with $\Delta T/T_\infty$ = .01, α = 6, ω = 6,000, s = 3.67m, z = 1.52m.

C - 3

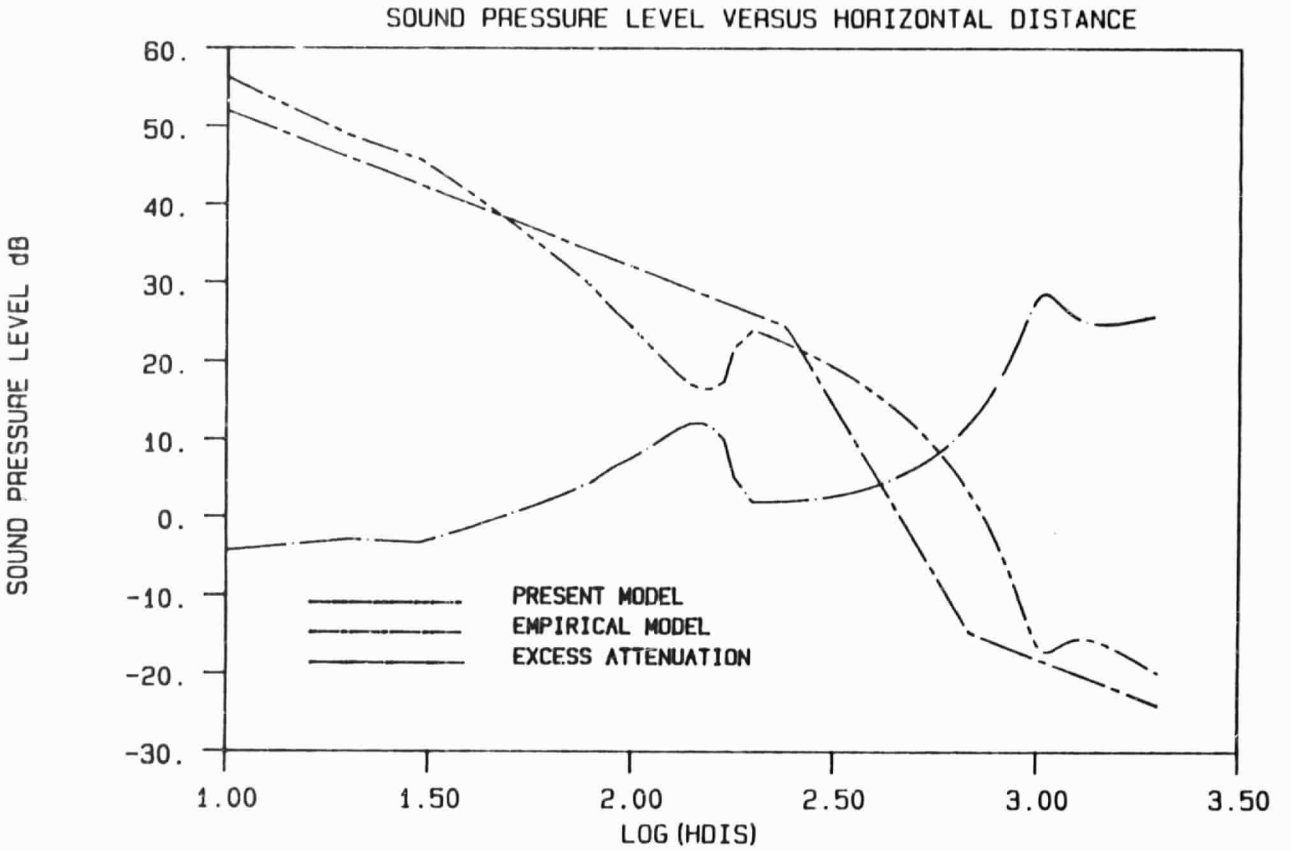

Figure 25. Sound pressure level versus horizontal distance with $\Delta T/T_\infty$ = .005, α = 6, ω = 4,000, s = 3.67m, z = 1.52m.

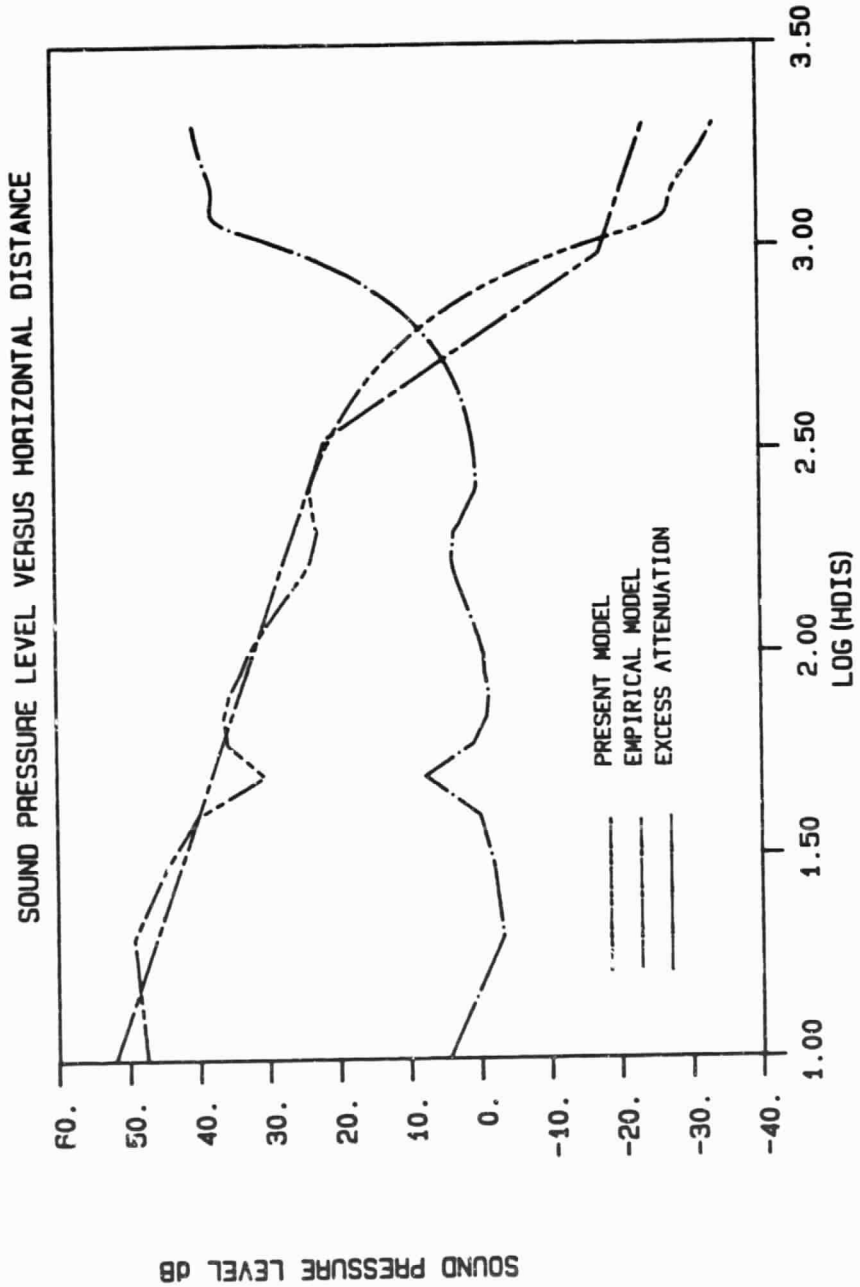

Figure 26. Sound pressure level versus horizontal distance with $\Delta T/T_\infty = 0.1$, $\alpha = 6$, $\omega = 4{,}000$, $s = 3.67$m, $z = 4.67$m.

term on the frequency has been shown in Figure 19. Figure 27 is a plot of the ground wave-like term versus height of the receiver. It is noticed that the pressure level of the ground wave-like term increases with the height of the receiver for height less than 1m, it then decreases with the continuous increase of the height. It also decays slower than the surface wave with the increase of the height (Figure 14 and Figure 27).

Since Wiener and Keast only conducted the experiments at a fixed receiver height and more than ±10 dB spread of the measured data exist in their experiments, this present mathematical model is believed to fit the experiments very well.

Embleton, Piercy and Olson [7] suggested that the ground wave term will be more dominant in the pressure field if the source and the receiver are both located very close to the ground. Figure 28, where the heights of the source and receiver are both .5 meters, shows a similar kind of behavior of the ground wave-like term. Over the whole horizontal distance range, this ground wave-like term dominate the sound pressure level, except for horizontal distance less than 100m, where the surface wave has a very strong effect.

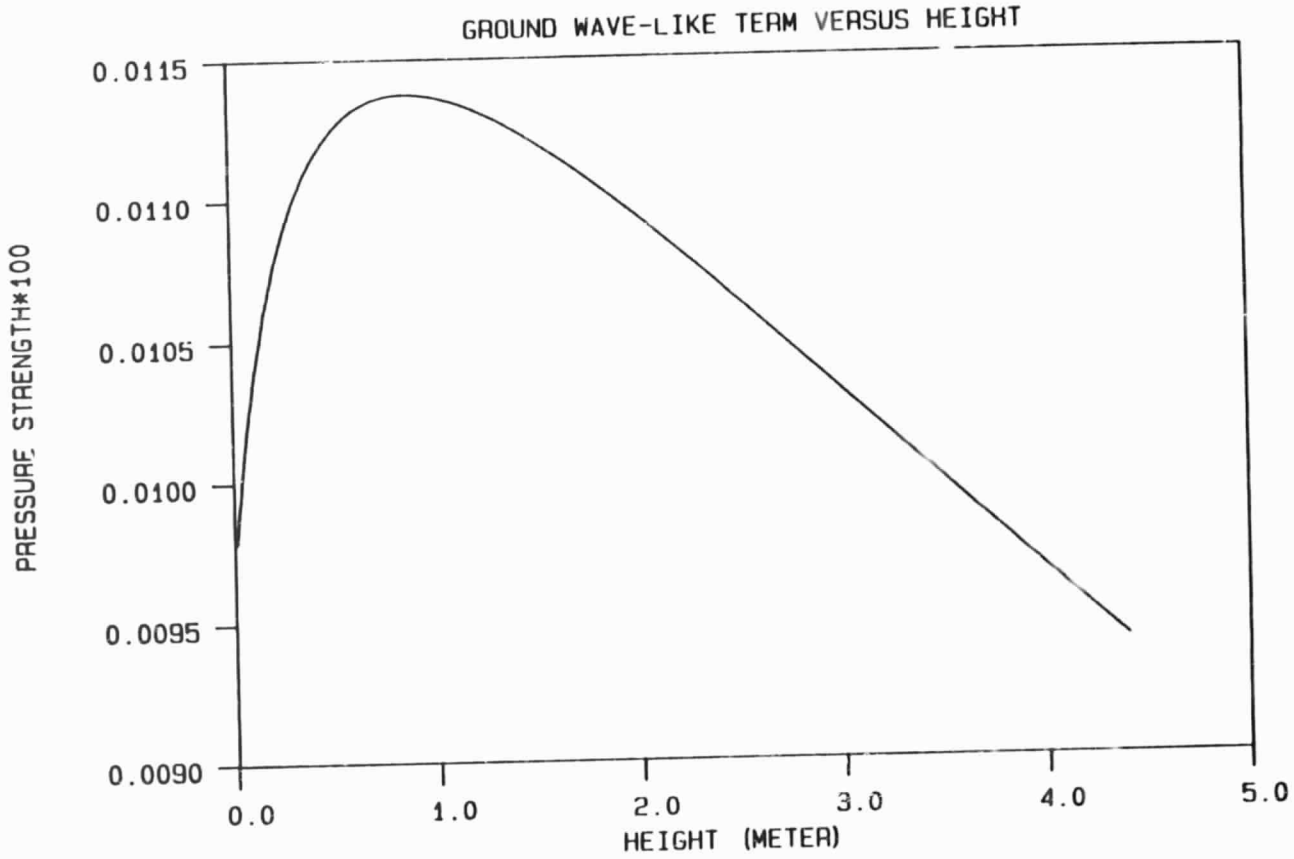

Figure 27. Ground wave-like term versus elevation with $\Delta T/T_\infty$ = .01, α = 6, ω = 2,000, s = 3m, r = 200m.

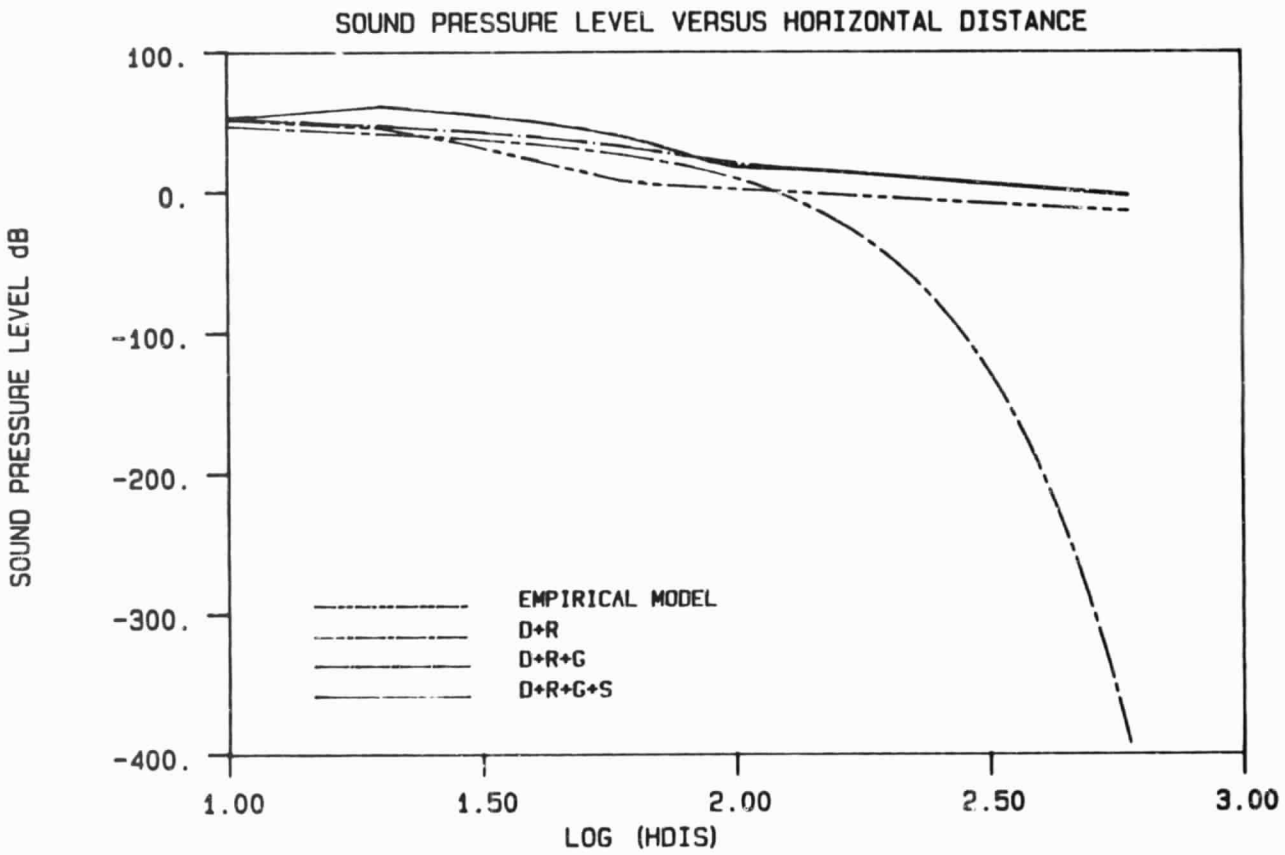

Figure 28. Sound pressure level versus horizontal distance with $\Delta T/T_\infty$ = .01, α = 6, ω =4,000, s = .5m, z = .5m.

7. CONCLUSIONS

In this project, the behavior of sound propagation under a temperature lase condition has been studied, especially the behavior inside the shadow region.

The surface wave has been found under certain combinations of temperature profile and ground impedance. Mathematically, it is the result of the pole which is located between the original integration path and the steepest descent integration path. This surface wave has been seen to be important in a range of the horizontal distance from the source when receiver is close to ground and the frequency is low. At large distance, no matter how low the frequency is the exponential decay behavior of this surface wave will be strong enough to quench it. The surface wave might also be the reason why we sense the negative excess attentuation in a certain range of horizontal distance at low frequency, which is observed in the experiments. Also this study shows that the surface wave is more important in the homogeneous atmosphere.

A term which decays as -3/2 power of the horizontal distance is also found. This term is required mathematically to keep the steepest descent integration path from running into a branch point. It is this term that gives the saturated excess attenuation inside the shadow region which was observed by Wiener and Keast. This term is believed to be a ground wave-like term.

The present mathematical model is seen not to give a strange

behavior at low frequency. More experiments are needed to prove the validity of this model at very low frequency. These can be achieved by carrying out the outdoor measurements over a wide range of frequencies, from several hundred to several thousand Hertz, under different temperature profiles.

A comparison between present model and the empirical model suggested by Wiener and Keast has been made, which shows a very good agreement between the theory and the experiments.

APPENDIX

PROGRAM

```
      PROGRAM PRESSURE
C
C     ************************************************************
C     ************************************************************
C     *                                                          *
C     *       THIS IS THE COMPUTER PROGRAM OF A MATHEMATICAL     *
C     *  MODEL FOR EVALUATING THE SOUND PRESSURE LEVEL AT ANY    *
C     *  POINT  IN THE PHYSICAL SPACE UNDER A TEMPERATURE        *
C     *  LAPSE CONDITION. THE PROGRAM CONSISTS OF 1 MAIN ROU-    *
C     *  TINE, 18 SUBROUTINES AND 10 FUNCTIONS.                  *
C     *       FOLLOWING IS A LIST OF STANDARD SYMBLES USED IN    *
C     *  THIS PROGRAM:                                           *
C     *                                                          *
C     *       S—— ELEVATION OF THE SOUND SOURCE                  *
C     *       Z—— ELEVATION OF THE RECEIVER                      *
C     *     HDIS—— HORIZONTAL DISTANCE OF THE RECEIVER FROM      *
C     *             THE SOURCE                                   *
C     *       Z1—— COMPLEX GROUND IMPEDANCE                      *
C     *       R1—— FLOW RESISTANCE                               *
C     *    OMEGA—— ANGULAR FREQUENCY OF THE SOURCE               *
C     *     DTOT—— ΔT/T∞                                         *
C     *    SPEED—— SPEED OF THE SOUND AT INFINITY                *
C     *    ALPHA—— CONSTANT                                      *
C     *   REGION—— THE REGION OF THE LOCATION OF THE RECEIVER    *
C     *             IN THE PHYSICAL SPACE                        *
C     *      BRW—— BRANCH POINT Bw                               *
C     *      BRS—— BRANCH POINT Bs                               *
C     *      BRZ—— BRANCH POINT Bz                               *
C     *      BRO—— BRANCH POINT Bo                               *
C     *   SADPOT—— SADDLE POINT ARRAY                            *
C     *       P—— SOUND PRESSURE STRENGTH                        *
C     *      SPL—— SOUND PRESSURE LEVEL PREDICTED BY SIMPLE      *
C     *             SOURCE MODEL                                 *
C     *                                                          *
C     ************************************************************
C
C     ************************************************************
C     *                                                          *
C     *    LIST OF INPUT:                                        *
C     *             DTOT: ΔT/T∞                                  *
C     *            ALPHA: TEMPERATURE PROFILE CONSTANT           *
C     *                S: HEIGHT OF SOURCE                       *
C     *               ZL: LOWER LIMIT OF RECEIVER'S HEIGHT       *
C     *               ZT: HIGHER LIMIT OF RECEIVER'S HEIGHT      *
C     *               NZ: NUMBER OF CALCULATING POINTS IN        *
C     *                    Z DIRECTION                           *
C     *           OMEGAL: LOWER LIMIT OF SOURCE ANGULAR          *
C     *                    FREQUENCY                             *
C     *           OMEGAT: HIGHER LIMIT OF SOURCE ANGULAR         *
C     *                    FREQUENCY                             *
C     *               NO: NUMBER OF CALCULATING POINTS OF        *
C     *                    DIFFERENT FREQUENCIES                 *
```

```
C     *            HDISL: CLOSEST DISTANCE OF RECEIVER'S       *
C     *                   LOCATION                             *
C     *            HDIST: FARTHEST DISTANCE OF RECEIVER'S      *
C     *                   LOCATION                             *
C     *               NH: NUMBER OF CALCULATING POINTS         *
C     *                   IN HORIZONTAL DIRECTION              *
C     *                                                        *
C     **********************************************************
C
      IMPLICIT DOUBLE PRECISION (A-H,O-Z)
      COMPLEX*16 BETA,Z1,P1,P2,P3,P4,P5,P,G32PI,RC2
      COMMON /BRANCH/BRO,BRS,BRZ,BRW
      COMMON /CONSTANT/SPEED,OMEGA,ALPHA,DTOT
      DIMENSION SADPOT(2)
      INTEGER REGION,FORM
      REAL *8 LEMDA
      TYPE *,'INPUT DTOT,ALPHA,S,ZL,ZT,NZ,OMEGAL,OMEGAT
     1        ,NO,HDISL,HDIST,NH'
      READ *, DTOT,ALPHA,S,ZL,ZT,NZ,OMEGAL,OMEGAT,NO,HDISL,
     1        HDIST,NH
      SPEED=340.
      PI=4.*DATAN(1.DO)
      R1=300.
      IF(OMEGAL.EQ.OMEGAT) THEN
            STEPO=.001
      ELSE
            STEPO=(OMEGAT-OMEGAL)/NO
      ENDIF
      DO 14 OMEGA=OMEGAL,OMEGAT,STEPO
      LEMDA=OMEGA/(SPEED*ALPHA)
      BRW=OMEGA/SPEED
      BRO=BRW*DSQRT(1./(1.+DTOT))
      BRS=BRW*DSQRT((1.+ALPHA*S)/(1.+ALPHA*S+DTOT))
      FR=OMEGA/(2.*PI)
      RATIO=FR/R1
      R=1.+9.08*RATIO**(-.75)
      X=-11.9*RATIO**(-.73)
      Z1=DCMPLX(R,X)
      ID=1
      ID1=0
      ID2=0
      IF(OMEGA.GT.6000) THEN
            ID=3
            GOTO 1
      ENDIF
      CALL POLE(P5,S,Z,HDIS,Z1,FC,ID)
1     IF(HDIST.EQ.HDISL) THEN
            STEPH=.001
      ELSE
            STEPH=(HDIST-HDISL)/NH
      ENDIF
      IF(ZT.EQ.ZL) THEN
```

```
              STEPZ=.001
      ELSE
              STEPZ=-(ZT-ZL)/NZ
      ENDIF
      NC=0
      DO 16 Z=ZT,ZL,STEPZ
      DO 16 HDIS=HDISL,HDIST,STEPH
      CHE=BRW*HDIS
      P1=.0
      P2=.0
      P3=.0
      P4=.0
      P5=.0
      P=.0
      BRZ=BRW*DSQRT((1.+ALPHA*Z)/(1.+ALPHA*Z+DTOT))
      CALL SAD(S,Z,HDIS,REGION,SADPOT,ID2)
      IF(ID2.EQ.4) GOTO 2
      IF(REGION.NE.7) THEN
              BETA=SADPOT(2)
      ELSE
              BETA=SADPOT(1)+SADPOT(2)*DCMPLX(.0,1.)
      ENDIF
      CALL FINFORM(BETA,Z,FC,HDIS,S,F2,FORM)
2     GOTO (10,20,10,20,30,40,50) REGION
10    CALL INTD(SADPOT(1),P1,S,Z,HDIS,Z1)
      BETA=SADPOT(2)
      CALL INTR(BETA,P2,S,Z,HDIS,Z1,1,1)
      GOTO 60
20    CALL INTD(SADPOT(1),P1,S,Z,HDIS,Z1)
      BETA=SADPOT(2)
      CALL INTR(BETA,P2,S,Z,HDIS,Z1,2,1)
      GOTO 60
30    BETA=SADPOT(1)
      CALL INTR(BETA,P2,S,Z,HDIS,Z1,1,1)
      BETA=SADPOT(2)
      CALL INTR(BETA,P1,S,Z,HDIS,Z1,2,2)
      GOTO 60
40    IF(NC.EQ.1) GOTO 41
      BETA=SADPOT(1)
      CALL INTR(BETA,P2,S,Z,HDIS,Z1,2,1)
      BETA=SADPOT(2)
      CALL INTR(BETA,P1,S,Z,HDIS,Z1,2,2)
41    CALL INTC(S,Z,HDIS,Z1,P3)
      IF(NC.EQ.0) THEN
       IF(CDABS(P1+P2).GE.CDABS(P3)) THEN
              NC=1
              P1=.0
              P2=.0
       ELSE
              P3=.0
       ENDIF
      ENDIF
```

```
      GOTO 60
50    CALL INTC(S,Z,HDIS,Z1,P1)
60    IF(ID1.EQ.1) THEN
              CALL CON(P4,S,Z,HDIS,Z1)
      ELSE
         IF(ABS(FC).LE.ABS(CHE)) THEN
              CALL CON(P4,S,Z,HDIS,Z1)
              ID1=1
              FC=CHE
       ENDIF
      ENDIF
61    IF(ID.EQ.0) GOTO 70
      IF(ID.EQ.1) ID=2
      IF(OMEGA.GT.6000) GOTO 70
      CALL POLE(P5,S,Z,HDIS,Z1,FC,ID)
70    P=P1+P2+P3+P4+P5
      ID2=ID+ID1
      SPL=1./(4*PI*HDIS)
      SPL1=20.*DLOG10(CDABS(P)/.00002)
      SPL2=20.*DLOG10(SPL/.00002)
      SPL3=SPL2-SPL1
      SPL4=20*DLOG10(CDABS(P1+P2+P3)/.00002)
      SPL5=20*DLOG10(CDABS(P1+P2+P3+P4)/.00002)
      SPL6=20*DLOG10(CDABS(P1+P2+P3+P4+P5)/.00002)
      IF(Z.GT.S) THEN
              BB=BRS
      ELSE
              BB=BRZ
      ENDIF
      CALL FIN(Z,S,BRO,BB,RC1)
      RC2=DCMPLX(RC1,.ODO)
      RC=CDABS(-G32PI(Z,RC2)-G32PI(S,RC2))
      IF(HDIS.GT.RC) THEN
              SPL21=SPL2-20.*DLOG10(HDIS/RC)/LOG10(2.)
              IF((SPL21-SPL2).LE.-30.) SPL21=SPL2-30.
              SPL2=SPL21
      ENDIF
      IF(OMEGAT.NE.OMEGAL) THEN
              WRITE(20,*)FR,SPL1,SPL2,SPL3
              WRITE(24,*)FR,SPL2,SPL4,SPL5,SPL6
      ENDIF
      IF(ZL.NE.ZT) THEN
              WRITE(20,*)Z,SPL1,SPL2,SPL3
              WRITE(24,*)Z,SPL2,SPL4,SPL5,SPL6
      ENDIF
      IF(HDISL.NE.HDIST) THEN
              WRITE(20,*)DLOG10(HDIS),SPL1,SPL2,SPL3
              WRITE(24,*)DLOG10(HDIS),SPL2,SPL4,SPL5,SPL6
      ENDIF
16    CONTINUE
14    CONTINUE
      STOP
```

```
      END
C
C     ************************************************************
C
      SUBROUTINE INTR(SADP,P,S,Z,HDIS,Z1,K,N)
C
C     ************************************************************
C     *                                                          *
C     *       THIS SUBROUTINE USES SADDLE POINT METHOD TO        *
C     *  CALCULATE THE INTEGRAL OF THE REFLECTED/REFRACTED       *
C     *  TERM.                                                   *
C     *                                                          *
C     ************************************************************
C
      IMPLICIT DOUBLE PRECISION (A-H,O-Z)
      COMPLEX*16 SADP,P,Q,BETA,AI,F,F1,F2,Z1,E,H2,GZ
      COMPLEX*16 G32PI2,C,GZZ,GZS,H2Z,H2S,H1
      COMMON /CONSTANT/SPEED,OMEGA,ALPHA,DTOT
      REAL *8 LEMDA
      INTEGER FORM
      P=DCMPLX(.O,.O)
      LEMDA=OMEGA/(SPEED*ALPHA)
      AI=DCMPLX(.O,1.)
      PI=4.*DATAN(1.DO)
      CALL FINFORM(SADP,Z,FF,HDIS,S,FFF,FORM)
      C=1.
      N1=1
      N2=1
      N3=1
      IF(FORM.EQ.3) THEN
             N3=2
             C=CDEXP(-AI*PI/3.)
      ENDIF
      IF(FORM.EQ.4) THEN
             N1=2
             N3=2
             C=CDEXP(-2.*AI*PI/3.)
      ENDIF
      IF(FORM.EQ.5) THEN
             N1=2
             C=CDEXP(-AI*PI/3.)
      ENDIF
      CALL FALL(Z,SADP,F,F1,F2,Z1,E,H2Z,GZZ,K,H1,N3)
      CALL FALL(S,SADP,F,F1,F2,Z1,E,H2S,GZS,K,H1,N1)
      CALL FALL(.O,SADP,F,F1,F2,Z1,E,H2,GZ,K,H1,N2)
      IF(K.EQ.1) THEN
       F1=2.*G32PI2(.O,SADP)-G32PI2(Z,SADP)-G32PI2(S,SADP)
      ELSE
       F1=-G32PI2(Z,SADP)-G32PI2(S,SADP)
      ENDIF
      F3=DSQRT(2.*PI/CDABS(F1))
      IF(N.EQ.1) THEN
```

```
            Q=PI*AI/4.
      ELSE
            Q=3.*PI*AI/4.
      ENDIF
      IF(DREAL(GZZ*GZS).LT..0.AND.DIMAG(GZZ*GZS).GT..0) THEN
            SS=-1.
      ELSE
            SS=1.
      ENDIF
      P=H2S*H2Z*SS*E*F3*CDEXP(Q)*CDSQRT(2.*SADP/(PI*HDIS))*C
     1      *CDEXP(-AI*SADP*HDIS+AI*PI/4.)/(24.*AI
     2      *CDSQRT(GZS*GZZ)*F*LEMDA**(2./3.))
      RETURN
      END
C
C     ********************************* *********************
C
      SUBROUTINE INTD(SADP,P,S,Z,HDIS,Z1)
C
C     ***********************************************************
C     *                                                         *
C     *       THIS SUBROUTINE USES SADDLE POINT METHOD TO       *
C     *  CALCULATE THE INTEGRAL OF THE DIRECT TERM              *
C     *                                                         *
C     ***********************************************************
C
      IMPLICIT DOUBLE PRECISION (A-H,O-Z)
      COMPLEX*16 P,Q,BETA,AI,F,F1,F2,Z1,E,H2,GZZ
      COMPLEX*16 G32PI2,GZS,H2Z,H2S,H1S,H1Z
      COMMON /CONSTANT/SPEED,OMEGA,ALPHA,DTOT
      REAL *8 LEMDA
      P=DCMPLX(.0,.0)
      LEMDA=OMEGA/(SPEED*ALPHA)
      AI=DCMPLX(.0,1.)
      PI=4.*DATAN(1.DO)
      BETA=SADP
      K=1
      CALL FALL(Z,BETA,F,F1,F2,Z1,E,H2Z,GZZ,K,H1Z,1)
      CALL FALL(S,BETA,F,F1,F2,Z1,E,H2S,GZS,K,H1S,1)
      IF(Z.GT.S) THEN
       F3=DREAL(-G32PI2(Z,BETA)+G32PI2(S,BETA))
       H2=H1S*H2Z
      ELSE
       F3=DREAL(G32PI2(Z,BETA)-G32PI2(S,BETA))
       H2=H2S*H1Z
      ENDIF
      F3=DSQRT(2.*PI/DABS(F3))
      Q=PI*AI/4.
      IF(DREAL(GZZ*GZS).LT..0.AND.DIMAG(GZZ*GZS).GT..0) THEN
            SS=-1.
      ELSE
            SS=1.
```

```
      ENDIF
      P=H2*SS*F3*CDEXP(Q)*DSQRT(2.*SADP/(PI*HDIS))
     1        *CDEXP(-AI*SADP*HDIS+AI*PI/4.)/(24.*AI
     2        *CDSQRT(GZS*GZZ)*LEMDA**(2./3.))
      RETURN
      END
C
C     ************************************************************
C
      SUBROUTINE INTC(S,Z,HDIS,Z1,P)
C
C     ************************************************************
C     *                                                          *
C     *       THIS SUBROUTINE USES THE NONUNIFORM ASYMPTOTIC     *
C     *  SOLUTION OF SACHS AND SILBIGER'S TO EVALUATE THE        *
C     *  PRESSURE LEVEL NEAR THE CAUSTIC.                        *
C     *                                                          *
C     ************************************************************
C
      IMPLICIT DOUBLE PRECISION (A-H,O-Z)
      COMPLEX*16 P,AIQ,BETA,AI,EN,F,F1,F2,Z1,E,H2,GZZ,GZS,H2Z,
     1        H21,H22,H23,H11,H12,H13,ARG,G32PI3,BIQ,
     2        AIP,BIP,G32PI,H2S,H1
      COMMON /BRANCH/BRO,BRS,BRZ,BRW
      COMMON /CONSTANT/SPEED,OMEGA,ALPHA,DTOT
      REAL *8 LEMDA
      IF(Z.GT.S) THEN
              B1=BRS
      ELSE
              B1=BRZ
      ENDIF
      CALL FIN(Z,S,BRO,B1,B)
      BETA=B
      P=DCMPLX(.0,.0)
      LEMDA=OMEGA/(SPEED*ALPHA)
      AI=DCMPLX(.0,1.)
      PI=4.*DATAN(1.DO)
      R1=CDABS(-G32PI(Z,BETA)-G32PI(S,BETA))
      DR=HDIS-R1
      K=1
      CALL FALL(Z,BETA,F,F1,F2,Z1,E,H2Z,GZZ,K,H1,1)
      CALL FALL(S,BETA,F,F1,F2,Z1,E,H2S,GZS,K,H1,1)
      Q43=DREAL(G32PI3(Z,BETA)+G32PI3(S,BETA))
      ARG=(2./Q43)**(1./3.)*DR
      CALL CGBAIR(ARG,AIQ,BIQ,AIP,BIP)
      IF(DREAL(GZZ*GZS).LT..0.AND.DIMAG(GZZ*GZS).GT..0) THEN
              SS=-1.
      ELSE
              SS=1.
      ENDIF
      P=H2Z*H2S*SS*DSQRT(2.*B/(PI*HDIS))
     1        *CDEXP(-AI*B*HDIS+AI*PI/4.)*ARG*2.*PI*AIQ/(24.*AI
```

```
     2        *CDSQRT(GZS*GZZ)*LEMDA**(2./3.)*DR)
      RETURN
      END
C
C     ************************************************************
C
      SUBROUTINE POLE(P5,S,Z,HDIS,Z1,CHE,ID)
C
C     ************************************************************
C     *                                                          *
C     *       THIS IS A SUBROUTINE TO EVALUATE THE CONTRIBU-     *
C     *  TION OF THE POLE.                                       *
C     *       BETA IS THE LOCATION OF THE POLE IN THE COMPLEX    *
C     *  BETA  SPACE.                                            *
C     *                                                          *
C     ************************************************************
C
      IMPLICIT DOUBLE PRECISION (A-H,O-Z)
      COMPLEX*16 AI,BETA,Z1,F,F1,F2,E,H2Z,H2S,GZZ,GZS,F11,E1,
     1        P5,G32,H1
      COMMON /BRANCH/BRO,BRS,BRZ,BRW
      COMMON /CONSTANT/SPEED,OMEGA,ALPHA,DTOT
      INTEGER REGION,FORM
      REAL *8 LEMDA
      LEMDA=OMEGA/(SPEED*ALPHA)
      PI=4.*DATAN(1.DO)
      AI=DCMPLX(.0,1.)
      N=1
      K=1
      P5=.0
      GOTO (1,20,30) ID
1     BETA=OMEGA/SPEED*CDSQRT(1.-(1./Z1)**2.)
10    CALL FALL(O.,BETA,F,F1,F2,Z1,E,H2Z,GZZ,N,H1,1)
      IF(CDABS(F).LT..000000000001) RETURN
      BETA=BETA-2.*F/(F1+CDSQRT(F1**2.-2.*F*F2))
      K=K+1
      IF(K.GE.500) RETURN
      GOTO 10
20    CALL FINFORM(BETA,Z,FF,HDIS,S,FFF,FORM)
      IF(FORM.NE.1) THEN
      ID=0
      RETURN
      ENDIF
      IF(DREAL(BETA).GT.BRW) THEN
       IF(DIMAG(BETA).GT..0.AND.ABS(FF).LE.ABS(CHE)) GOTO 30
       IF(DIMAG(BETA).LE..0.AND.ABS(FF).GE.ABS(CHE)) GOTO 30
      ELSE
       IF(DREAL(BETA).LT.BRO) THEN
        IF(DIMAG(BETA).GT..0.AND.ABS(FF).GE.ABS(CHE)) GOTO 30
        IF(DIMAG(BETA).LE..0.AND.ABS(FF).LE.ABS(CHE)) GOTO 30
       ENDIF
      ENDIF
```

```
      RETURN
30    CALL FALL(Z,BETA,F,F11,F2,Z1,E1,H2Z,GZZ,N,H1,1)
      CALL FALL(S,BETA,F,F11,F2,Z1,E1,H2S,GZS,N,H1,1)
      ID=3
      P5=CDEXP(-AI*BETA*HDIS+AI*PI/4.)*H2S*H2Z*E*CDSQRT(2*BETA
     1        /(PI*HDIS))/(24.*DCMPLX(.0,.1)*LEMDA**(2./3.)
     1        *CDSQRT(GZZ*GZS)*F1)*(-2*PI*AI)
      RETURN
      END
C
C     ************************************************************
C
      SUBROUTINE CON(P4,S,Z,HDIS,Z1)
C
C     ************************************************************
C     *                                                          *
C     *       SUBROUTINE CON EVALUATES THE INTEGRATION ALONG     *
C     *  THE MODIFIED INTEGRATION PATH, WHICH IS REQUIRED TO     *
C     *  KEEP THE INTEGRATION PATH FROM RUNNING INTO THE         *
C     *  BRANCH POINT Bw.                                        *
C     *                                                          *
C     ************************************************************
C
      IMPLICIT DOUBLE PRECISION (A-H,O-Z)
      REAL*8 LEMDA
      COMPLEX*16 P4,D,AI,F,F1,F2,Z1
      COMMON /CONSTANT/SPEED,OMEGA,ALPHA,DTOT
      LEMDA=OMEGA/(SPEED*ALPHA)
      AI=DCMPLX(.0,1.)
      PI=4.*DATAN(1.DO)
      A=DSQRT(2.*OMEGA/(PI*HDIS*SPEED*DTOT))
      B=(1+ALPHA*Z+DTOT)
      C=(1+ALPHA*S+DTOT)
      D=A*(B*C)**(1./4.)/(8*ALPHA*LEMDA*PI*(-AI*HDIS-2*SPEED/(3.
     1  *OMEGA*DSQRT(DTOT))*(B**(3/2)+C**(3/2)-2*(1+DTOT)**(3/2))))
      F=-AI*OMEGA*HDIS/SPEED-2*LEMDA*DSQRT(DTOT)*(SQRT(B)+SQRT(C)
     1  -2*SQRT(1+DTOT))+AI*PI/4
      F1=1+AI*Z1/(4*(1+DTOT)*LEMDA)
      F2=-AI*Z1*DSQRT(DTOT/(1+DTOT))
      P4=D*((F1-F2)/(F1+F2))*CDEXP(F)
      RETURN
      END
C
C     ************************************************************
C
      SUBROUTINE SAD(S,Z,HDIS,REGION,SADPOT,ID)
C
C     ************************************************************
C     *                                                          *
C     *       SUBROUTINE SAD IS USED TO FIND THE SADDLE POINT    *
C     *  OF THE INTEGRATION.                                     *
```

```
C     *                                                              *
C     ****************************************************************
C
      IMPLICIT DOUBLE PRECISION (A-H,O-Z)
      DIMENSION SADPOT(2)
      COMMON /CONSTANT/SPEED,OMEGA,ALPHA,DTOT
      COMMON /BRANCH/BRO,BRS,BRZ,BRW
      INTEGER REGION,FORM
      CALL FINREG(S,Z,HDIS,REGION)
      GOTO (10,20,10,20,30,40,50) REGION
10    CALL FINDRL(S,Z,HDIS,SADPOT(1),1)
      CALL FINDRL(S,Z,HDIS,SADPOT(2),2)
      RETURN
20    CALL FINDRL(S,Z,HDIS,SADPOT(1),1)
      CALL FINRFC(S,Z,HDIS,REGION,SADPOT)
      RETURN
30    CALL FINDRL(S,Z,HDIS,SADPOT(1),2)
      CALL FINRFC(S,Z,HDIS,REGION,SADPOT)
      RETURN
40    CALL FINRFC(S,Z,HDIS,REGION,SADPOT)
      RETURN
50    IF(ID.EQ.4) RETURN
      IF(Z.GT.S) THEN
             CALL FIN(Z,S,BRO,BRS,B)
      ELSE
             CALL FIN(Z,S,BRO,BRZ,B)
      ENDIF
      CALL FINCPX(Z,S,HDIS,B,SADPOT)
60    RETURN
      END
C
C     ************************************************
C
        SUBROUTINE FINDRL(S,Z,HDIS,SAD,I)
C
C     ************************************************
C     *                                              *
C     *       SUBROUTINE FINDRL IS USED TO FIND THE  *
C     *  SADDLE POINT FOR THE DIRECT AND REFLECTED   *
C     *  WAVES.                                      *
C     *                                              *
C     ************************************************
C
      IMPLICIT DOUBLE PRECISION (A-H,O-Z)
      COMPLEX*16 G1C,G2C,GC,G32PI
      COMMON /CONSTANT/SPEED,OMEGA,ALPHA,DTOT
      G1=.0
      IF(I.EQ.1) THEN
       IF(Z.GT.S) THEN
             SS=S
       ELSE
             SS=Z
```

```
      ENDIF
     ELSE
             SS=0.
     ENDIF
     G2=OMEGA*DSQRT((1.+ALPHA*SS)/(1.+ALPHA*SS+DTOT))/SPEED
     G1C=DCMPLX(G1,.0D0)
     G2C=DCMPLX(G2,.0D0)
     IF(I.EQ.1) THEN
      IF(Z.GT.S) THEN
      F1=-HDIS+DREAL(G32PI(S,G1C)-G32PI(Z,G1C))
      F2=-HDIS+DREAL(G32PI(S,G2C)-G32PI(Z,G2C))
      ELSE
      F1=-HDIS-DREAL(G32PI(S,G1C)+G32PI(Z,G1C))
      F2=-HDIS-DREAL(G32PI(S,G2C)+G32PI(Z,G2C))
      ENDIF
     ELSE
      F1=-HDIS+2.*DREAL(G32PI(.0,G1C)-G32PI(Z,G1C)-G32PI(S,G1C))
      F2=-HDIS+2.*DREAL(G32PI(.0,G2C)-G32PI(Z,G2C)-G32PI(S,G2C))
     ENDIF
     IF(DABS(F1).LT..1D-8) GOTO 11
     IF(DABS(F2).LT..1D-8) GOTO 21
     IF(F1*F2.GT..0) GOTO 41
     K=0
10   K=K+1
     IF(K.GT.500) GOTO 31
     G=(G1+G2)/2.
     GC=DCMPLX(G,0.D0)
     IF(I.EQ.1) THEN
      IF(Z.GT.S) THEN
       F=-HDIS+DREAL(G32PI(S,GC)-G32PI(Z,GC))
      ELSE
       F=-HDIS-DREAL(G32PI(S,GC)+G32PI(Z,GC))
      ENDIF
     ELSE
       F=-HDIS+2.*DREAL(G32PI(.0,GC)-G32PI(Z,GC)-G32PI(S,GC))
     ENDIF
     IF(DABS(F).LT..1D-10) GOTO 31
     IF(F1*F.GT..0) THEN
             G1=G
             GOTO 10
     ELSE
             G2=G
             GOTO 10
     ENDIF
11   SAD=G1
     F=F1
     RETURN
21   SAD=G2
     F=F2
     RETURN
31   SAD=G
41   RETURN
```

```
      END
C
C     ************************************************
C
        SUBROUTINE FINRFC(S,Z,HDIS,REGION,SADRFC)
C
C     ************************************************
C     *                                              *
C     *       SUBROUTINE FINRFC IS USED TO FIND THE  *
C     *  SADDLE POINTS OF THE REFRACTED TERM.        *
C     *                                              *
C     ************************************************
C
      IMPLICIT DOUBLE PRECISION (A-H,O-Z)
      INTEGER REGION
      COMPLEX*16 G1C,G2C,GC,GSC,GLC,G32PI
      DIMENSION SADRFC(2),RFC(2)
      COMMON /CONSTANT/SPEED,OMEGA,ALPHA,DTOT
      G1=OMEGA*DSQRT(1./(1.+DTOT))/SPEED
      IF(Z.GT.S) THEN
              SS=S
      ELSE
              SS=Z
      ENDIF
      G2=OMEGA*DSQRT((1.+ALPHA*SS)/(1.+ALPHA*SS+DTOT))/SPEED
      G1C=DCMPLX(G1,0.D0)
      G2C=DCMPLX(G2,0.D0)
      F1=-HDIS-DREAL(G32PI(Z,G1C)-G32PI(S,G1C))
      F2=-HDIS-DREAL(G32PI(Z,G2C)-G32PI(S,G2C))
      IF(REGION.EQ.6) GOTO 71
      IF(DABS(F1).LT..1D-8) GOTO 11
      IF(DABS(F2).LT..1D-8) GOTO 21
      IF(F1*F2.GT..0) GOTO 41
      K=0
10    K=K+1
      IF(K.GT.500) GOTO 51
      G=(G1+G2)/2.
      GC=DCMPLX(G,.0D0)
      F=-HDIS-DREAL(G32PI(Z,GC)-G32PI(S,GC))
      IF(DABS(F).LT..1D-10) GOTO 31
      IF(F1*F.GT..0) THEN
              G1=G
              GOTO 10
      ELSE
              G2=G
              GOTO 10
      ENDIF
11    SADRFC(2)=G1
      F=F1
      RETURN
21    SADRFC(2)=G2
      F=F2
```

```
      RETURN
31    SADRFC(2)=G
41    RETURN
51    SADRFC(2)=G
      RETURN
71    IF(F1*F2.LT..0) GOTO 81
      CALL FIN(Z,S,G1,G2,G)
      GC=DCMPLX(G,.0D0)
      F=-HDIS-DREAL(G32PI(Z,GC)-G32PI(S,GC))
      IF(DABS(F).LT..1D-10) GOTO 72
      IF(F1*F.GT..0) GOTO 81
      IF(G2.EQ.G.OR.G1.EQ.G) GOTO 72
      GG=G
      K=0
20    K=K+1
      IF(K.GT.500) GOTO 73
      GS=(GG+G1)/2.
      GSC=DCMPLX(GS,.0D0)
      FS=-HDIS-DREAL(G32PI(Z,GSC)-G32PI(S,GSC))
      IF(DABS(FS).LT..1D-10) GOTO 73
      IF(FS*F1.GT..0) THEN
              G1=GS
      ELSE
              GG=GS
      ENDIF
      GOTO 20
73    SADRFC(1)=GS
      K=0
30    K=K+1
      IF(K.GT.500) GOTO 74
      GL=(G+G2)/2.
      GLC=DCMPLX(GL,.0D0)
      FL=-HDIS-DREAL(G32PI(Z,GLC)-G32PI(S,GLC))
      IF(DABS(FL).LT..1D-10) GOTO 74
      IF(FL*F2.GT..0) THEN
              G2=GL
      ELSE
              G=GL
      ENDIF
      GOTO 30
74    SADRFC(2)=GL
      RETURN
72    SADRFC(1)=G
      SADRFC(2)=G
81    RETURN
      END
C
C     ************************************************
C
      SUBROUTINE FINCPX(Z,S,HDIS,G,SADPOT)
C
C     ************************************************
```

```
C     *                                                    *
C     *       SUBROUTINE FINCPX IS USED TO FIND THE        *
C     *  SADDLE POINTS OF A POINT INSIDE THE SHADOW        *
C     *  REGION.                                           *
C     *                                                    *
C     ****************************************************
C
      IMPLICIT REAL*8 (A-H,O-Z)
      COMMON /CONSTANT/SPEED,OMEGA,ALPHA,DTOT
      COMMON /BRANCH/BRO,BRS,BRZ,BRW
      DIMENSION SADPOT(2)
      COMPLEX*16 G32PI,G32PI2,G32PI3,B,F,FP,FP2
      COMPLEX*16 GG,G1,G2,GC
      GC=DCMPLX(G,.0D0)
      FF=-HDIS-DREAL(G32PI(Z,GC)-G32PI(S,GC))
      IF(DABS(FF).LT..1D-6) GOTO 710
      K=0
      GG=G*DCMPLX(1.,.0)+.1D-4*DCMPLX(.0,1.)
      FG=-HDIS-DREAL(G32PI(Z,GG)+G32PI(S,GG))
11    G1=GG+.01*DCMPLX(.0,1.)
      F1=-HDIS-DREAL(G32PI(Z,G1)+G32PI(S,G1))
      IF(DABS(F1).LT..1D-6) GOTO 720
      IF(K.GT.500) GOTO 900
      IF((FF-FG)*(FF-F1).GT..0) THEN
              GG=G1
              K=K+1
              GOTO 11
      ELSE
      ENDIF
20    G2=(GG+G1)/2.
      F2=-HDIS-DREAL(G32PI(Z,G2)+G32PI(S,G2))
      IF(DABS(F2).LT..1D-6.OR.K.GT.200) GOTO 730
      IF((FF-FG)*(FF-F2).GT..0) THEN
              GG=G2
              K=K+1
      ELSE
              G1=G2
              K=K+1
      ENDIF
      GOTO 20
720   GG=G1
      GOTO 900
730   GG=G2
      GOTO 900
710   SADPOT(1)=G
      SADPOT(2)=.0
      RETURN
900   B=GG
      K=0
10    F=-HDIS-G32PI(Z,B)-G32PI(S,B)
      FP=-G32PI2(Z,B)-G32PI2(S,B)
      FP2=-G32PI3(Z,B)-G32PI3(S,B)
```

```
      IF(CDABS(F).LT..1D-6) GOTO 100
      B=B-2.*F/(FP+CDSQRT(FP**2.-2.*F*FP2))
      K=K+1
      IF(K.GT.500) GOTO 200
      GOTO 10
100   SADPOT(1)=DREAL(B)
      SADPOT(2)=DIMAG(B)
      IF(DREAL(B).LE.BRS.AND.DREAL(B).LE.BRZ)
     1        SADPOT(2)=ABS(SADPOT(2))
200   RETURN
      END
C
C     ************************************************
C
      SUBROUTINE FIN(Z,S,G1,G2,G)
C
C     ************************************************
C     *                                              *
C     *       SUBROUTINE FIN IS USED TO FIND THE     *
C     *  BETA WHICH CORRESPONDS TO THE CAUSTIC AT    *
C     *  RECEIVER HEIGHT Z.                          *
C     *                                              *
C     ************************************************
C
      IMPLICIT DOUBLE PRECISION (A-H,O-Z)
      COMPLEX*16 G1C,G2C,GC,G32PI2
      COMMON /CONSTANT/SPEED,OMEGA,ALPHA,DTOT
      C=.1D-6
      G1C=DCMPLX(G1,0.DO)
      F1=DREAL(G32PI2(Z,G1C)+G32PI2(S,G1C))
11    G2=G2-C
      G2C=DCMPLX(G2,0.DO)
      F2=DREAL(G32PI2(Z,G2C)+G32PI2(S,G2C))
      IF(DABS(F1).LT..1D-8) GOTO 100
      IF(DABS(F2).LT..1D-8) GOTO 200
      IF(F1*F2.GT..0) GOTO 400
      K=0
      GL=G1
      GR=G2
      G2=G2+C
10    K=K+1
      IF(K.GT.200) RETURN
      G=(GL+GR)/2
      GC=DCMPLX(G,0.DO)
      F=DREAL(G32PI2(Z,GC)+G32PI2(S,GC))
      IF(DABS(F).LT..1D-8) RETURN
      IF(F*F1.GT..0) THEN
             GL=G
      ELSE
             GR=G
      ENDIF
      GOTO 10
```

```
100   G=G1
      RETURN
200   G=G2
      G2=G2+C
      RETURN
400   C=C*.1
      GOTO 11
      END
C
C     ************************************************************
C
      SUBROUTINE FINREG(S,Z,HDIS,REGION)
C
C     ************************************************************
C     *                                                          *
C     *       THIS IS A SUBROUTINE TO FIND THE REGION IN THE     *
C     *  PHYSICAL SPACE WHERE A SPECIFIC POINT IS LOCATED.       *
C     *                                                          *
C     ************************************************************
C
      IMPLICIT DOUBLE PRECISION (A-H,O-Z)
      INTEGER REGION
      COMMON /CONSTANT/SPEED,OMEGA,ALPHA,DTOT
C     THE FOLLOWING STATEMENT IS USED BECAUSE OF THE
C     PROBLEM ARISED FROM THE DOUBLE PRECISION.
      IF(ABS(Z-S).LT.0.1E-10)GOTO 5
      IF(Z.LE.S) THEN
       IF(Z.LT.1E-5)GOTO 8
5       ANGLE2=DACOS(DSQRT((1.+ALPHA*S+DTOT)/((1.+DTOT)
     1     *(1.+ALPHA*S))))
        BOUND2=FNRAY(Z,ANGLE2,S)+FNRAY(S,ANGLE2,S)
8       IF((Z.GT.2.99999).AND.(Z.LT.3.00001))THEN
              BOUND3=0.0
              GOTO 10
        ENDIF
        ANGLE3=DACOS(DSQRT((1.+ALPHA*S+DTOT)*(1.+ALPHA*
     1      Z)/((1.+ALPHA*Z+DTOT)*(1.+ALPHA*S))))
        BOUND3=FNRAY(S,ANGLE3,S)
        IF(Z.LT.1E-5)BOUND2=BOUND3
10      IF((HDIS.GT.BOUND2).AND.(HDIS.GT.BOUND3)) THEN
              CALL EVALB4(S,Z,ANGLE4,BOUND4)
              IF(HDIS.LE.BOUND4) THEN
                  REGION=6
              ELSE
                  REGION=7
              ENDIF
         ELSE
            IF((HDIS.GT.BOUND2).AND.(HDIS.LT.BOUND3)) THEN
                  REGION=4
            ELSEIF((HDIS.GT.BOUND3).AND.(HDIS.LT.BOUND2)) THEN
                  REGION=5
            ELSE
```

```
                REGION=3
              ENDIF
             ENDIF
            ELSE
             ZERO=0.0
             BOUND1=FNRAY(Z,ZERO,S)
             ANGLE2=DACOS(DSQRT((1.+ALPHA*S+DTOT)/((1.+DTOT)
     1        *(1.+ALPHA*S))))
             BOUND2=FNRAY(Z,ANGLE2,S)+FNRAY(S,ANGLE2,S)
             IF((HDIS.LT.BOUND2).AND.(HDIS.LT.BOUND1)) THEN
                  REGION=1
             ELSEIF((HDIS.LT.BOUND1).AND.(HDIS.GT.BOUND2)) THEN
                  REGION=2
             ELSEIF((HDIS.LT.BOUND2).AND.(HDIS.GT.BOUND1)) THEN
                  REGION=5
             ELSE
                  CALL EVALB4(S,Z,ANGLE4,BOUND4)
                  IF(HDIS.LT.BOUND4) THEN
                      REGION=6
                      GOTO 20
                  ENDIF
                  REGION=7
             ENDIF
            ENDIF
20          RETURN
            END
C
C     ************************************************
C
        SUBROUTINE EVALB4(S,Z,ANGLE4,BOUND4)
C
C     ************************************************
C     *                                              *
C     *       SUBROUTINE EVALB4 IS USED TO EVALUATE  *
C     *  THE SHADOW BOUNDARY.                        *
C     *                                              *
C     ************************************************
C
        IMPLICIT DOUBLE PRECISION (A-H,O-Z)
        COMPLEX*16 GU1,GU2,G32PI2
        COMMON /CONSTANT/SPEED,OMEGA,ALPHA,DTOT
        GUESS2=(OMEGA/SPEED)*DSQRT(1./(1.+DTOT))
        IF(Z.GT.S) THEN
           GUESS1=(OMEGA/SPEED)*DSQRT((1.+ALPHA*S)/
     1      (1.+ALPHA*S+DTOT))-0.00001
        ELSE
           GUESS1=(OMEGA/SPEED)*DSQRT((1.+ALPHA*Z)/
     1      (1.+ALPHA*Z+DTOT))-0.00001
        ENDIF
        ICOUNT=0
10      GU1=DCMPLX(GUESS1,0.D0)
        Y=DREAL(G32PI2(Z,GU1)+G32PI2(S,GU1))
```

```
      IF(Y.LT.0.0) THEN
         GOTO 20
      ELSE
         TEMP=Y
       IF(Z.LT.25.0) THEN
            GUESS1=GUESS1-.001
       ELSE
            GUESS1=GUESS1-.0001
       END IF
         GOTO 10
      END IF
20    IF(Z.LT.25.0) THEN
         GUESS1=GUESS1+.001
      ELSE
         GUESS1=GUESS1+.0001
      END IF
      FF=TEMP
30    GU2=DCMPLX(GUESS2,0.D0)
      HDIS=DREAL(G32PI2(Z,GU2)+G32PI2(S,GU2))
      GG=HDIS
      DELTA=GUESS2-(GUESS2-GUESS1)/(GG-FF)*GG
      IF(ABS(DELTA-GUESS2).LT..000001) THEN
         GOTO 40
      ELSE
         ICOUNT=ICOUNT+1
       IF(ICOUNT.GT.1000) THEN
              GOTO 50
       ELSE
            GUESS2=DELTA
            GOTO 30
       END IF
      END IF
40    ABETA=DELTA
      ANGLE4=DACOS((ABETA*SPEED)/(OMEGA*DSQRT((1.+
     1  ALPHA*S)/(1.+ALPHA*S+DTOT))))
      BOUND4=FNRAY(Z,ANGLE4,S)+FNRAY(S,ANGLE4,S)
50    RETURN
      END
C
C     ************************************************************
C
      SUBROUTINE FALL(Z,BETA,F,F1,F2,Z1,E,H2,GZ,K,H1,N)
C
C     ************************************************************
C     *                                                          *
C     *       THIS SUBROUTINE EVALUATES THE REFLECTED/REFRA-     *
C     *  CTED COEFFICIENTS AND THE FIRST AND SECOND DERIVA-       *
C     *  TIVES OF THE DENOMINATOR OF THE COEFFICIENT.            *
C     *                                                          *
C     ************************************************************
C
      IMPLICIT REAL*8(A-H,O-Z)
```

```
      COMPLEX *16 BETA,F,F1,F2,A,GZ,GZZ,GZ1,GZ2,GZZ1,GZZ2
     1        EN,EN1,EN2,A1,A2,AI,Z1,B,B1,B2,E,H1,H11,H12,H2,H21
     2        ,H13,C,AIQ,H22,H23
      COMMON /CONSTANT/SPEED,OMEGA,ALPHA,DTOT
      CALL GZALL1(Z,BETA,GZ,GZ1,GZ2,GZZ,GZZ1,GZZ2,EN,EN1,EN2)
      PI=4.*DATAN(1.DO)
      AI=DCMPLX(0.,1.)
      IF(N.EQ.2) EN=EN*CDEXP(2.*AI*PI/3.)
      CALL HALL(EN,H2,H21,H22,H23,H1,H11,H12,H13,AIQ)
      A=1.-AI*SPEED*Z1*GZZ/(2.*OMEGA*GZ)
      A1=(A-1.)*GZZ1/GZZ+(1.-A)*GZ1/GZ
      A2=(A-1.)*GZZ2/GZZ+(1.-A)*GZ2/GZ-2.*A1*GZ1/GZ
      B=AI*SPEED*Z1*(3.*OMEGA/(2.*SPEED*ALPHA))**(2./3.)*GZ/OMEGA
      B1=B*GZ1/GZ
      B2=B*GZ2/GZ
      IF(K.EQ.2) GOTO 10
      F=A*H2+B*H21
      E=-(A*H1+B*H11)
      F1=A*H21*EN1+H2*A1+B*H22*EN1+B1*H21
      F2=(A*H22+B*H23)*EN1**2+(A*H21+B*H22)*EN2+
     1        (H21*A1+H22*B1)*2.*EN1+H2*A2+H21*B2
      RETURN
10    PI=4.*DATAN(1.DO)
      C=CDEXP(PI*AI/3.)
      F=A*(H2+C*H1)+B*(H21+C*H11)
      E=CDEXP(-PI*AI/3.)*(A*H2+B*H21)
      F1=A*(H21+C*H11)*EN1+(H2+C*H1)*A1+B*(H22+C*H12)*EN1+B1
     1        *(H21+C*H11)
      F2=(A*(H22+C*H12)+B*(H23+C*H13))*EN1**2+(A*(H21+C*H11)
     1  +B*(H22+C*H12))*EN2+((H21+C*H11)*A1+(H22+C*H12)*B1)*2.*EN1
     2  +(H2+C*H1)*A2+(H21+C*H11)*B2
      RETURN
      END
C
C     ***************************************************************
C
      SUBROUTINE HALL(Z,H2,H21,H22,H23,H1,H11,H12,H13,AI)
C
C
C     *  HALL USES SUBROUTINE CGBAIR TO CALCULATE 1/3 ORDER  *
C     *  HANKLE  FUNCTIONS FROM AIRY FUNCTIONS.              *
C
C
        IMPLICIT REAL*8 (A-H,O-Z)
        COMPLEX*16 Z,AI,BI,AIP,BIP,K,KS,H1,H2,H11,H21,ARG,CI,H12
        COMPLEX*16 H23,H13,H22
        CI= DCMPLX(0.DO,1.DO)
        PI= 3.141592654DO
        ARG= DCMPLX(0.DO,-PI/6.DO)
        K= (12.DO)**(1.DO/6.DO)*CDEXP(ARG)
        KS= DCONJG(K)
```

```
      CALL CGBAIR(-Z,AI,BI,AIP,BIP)
      H1= K*(AI-CI*BI)
      H2= KS*(AI+CI*BI)
      H11= -K*(AIP-CI*BIP)
      H21= -KS*(AIP+CI*BIP)
      H22=-Z*H2
      H12=-Z*H1
      H23=-H2-Z*H21
      H13=-H1-Z*H11
      RETURN
      END
C
C     ***************************************************************
C
      SUBROUTINE CGBAIR(Z,AI,BI,AIP,BIP)
C
C     ***************************************************************
C     *                                                             *
C     *       SUBROUTINE CGBAIR EVALUATES THE AIRY FUNCTIONS.       *
C     *                                                             *
C     ***************************************************************
C
      IMPLICIT REAL*8 (A-H,O-Z)
      COMPLEX*16 Z,AI,BI,AIP,BIP,ZETA,CZETA,Z14,SUM1,SUM2,
     1 SUM3,SUM4,ZETAP,FACT1,FACT2,SN,CS,FTERM,FPTERM,GTERM,
     2 GPTERM,F,FP,G,GP,Z3
      DIMENSION C(21),D(21)
C
      DATA C1,C2,PIRT,PI4/.3550280539D0,.2588194038D0,
     + 1.772453851D0,.7853981635D0/
C
      DATA C/1.D0,.069444444444444D0,
     + .037133487654321D0,.0379930591278OOD0,
     1 .0576491904126690,.11609906402551D0,
     + .291591399230740,.87766696950998D0,
     2 3.0794530301731D0,12.341573332345D0,
     + 55.622785365914D0,278.46508077759D0,
     3 1533.1694320127D0,9207.2065997258D0,
     + 59892.513565875D0,419524.87511653D0,
     4 3148257.4178666D0,25198919.871601D0,
     + 214288036.96366D0,1929375549.1823D0,
     5 18335766937.889D0/
C
      DATA D/1.D0,-.097222222222221D0,
     + -.043885030864197D0,-.042462830789894D0,
     1 -.062662163492031D0,-.12410589602727D0,-.30825376490107D0,
     2 -.92047999241291D0,-3.2104935846485D0,-12.807293080735D0,
     3 -57.508303513911D0,-287.03323710920D0,-1576.3573033370D0,
     4 -9446.3548230953D0,-61335.706663847D0,-428952.40040004D0,
     5 -3214536.5214006D0,-25697908.383909D0,-218293420.83214D0,
     6 -1963523788.9909D0,-18643931088.105D0/
C
```

```
      ABSZ=ABS(Z)
      IF(ABSZ.EQ.0) GOTO 3
      IF(ABS(DIMAG(Z)).LE.1.D-12.AND.DREAL(Z).LT.0.DO) GOTO 5
      ARGZ=ATAN2(DIMAG(Z),DREAL(Z))
      GOTO 4
3     ARGZ=0.DO
      GOTO 4
5     ARGZ=3.1415926535898DO
4     CONTINUE
      IF(ABSZ.GT.6.DO) GOTO 10
C
C     ASCENDING SERIES
C     EQS. 10.4.2,10.4.3
C
      Z3=Z**3
      FTERM=1.DO
      FPTERM=Z*Z/2.DO
      GTERM=Z
      GPTERM=1.DO
      GLIM=1.D-13*ABSZ
      F=FTERM
      FP=FPTERM
      G=GTERM
      GP=GPTERM
      DO 1 I=1,100
      I3=3*I
      FTERM=FTERM*Z3/((I3-1.DO)*I3)
      FPTERM=FPTERM*Z3/(I3*(I3+2.DO))
      GTERM=GTERM*Z3/(I3*(I3+1.DO))
      GPTERM=GPTERM*Z3/((I3-2.DO)*I3)
      F=F+FTERM
      FP=FP+FPTERM
      G=G+GTERM
      GP=GP+GPTERM
      IF(ABS(GTERM).LE.GLIM) GOTO 2
1     CONTINUE
2     AI=C1*F-C2*G
      AIP=C1*FP-C2*GP
      BI=1.732050808DO*(C1*F+C2*G)
      BIP=1.732050808DO*(C1*FP+C2*GP)
      GOTO 999
C
C     ASYMPTOTIC EXPANSION FOR /Z/ LARGE
C
10    SIGN=1.DO
      SUM1=0.DO
      SUM2=0.DO
      SUM3=0.DO
      SUM4=0.DO
      IF(ABS(ARGZ).GE.1.3DO) GOTO 20
C
C     /ARG(Z)/ LE PI/3
```

```
C       EQS. 10.4.59, 10.4.61, 10.4.63, 10.4.66
C
        ZETA=CZETA(ABSZ,ARGZ)
        DO 11 I=1,12
        K=I-1
        ZETAP=ZETA**K
        SUM1=SUM1+SIGN*C(I)/ZETAP
        SUM2=SUM2+SIGN*D(I)/ZETAP
        SUM3=SUM3+C(I)/ZETAP
        SUM4=SUM4+D(I)/ZETAP
11      SIGN=-SIGN
        Z14=ABSZ**.25D0*DCMPLX(COS(ARGZ/4.D0),SIN(ARGZ/4.D0))
        FACT1=.5D0*EXP(-ZETA)/(PIRT*Z14)
        FACT2=.5D0*EXP(-ZETA)*Z14/PIRT
        AI=FACT1*SUM1
        AIP=-FACT2*SUM2
        FACT1=EXP(ZETA)/(PIRT*Z14)
        FACT2=EXP(ZETA)*Z14/PIRT
        BI=FACT1*SUM3
        BIP=FACT2*SUM4
        GOTO 999
C
C       /ARG(Z)/ GT PI/3
C       EQS. 10.4.60, 10.4.62, 10.4.64, 10.4.67
C
20      ARGZ=ATAN2(-DIMAG(Z),-DREAL(Z))
        ZETA=CZETA(ABSZ,ARGZ)
        DO 21 I=1,10
        K2=(I-1)*2
        J=K2+1
        ZETAP=ZETA**K2
        SUM1=SUM1+SIGN*C(J)/ZETAP
        SUM2=SUM2+SIGN*C(J+1)/(ZETAP*ZETA)
        SUM3=SUM3+SIGN*D(J)/ZETAP
        SUM4=SUM4+SIGN*D(J+1)/(ZETAP*ZETA)
21      SIGN=-SIGN
        Z14=ABSZ**.25D0*DCMPLX(COS(ARGZ/4.D0),SIN(ARGZ/4.D0))
        FACT1=1.D0/(PIRT*Z14)
        FACT2=Z14/PIRT
        SN=SIN(ZETA+PI4)
        CS=COS(ZETA+PI4)
        AI=FACT1*(SN*SUM1-CS*SUM2)
        AIP=-FACT2*(CS*SUM3+SN*SUM4)
        BI=FACT1*(CS*SUM1+SN*SUM2)
        BIP=FACT2*(SN*SUM3-CS*SUM4)
999     RETURN
        END
C
C       ************************************
C
        FUNCTION CZETA(ABSZ,ARGZ)
        IMPLICIT REAL*8 (A-H,O-Z)
```

```
      COMPLEX*16 CZETA
      ARG=ARGZ*1.5D0
      CZETA=(ABSZ**1.5D0)*DCMPLX(COS(ARG),SIN(ARG))
     1      *.66666666666667D0
      RETURN
      END
C
C     ************************************************
C
      SUBROUTINE FINFORM(BETA,Z,F1,HDIS,S,F2,FORM)
C
C     ************************************************
C     *                                              *
C     *       SUBROUTINE FINFORM DECIDES THE FORM OF *
C     *  THE SOLUTION TO BE USED.                    *
C     *                                              *
C     ************************************************
C
      IMPLICIT REAL*8 (A-H,O-Z)
      COMPLEX*16 BETA,G320,G32S,G32Z,G32,G321,F
      INTEGER FORM
      REAL *8 LEMDA
      COMMON /BRANCH/BRO,BRS,BRZ,BRW
      COMMON /CONSTANT/SPEED,OMEGA,ALPHA,DTOT
      PI=4.*DATAN(1.D0)
      LEMDA=OMEGA/(SPEED*ALPHA)
      G320=G32(.0,BETA)
      G32S=G32(S,BETA)
      G32Z=G32(Z,BETA)
      FORM=1
      IF(DIMAG(BETA).GT..0) THEN
         IF(DREAL(G320).LT..0.AND.DIMAG(G320).GT..0) FORM=2
       IF(Z.GT.S) THEN
          IF(DREAL(G32S).LT..0.AND.DIMAG(G32S).GT..0) FORM=5
        IF(DREAL(G32Z).LT..0.AND.DIMAG(G32Z).GT..0) FORM=4
       ELSE
        IF(DREAL(G32Z).LT..0.AND.DIMAG(G32Z).GT..0) FORM=3
        IF(DREAL(G32S).LT..0.AND.DIMAG(G32S).GT..0) FORM=4
       ENDIF
      ELSE
       IF(DREAL(BETA).LT.BRW) FORM=4
       IF(Z.GT.S) THEN
          IF(DREAL(BETA).LT.BRZ) FORM=5
          IF(DREAL(BETA).LT.BRS) FORM=2
       ELSE
          IF(DREAL(BETA).LT.BRS) FORM=3
          IF(DREAL(BETA).LT.BRS) FORM=2
       ENDIF
          IF(DREAL(BETA).LT.BRO) FORM=1
      ENDIF
      GOTO (10,20,30,40,50) FORM
10    F=(-BETA*HDIS+LEMDA*(2.*G321(.0,BETA,S,FORM)
```

```
     1        -G321(Z,BETA,S,FORM)-G321(S,BETA,S,FORM)))
      GOTO 55
20    F=(-BETA*HDIS-LEMDA*(G321(Z,BETA,S,FORM)
     1        +G321(S,BETA,S,FORM)))
      GOTO 55
30    F=(-BETA*HDIS-LEMDA*(G321(Z,BETA,S,FORM)
     1        +G321(S,BETA,S,FORM))-PI/3.)
      GOTO 55
40    F=(-BETA*HDIS-LEMDA*(G321(Z,BETA,S,FORM)
     1        +G321(S,BETA,S,FORM))-2.*PI/3.)
      GOTO 55
50    F=(-BETA*HDIS-LEMDA*(G321(Z,BETA,S,FORM)
     1        +G321(S,BETA,S,FORM))-PI/3.)
      GOTO 55
51    F=(-BETA*HDIS-LEMDA*(G321(Z,BETA,S,FORM)
     1        +CDABS(G321(.0,BETA,S,FORM))
     2        +G321(S,BETA,S,FORM))+PI/4.)
55    F1=DREAL(F)
      F2=DIMAG(F)
60    RETURN
      END
C
C     ***********************************************************
C
      SUBROUTINE GZALL1(Z,BETA,GZ,GZ1,GZ2,GZZ,GZZ1,GZZ2,EN,EN1,EN2)
C
C     ***********************************************************
C     *                                                         *
C     *       GZALL1 CALCULATES ALL THE PARTIAL DERIVATIVES     *
C     *  OF THE G FUNCTION WITH RESPECT TO Z.                   *
C     *                                                         *
C     ***********************************************************
C
      IMPLICIT REAL*8(A-H,O-Z)
      COMPLEX *16 BETA,GZ,GZ1,GZ2,GZZ,GZZ1,GZZ2,G,GB,GBB,SQRT1,
     1        EN,EN1,EN2
      COMMON /CONSTANT/SPEED,OMEGA,ALPHA,DTOT
      CALL GALL(Z,BETA,G,GB,GBB)
      A=1.+ALPHA*Z+DTOT
      BRAN=OMEGA/SPEED*DSQRT((A-DTOT)/A)
      IF(DREAL(G).LE..0.AND.DIMAG(G).GE.0.) THEN
            SI=-1.
      ELSE
            SI=1.
      ENDIF
      GZ=SI*2.*ALPHA*SQRT1(BETA,Z)/(3.*CDSQRT(G*A))
      C=2.*ALPHA**3*DTOT/(9*A**2)
      GZZ=C/(GZ*G)-.5*GZ**2/G
      B=-(2.*ALPHA*SPEED/(3.*OMEGA))**2
      GZ1=B*BETA/(GZ*G)-.5*GZ*GB/G
      GZ2=B*(GZ*G-BETA*(GZ1*G+GZ*GB))/(GZ*G)**2-.5*(G*(GZ1*GB+
     1  GZ*GBB)-GZ*GB**2)/G**2
```

```
      GZZ1=-C*(GZ*GB+GZ1*G)/(GZ*G)**2-.5*(2.*G*GZ*GZ1-GZ**2*GB)
     2  /G**2
      GZZ2=-C*(GZ*G*(GZ*GBB+2.*GZ1*GB+G*GZ2)-2.*(GZ*GB+GZ1*G)**2)
     3  /(GZ*G)**3-.5*(G*(2.*G*GZ1**2+2.*G*GZ*GZ2-GZ**2*GBB)-2.*GB*
     4  (2.*G*GZ*GZ1-GZ**2*GB))/G**3
      T=(3.*OMEGA/(2.*ALPHA*SPEED))**(2./3.)
      EN=T*G
      EN1=T*GB
      EN2=T*GBB
      RETURN
      END
C
C     ************************************************
C
      SUBROUTINE GALL(Z,BETA,G,GPI,GPI2)
C
C     ************************************************
C     *                                              *
C     *       GALL EVALUATES THE G FUNCTION AND ITS  *
C     *  PARTIAL DERIVATIVES WITH RESPECT TO BETA.   *
C     *                                              *
C     ************************************************
C
      IMPLICIT REAL*8 (A-H,O-Z)
      COMPLEX *16 G,GPI,GPI2,BETA,G32,G32PI,G32PI2
      COMMON /CONSTANT/SPEED,OMEGA,ALPHA,DTOT
      G=CDEXP(2./3.*CDLOG(G32(Z,BETA)))
      IF(DREAL(G).LE..0.AND.DIMAG(G).GE..0) THEN
            S=-1.
        ELSE
            S=1.
      ENDIF
      GPI=2.*SPEED*ALPHA*S*G32PI(Z,BETA)/(3.*OMEGA*CDSQRT(G))
      GPI2=GPI*G32PI2(Z,BETA)/G32PI(Z,BETA)-.5*GPI**2/G
      RETURN
      END
C
C     ************************************************************
C
      FUNCTION G321(Z,BETA,S,FORM)
C
C     ************************************************************
C     *                                                          *
C     *       THIS FUNCTION IS REQUIRED BECAUSE OF DIFFERENT     *
C     *  BRANCH CUTS INVOLVED  WITH HANKEL FUNCTIONS.            *
C     *                                                          *
C     ************************************************************
C
      IMPLICIT REAL*8 (A-H,O-Z)
      COMPLEX*16 BETA,G321,G,G32,C
      INTEGER FORM
      PI=4.*DATAN(1.DO)
```

```
      C=CDEXP(2.*PI*DCMPLX(.0,1.)/3.)
      G=CDEXP(2./3.*CDLOG(G32(Z,BETA)))
      G321=(CDSQRT(G))**3.
      IF(FORM.EQ.3.AND.Z.LT.S.OR.FORM.EQ.5.AND.Z.EQ.S
     1        .OR.FORM.EQ.4) THEN
       IF(DIMAG(BETA).LT..0)THEN
             G321=-(CDSQRT(C*G))**3.
       ELSE
            G321=(CDSQRT(C*G))**3.
       ENDIF
      ENDIF
      RETURN
      END
C
C     ************************************************
C
      FUNCTION G32(Z,BETA)
C
C     ************************************************
C     *                                              *
C     *       THIS FUNCTION CALCULATES THE G TO THE  *
C     *  3/2 POWER.                                  *
C     *                                              *
C     ************************************************
C
      IMPLICIT REAL*8 (A-H,O-Z)
      COMPLEX*16 BETA,PHI,SQRT1,SQRT2,FOO,G32,MODLOG
      COMPLEX*16 S1,S,B
      COMMON /CONSTANT/SPEED,OMEGA,ALPHA,DTOT
      AA=1.+ALPHA*Z+DTOT
      B=1.-(SPEED*BETA/OMEGA)**2
      S1=SQRT1(BETA,Z)
      S=SQRT2(BETA)
      PHI=S1/(S*DSQRT(AA))
      IF(DTOT.EQ..0) THEN
             FOO=.0
      ELSE
        FOO=MODLOG((1.+PHI)/(1.-PHI))
      ENDIF
      G32=DSQRT(AA)*S1-.5*DTOT*FOO/S
      RETURN
      END
C
C     ************************************************
C
        FUNCTION G32PI(Z,BETA)
C
C     ************************************************
C     *                                              *
C     *       THE FIRST DERIVATIVE OF G32 WITH RESPECT *
C     *  TO BETA IS CALCULATED.                      *
C     *                                              *
```

```
C     ************************************************
C
      IMPLICIT REAL*8 (A-H,O-Z)
      COMPLEX*16 BETA,PHI,SQRT1,SQRT2,FOO,MODLOG,G32PI,S1,S,A,B
      COMMON /CONSTANT/SPEED,OMEGA,ALPHA,DTOT
      AA=1.+ALPHA*Z+DTOT
      B=1.-(SPEED*BETA/OMEGA)**2
      S1=SQRT1(BETA,Z)
      S=SQRT2(BETA)
      PHI=S1/(S*DSQRT(AA))
      IF(DTOT.EQ..0) THEN
            FOO=.0
      ELSE
        FOO=MODLOG((1.+PHI)/(1.-PHI))
      ENDIF
      A=-1.*SPEED*BETA/(ALPHA*OMEGA*B)
      G32PI=A*(DSQRT(AA)*S1+.5*DTOT*FOO/S)
      RETURN
      END
C
C     ************************************************
C
      FUNCTION G32PI2(Z,BETA)
C
C     ************************************************
C     *                                              *
C     *       THE SECOND DERIVATIVE OF G32 WITH      *
C     *  RESPECT TO BETA IS CALCULATED.              *
C     *                                              *
C     ************************************************
C
      IMPLICIT REAL*8 (A-H,O-Z)
      COMPLEX*16 BETA,PHI,SQRT1,SQRT2,FOO,MODLOG,PRT2,PRT3
      COMPLEX*16 G32PI2,S1,S,A,B,B1,A0,A1,A2,A3,PRT0,PRT1
      COMMON /CONSTANT/SPEED,OMEGA,ALPHA,DTOT
      AA=1.+ALPHA*Z+DTOT
      B=1.-(SPEED*BETA/OMEGA)**2
      S1=SQRT1(BETA,Z)
      S=SQRT2(BETA)
      PHI=S1/(S*DSQRT(AA))
      IF(DTOT.EQ..0) THEN
            FOO=.0
      ELSE
            FOO=MODLOG((1.+PHI)/(1.-PHI))
      ENDIF
      B1=1.+2.*(SPEED*BETA/OMEGA)**2.
      G32PI2=-SPEED/(ALPHA*OMEGA*B**2)*((B*AA**2-B1*DTOT*AA)/
     1  (DSQRT(AA)*S1)+.5*DTOT*B1*FOO/S)
        RETURN
        END
C
C     ************************************************
```

```
C
      FUNCTION G32PI3(Z,BETA)
C
C     ************************************************
C     *                                              *
C     *       THE THIRD DERIVATIVE OF G32 WITH RESPECT *
C     *  TO BETA IS CALCULATED.                      *
C     *                                              *
C     ************************************************
C
      IMPLICIT REAL*8 (A-H,O-Z)
      COMPLEX*16 BETA,PHI,SQRT1,SQRT2,FOO,MODLOG,G32PI2,PRT3
      COMPLEX*16 G32PI3,S1,S,A,B,B1,A0,A1,A2,A3,PRT0,PRT1,PRT2
      COMMON /CONSTANT/SPEED,OMEGA,ALPHA,DTOT
      AA=1.+ALPHA*Z+DTOT
      B=1.-(SPEED*BETA/OMEGA)**2
      S1=SQRT1(BETA,Z)
      S=SQRT2(BETA)
      PHI=S1/(S*DSQRT(AA))
      IF(DTOT.EQ..0) THEN
            FOO=.0
      ELSE
            FOO=MODLOG((1.+PHI)/(1.-PHI))
      ENDIF
      A1=(SPEED*BETA/OMEGA)**2
      A0=A1/BETA
      A2=1.+2.*A1
      A3=5.-2.*A1
      PRT0=-(SPEED/(ALPHA*OMEGA))/B**2
      PRT1=A0*AA**2*(2.*A1*DTOT*AA+4.*DTOT**2-B*AA**2-3.*DTOT*AA)
      PRT2=(B*AA**2-DTOT*AA)*S1*DSQRT(AA)
      PRT3=FOO*A0*A3/B*S-2.*A0*A2*DSQRT(AA)/
     1      (B*S1)
      PRT4=4.*A0/B*G32PI2(Z,BETA)
      G32PI3=PRT0*(PRT1/PRT2+0.5*DTOT*PRT3)+PRT4
      RETURN
      END
C
C     ************************************************************
C
      FUNCTION SQRT1(BETA,Z)
      IMPLICIT REAL*8 (A-H,O-Z)
      COMPLEX*16 BETA,AA,SQRT1
      COMMON /CONSTANT/SPEED,OMEGA,ALPHA,DTOT
      AA=1.-((SPEED/OMEGA)*BETA)**2.
      BB=1.+ALPHA*Z+DTOT
      BRAN1=(OMEGA/SPEED)*DSQRT((1.+ALPHA*Z)/(1.+ALPHA*Z+DTOT))
      IF((DREAL(BETA) .GE. BRAN1) .AND.
     1  (DIMAG(BETA) .LE. 0.0)) THEN
           SQRT1=-CDSQRT(AA*BB-DTOT)
      ELSE
           SQRT1=CDSQRT(AA*BB-DTOT)
```

```
      END IF
      RETURN
      END
C
C     ************************************************
C
      FUNCTION SQRT2(BETA)
      IMPLICIT REAL*8 (A-H,O-Z)
      COMPLEX*16 BETA,AA,SQRT2
      COMMON /BRANCH/BRO,BRS,BRZ,BRW
      COMMON /CONSTANT/SPEED,OMEGA,ALPHA,DTOT
      AA=1.-((SPEED/OMEGA)*BETA)**2.
      IF((DREAL(BETA) .GE. BRW) .AND.
     1        (DIMAG(BETA) .LE..0)) THEN
           SQRT2=-CDSQRT(AA)
      ELSE
           SQRT2=CDSQRT(AA)
      END IF
      RETURN
      END
C
C     ************************************************
C
      FUNCTION MODLOG(QUAN)
      IMPLICIT REAL*8 (A-H,O-Z)
      COMPLEX*16 QUAN,MODLOG
      IF((DREAL(QUAN) .LE. 0.0) .AND. (DIMAG(QUAN)
     1        .GE. 0.0)) THEN
       MODLOG=CDLOG(QUAN)+DCMPLX(0.0,-2*3.1415927)
      ELSE
       MODLOG=CDLOG(QUAN)
      END IF
      RETURN
      END
C
C     ************************************************************
C
      FUNCTION FNRAY(Z,ANGLE,S)
      IMPLICIT REAL*8 (A-H,O-Z)
      COMPLEX*16 G32PI,BC
      COMMON /CONSTANT/SPEED,OMEGA,ALPHA,DTOT
      IF(ANGLE.EQ..0) ANGLE=.000001
      BETA=OMEGA/SPEED*DSQRT((1.+ALPHA*S)/(1.+ALPHA*S+DTOT))
     1        *DCOS(ANGLE)
      BC=DCMPLX(BETA,.0D0)
      FNRAY=-DREAL(G32PI(Z,BC))
      RETURN
      END
```

REFERENCES

1. U. Ingard, "On the Reflection of a Sperhical Sound Wave From an Infinite plane," J. Acoust. Soc. Am., Vol. 23, 1951, pp. 329-335.

2. R.B. Lawhead and I. Rundick, "Measurements on an Acoustic Wave Propagated Along a Boundary," J. Acoust. Soc. Am., Vol. 23, 1951, pp. 541-545.

3. R.B. Lawhead and I. Rundick, "Acoustic Wave Propagation Along a Constant Normal Impedance Boundary," J. Acoust. Soc. Am., Vol. 23, 1951, pp. 546-549.

4. A.R. Wenzel, "Propagation of Waves Along an Impedance Boundary," J. Acoust. Soc. Am., Vol. 55, 1974, pp. 956-963.

5. C.F. Chien and W.W. Soroka, "Sound Propagation Along an Impedance Plane," J. Sound Vib., Vol. 43, 1975, pp. 9-20.

6. S. Thomasson, "Reflection of Waves From a Point Source by an Impedance Boundary," J. Acoust. Soc. Am., Vol. 59, 1976, pp. 780-785.

7. T.F. Embleton, J.E. Piercy and N. Olson, "Effect of the Ground on Near-horizontal Sound Propagation," J. Acoust. Soc. Am., Vol. 53, 1973, pg. 340(A).

8. T.F. Embleton, J.E. Piercy and N. Olson, "Outdoor Sound Progagation Over Ground of Finite Impedance," J. Acoust. Soc. Am., Vol. 59, 1976, pp. 267-277.

9. F.M. Wiener and D.N. Keast, "Experimental Study of the Propagation of Sound Over Ground," J. Acoust. Soc. Am., Vol. 31, 1959, pp. 724-733.

10. P.H. Parkin and W.E. Scholes, "The Horizontal Propagation of Sound From a Jet Engine Close to Ground, at Radlett," J. Sound Vib., Vol. 1, 1964, pp. 1-13.

11. P.H. Parkin and W.E. Scholes, "The Horizontal Propagation of Sound From a Jet Engine Close to Ground, at Hatfield," J. Sound Vib., Vol. 2, 1965, pp. 353-374.

12. S.P. Pao and L.B. Evans, "Sound Attenuation Over Simulated Ground Cover," J. Acoust. Soc. Am., Vol. 49, 1971, pp. 1069-1075.

13. H.G. Jonasson, "Sound Reduction by Barriers on the Ground," J. Sound Vib., Vol. 22, 1972, pp. 113-126.

14. A. Cheng, Unpublished manuscript, Mechanical and Industrial Engineering Department, University of Utah, Salt Lake City, Utah.

15. W.K. Van Moorhem, "An Investigation of Acoustic Propagation in a Thermally Inhomoheneous Atmosphere," UTEC ME82-015, Mechanical and Industrial Engineering Department, University of Utah, Salt Lake City, Utah.

16. W.K. Van Moorhem, "Acoustic Propagation in a Thermally Stratified Atmosphere," "Fourth Seminannual Report to the National Aeronautic and Space Agency-Grant NAG-1-283," UTEC ME 84-075, Mechanical and Industrial Engineering Department, University of Utah, Salt Lake City, Utah.

17. J. Mathews and R.L. Walker, Mathematical Methods of Physics, (W.A. Benjamin, Inc., New York), 1964.

18. L.P. Smith, Methods for Scientists and Engineers, (Prentice-Hall, Inc., New York), 1953.

19. D.A. Sachs and A. Silbiger, "Focusing and Refraction of Harmonic Sound and Transient Pulses in a Stratified Media," J. Acoust. Soc. Am. Vol. 49, 1971, pp. 824-840.

20. D.W. While and M.A. Pedersen, "Evaluation of Shadow Zone Fields by Uniform Asymptotics and Complex Rays," J. Acoust. Soc. Am. Vol. 69, 1981, pp. 1029-1058.

21. C.I. Chessell, "Propagation of Noise Along a Finite Impedance Boundary," J. Acoust. Soc. Am., Vol. 62, 1977, pp. 825-834.

22. J.E. Piercy and R.F. Embleton, "Noise Testing of Vehicles-Acoustic Propagation Phenomena," S.A.E. Special Publication 456, 1980, pp. 13-19.

23. J.E. Piercy, R.F. Embleton, and L.C. Sutherland, "Review of Noise Propagation in the Atmosphere," J. Acoust. Soc. Am., Vol. 61, pp. 1403-1418.

24. S.P. Pao, A.R. Wenzel and P.B. Oncley, "Prediction of Ground Effects on Aircraft Noise," NASA Technical Paper 1104.

25. W.K. Van Moorhem, personal communication.

APPENDIX C

The propagation of plane waves in a thermally stratified atmosphere

W. K. Van Moorhem and Gregory K. Landheim
Mechanical and Industrial Engineering Department, University of Utah, Salt Lake City, Utah 84112

(Received 28 July 1983; accepted for publication 2 June 1984)

The behavior of a plane wave reflecting from a finite impedance surface with a realistic atmospheric temperature profile is investigated. An approximate solution has been implemented on a digital computer and this solution is presented graphically for a number of cases at low incidence angles.

PACS numbers: 43.28.Kt, 43.28.Fb, 43.20.Bi

INTRODUCTION

The atmosphere is not isothermal under normal conditions, yet most acoustic propagation models make that assumption. Temperature inhomogeneity can occur as random fluctuations resulting from convection cells and turbulence or as slow diurnal variations in the atmosphere immediately adjacent to the ground surface. It is the latter case that this paper addresses.

During daylight hours when sufficient insolation is present, the atmosphere is typically warmer near the ground surface than far above it, a lapse condition. Although these regions of strong temperature gradients extend, at most, only a few meters above the ground, most acoustic receivers are also in this range of altitude. Ground mounted microphones, which are sometimes used to avoid ground reflections, are unfortunately located so as to receive the maximum effects of refraction due to temperature gradients.

I. TEMPERATURE PROFILE

Any study of the effects of thermal gradients on near-earth sound propagation requires the selection of a temperature profile which is both realistic and mathematically tractable. Geiger[1] gives some experimental results which indicate that the variation of temperature with altitude behaves as the logarithm of the height above the ground. Tenekes and Lumley[2] give an argument based on turbulence theory that leads to the same conclusion.

Logarithmic profiles are difficult to deal with mathematically. Most previous work (e.g., Pekeris[3]) on the problem of acoustic propagation in a stratified atmosphere have considered the profile

$$T = T_0/(1 + \alpha z), \tag{1}$$

which yields an exact solution to the resulting differential equation. The vertical temperature profile used here

$$\frac{T}{T_\infty} = 1 + \frac{\Delta T}{T_\infty}\left(\frac{1}{1+\alpha z}\right) \tag{2}$$

is similar to Eq. (1) in its behavior near the ground ($z = 0$) in that it allows a steep gradient, but, more realistically, asymptotically approaches a constant value high above the ground. Using data obtained by Willshire[4] and by Butterworth[5] and fitting Eq. (2) to this data, typical values for α ranged from 1.2 to 5.9 m^{-1} and for $\Delta T/T_\infty$ from 0.0032 to 0.0342 for lapse conditions. Similar values of α and magnitude of $\Delta T/T_\infty$ were obtained for inversion conditions. In other cases, particularly where a lapse condition is being replaced by an inversion or vice versa, the fit can be very poor.

II. ANALYSIS

Consideration of the problem of propagation of plane waves in a thermally inhomogeneous atmosphere yields considerable insight into the more complex problem of propagation of waves from a point source. The problem is also interesting in its own right as a model of the propagation of waves from a point source when the source is very far from the refracting region.

The problem considered is governed by the equation

$$\frac{1}{c^2(z)}\frac{\partial^2 P}{\partial t^2} + \nabla^2 P = 0, \tag{3}$$

with the sound speed $c(z)$ given by

$$c^2(z) = c_\infty^2\left[1 + \frac{\Delta T}{T_\infty}\left(\frac{1}{1+\alpha z}\right)\right]. \tag{4}$$

At the surface ($z = 0$) the boundary condition

$$-Zw = P, \tag{5}$$

where w is the vertical component of the acoustic fluid velocity and Z the acoustical impedance of the surface, is applied. The solution is assumed to behave as

$$P = \exp\left[i\left(\omega t - \frac{\omega}{c_\infty}x\cos\theta + \frac{\omega}{c_\infty}z\sin\theta\right)\right] + R(\theta)\exp\left[i\left(\omega t - \frac{\omega}{c_\infty}x\cos\theta - \frac{\omega}{c_\infty}z\sin\theta\right)\right] \tag{6}$$

as $z \to \infty$. This condition implies the solution behaves as plane waves in a homogeneous atmosphere outside the region of strong gradients. The subscript ∞, indicating evaluation as $z \to \infty$, is omitted below to simplify notation. The subscript zero will be used to indicate evaluation at the ground surface.

Taking

$$P = F(z)\exp\{i[\omega t - (\omega/c)x\cos\theta]\} \tag{7}$$

and substituting into Eq. (3) yields

$$\frac{d^2F}{dz^2} + \frac{\omega^2}{c^2}\left(\frac{1+\alpha z}{1+\alpha z+\Delta T/T} - \cos^2\theta\right)F = 0, \tag{8}$$

a second-order differential equation with a turning point at

$$z_{TP} = (1/\alpha)[(\Delta T/T)\cot^2\theta - 1]. \tag{9}$$

Nayfeh[6] gives a method of obtaining an approximate solution of this equation which is valid when $\gamma = \omega/(\alpha c) \gg 1$. This requirement is the same as that found for Eq. (3) to be valid, so no new approximations are required. The approximate solution can be expressed as

$$F = \frac{K_1}{[g'(z)]^{1/2}} h_1(\eta(z)) + \frac{K_2}{[g'(z)]^{1/2}} h_2(\eta(z)) \tag{10}$$

where

$$\eta(z) = (\tfrac{3}{2}\gamma)^{2/3} g(z), \tag{11}$$

$$K_1 = \begin{cases} A, & 0 < \cos\vartheta \leqslant (1+\Delta T/T)^{-1/2}, \\ A, & \cos\theta \geqslant (1+\Delta T/T)^{-1/2} \\ & \text{and } z \geqslant z_{TP}, \\ \dfrac{Ae^{i(\pi/6)}}{e^{i(\pi/6)} - iR}, & \cos\theta \geqslant (1+\Delta T/T)^{-1/2} \\ & \text{and } 0 \leqslant z \leqslant z_{TP}, \end{cases} \tag{12}$$

$$K_2 = \begin{cases} A \cdot R, & 0 < \cos\theta \leqslant (1+\Delta T/T)^{-1/2}, \\ \dfrac{Ae^{-(\pi/6)}}{e^{i(\pi/6)} - iR}, & \cos\theta \geqslant (1+\Delta T/T)^{-1/2} \\ & \text{and } z \geqslant z_{TP}, \\ \dfrac{ARe^{i(\pi/6)}}{e^{i(\pi/6)} - iR}, & \cos\theta \geqslant (1+\Delta T/T)^{-1/2} \\ & \text{and } 0 \leqslant z \leqslant z_{TP}, \end{cases} \tag{13}$$

$$A = \sqrt{\pi/3}\,\sin^{1/2}(\theta)\gamma^{1/6}\alpha^{1/2}e^{i(5\pi/12)}, \tag{14}$$

$$R = -\frac{\tau h_1(\eta(0)) + i\psi h_1'(\eta(0))}{\tau h_2(\eta(0)) + i\psi h_2'(\eta(0))}, \tag{15}$$

$$\tau = \alpha\gamma - \frac{i}{2}\frac{Z}{\rho_0 c_0}\frac{g''(0)}{g'(0)}, \tag{16}$$

$$\psi = (Z/\rho_0 c_0)\gamma^{2/3} g'(0)(\tfrac{3}{2})^{2/3}, \tag{17}$$

$$g^{3/2}(z) = \left[\sin^2\theta\left(1 + \alpha z + \frac{\Delta T}{T}\right)^2 - \frac{\Delta T}{T}\left(1 + \alpha z + \frac{\Delta T}{T}\right)\right]^{1/2} - \frac{1}{2}\frac{\Delta T}{T}\frac{1}{\sin\theta}\ln\left(\frac{1+\phi}{1-\phi}\right), \tag{18}$$

$$\phi = \left(\frac{\sin^2\theta(1+\alpha z + \Delta T/T) - \Delta T/T}{\sin^2\theta(1+\alpha z + \Delta T/T)}\right)^{1/2}, \tag{19}$$

$$h_1(\xi) = (\tfrac{2}{3})^{1/3}\xi^{1/2}H_{1/3}^{(1)}(\tfrac{2}{3}\xi^{3/2}), \tag{20}$$

and

$$h_2(\xi) = (\tfrac{2}{3})^{1/3}\xi^{1/2}H_{1/3}^{(2)}(\tfrac{2}{3}\xi^{3/2}). \tag{21}$$

Values of the modified one-third order Hankel functions, h_1 and h_2, have been tabulated and their properties discussed.[7] For the numerical analysis the functions h_1 and h_2 have been expressed in terms of Airy functions, Ai and Bi, where

$$h_1(\xi) = k\,[\mathrm{Ai}(-\xi) - i\,\mathrm{Bi}(-\xi)] \tag{22}$$

and

$$h_2(\xi) = k^*[\mathrm{Ai}(-\xi) + i\,\mathrm{Bi}(-\xi)], \tag{23}$$

where $k = (12)^{1/6}e^{-i\pi/6}$ and k^* is the complex conjugate of k.

The asymptotic expressions for the modified Hankel functions are available,[7] and if the parameter γ is sufficiently large the usual result for the reflection of plane waves from a plane surface in a homogeneous atmosphere is obtained.

The form and behavior of the solution depends upon whether the waves which are initially traveling downward, toward the ground, are reflected upward from the ground or if refraction turns the waves upward before the ground is reached. If $\cos\theta < [(1+\Delta T/T)]^{-1/2}$ the turning point is below the ground surface and reflection from the ground surface occurs. In the opposite case the turning point is above the ground surface and the wave is refracted upward before the ground is reached.

Based on meteorological data where $\Delta T/T$ ranged up to 0.0342, rays with incidence angles less than about 10° could be refracted upwards before reflection from the ground could occur. Although these angles are quite small, they are within the range of common "look angles" for aircraft noise testing and refractive effects can be expected to play a significant role in this case.

If the waves are refracted into upward propagation at the turning point, the solution depends upon whether the receiver is above or below the turning point. Above the turning point the solution describes an interference pattern similar to that in a uniform atmosphere. Below the turning point exponential growth or decay occurs for large values of η.

The first term in Eq. (10) decays as the receiver moves downward, away from the turning point, if $\sqrt{-1}$ is taken to equal $-i$ and, similarly, the acoustic field below the turning point is reduced as θ goes to zero and the turning point moves upward, if $\ln(-1) = -i\pi$ is chosen. The second term in Eq. (10) also decays with decreasing θ, but grows as z decreases from the turning point value. This behavior occurs since the second term represents the reflection from the ground surface of the exponentially decreasing first term.

III. RESULTS

Numerical evaluation of the solution for the propagation of plane waves in a temperature gradient has been performed on a digital computer. Figure 1 is a typical example and is intended as the referent as parameters are varied in other drawings. Surface impedance values given by Chessell's[8] relationship for grass have been used, with specific flow resistance chosen as 300 cgs units. A value of $\gamma = 10$ corresponds to a frequency of approximately 1000 Hz with $\alpha = 2\,\mathrm{m}^{-1}$. Although this value of γ and the additional value discussed below are not extremely large they are given as examples and experiments will be required to demonstrate the applicability of the theory of these values. Figures 1 to 3 show plots of height above the ground versus sound pressure level in decibels. The reference level is assumed equal to the amplitude of the incoming wave at an infinite height. Thus the plots show the difference between the sound pressure

level of the incident wave in an isothermal atmosphere which is neither reflected nor refracted and the levels resulting from the refraction/reflection process in a nonisothermal atmosphere.

For the conditions used to calculate Fig. 1(a), $\gamma = 10$, $\Delta T/T = 0.2$, $\theta = 5°$, and $\alpha = 2\ \mathrm{m}^{-1}$ the turning point and caustic is located at a height of about 0.8 m. Note that the maximum sound pressure level occurs somewhat above this. Above the turning point an interference pattern occurs with a slowly decreasing sound level in successively higher maxima. Since the ratio of amplitudes of the incident and refracted waves is near unity, values of the sound levels above approximately 6 dB must be due to increased amplitude of the waves beyond the values occurring far above the ground. The similar amplitude of the two waves also leads to the strong cancellation observed in the interference pattern. Below the turning point a rapid decay occurs as the shadow region is entered.

Figure 1(b) is for the same conditions but with an isothermal atmosphere, $\Delta T/T = 0$. In this case the reflected wave is somewhat weaker than the incident wave and this is apparent from the levels reached in the interference maxima and minima. Comparison of Fig. 1(a) and (b) clearly points out the increased sound levels and variable spacing of the interference pattern in the thermally inhomogeneous case.

Figure 2(a) shows a similar case but with the incidence angle increased to 10°. In this case the turning point would be below the ground surface and reflection at the ground occurs. The reflected wave is weaker than the incident wave in

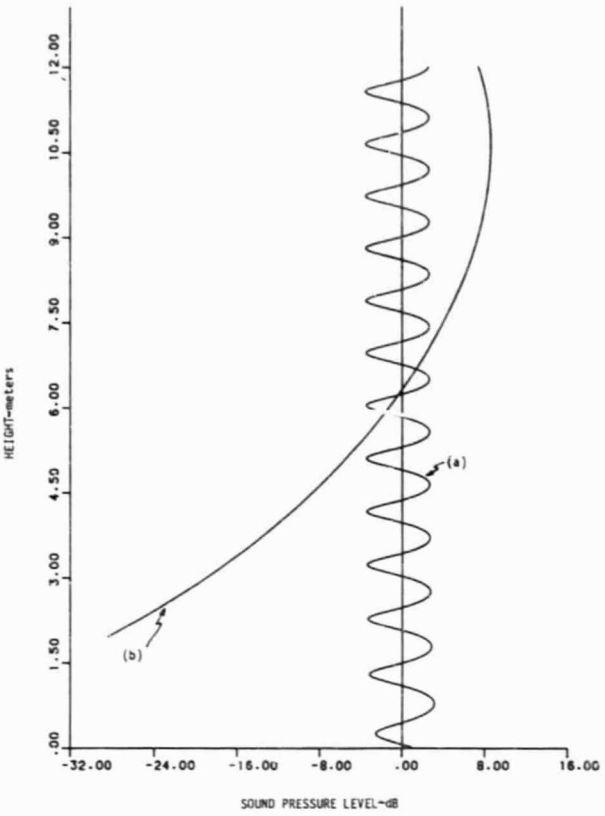

FIG. 2. Height versus sound pressure level for: (a) $\gamma = 10$, $\Delta T/T_\infty = 0.02$, $\theta = 10°$, $\alpha = 2\ \mathrm{m}^{-1}$; (b) $\gamma = 10$, $\Delta T/T_\infty = 0.02$, $\theta = 2°$, $\alpha = 2\ \mathrm{m}^{-1}$.

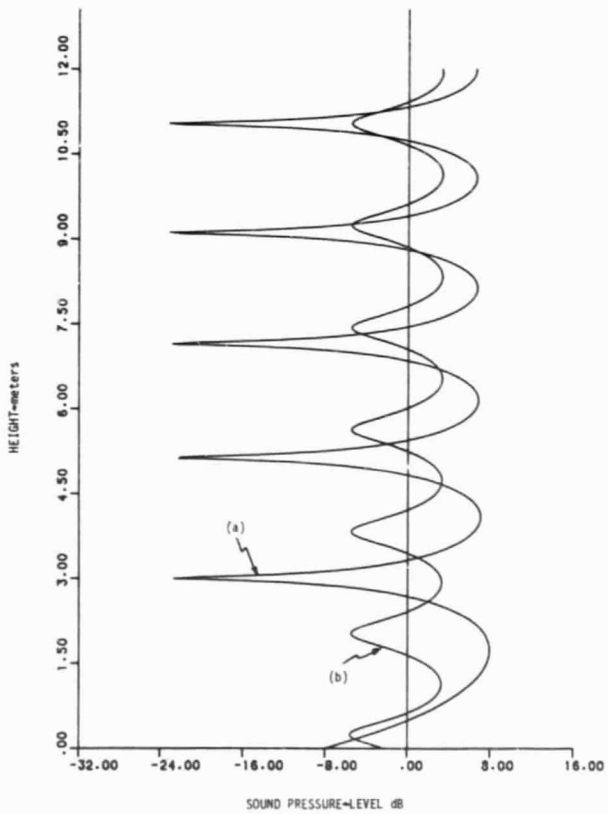

FIG. 1. Height versus sound pressure level for: (a) $\gamma = 10$, $\Delta T/T_\infty = 0.02$, $\theta = 5°$, $\alpha = 2\ \mathrm{m}^{-1}$; (b) $\gamma = 10$, $\Delta T/T_\infty = 0$, $\theta = 5°$, $\alpha = 2\ \mathrm{m}^{-1}$.

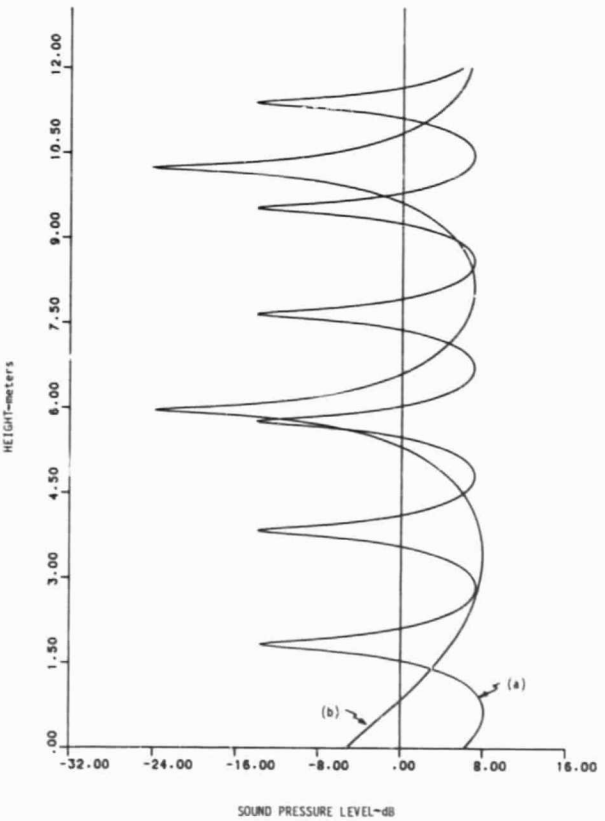

FIG. 3. Height versus sound pressure level for: (a) $\gamma = 10$, $\Delta T/T_\infty = 0.01$, $\theta = 5°$, $\alpha = 2\ \mathrm{m}^{-1}$; (b) $\gamma = 10$, $\Delta T/T_\infty = 0.02$, $\theta = 5°$, $\alpha = 1\ \mathrm{m}^{-1}$.

this case and this is indicated by the levels occurring in the interference pattern. Figure 2(b) again shows a similar case but with $\theta = 2°$. In this case the turning point is at a height of about 7.7 m above the ground and the rapid decay below the turning point is more apparent than in Fig. 1(a).

In Fig. 3(a) $\Delta T/T$ has been decreased to 0.01 yielding a turning point at about 0.15 m. Comparison to Fig. 1(a) shows that this change has reduced the envelope of the sound level maxima, and that the interference minima are at a higher sound level, both due to a slightly weaker reflected wave than in Fig. 1(a), but stronger than the isothermal case shown in Fig. 1(b). Figure 3(b) has the parameter α decreased to 1 m^{-1} spreading the region of significant temperature variation upward and decreasing the temperature gradient. The parameter λ is held constant at ten but since α was decreased this corresponds to a decreased frequency as is apparent from the interference pattern. The turning point for this case is at a height of about 1.6 m.

IV. CONCLUSIONS

The situation investigated here, plane waves approaching a finite impedance boundary at an arbitrary angle through a lapse temperature gradient is seen to demonstrate the major phenomena occurring at a large distance from a point source. The interference pattern is seen to be significantly distorted from the isothermal situation by an inhomogeneous layer about 0.5 m thick ($\alpha = 2$ m^{-1}) and with a temperature increase of about 6 °C near the ground ($\Delta T/T = 0.02$).

ACKNOWLEDGMENTS

The authors would like to acknowledge the support of the National Research Council which allowed one of the authors (WKV) to develop the model presented here while a Senior Research Associate at NASA Langley Research Center and of NASA under grant NAG-1-283 which allowed numerical evaluation. The assistance of Alex Cheng in carrying out some of the calculations is also greatly appreciated.

[1] R. Geiger, *The Climate Near the Ground* (Harvard U. P., Cambridge, MA, 1965).

[2] H. Tenekes and J. L. Lumley, *A First Course in Turbulence* (M.I.T., Boston, MA, 1972).

[3] C. L. Pekeris, "Theory of Propagation of Sound in a Half-space of Variable Sound Velocity under Conditions of Formation of a Shadow Zone," J. Acoust. Soc. Am. **18**, 295–315 (1946).

[4] W. L. Willshire (private communication, 1980).

[5] J. Butterworth, "An Investigation of Sound Pressure Levels in an Acoustic Shadow," M.S. thesis, University of Utah (1979).

[6] A. H. Nayfeh, *Perturbation Methods* (Wiley, New York, 1973).

[7] *Tables of the Modified Hankel Functions of Order One-Third and of Their Derivatives* (Harvard U. P., Cambridge, MA, 1945).

[8] C. I. Chessell, "Propagation of Noise along a Finite Impedance Boundary," J. Acoust. Soc. Am. **62**, 825–834 (1977).